

PETE 611

**RESERVOIR SIMULATION
APPLICATION**

Class Notes

Spring 2000

R. A. Wattenbarger

Texas A&M University

Contents

Chapter 1 Three-Phase Relative Permeability

Introduction
Driving Forces
Gravity Segregation - Homogeneous
Stratified Reservoir - High Rate (Hearn)
Stratified Reservoir - Low Rate
Vertical Equilibrium
Dynamic Pseudo Relative Permeability (Jacks, *et al.*)
Dynamic Pseudo Relative Permeability (Kyte & Berry)

Chapter 1A Equilibration

Geologic Equilibration
Initialization of Gridblocks
Effect of Heterogeneity

Chapter 2 Repressuring with Variable Bubble Point

Introduction
Vertical Variation of Initial Bubble Point Pressure
Laboratory Behavior
Reservoir Behavior
Effect of Re-solution on Compressibility
A case of Re-solution History Matching
Gas Injection above the Bubble Point
Water Flooding Depleted Reservoirs
Diffusion Effect
Illustrative Case of Repressuring of Secondary Gas Cap with Limited
Resolution
A Simplified Waterflood of Depleted Reservoir

Chapter 3 History Matching

Technique
Purpose

Quality of Data
Production Allocation
Wrong Rate Problem
Pressure Analysis
Determining OOIP from Depletion History
Continuity Problem
Parameters to be Changed in History Matching
History Matching Procedures

Chapter 4 Coning

Introduction
Analysis of Forces
Critical Coning Rate
Coning Simulation
Addington's Method
References
Exercises
Appendix

Chapter 5 Compositional Simulation

Introduction
Applications
PVT Behavior
Equations for Compositional Simulation
Regression of EOS Parameters
Modeling of Surface Facilities
Lab Tests
Gas Cycling in Volatile Oil and Gas Condensate Reservoir
Vaporizing Gas Drive (VGD)
Field Examples
Fundamentals
 Heavy Fraction Characterization
 Pseudoization
 Regrouping Scheme of Heavy Components
Compositional Simulation
 Heavy Ends Characterization
 Default Fluid Predictions
 Pre-Regression
 Component Pseudoization
 Regression
 Initialization Data for VIP
 Run Data for VIP
Data Files

CHAPTER 1

Pseudo Relative Permeability Curves

- Introduction
- Driving Forces
- Gravity Segregation - Homogeneous
- Stratified Reservoir - High Rate (Hearn)
- Stratified Reservoir - Low Rate
- Vertical Equilibrium
- Dynamic Pseudo Relative Permeability (Jacks, *et al.*)
- Dynamic Pseudo Relative Permeability (Kyte & Berry)

Pseudo Relative Permeability Curves

Introduction

Numerical reservoir simulation is an important engineering tool to predict reservoir performance and plan future field development. For a fieldwide reservoir simulation, a finely gridded, three-dimensional model might be needed to adequately simulate reservoir performance under natural depletion, or waterflood conditions. However, the large areal extent of the field may require too many grid blocks, which result in computation very complex and time consuming. In addition, reservoir data control in most of fields is often too sparse to justify a finely gridded model. For these reasons, it is often desirable to simulate reservoir performance with 2-D areal model instead of a 3-D model. To give realism to the results, the pseudo relative permeability treatment is developed. By using pseudo relative permeabilities, we can obtain essentially the same results with 2-D areal model. There are two purposes of this transformation. The first is to reduce computing cost and complexity. The second relates to the importance of pseudo relative permeability. In most cases, the use of rock curve in coarse vertical gridding will produce incorrect results. For example, unrealistically optimistic gas saturation profile and much later gas breakthrough because it did not account for gas overriding.⁶

Pseudo relative permeabilities result from averaging the flow properties and the fluid saturations in the vertical direction. In order to compress a 3-D model to a 2-D areal model, we must account for everything that is happening in the vertical direction of the 3-D model and average that into our pseudo relative permeabilities. **Fig. 1** illustrates a transformation of 3-D fine grid model to coarse 2-D areal model, and **Fig. 2** shows an example of those two model performances.

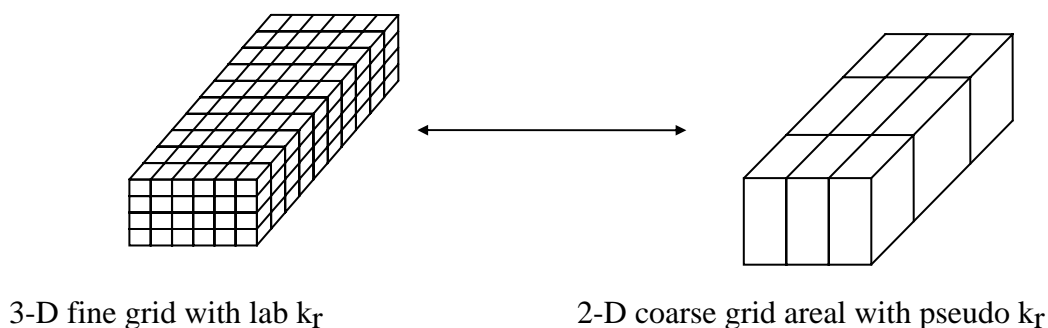


Fig. 1 - Transformation of 3-D model to 2-D model.

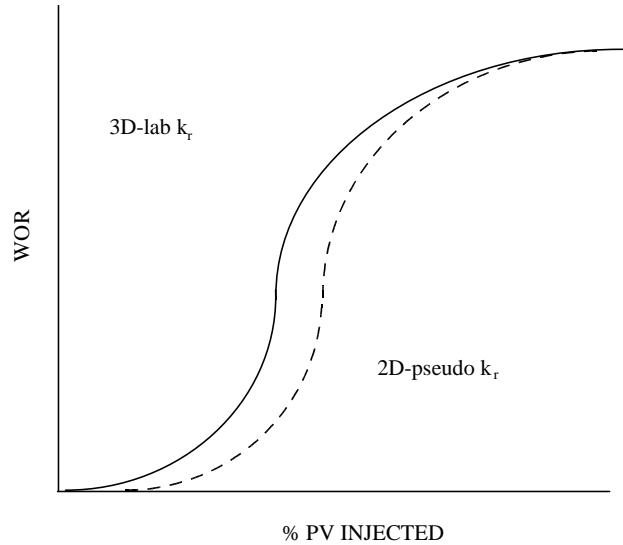


Fig. 2 - Example of performances of 3-D fine grid using lab k_r and 2D coarse grid with pseudo k_r .

In this chapter, we present three kinds of static analyses of pseudo relative permeabilities, each analysis based on the particular driving force or forces dominating in the reservoir. We begin by discussing the three driving forces which control fluid flow in the reservoir. Then, the pseudo relative permeabilities for the segregated case for flows dominated by the gravity force is presented, followed by Hearn's method for flows dominated by the viscous force, and finally presented is the vertical equilibrium method, where capillary and gravity forces are assumed to be in equilibrium.

Driving Forces

The movement of the fluids in a typical reservoir is controlled by three kinds of forces. Table 1.1 shows those three forces. The gravity forces tend to segregate the fluid vertically and is proportional to the difference in densities. Viscous forces, induced by production and injection, tend to move the fluids in the direction of the induced movement and the forces are proportional to the Darcy velocity and inversely proportional to mobility. The capillary forces tend to spread out the saturations according to the slope of the capillary pressure curve and the saturation gradients. In the segregated flow case, the saturation gradients of interest are vertical.

Table 1
Forces in fluid movement

Forces	Magnitude
(a) gravity	$\frac{\Delta\rho}{144}$
(b) viscous	$\frac{\mu}{0.00633k} u$
(c) capillary	$\frac{dP_c}{dS} \frac{\partial S}{\partial x}$

The ratio of gravity forces to viscous forces is known as Gravity Number. This number is calculated by the following equation for an oil-water system:

$$N_{grav} = \frac{(\rho_w - \rho_o)/144}{(q_w / A) \frac{\mu_w}{0.00633 \bar{k} k_{rw@S_{or}}} \quad (1)$$

where

$$\bar{k} = (\Sigma k_i h_i) / \Sigma h_i$$

Gravity Segregation - Homogeneous

Methodology. Segregated flow is a special case in homogeneous reservoir that requires certain assumptions to be met. It is assumed that

- (a) gravity forces dominate.
- (b) viscous and capillary forces are negligible.
- (c) if a transition zone is present, it is negligible compared to the thickness of the reservoir.
- (d) there is a good vertical communication so that the fluids are free to segregate vertically.

For an oil/water reservoir under assumptions, the free water segregates to the bottom by gravity. Above the water/oil contact, we assume that only connate water saturation exists. while below the water/oil contact, only residual oil saturation exists. Water flows near the bottom and oil flows near the top.

Given a particular location of the water/oil contact, we can calculate the average saturation and the average flow coefficient (pseudo relative permeability). Fig. 3 shows the physical process of segregation for homogeneous reservoirs.

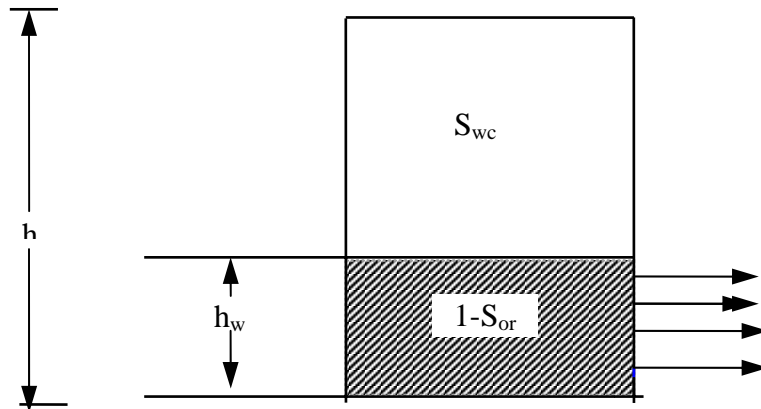


Fig. 3 - Gravity segregation case.

The equations that express the average water saturation, and the oil and water pseudo relative permeability, are all linear with the water height. Consequently, the pseudo relative permeabilities are linear with saturation as can be seen in these following equations :

$$\tilde{S}_w = \frac{h_w}{h}(1 - S_{or}) + \frac{h - h_w}{h}S_{wc} \quad (2)$$

$$\tilde{k}_{rw} = \frac{h_w}{h}k_{rw@ (1 - s_{or})} \quad (3)$$

$$\tilde{k}_{ro} = \frac{h - h_w}{h}k_{ro@ (1 - s_{wc})} \quad (4)$$

If we investigate the "end points" of the flow conditions, we note that when the water/oil contact is at the bottom, there is no water flow. Water saturation is at the connate water saturation value and the oil pseudo relative permeability is the value at connate water saturation. When the water/oil contact is at the top, no oil flows, water flows at the relative permeability at residual oil saturation and the water saturation, has a value with residual oil saturation present.

Calculation Procedure. The calculation procedures are summarized in the following steps:

- (1) Characterize thickness, connate water saturation, and residual oil saturation.
- (2) Find end-point water relative permeability and end-point oil relative permeability.
- (3) For a value of h_w calculate \tilde{S}_w , \tilde{k}_{rw} and \tilde{k}_{ro} .
- (4) Repeat step 3 for different values of h_w .

Application. The equation that express pseudo relative permeabilities and average water saturations for the segregated case are linear. If we look at the shape of the pseudo relative permeability curves, we notice that these are straight lines connecting the end points of the laboratory relative permeability curves as shown in Fig. 4. If the segregated assumptions supply, then we can input these straight line as relative permeabilities in a 2-D model and obtain about the same results as the lab curves produce in a 3-D model.

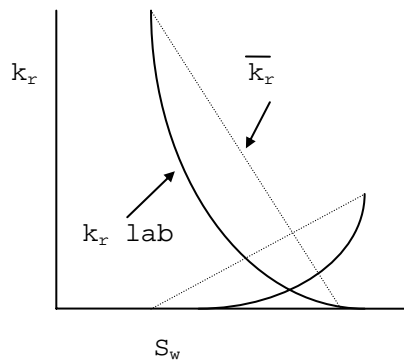


Fig. 4 - k_r curves for homogeneous gravity segregated case.

Stratified Reservoir - High Rate (Hearn)⁴

A common method for approximating the effect of vertical permeability variation in displacement projects such as waterflooding or aquifer encroachment is to assume that the reservoir is stratified. At high rates, the vertical sweep may not be dominated by gravity forces, but by viscous flow forces. Rather than the water falling to the bottom of the reservoir because of slow movement, the water in this case moves to the high permeability layers due to vertical permeability variation.

Hearn (1971) studied this case and compared the assumptions to the Stiles waterflood calculations which are used to predict water/oil ratio by layer floodout. This is still an important concept to understand even though these assumptions are somewhat simplified.

..

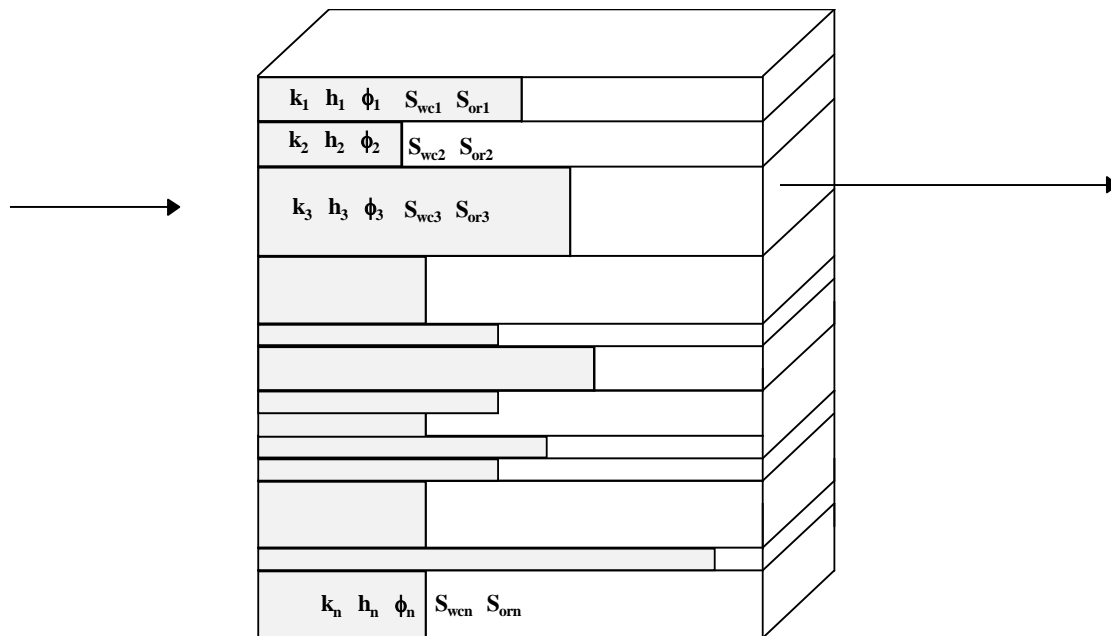


Fig. 5 - Stratified reservoir model.

Methodology. The pseudo relative permeability functions are based on a mathematical model for calculating vertical efficiency using a stratified concept as shown in Fig. 5. The assumptions are listed as follows:

- (a) Uniform layers.
- (b) Piston-like displacement.
- (c) Oil and water phases present.
- (d) Good vertical communication.
- (e) Viscous forces dominate (ignore gravity, P_c forces)

Now we consider a layered case in which water injection has begun and established different fronts according to the permeability of the layers. The order of breakthrough is determined by the properties of each layer. After each layer has broken through, we can calculate the average relative permeabilities and average saturations. These calculations will give us points on a pseudo relative permeability curve which we can then smooth to obtain a continuous curve.

Calculation Procedures. The calculation procedures are summarized in the following steps.

- (1) The layers are characterized by thickness, porosity, connate water saturation, and residual oil saturation.
- (2) The layers are arranged in order of decreasing breakthrough of water-oil displacement front according to the values of the factor $k_i / \phi_i \Delta S_i$, where $\Delta S_i = (1 - S_{wci} - S_{ori})$
- (3) Calculate the average water saturation at the outflow end at the system before breakthrough of the first layer, and after breakthrough of each layer
- (4) For each, values of \tilde{k}_{rw} and \tilde{k}_{ro} , the pseudo relative permeabilities to water and to oil, respectively, are calculated. The resulting equations are summarized as follows:

For $n = 0$ (before breakthrough):

$$\tilde{S}_w = \frac{\sum_{i=1}^N (\phi h S_{wc})_i}{\sum_{i=1}^N (\phi h)_i} \quad (5)$$

$$\tilde{k}_{rw} = 0 \quad (6)$$

$$\tilde{k}_{ro} = \frac{\sum_{i=1}^N (kh k_{ro@S_{wc}})_i}{\sum_{i=1}^N (kh)_i} \quad (7)$$

After each layer breakthrough (For $n = 1, 2, 3, \dots, N-1$), then calculate:

$$\tilde{S}_w = \frac{\sum_{i=1}^n (\phi h (1 - s_{or}))_i + \sum_{i=n+1}^N (\phi h s_{wc})_i}{\sum_{i=1}^N (\phi h)_i} \quad (8)$$

$$\tilde{k}_{rw} = \frac{\sum_{i=1}^n (kh)_i k_{rw@}(1-S_{or})}{\sum_{i=1}^N (kh)_i} \quad (9)$$

$$\tilde{k}_{ro} = \frac{\sum_{i=n+1}^N (khk_{ro@S_{wc}})_i}{\sum_{i=1}^N (kh)_i} \quad (10)$$

For n = N

$$\tilde{S}_w = \frac{\sum_{i=1}^N (\phi h(1 - S_{or}))_i}{\sum_{i=1}^N (\phi h)_i} \quad (11)$$

$$\tilde{k}_{rw} = k_{rw@(1-S_{or})} \quad (12)$$

$$\tilde{k}_{ro} = 0 \quad (13)$$

where,

N= total layers

n= layers with breakthrough

Application. Fig. 6 shows the comparison of the pseudo and lab relative permeability curves. The pseudo relative permeabilities to water are generally very different from lab relative permeability.

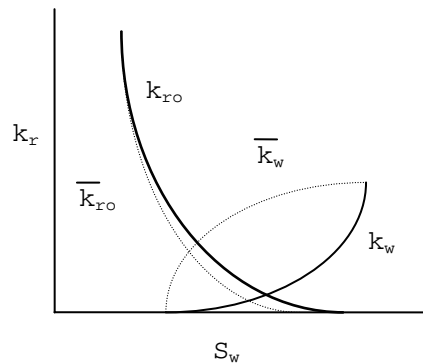


Fig. 6 - Pseudo k_r curves for Hearn's method

Stratified Reservoir - Low Rate

Hearn's method and procedures for calculating pseudo relative permeability of stratified reservoir are applied but with layers ordered as they actually occur in the vertical sequence. Gravity forces will have more influence on fluid movement than viscous force. Fig. 7 shows the performances of both low rate and high rate cases.

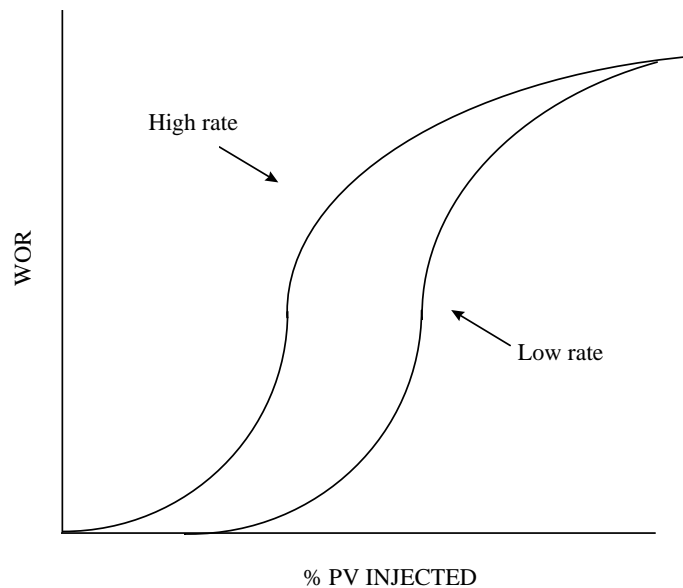


Fig. 7 - Performance of stratified reservoir for low rate and high rate cases.

Vertical Equilibrium

The vertical equilibrium case (VE) is similar to the segregated case except that it is modified to include the effects of capillary pressure. The VE concept is the differences between the pressures in the oil and water (or oil and gas) phases is exactly balanced by capillary pressure. This is the same as having potentials of each phase constant vertically.⁶ The factors which favor VE are:

- (1) low resistance to flow normal to the bedding planes,
- (2) sands thin in the direction normal to the bedding planes,
- (3) low areal rates of fluid movement, and
- (4) if there is capillary pressure in transition zone, the capillary and gravity forces are balanced.

Fig. 8 illustrates equilibrium between capillary forces and gravity forces. The P_C curve translated to elevation above the *free water level* ($P_C = 0$) by $P_C = (Z - Z_{FWL})(\rho_w - \rho_o)/144$.

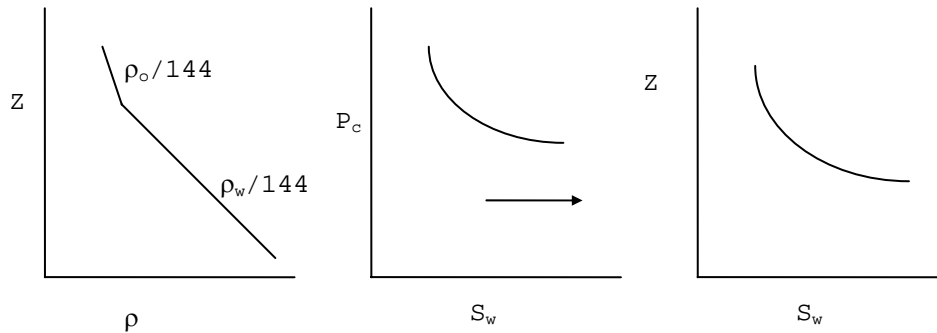


Fig. 8 - P_C forces balance gravity forces.

Methodology. The calculation of the saturation profile at any moment depends on the translation of the capillary pressure curve (imbibition curve) by multiplying the difference in hydrostatic gradients. Given a particular saturation profile, the integration is performed from top to bottom of the formation. The saturations are averaged with a porosity-thickness weighting and the pseudo relative permeabilities are averaged with a permeability-thickness weighting.

Equations 14 and 15 illustrate how the integration process is applied to obtain a volumetrically- averaged saturation and relative permeability for wetting phase flow parallel to the x-z plane at any areal point on the reference surface.

$$\tilde{S}_w = \frac{\int_0^h \phi(Z) S_w(Z) dZ}{\int_0^h \phi(Z) dZ} \quad (14)$$

$$\tilde{k}_{rw} = \frac{\int_0^h k(Z)k_{rw}(Z)dZ}{\int_0^h k(Z)dZ} \quad (15)$$

The shape of the pseudo relative permeability and capillary pressure curves are affected by:

- (1) density difference,
- (2) dip angle,
- (3) sand thickness h, and
- (4) stratification (k(Z) and p(Z)).

So the resulting pseudo relative permeability curves are not straight lines unless the assumptions of the homogeneous segregated cases are met. Otherwise, the VE curves will be somewhere between the laboratory curves and the segregated case curves.

Application. Results summarized in Fig. 9 demonstrate that simulations using correct 1-D, VE pseudo curves agree closely with the correct behavior.⁶

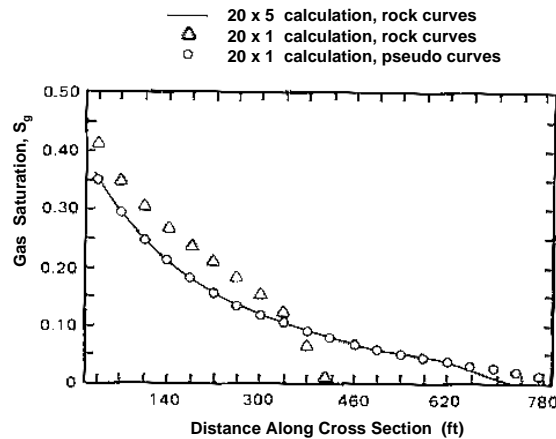


Fig. 9 - Comparison of saturation profiles in 2-D cross-sectional and 1-D areal models⁶ (from Fig. 3.23, SPE Monograph 13)

Dynamic Pseudo Relative Permeability (Jacks *et al*)⁵

The purpose of pseudo relative permeabilities is to reduce the number of cells required to perform reservoir simulation studies. The vertical definition of the reservoir is a very important factor that affects the results of numerical simulation. Three-dimensional reservoir simulation models can be replaced by two-dimensional models using the pseudo functions. The transformation from 3-D to 2-D and from 2-D to 1-D models can reduce the cost of running the simulator. But to obtain good results from 2-D and 1-D simulators, the third dimension (vertical dimension) must be properly described by modeling the nonuniform distribution and flow of fluids.

The transformation can be achieved through the use of special saturation-dependent functions. These functions are derived from conventional laboratory-measured values.

Two types of reservoir models have been developed: the vertical equilibrium (VE) model of Coats *et al.*,¹⁻³ which is based on capillary-gravity equilibrium in the vertical direction. The second is the stratified model of Hearn⁴, which assumes that viscous forces dominate vertical fluid distribution.

The effect of large changes in flow rate have not been taken into consideration in the two models mentioned above. An alternative method for developing pseudo functions that is applicable to a wide ranges of flow rates and initial fluid saturations was introduced by Jacks *et al.*⁵. The new functions are both space and time-dependent. The functions are called dynamic pseudo functions.

Dynamic pseudo relative permeability functions are based on the vertical saturation distribution. The VE model is often not appropriate in actual field situations. In this case, one of the following techniques should be used:

- (1) A third dimension should be added to the model in order to take into account the vertical saturation distribution.
- (2) Dynamic pseudo relative permeabilities should be used to more accurately model the vertical saturation distribution.

Dynamic pseudo relative permeability functions are derived from the results of cross-sectional models⁶. Dynamic pseudo-functions are used:

- (1) to reduce a fine grid 3-D model to a coarser 2-D model.
- (2) to reduce a 2-D model to a coarser 1-D model.
- (3) to reduce the number of blocks in the vertical direction in a 3-D model.

Use of dynamic pseudo permeabilities in 1-D models can simulate accurately the performance of 2-D cross-sectional models. The technique for deriving the vertical saturation distribution is summarized in the following steps:

- (1) Detailed simulation of the fluid displacement is performed in a vertical cross-sectional (RZ) model of the reservoir.
- (2) Results of the simulation runs are then processed to produce the depth-averaged fluid saturations.
- (3) Saturations are then used to produce dynamic pseudo relative permeability values for each column in the cross-sectional model at each time.
- (4) The results are a different set of dynamic pseudo functions for each column due to differences in initial saturations and reservoir heterogeneity.

The objective of the procedure is to produce separate pseudo relative permeability curves for different areas of the field. Once the dynamic pseudo relative permeability curves have been calculated, the correlations can be used in a one-dimensional simulation of the cross-sectional calculations.

The pseudo relative permeability can be determined by studying the results of cross-section runs. Dynamic pseudo relative permeability functions depend on both initial water saturation and flow rate. At each output, the following should be calculated for each column in the cross-sectional model:

- (1) Average water saturation.
- (2) Oil pseudo relative permeability.
- (3) Water pseudo relative permeability.

Calculation Procedure. The following is a step-by-step procedure to calculate the dynamic pseudo relative permeability curves from the laboratory data for an areal model block⁵:

- (1) Layer properties should be studied.
- (2) Determine fractional thickness for each zone.
- (3) Determine porosity-thickness for each zone.
- (4) Determine permeability-thickness for each zone
- (5) Determine the average water saturation of the block using:

$$\tilde{S}_w = \frac{\sum_{j=i}^{JMAX} (\phi h S_w)_j}{\sum_{j=i}^{JMAX} (\phi h)_j} \quad (16)$$

- (6) Calculate average water saturation in the oil zone.
- (7) Calculate dynamic pseudo relative permeability for water in the oil zone using:

$$\tilde{k}_{rw} = \frac{\sum_{j=1}^{JMAX} (khk_{rw})_j}{\sum_{j=1}^{JMAX} (kh)_j} \quad (17)$$

(8) Calculate dynamic pseudo relative permeability for oil in the oil zone using:

$$\tilde{k}_{ro} = \frac{\sum_{j=1}^{JMAX} (khk_{ro})_j}{\sum_{j=1}^{JMAX} (kh)_j} \quad (18)$$

(9) The pseudo relative permeabilities to oil and water in the oil zone are then averaged with values for zones in the remainder of the block thickness. These values are the dynamic pseudo relative permeabilities.

Fig. 10 illustrates a cross-sectional model which is used to develop dynamic pseudo relative permeabilities for each column, and Fig. 11 shows the results of the calculation. Higher rates move the dynamic pseudo relative permeability curves closer to the rock curve.

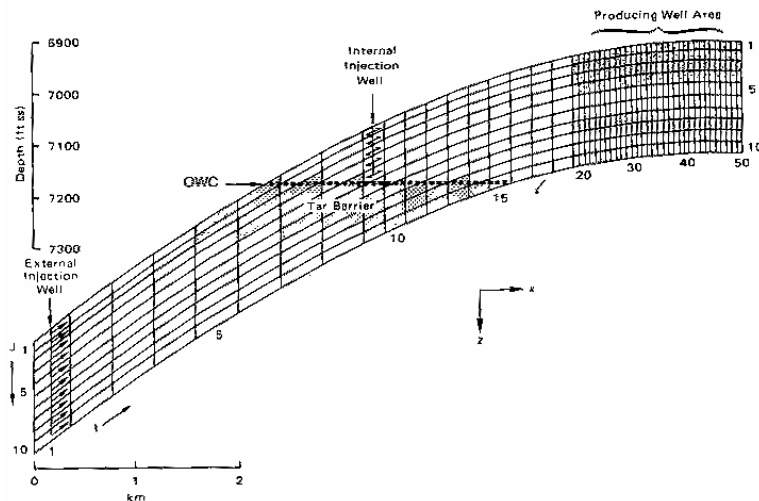


Fig. 10 - Cross-sectional model used to develop dynamic pseudo functions.⁶
(from Fig 3.25, SPE Monograph 13)

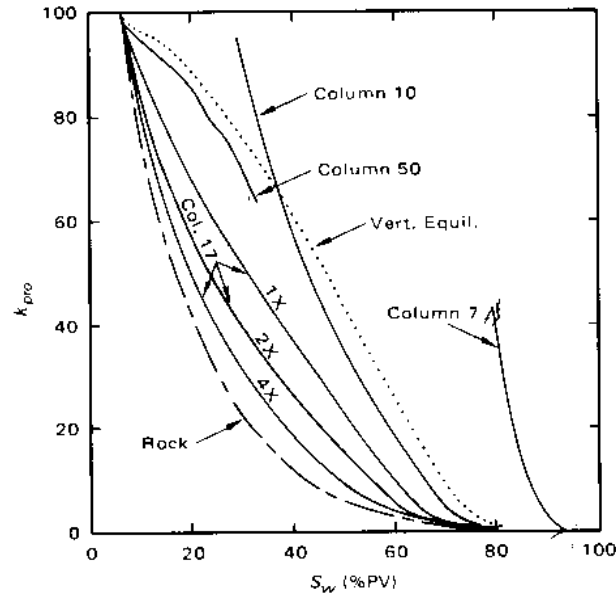


Fig. 11- Example of dynamic pseudo relative permeabilities.⁶
(from Fig. 3.24, SPE Monograph)

The effect of variations in initial water saturation on pseudo-relative permeabilities is shown by the curves for columns 7, 10 and 17 in Fig 11. Columns 7 ($S_{wi} = 81\%$) and 10 ($S_{wi} = 30\%$) are located in the oil-water transition zone area, whereas Column 17 is located entirely above the original contact and contains only clean oil at 7% PV connate water. The effect of rate on the dynamic pseudo-relative permeability to oil is shown in Fig 11 by the shift in curves obtained at the three rates (1x, 2x and 4x) in Column 17 and by the single curve representing all data from Column 50 of the cross-section model. Oil in Column 17 was displaced during the peak rate period but oil in Column 50 was displaced at much lower rates immediately prior to shut-in of the last well in the model.

Dynamic Pseudo Relative Permeability (Kyte & Berry)⁷

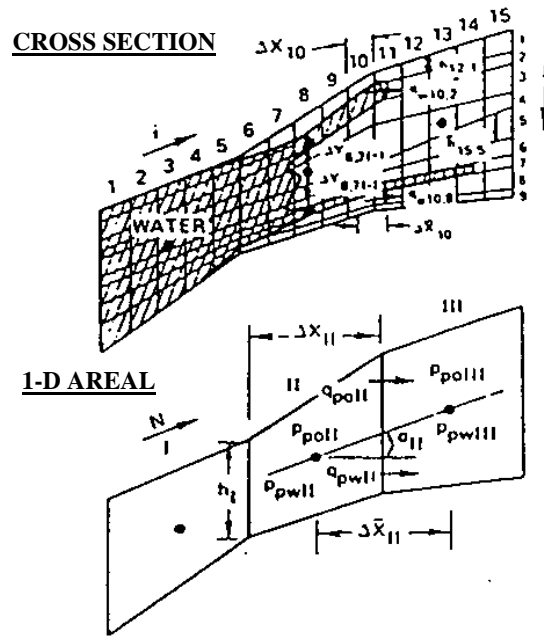
The objective of Kyte & Berry's method is to improve the dynamic pseudo relative permeability procedure, including a dynamic pseudo capillary pressure. These pseudo relative permeabilities differ because:

- they account for differences in computing block lengths between the cross-sectional and areal models, and
- they transfer the effects of different flow potentials in different layers of the cross-sectional model to the areal model.

Methodology. Dynamic pseudo functions are calculated for each areal block at different times during the cross-sectional run. This means pseudo functions are generated for each block in the one-dimensional areal model. The technique for calculating the pseudos are summarized in the following list:

- (a) Darcy's equation is used to calculate dynamic pseudo relative permeabilities of oil and water.
- (b) Pseudo capillary pressure, which is included, accounts for any phenomenon other than the gravity component in the direction of flow. This gravity component is included in the areal model flow calculations.
- (c) Upstream relative permeabilities will be used in the areal model to calculate flow between blocks.
- (d) Areal model porosity is defined as the ratio of the total void volume of all the cross-sectional blocks represented by the given areal block to the total bulk volume of these same cross-sectional blocks.
- (e) Areal block permeability is a type of harmonic average.
- (f) Densities and viscosities are evaluated at the arithmetic average pressure.

Calculation Procedure. Fig. 12 below compares a cross-sectional model with the corresponding one-dimensional areal model to help define symbols used in the equations.



NOTE: BOTH MODELS ARE 1 FT. THICK

Fig. 12 - Comparison of a cross-sectional model with the corresponding one-dimensional areal model. (from Fig. 9, p. 16, SPE Monograph Reprint 20)

Before developing equations for calculating pseudo functions, we need to define the relationship between porosities and permeabilities for the cross-sectional and areal models. Areal model block porosity is defined as shown below :

$$\phi_{II} = \frac{\sum_{i=6}^{i=10} (\bar{h} \phi \Delta X)_i}{\frac{1}{2} (h_I + h_{II}) \Delta X_{II}} \quad (19)$$

and areal block permeability is defined as :

$$k_{II} = \frac{\Delta \bar{x}_{II}}{h_{II} \sum_{i=8}^{i=12} \frac{\Delta \bar{x}_i}{h_i k_i}} \quad (20)$$

The steps of the procedure are as follows:

- (1) Calculate the pseudo water saturation using Equation 21 below:

$$S_{pwII} = \frac{\sum_{i=6}^{i=10} (\bar{h} \phi \Delta x S_w)_i}{\frac{1}{2} [h_I + h_{II}] \Delta x_{II} \phi_{II}} \quad (21)$$

- (2) Calculate pseudo flow rates for water and oil across the boundary between areal blocks II and III using Equations 22 and 23 below:

$$q_{pwII} = \sum_{j=1}^{j=9} q_{w10,j} \quad (22)$$

$$q_{poII} = \sum_{j=1}^{j=9} q_{o10,j} \quad (23)$$

- (3) Calculate dynamic pseudo pressures for water and oil using Equations 24 and 25 below:

$$P_{pwII} = \frac{\sum_{j=1}^{j=9} [p_{w8,j} + \frac{\rho_{w8,j} \Delta y_{8,j}}{144}] k_{8,j} k_{rw8,j} h_{8,j}}{\sum_{j=1}^{j=9} k_{8,j} k_{rw8,j} h_{8,j}} \quad (24)$$

$$P_{poII} = \frac{\sum_{j=1}^{j=9} [p_{o8,j} + \frac{\rho_{o8,j} \Delta y_{8,j}}{144}] k_{8,j} k_{ro8,j} h_{8,j}}{\sum_{j=1}^{j=9} k_{8,j} k_{ro8,j} h_{8,j}} \quad (25)$$

- (4) Calculate dynamic pseudo capillary pressure using Equation 26 below:

$$P_{pcII} = P_{poII} - P_{pwII} \quad (26)$$

Application. Two sets of example calculations are presented. Case 1 uses cross-sectional results from an actual reservoir study and illustrates how the dynamic pseudo relative permeabilities account for differences between cross-sectional and one-dimensional areal block lengths. Case 2 is a hypothetical example to illustrate the applicability of both the dynamic

pseudo relative permeability and pseudo capillary pressure functions in duplicating cross-sectional results.

Fig. 13 shows the cross-sectional and one dimensional areal models for Case 1. The lengths of the blocks in the areal model are three times the lengths of the blocks in the cross-sectional model, and each areal block represents 60 cross-sectional blocks. The resulting saturation profiles at breakthrough of this case are shown in Fig. 14.

Fig. 15 shows the cross-sectional and one-dimensional areal models for Case 2. There is limited communication between the upper and lower zones, a high-permeability zone in the lower half of the model, and an oil-water viscosity ratio of about 10:1. Fig. 16 compares the reliability of the dynamic pseudos using Kyte and Berry's method with the previous method.

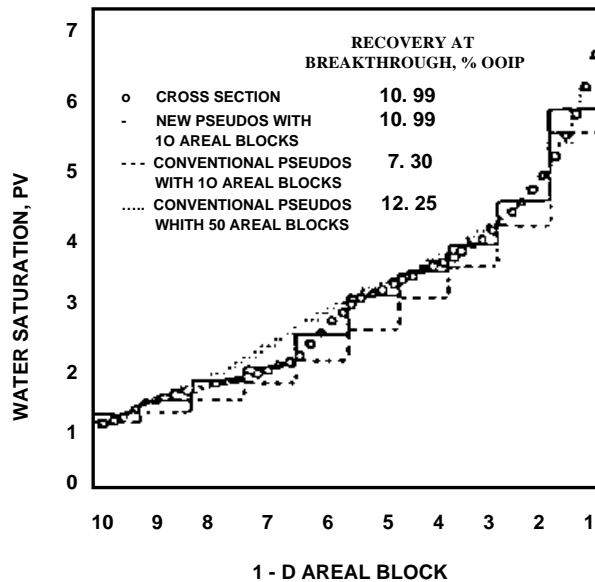


Fig. 13 - Cross-sectional and one dimensional models of Case 1.
(from Fig. 8, p. 15, SPE Monograph, Reprint 20)

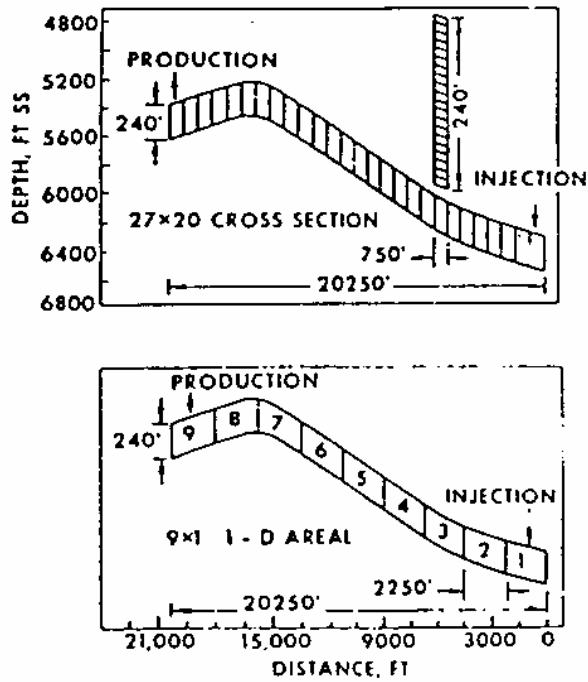


Fig. 14 - Saturation profiles at breakthrough of Case 1.
(from Fig. 5.16 (b), SPE Monograph 13)

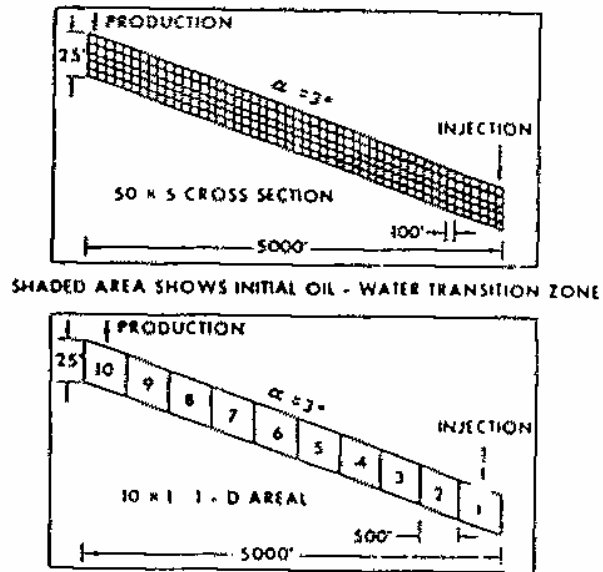


Fig. 15 - Cross-sectional and one dimensional models of Case 2.
(From Fig. 5, p. 16, SPE Monograph, Reprint 20)

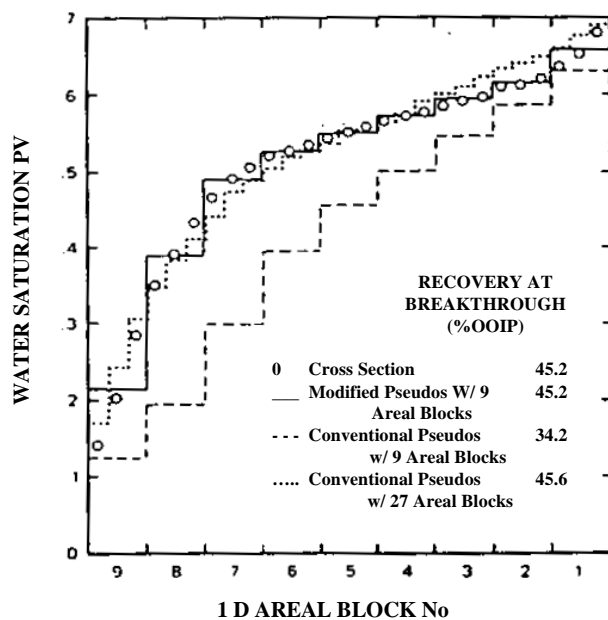


Fig. 16 - Saturation profiles at breakthrough of Case 2.
 (From Fig. 4, p.13. SPE Monograph, Reprint 20)

Using this method, the number of computing blocks in the two-dimensional areal model is reduced by a factor equal to the square of the ratio of the block lengths for the cross-sectional and areal models.

NOMENCLATURE

dP_c	=	capillary pressure difference, psia
dS	=	fluid saturation difference, fraction
dZ	=	elevation difference, ft
N_{grav}	=	gravity number, dimensionless
h	=	thickness, ft
J_{MAX}	=	maximum number of grid in column direction
k	=	absolute permeability, md
$k(Z)$	=	absolute permeability as a function of elevation, md
k_o	=	oil effective permeability, md
k_r	=	relative permeability, fraction
$k_{rw}(Z)$	=	water relative permeability function of elevation, frac.
k_w	=	water effective permeability, md
k_r	=	pseudo relative permeability, fraction
$k_{ro} @ 1-S_{wc}$	=	oil relative permeability at $S_w=1-S_{wc}$, fraction
$k_{rw} @ 1-S_{or}$	=	water relative permeability at $S_w=1-S_{or}$, fraction
p	=	pressure, psia
P_c	=	capillary pressure, psi
S	=	saturation, fraction
S_{or}	=	residual oil saturation, fraction
S_{wc}	=	connate water saturation, fraction
S_w	=	pseudo water saturation, fraction
S_{wc}	=	pseudo connate water saturation, fraction
u	=	Darcy fluid velocity, ft/day
Z	=	elevation, ft

Symbols

i	=	layer
ρ	=	density, lb_m/ft^3
$\Delta\rho$	=	density difference, lb_m/ft^3
ϕ	=	porosity, fraction
$\phi(z)$	=	porosity function of depth, fraction
μ	=	viscosity, cp

Subscripts

o	=	oil
w	=	water
n	=	layers with breakthrough
N	=	total layers

REFERENCES:

1. Coats, K.H., Neilson, R.L., Terhune, M.H., and Weber, A.G.: "Simulation of Three-Dimensional, Two-Phase Flow in Oil and Gas Reservoirs," *SPEJ* (Dec. 1967) 377-388.
2. Martin, J.C.: "Partial Integration of Equations of Multiphase Flow," *SPEJ* (Dec. 1968) 370-380; *Trans.*, AIME, **243**.
3. Coats, K.H., Dempsey, J.R., and Henderson, J.H.: "The Use of Vertical Equilibrium in Two-Dimensional Simulation of Three-Dimensional Reservoir Performance," *SPEJ* (March 1971) 63-71; *Trans.*, AIME, **251**.
4. Hearn, C.L.: "Simulation of Stratified Waterflooding by Pseudo Relative Permeability Curves," *JPT* (July 1971) 805-813.
5. Jacks, H.H., Smith, O.J.E., and Mattax, C.C.: "The Modeling of a Three-Dimensional Reservoir with a Two-Dimensional Reservoir Simulator-The Use of Dynamic Pseudo Functions," *SPEJ* (June 1973) 175-85.
6. Mattax, C.C. and Dalton, R.L.: *Reservoir Simulation*, Monograph Series, SPE, Richardson, TX (1990) 20, **13**.
7. Kyte, J.R. and Berry, D.W. : "New Pseudo Functions To Control Numerical Dispersion," *SPEJ* (Aug. 1975) 269-76.

Exercises

Class Problem No. 20 (Pseudo Relative Permeability)

Attached is a plot of a laboratory oil-water relative permeability curve. This relationship applies to the rock where oil and water both flow. We also have measured that $k_{rw} = 1.0$ at $S_w = 1.0$.

Our 2-D model includes some parts of a reservoir with an initial water-oil contact. Below this initial water-oil contact $S_w = 1.0$.

Construct pseudo relative permeability curves for cells which have 0%, 25%, 50%, and 75% of their thickness below the initial water-oil contact.

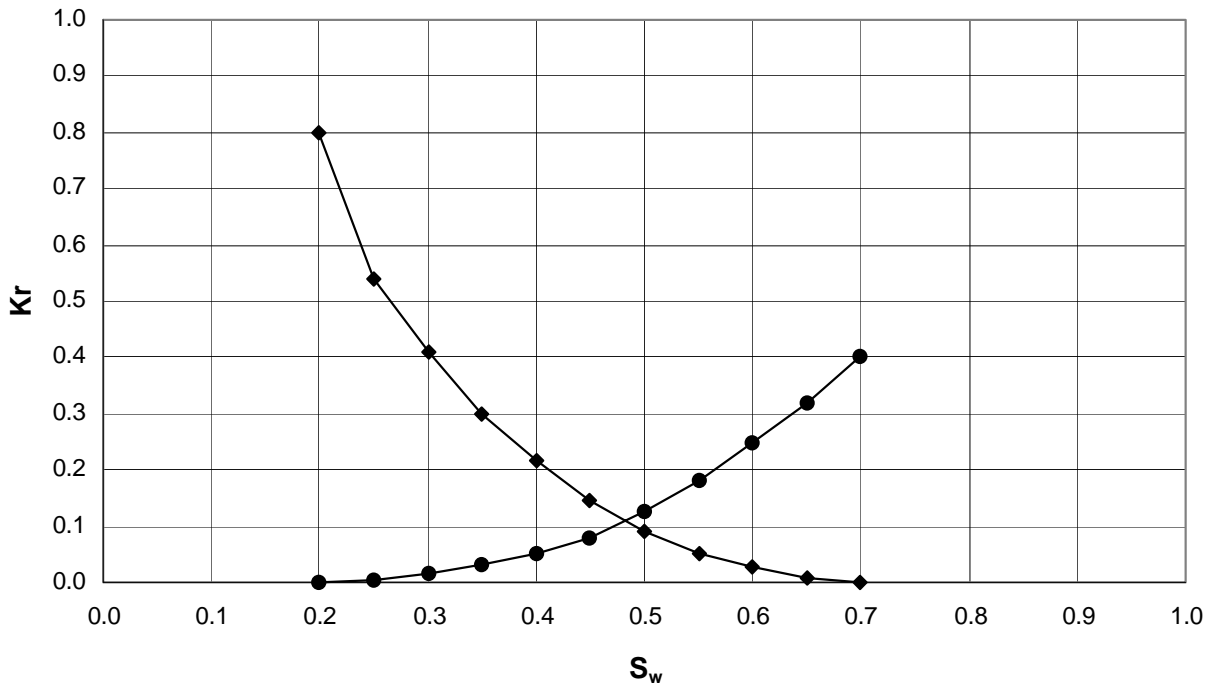
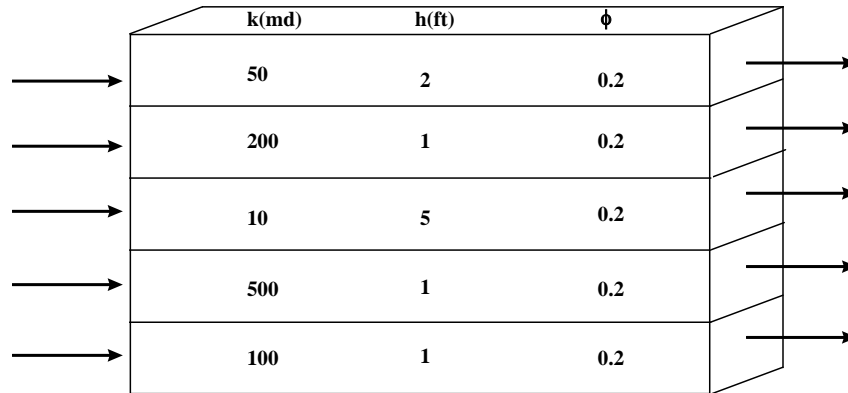


Fig. 17 - Relative Permeability Curve for Problem No. 20

Class Problem No. 24 (Pseudo Relative Permeability)



Assume:

(1) Vertical fluid saturation distribution is controlled by viscous flow forces resulting from vertical permeability variation (gravity and capillary forces are negligible relative to viscous effect)

$$\begin{aligned} (2) \quad S_{wc} &= 0.25 & k_{ro} &= 0.9 \\ S_{or} &= 0.35 & k_{rw} &= 0.3 \end{aligned}$$

- Calculate the pseudo relative permeability curves using Hearn's approach.
- Plot the resulting curves on the attached graph paper.
- Plot another pseudo relative permeability curve using the data with an assumption of gravity segregation. Remember that the system is not homogeneous.
-

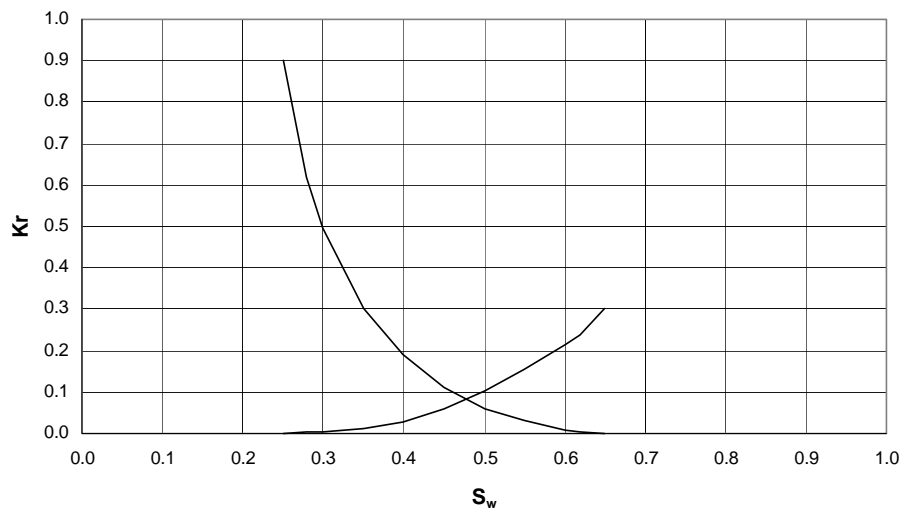


Fig. 18 - Relative Permeability Curve for Problem No. 24

Class Problem No. 28 (Vertical Equilibrium)

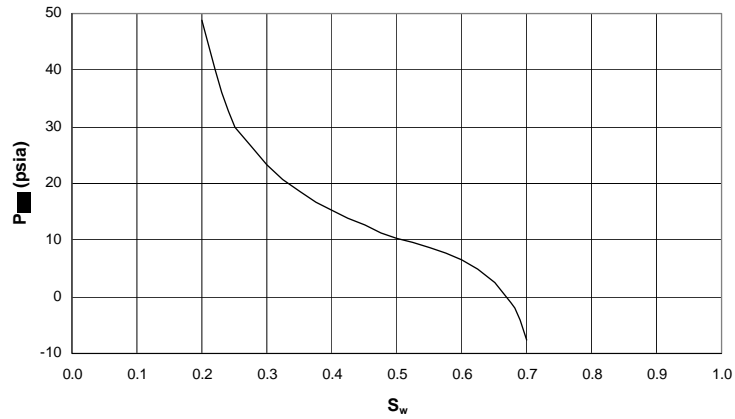


Fig. 19 - Relative Permeability Curve for Problem No. 28

Attached are lab k_r curve and P_c curve for an oil/water system. Develop a V.E. pseudo k_{rw} curves.

- Density of water is 62.4 lbs/res. cf.
Density of oil is 48.0 lbs/res. cf.
Formation thickness is 100 ft.
- Choose three intervals (each 100 ft) with different capillary pressure P_c , each interval will represent intermediate saturations for the V.E curve.
- Draw saturation vs height profiles for the formation for each of the three saturation conditions of (b)
- Draw k_{rw} vs height profiles to match (c).
- Calculate pseudo k_{rw} points for these conditions and draw the pseudo k_{rw} curve.

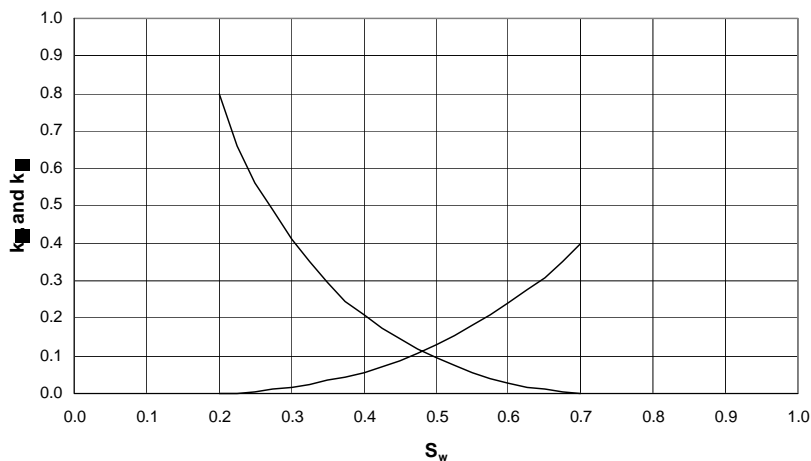


Fig. 20 - Capillary Pressure Curve for Problem No. 28

Class Problem No. 32 (Pseudo Relative Permeability)

We are modelling a waterflood in which we observe a sharp oil bank. The formation is homogeneous and there is no gas saturation.

Our model runs are exhibiting numerical dispersion, which is showing early breakthrough and giving the wrong shape to WOR curves.

Modify the attached laboratory relative permeability curve to give a Buckley-Leverett front as water leaves a cell. Construct a fractional flow curve and calculate the proper relative permeabilities at breakthrough. Sketch the rest of the relative permeability curves.

Water viscosity = 0.6 cp
Oil viscosity = 2.5 cp

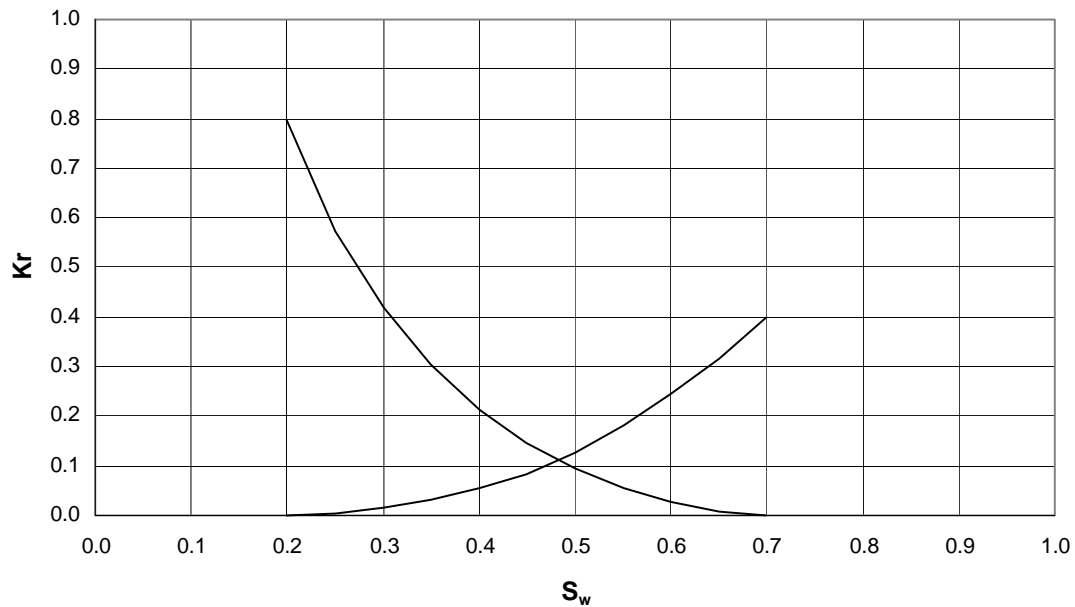


Fig. 21 - Relative Permeability Curve for Problem No. 32

RESERVOIR SIMULATION
CLASS PROBLEM No. 28 (SOLUTION)

(a) First we change P_C vs S_W curve to h vs S_W curve. Given a capillary pressure P_C , the relevant water column height 'h' could be calculated by the following formula:

$$P_c = \frac{(\rho_w - \rho_o)h}{144}$$

or in the form:

$$h = \frac{144 P_c}{(\rho_w - \rho_o)}$$

where:

ρ = lb/cu ft

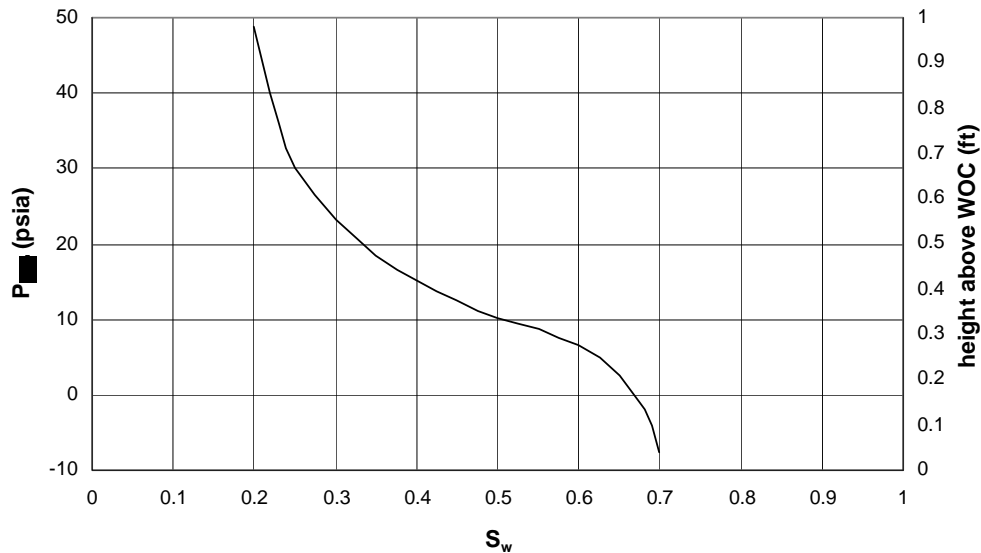
P_C = psi

h = ft

Substitute the given values of variables into the formula:

$$h = 144 (P_C) / (62.4 - 48.0) = 10.0 P_C \text{ ft.}$$

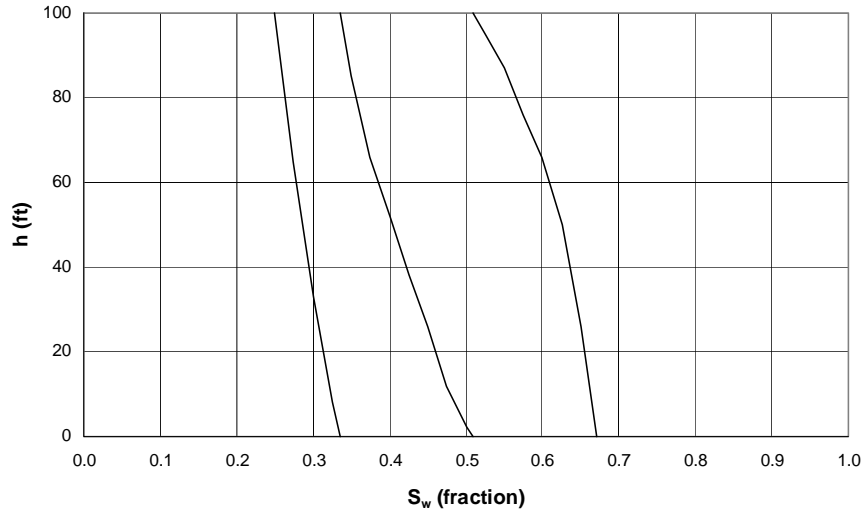
h vs S_W curve is shown in Fig. 1:



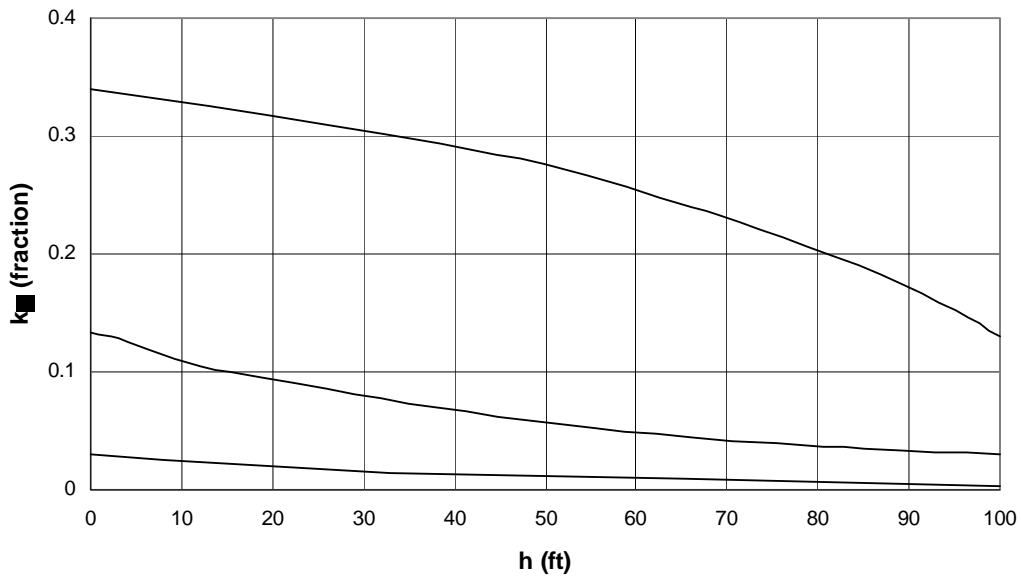
(b) Three 100 ft intervals are chosen from different capillary pressures as:

- Case 1: $P_C = 0.0 - 10.0$ psi.
- Case 2: $P_C = 10.0 - 20.0$ psi.
- Case 3: $P_C = 20.0 - 30.0$ psi.

(c) Saturation vs height profiles for the above three cases are shown in Fig. 2:



(d) k_{rw} vs height profiles for the three cases are shown in Fig. 3:



(e) The pseudo k_{rw} and S_w for the three cases are calculated by the formulas:

$$S_w = \frac{\int_0^h \phi(Z) S_w dZ}{\int_0^h \phi(Z) dZ}$$

$$k_{rw} = \frac{\int_0^h k(Z)k_{rw}(Z)dZ}{\int_0^h k(Z)dZ}$$

In this problem, $h = 100$ ft and we assume $k(Z) = \text{const.}$, $p(Z) = \text{const.}$ so the formulas are simplified:

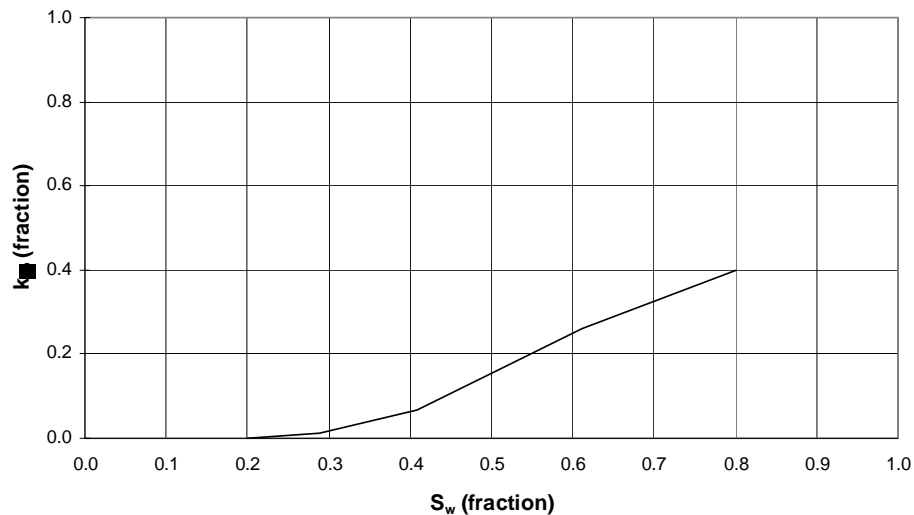
$$S_w = \frac{\int_0^h S_w(Z)dZ}{100}$$

$$k_{rw} = \frac{\int_0^h k_{rw}(Z)dZ}{100}$$

The trapezoidal rule is used for the above integration and the results are shown in the following table:

	<u>Case 1</u>	<u>Case 2</u>	<u>Case 3</u>
S_w	0.6121	0.4084	0.2884
k_{rw}	0.2612	0.06538	0.01348

The pseudo-curve from the above results is plotted and shown in Fig. 4:



CHAPTER 1A

Equilibration

- Geologic Equilibration
- Initialization of Gridblocks
- Effect of Heterogeneity

Equilibration

Geologic Equilibration

Equilibration is the initialization of fluid saturations for all gridblocks in a numerical reservoir simulator such that the fluid potential gradients are equal to zero.

Fig. 1 shows a schematic of a reservoir along with the corresponding capillary pressure curves, depth and water saturation relationships.

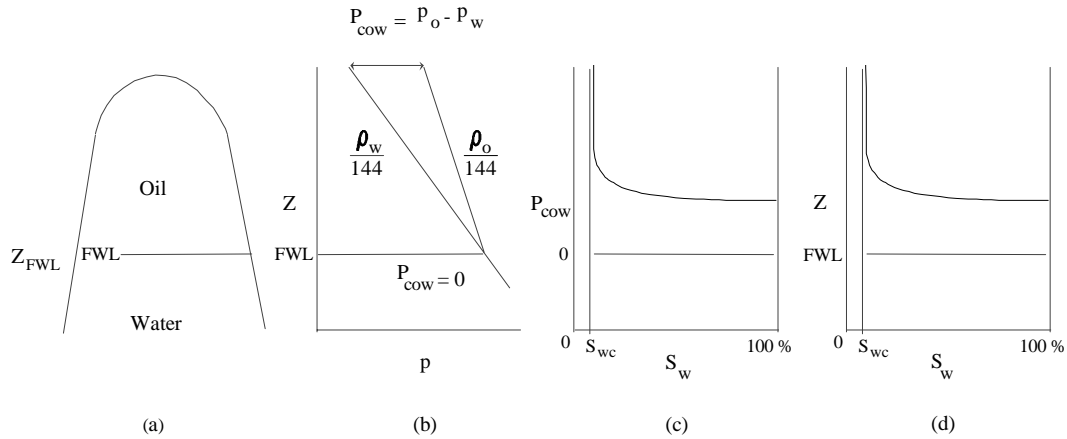


Fig. 1 - (a) Schematic of an oil-water reservoir system. (b) Oil and water phase pressures versus depth. (c) Oil-water capillary pressure as a function of water saturation. (d) Water saturation versus depth.

Consider an oil-water reservoir system, Fig. 1.a, with a maximum water saturation at Z_{FWL} at which $P_{cow} = 0$. If the imbibition capillary pressure curve has a distinct capillary transition zone, as shown in Fig. 1.c, then above Z_{FWL} , the water saturation will be distributed in accordance with the capillary pressure-saturation relationship. In particular, the capillary pressure at a distance h above the free water level (FWL) can be calculated as,

$$\begin{aligned}
 P_{ow}(S_w) &= P_o - P_w \\
 &= \frac{\Delta\rho}{144} (Z - Z_{FWL})
 \end{aligned} \tag{1}$$

or,

$$Z = Z_{FWL} \left(\frac{144}{\Delta\rho} \right) P_{CO_2}(S_w) \quad (2)$$

where,

$$P_o = P_{FWL} - \frac{\rho_o}{144} (Z - Z_{FWL}) \quad (3)$$

$$P_w = P_{FWL} - \frac{\rho_w}{144} (Z - Z_{FWL}) \quad (4)$$

To satisfy the condition for fluid potential equilibrium, we have,

$$\nabla\Phi = 0$$

Determination of water saturation as a function of reservoir thickness can also be applied to reservoirs with water influx or water injection. The maximum water saturation plane can be allowed to rise incrementally in Fig. 1.a to give a different water saturation distribution above Z_{FWL} . Dynamic displacement can be viewed as a series of static positions of the maximum water saturation plane as the water flood moves through the reservoir, each position leading to a new water saturation distribution dictated by the capillary pressure-saturation relationship.

Initialization of Gridblocks

The most commonly used initialization method "initializes on the oil phase." Oil pressure is calculated for each gridblock. The saturations and other phase pressures are derived from capillary pressures and phase pressure gradients. The following steps are involved.

1. Select an oil-phase reference pressure, p_1 , a reference water/oil capillary pressure, P_{C2} , a reference gas/oil capillary pressure P_{C3} , and the depths at which these reference pressures apply (D_1 , D_2 and D_3).
2. Calculate oil pressures at the center of all gridblocks.
3. Calculate water pressures at the centers of all blocks with the oil pressure at D_2 , capillary pressure P_{C3} , and the water pressure gradient.
4. Calculate gas pressures with the oil pressure at D_3 , capillary pressure P_{C3} , and the gas pressure gradient.
5. Having established block-centered pressures for oil, gas, and water, read the oil, gas, and water saturations at block centers from the appropriate capillary-pressure curves.

Initialization methods become more complicated for reservoirs with multiple WOC's or GOC's and rock/fluid properties that vary with depth. The J function can be applied for initialization of saturations for heterogeneous reservoirs. Application of the J function is discussed in the following section.

Effect of Heterogeneity

J Function

The J function is a term for correlating capillary-pressure data of rock formations of similar geological characteristics. The correlating procedure is a dimensionless grouping of the physical properties of the rock and saturating fluids. The J function can be expressed as,

$$J(S_w) = \frac{P_{cow}}{\sigma \cos \theta} \sqrt{\frac{k}{\phi}} \quad (5)$$

where,

- S_w = Water saturation, fraction of pore volume
- P_{cow} = Capillary pressure, dyne/cm²
- σ = Interfacial tension, dyne/cm
- k = Permeability, cm²
- ϕ = Porosity, fraction
- θ = Contact angle, degree

The J function was originally proposed for converting all capillary pressure data to a universal curve. There are significant differences in correlation of the J function with water saturation from formation to formation, so that no universal curve can be obtained. The J function can be used as a correlating device for capillary pressure-water saturation data on a reservoir basis. Correlation can be improved by dividing rock sample data on a textural basis.

To illustrate the use of the J function, we will consider a heterogeneous reservoir for which three core samples have been obtained with k/f values of 250, 500 and 1000 millidarcies. Each core sample has a different capillary pressure-saturation curve as shown in Fig. 2. A single J function-water saturation correlation curve as shown in Fig. 3, is constructed using the J function and capillary pressure-water saturation data of the core samples.

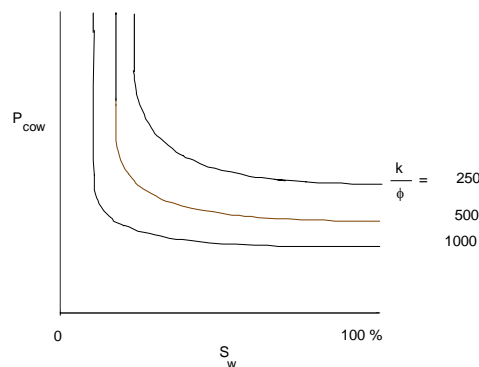


Fig. 2 - Capillary pressure (P_{cow}) versus water saturation (S_w).

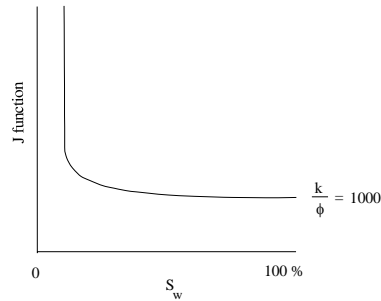


Fig. 3 - J function versus water saturation (S_w).

It is often difficult to obtain all capillary pressure-water saturation data from direct laboratory measurements for all k/f values of a heterogeneous reservoir due to data availability and costs. The following example illustrates the use of the J function to obtain a vertical water saturation profile for a heterogeneous reservoir with laboratory measurements available for only one layer.

Fig. 4 shows a three layered reservoir with k/f values of 1000, 250 and 1000. Laboratory capillary pressure-water saturation measurements are only available for the top layer. To obtain a vertical water saturation profile for the reservoir, we first convert the top layer's capillary pressure data to the J function for various water saturations to obtain a J function-water saturation curve as shown in Fig. 3.

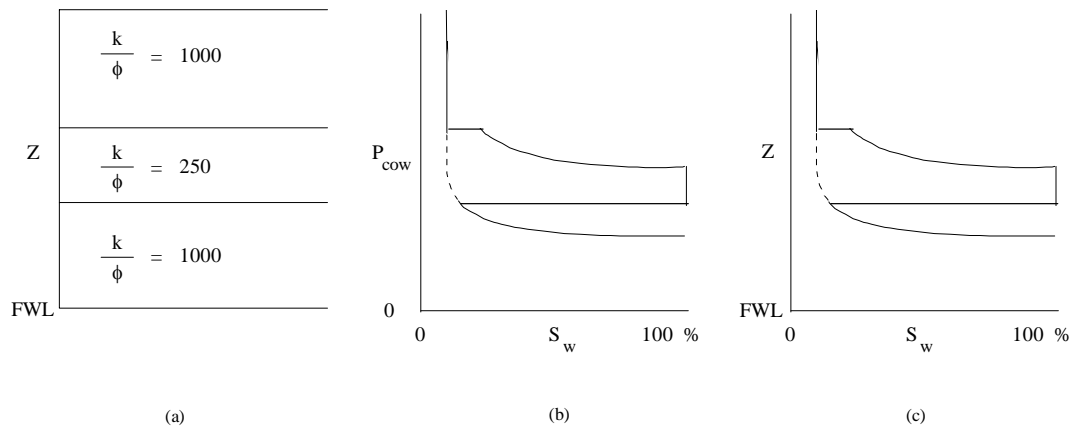


Fig. 4 - (a) Three layered reservoir. (b) Profile of capillary pressure (P_{cow}) versus water saturation (S_w). (c) Profile of elevation (Z) versus water saturation (S_w).

We can calculate J function values for the lower layers since we know the k/f values and P_{cow} from the capillary pressure equation. With this information we can find the water saturation values from the J function-water saturation correlation curve obtained from the top layer. The results can be plotted as shown in Fig. 4.b. Depth versus water saturation can also be plotted as shown in Fig. 4.c since the capillary pressure and depth are linearly related. If all three layers of the reservoirs are fully perforated, we can see from the vertical saturation profile, Fig. 4.c, that the top layer will produce oil, the middle layer will produce water and the bottom layer will produce oil and water.

References:

1. Mattax, C.C., and Dalton, R.L.: "Reservoir Simulation," Monograph Vol. 13 SPE. Chap.4, p. 41.

CHAPTER 2

Repressuring with Variable Bubble Point

- Introduction
- Vertical Variation of Initial Bubble Point Pressure
- Laboratory Behavior
- Reservoir Behavior
- Effect of Re-solution on Compressibility
- A Case of Re-solution History Matching
- Gas Injection above the Bubble Point
- Diffusion Effect
- Water Flooding Depleted Reservoirs
- Illustrative Case of Repressuring of Secondary Gas Cap
with Limited Resolution
- A Simulated Waterflood of Depleted Reservoir

Repressuring with Variable Bubble Point

Introduction

The bubble point pressure of an undersaturated oil is the pressure at which the first bubble of gas evolves as the pressure is decreased (Depletion). This is also the pressure at which all of the gas in a gas-liquid system is dissolved (or goes into solution) as the pressure is increased (Resolution). Generally, in the three-phase flow equations it is assumed that unique R_s and B_o curves can be used everywhere in the reservoir. This is true for example if the pressure decreases everywhere during the life of the reservoir. There are, however, several instances when this assumption is not satisfied.

Reservoir simulation usually involves the assumption of a Black-Oil System. All changes in the system are determined mainly as a function of pressure. Depending on their properties, all components in the system are grouped into two pseudo-components, vapor and liquid. At stock tank conditions, gas exists both as vapor and dissolved in solution. The oil is in the liquid phase only. Fig.1 is an illustration of the components and phases in a black oil system.

Components	Phases	
	Vapor	Liquid
Stock Tank Gas	X	X
Stock Tank Oil		X

Fig. 1 - Components and phases

Often reservoir problems are treated as constant bubble point cases. During a pressure maintenance process such as gas injection, the pressure at the beginning of injection is the "initial" bubble point pressure. Once the solution GOR corresponding to this pressure is reached, the oil is saturated and can no longer dissolve any more gas. Continued injection of gas leads to the formation of a secondary gas cap. However most reservoir simulation problems involve treating the reservoir as a variable bubble point system. When gas is injected into an undersaturated reservoir, gas will go into solution changing the bubble point, that is, the bubble point is a function of the available gas. During waterfloods of saturated reservoirs, the gas saturations in regions near the injectors frequently reduce to zero at pressures below the original bubble point.

Repressuring processes refer to processes in which the depletion is reversed by fluid injection. Two stages will be considered to describe the meaning and to understand the expected behavior of repressuring processes : liberation of gas, and repressuring itself. In addition, some technical considerations in simulating this process will be discussed.

Vertical Variation of Initial Bubble Point Pressure

The amount of solution gas in the oil is a function of temperature and oil-gas composition. Higher the temperature, less is the gas dissolved in oil because the gas molecules have more free energy at higher temperatures. Higher the density difference between oil and gas, higher is the gas content in oil. Fig. 2(a) shows the expected solution GOR vs. Pressure curves for different temperatures and fluid compositions. However the behavior shown in Fig. 2(b) is definitely possible for certain reservoirs. Fig. 2(c) shows the R_s curves used most commonly in simulation.

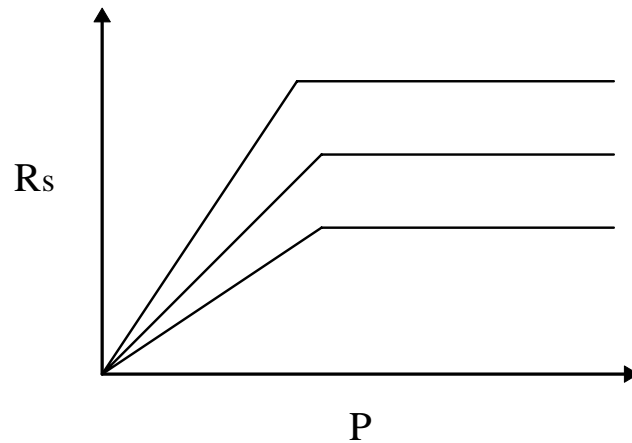


Fig. 2(a) - Typical R_s curves.

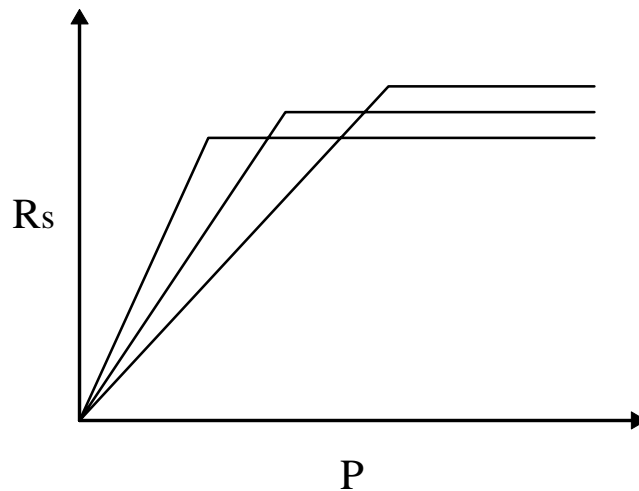


Fig. 2(b) - Possible R_s curves.

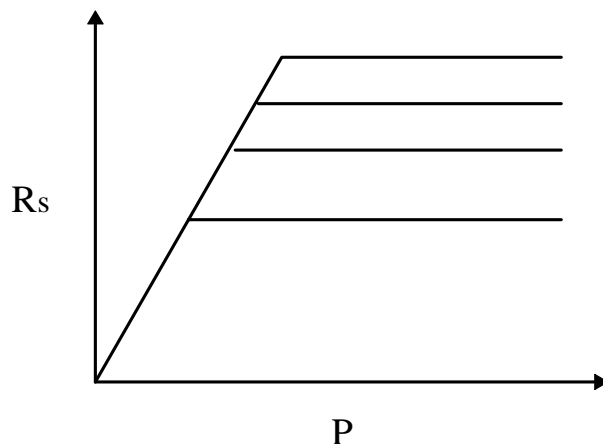


Fig. 2(c) - R_s curves used in simulation.

In a reservoir, gravity segregation causes the gas move to the top and oil to settle down to the bottom of the reservoir. At the gas-oil contact (GOC), there is a sharp change in the pressure gradient depending on the densities of the fluids. Throughout the gas cap, the pressure is the same (because of the low density). In the oil zone, an increase in pressure is expected with depth. This is because the heavier ends settle to the bottom. At the GOC, the fluids are in equilibrium and the oil is saturated. This is the true bubble point of the reservoir, and is less than the average value of bubble point determined using a tank model. Fig. 3 shows the possible variation in pressure in the oil zone. Contrary to popular belief, it has been observed for many field cases that the oil zone pressure could see a decrease with depth. This was reported by Standing¹ from his study of oil expansion due to solution gas.

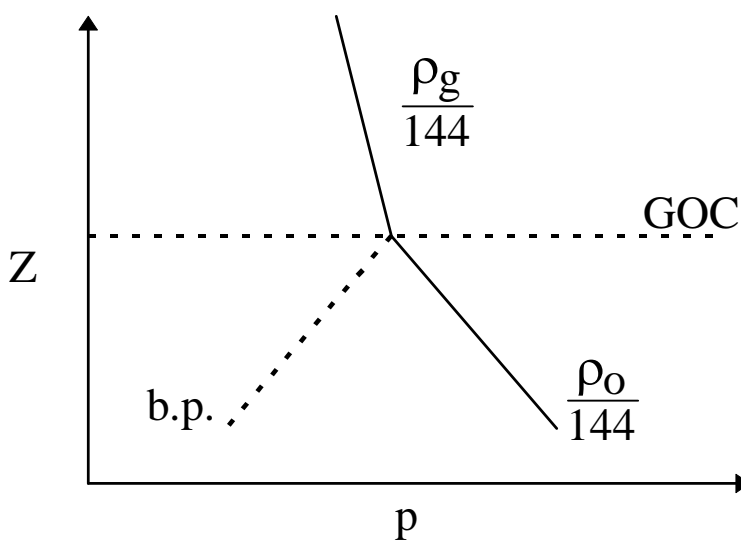


Fig. 3 - Bubble point curves.

For a constant API and temperature oil reservoir, we know that the structurally higher wells will produce with a higher GOR, as illustrated in Fig.4.

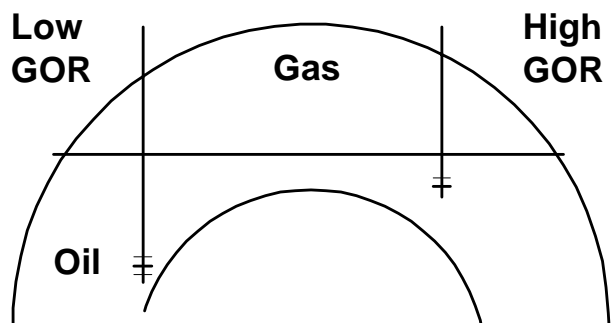


Fig. 4 - Varying producing GOR with well location.

In the above diagram, the well near the GOC produces with a high GOR and the well completed at a much lower depth produces with a low GOR. Using these values of produced GOR, we can find the corresponding bubble point pressures by plotting GOR produced vs. pressure. Naturally it follows that the bubble point pressure at the GOC depth lies somewhere above the two values. This is illustrated in Fig. 5.

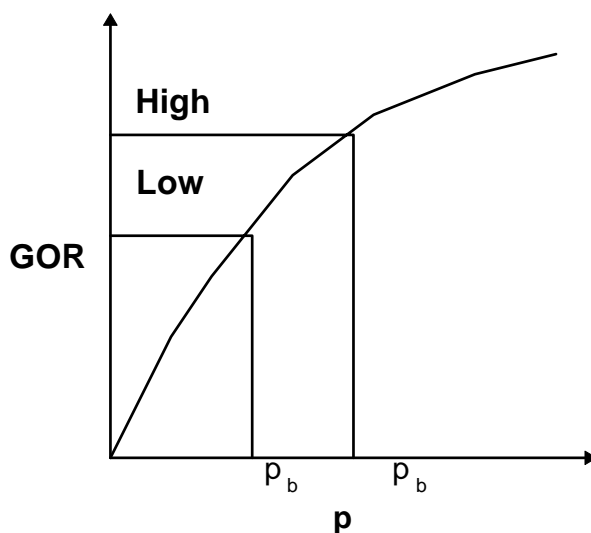


Fig. 5 - Relationship between producing GOR and bubble point.

This plot can be generalized to give a range of possible bubble point pressures and the solution GOR values at different depths. Thus we have a family of curves as shown in Fig. 6 and Fig. 7 respectively.

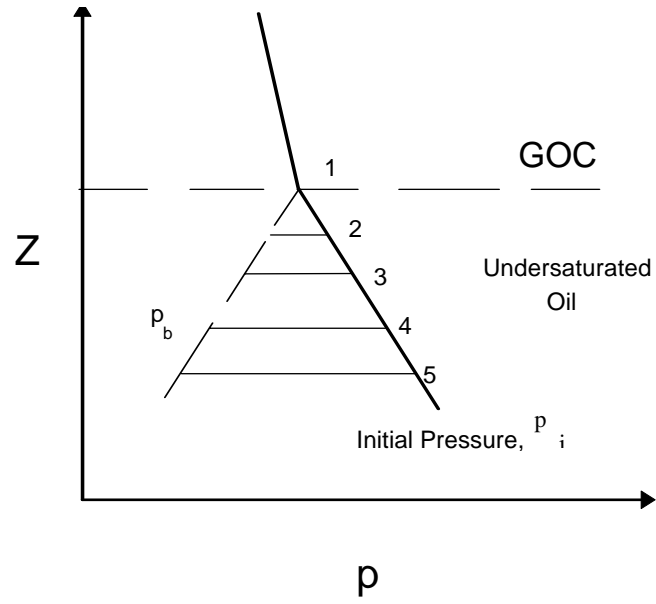


Fig. 6 - Oil becomes more undersaturated at lower depths.

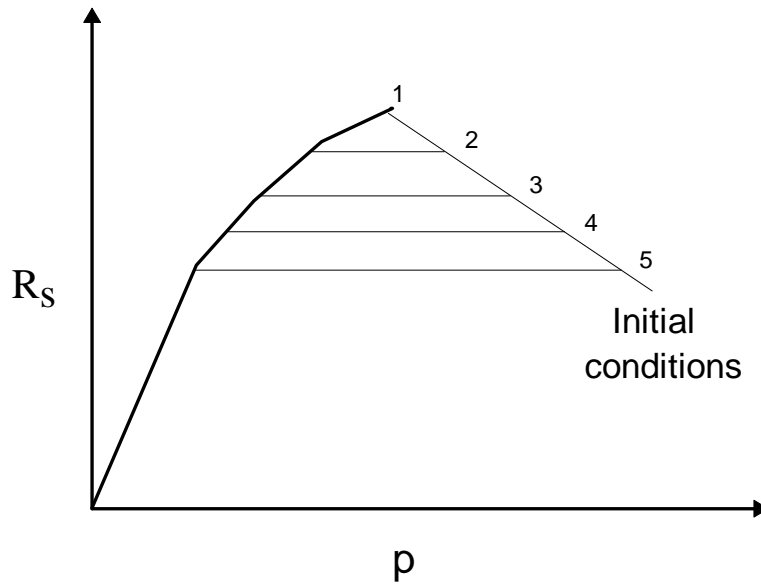


Fig. 7 - Varying R_s with depth.

Laboratory Behavior

To describe the two processes, a PVT cell will be considered as laboratory model of what happens in the reservoir.

Gas Liberation. First, reservoir oil above the bubble point is placed into a PVT cell. A pressure decrease above the bubble point results in an expansion of the oil which is controlled by the oil compressibility. After the bubble point is reached, any further decrease in pressure will cause gas to evolve from solution. As the pressure declines, the gas volume keeps increasing and the oil volume keeps decreasing. Fig. 8 presents the PVT cell behavior during depletion process.

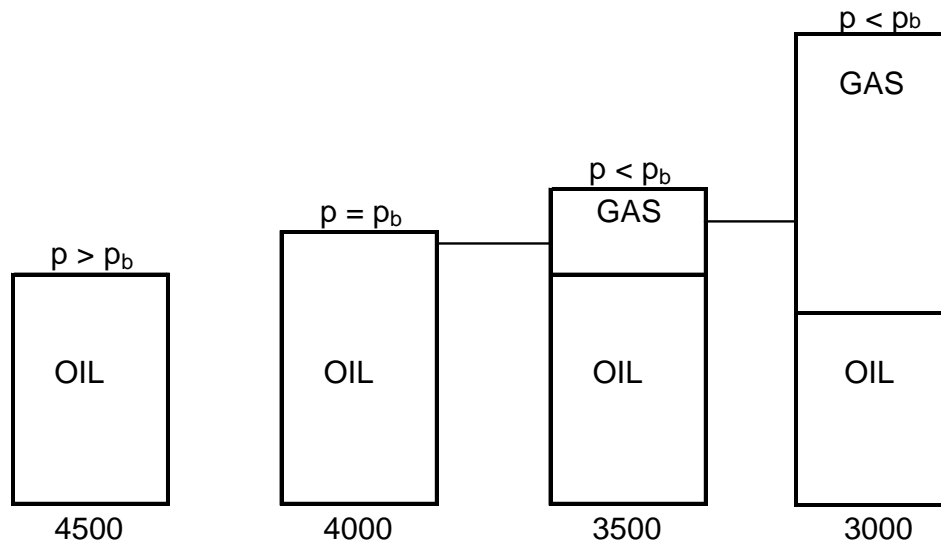


Fig. 8 - Constant composition (Flash) liberation

Gas Redissolving. It could be thought that this constant composition expansion is reversible. That is, if the process is reversed in the PVT cell, the gas will redissolve and all the fluid properties can be considered to be single valued functions of pressure. This re-solution process might not be so simple. With time the fluid volume in the container decreases, the PVT cell may have to be agitated and sufficient time has to be allowed for the process to take place. It would be found that the re-solution process would have a hysteresis.

Reservoir Behavior

The process of redissolving gas in the field is more complicated. As a solution gas drive reservoir below the bubble point is produced, it is found that the gas/oil ratio increases. While this is happening, the ratio of total gas and oil remaining in the reservoir is changed. In addition to the amount of gas available, the characteristics of the porous media and the reservoir geometry (dip angle etc.), make the resolution process more complicate than it was in the laboratory.

Properties Behavior. During the production period the gas/oil ratio of the produced fluids increases because of the increasing gas saturations and relative permeabilities. Later, after the gas/oil ratio has peaked, the gas/oil ratio decreases because of the increase of formation volume factor.

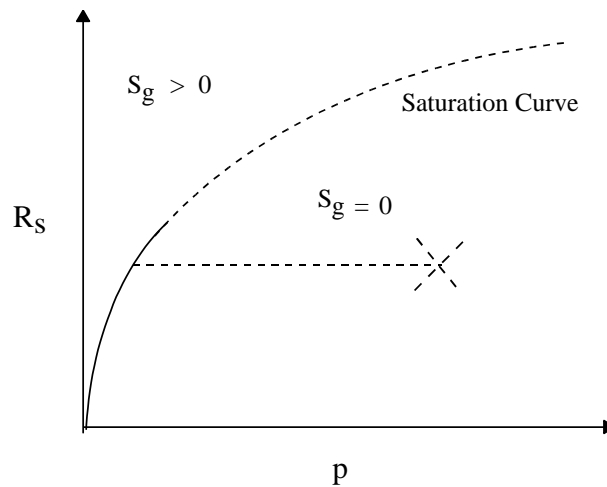


Fig. 9 - Example of an undersaturated gridblock

The bubble point is determined by monitoring the value of gas/oil ratio in the simulator cell. During repressuring, the simulator will retrace the original fluid property curves until it reaches a new bubble point. During the timestep where the new bubble point is reached, a negative gas saturation will be calculated unless the simulator calculations are modified. The simulator is modified to solve for 5 rather than 4 unknowns. In addition to the pressure and three saturations in each cell, we must also solve for the bubble point. The gas-in-place and oil-in-place are calculated independently according to the values at the beginning of the timestep, the flow in during the timestep and the production in the cell during the timestep. When these calculations are made, a ratio is calculated that represent the existing gas/oil ratio in the cell. The gas/oil ratio in the cell is compared with the original solubility curve. If this ratio is higher than the value from the curve, then more gas is available in the cell than can be dissolved in the oil at that pressure. In this case we have a positive free gas saturation. On the other hand, if the calculated value of gas/oil ratio is less than the value on the curve at that pressure, then we have established a new bubble point which corresponds to the existing gas/oil ratio for the cell.

Calculation procedure:

Oil in place:

$$OIP^{n+1} = OIP^n + Net\ Inflow - Production \quad (1)$$

where,

$$OIP = \frac{V_p S_o}{B_o} \quad (2)$$

Gas in place:

$$GIP^{n+1} = GIP^n + Net\ Inflow - Production \quad (3)$$

where,

$$GIP = GIP_{free} + GIP_{sol} = \frac{V_p S_g}{B_g} + \frac{V_p S_o R_s}{5.615 B_o} \quad (4)$$

Solubility:

$$R_{cell} = \frac{GIP(S.T.)}{OIP(S.T.)} \quad (5)$$

With this new solubility in the cell go to the curve R_s vs. P and find the pressure that corresponds to this new solubility. This is the new bubble point pressure of the cell.

To find the other properties above the new bubble point (oil volumetric factor and viscosity of oil) draw a line from the new bubble point pressure using the same slope that the properties followed with the original bubble point.

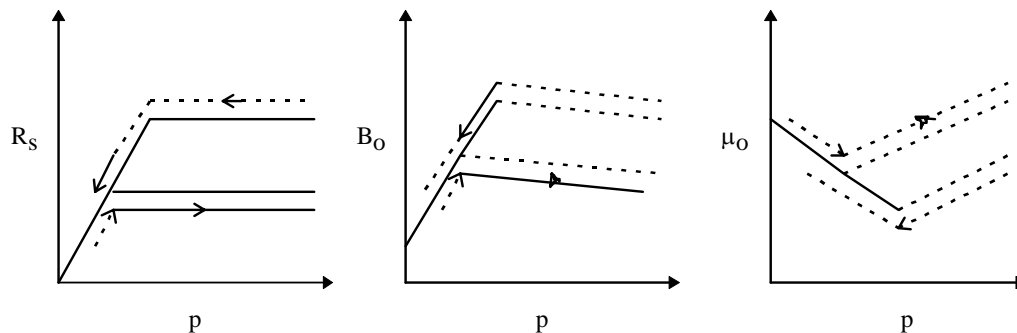


Fig. 10 - Repressuring after depletion

Effect of Re-solution on Compressibility

We have considered Cases A, B, and C. These represent three possible scenarios for gas redissolving. Each of these cases has different effects on the pressure behavior of the reservoir. The rate of pressure increase during repressuring is going to depend on the total system compressibility. The oil compressibility is still determined by the same equation as during the depletion. However, the slopes of the formation volume factor curve and the gas solubility depends on which case is being modeled. Two cases of gas solubility curves are shown which represent the original data and the data modified for Case B.

The total compressibility is defined as:

$$c_t = c_f + c_o S_o + c_w S_w + c_g S_g \quad (6)$$

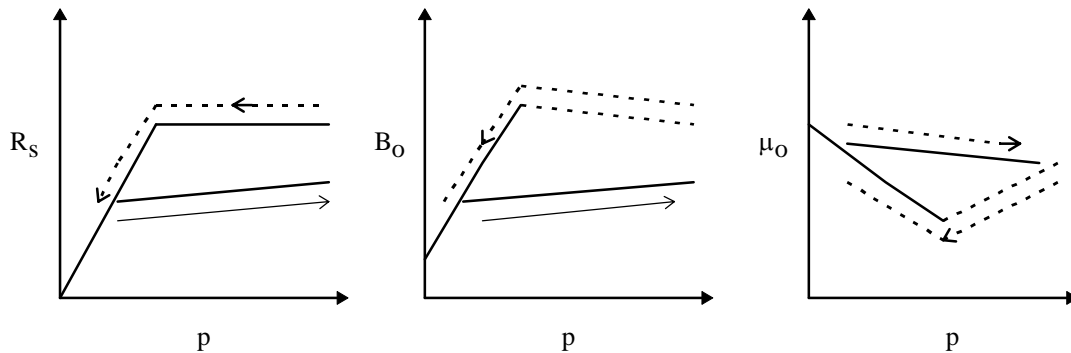


Fig. 11 - Effect of re-solution on compressibility

where for case A, C_o is defined as:

$$c_o = - \frac{1}{B_o} \frac{dB_o}{dp} + \frac{B_g}{B_o} \frac{dR_s}{dp} \quad (7)$$

For case B, C_o is defined as:

$$c_o = - \frac{1}{B_o} \frac{dB_o}{dp} \quad (8)$$

and

$$c_w = - \frac{1}{B_w} \frac{dB_w}{dp} \quad (9)$$

$$c_g = - \frac{1}{B_g} \frac{dB_g}{dp} \quad (10)$$

There are three different ways in which the resolution of gas could occur in the reservoir.

Case A (Complete Gas Re-solution). This case is in agreement with the Odeh's repressuring case (Case 2). If a reservoir is depleted to a low pressure and then the reservoir is repressured by fluid injection, it can be expected that the gas/oil ratio remaining in the reservoir will be considerably less than the initial gas/oil ratio. For this case, it will be assumed that gas redissolves along the original curve present.

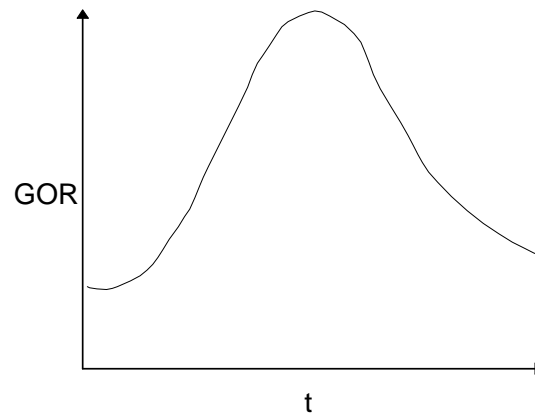


Fig. 12 - GOR behavior during depletion.

Therefore, gas redissolves just like PVT cell until all the free gas is back in solution. Since the gas/oil ratio is lower than original, all of the remaining gas redissolves before the original bubble point is reached. When this occurs, a new bubble point is reached which depends on the gas/oil ratio remaining in the reservoir. As pressure is increased from this new bubble point, the fluid properties reflect the new bubble point. The reservoir may be pressured to the original pressure above the original bubble point. In this case it will be found that the oil properties are different than the original oil properties. The oil viscosity is higher and the formation volume factor is lower.

Case B (Gas does not Redissolve). Following Odeh's notation this corresponds to Case 1. In this case the lowest pressure which is achieved in the reservoir becomes the bubble point during repressuring. Even though free gas is available, it is considered not to redissolve. If this is the case, the oil properties resemble a "dead" oil even at higher pressures. The oil compressibility is liquid-like. The oil viscosity also resembles a "dead" oil at higher pressures.

One reason for having this case in the field is that gas might freely migrate to a secondary gas cap, or at least to the top of the layer from which it evolves. We can readily see that the gas is no longer in intimate contact with the oil in this case. For that reason there is very little resolution of the gas during repressuring. The gas has been physically removed from the oil. To achieve this scenario in a simulator requires that the user specify that gas does not redissolve. It may be necessary to change the fluid properties during a re-start run input the fluid properties at a lower bubble point. To calculate the new properties (oil FVF and viscosity), using the lowest pressure reached in the

reservoir as new bubble point pressure. From this point draw lines following the same slope that they have above the original bubble point.

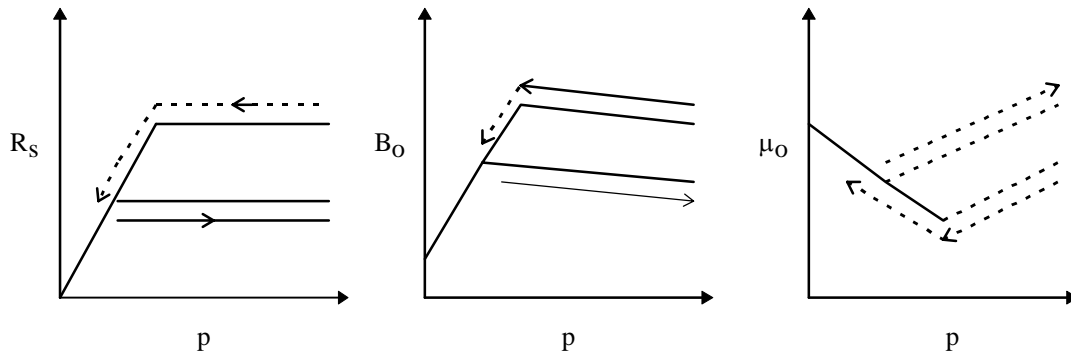


Fig. 13 - Repressuring without redissolving

Case C (Partial Re-solution). Cases A and B are extreme cases of a gas resolution. Either all of the gas goes to solution, or none of the gas goes into solution. It is likely that something in between these cases occurs in the reservoir. There is probably going to be some reluctance of gas to redissolve. For the partial resolution case, the fluid property curves during repressuring must be reconstructed to show the partial resolution.

It can be seen that the solubility curve is no longer a fundamental relationship between reservoir oil and gas. Instead the solubility curve reflects some combination of fluid behavior and the actual mechanics of gas going into solution. Once it is decided how this curve should be constructed, it is important that the formation volume curve and the oil viscosity curve be constructed, not just drawn, to be consistent with the amount of gas in solution at various pressures.

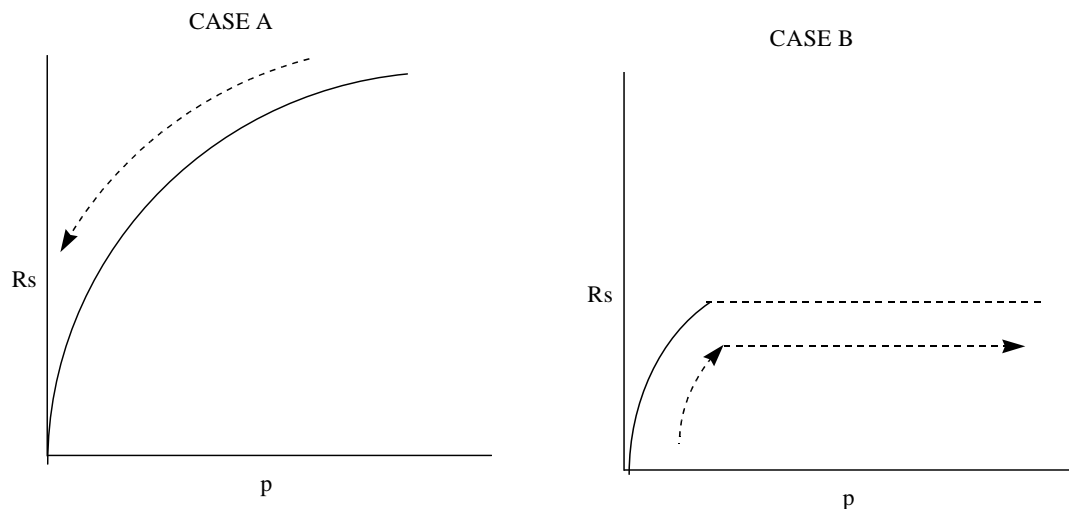


Fig. 14 - Repressuring with partial re-solution

A Case of Re-solution History Matching

Although it is difficult to predict how a reservoir might behave regarding resolution, the proper construction of re-solution curves might be necessary to model the history of an existing reservoir. In the case shown, the actual reservoir behavior is indicated by the solid line during repressuring. This behavior must be bracketed by first modeling the "all gas redissolving" case and then modeling the no re-solution case. For Case A the total system compressibility will be too low and the pressure rises too rapidly. The proper pressure behavior must be modeled trial-and-error, by assuming different solubility curves.

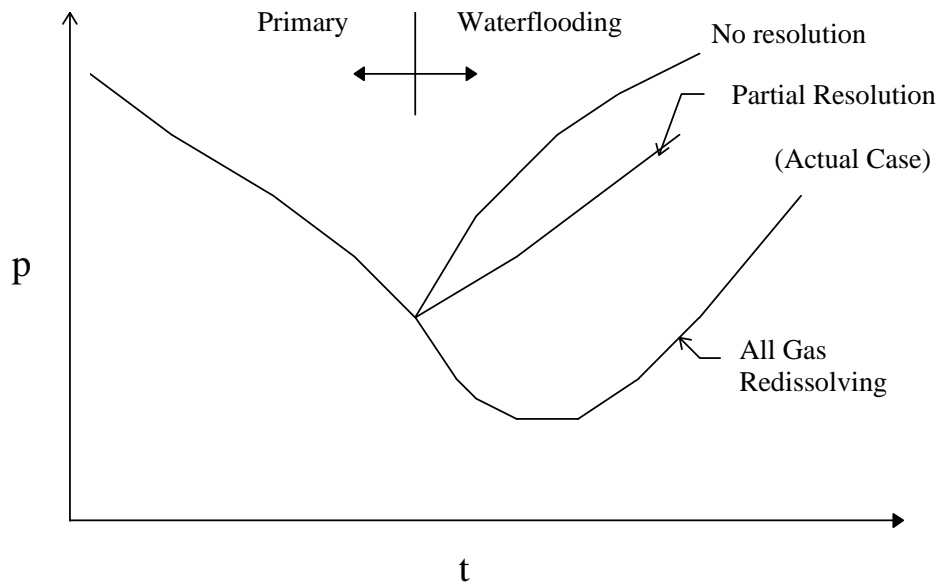


Fig. 15 - History matching with partial resolution

Gas Injection Above the Bubble Point

Another case where fluid properties must be modified is for gas injected into an under-saturated oil.

It is necessary to define the solubility properties of the gas and oil system above the original bubble point. It is important to obtain this data in the laboratory, if possible. The gas/oil ratio in the injection cell increases when gas is injected into an under-saturated oil. While this solubility increases, the oil swells and the oil viscosity reduces according to these relationships with gas/oil ratio. The limit of gas/oil ratio is reached when the solubility curve is reached. At this point the oil can dissolve no more gas and free gas saturation appears.

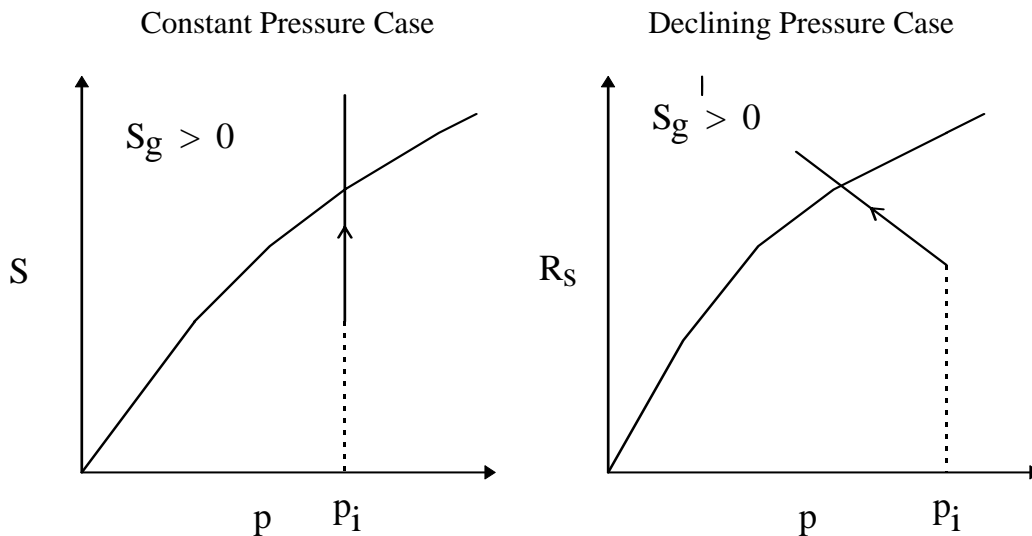


Fig. 16 - Gas injection above the bubble point

The same general process occurs even if pressure is not held constant. The usual case will be that pressure is either increasing or decreasing during the injection period. The trace of the points on the gas/oil ratio versus pressure curve for different timesteps depends on the history of pressure and gas injection into the cell. It is important that the simulator be programmed to properly account for this gas injection above the bubble point. It is also important that user understand how the simulator behaves and input the proper solubility and fluid property data into the simulator.

Diffusion Effect

The movement of gas in porous media during reservoir repressurizing is explained by molecular diffusion. Molecular diffusion is effective in miscible displacement of oil by an enriched gas or in gas-cycling operation.

The rate of molecular diffusion in porous media is very slow. This may explain why the gas does not redissolve in the oil when the reservoir is repressurized. An estimate of the time needed for the movement of the gas is determined by the following equation,

$$t = \frac{\tau}{13.1 D} \Delta L_c^2 \quad (11)$$

where,

ΔL_c	=	length between the 10% and 90% concentration levels, ft
D	=	diffusion coefficient, ft ² /D (typical value, D=4.48E-3 ft ² /D)
τ	=	tortuosity factor (typical value, $\tau=2$)
t	=	time, days

For the gas to move 10 ft in porous media using the above equation, it needs 9.33 years, but for 20 ft, it needs 37.3 years.

Waterflooding Depleted Reservoirs

This case involves water injection into a depleted oil reservoir with an initial gas saturation. As oil is displaced across the reservoir the bubble point pressure at a particular location will increase because of mixing. The bubble point pressures will be highest in the vicinity of the injectors and lowest at the producers.

Illustrative Case of Repressuring of Secondary Gas Cap with Limited Resolution

Introduction. This study investigates the effects of repressuring a secondary gas cap with limited resolution, and is analogous to a field in the Middle East. In general, the history of this field showed a period of rapid depletion, resulting in the formation of a secondary gas cap. This was followed by a period of repressuring during which the pressure at the gas/oil contact exceeded the bubble point pressure. In this unusual case, the gas cap did not dissipate because the gas dissolving mechanism was limited to molecular diffusion of gas into the oil.

Data for this study was taken from the Second SPE Comparative Study written by Weinstein, H.G., Chappellear, J.E., and Nolen, J.S. Their data was intended to simulate three phase coning.

Problem Statement. To determine the effect of grid size on the dissolution of a secondary gas cap during repressuring.

Reservoir Description. The prototype field consisted of a homogenous dipping reservoir (2.8°) with a formation thickness of 100 feet, total length of 2000 feet and width of 500 feet. Constant porosity and permeability were 13.0 % and 500 md respectively. Permeability in the z-direction measured 50 md, while the y-direction permeability measured 500 md. The field maintained one production and one injection well (Fig. 1).

The top right hand corner of the reservoir was located at an elevation of -9000 feet, which corresponded to the depth of the initial gas/oil contact. Set at -9300 feet, the water/oil contact was not a factor in production.

Total Pore Volume	=	2.316 MMRB
Hydrocarbon Pore Volume	=	1.797 MMRB
Original Oil in Place	=	1.620 MMSTB ($B_{oi} = 1.12$ RB/STB)

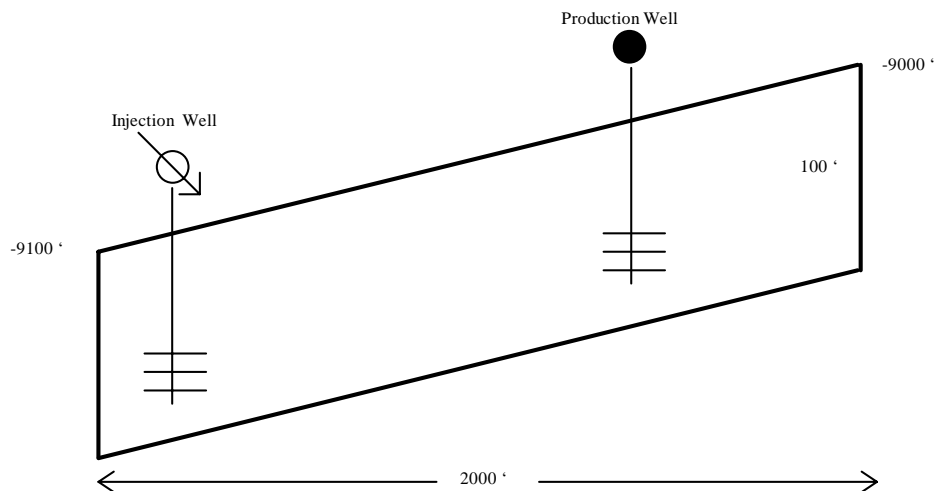


Fig.17 .

Grid. Grid dimensions, well locations and rate schedules used in simulation are shown below.

Grid Dimensions and Well Locations

Grid Size	Δx Feet	Δy Feet	Δz Feet	Number of Cells	Producer Location	Injector Location
10x5x1	200	500	20	50	8,1,1	4,1,1
25x10x1	80	500	10	250	20,1,1	7,1,1
50x20x1	40	500	5	1000	40,1,1	14,1,1
50x40x1	40	500	2.5	2000	40,1,1	14,1,1

Rate Schedule

Time (Days)	q_o STB/D	q_{wi} STB/D	N_p MSTB	W_{pi} MSTB	Stage
0.0	500	0.0	0.0		Depletion Phase
365	250	600	182.499	0.0	Repressuring Phase
850			303.749	291.000	

Procedure. Producing approximately 10% of the OOIP/Year resulted in a daily flowrate of 500 STB/D. Production remained constant for one year in order to form a secondary gas cap which occupied approximately one third of the total reservoir (Fig. 2). In order to increase the average reservoir pressure, water was injected at a rate of 600 STB/D while production was reduced to 250 STB/D. As the pressure increased, a fraction of the gas redissolved into the oil, but the major portion of gas become compressed at pressures in excess of the bubble point pressure (Fig. 3). Rates were held constant throughout the simulation of the reservoir, which ended when reservoir pressures surpassed the available data (out of table).

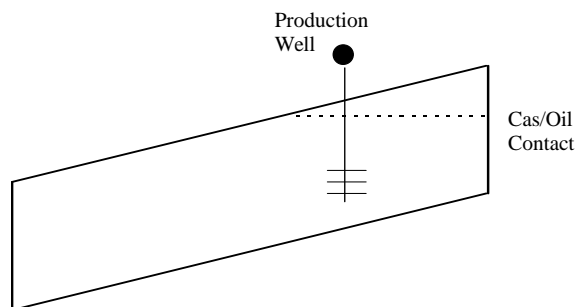


Fig. 18 - GOC after 1 year

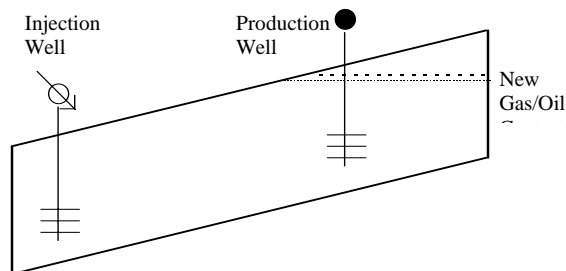


Fig. 19 - GOC at 850 days (after injection)

Results and Conclusions. Fig. 20 illustrates the pressure and depth of the gas/oil contact as the reservoir was depleted and repressured. It is apparent that during repressuring, the gas/oil contact only slightly rises while the pressure at the contact increases dramatically. During the depletion phase, the pressure at the GOC dropped from 3584 psi to 2923 psi ($\Delta P = -661$ psi), while the elevation of the GOC fell from -9000 ft to -9049 ft ($\Delta E = -49$ ft). At 850 days, after repressuring to 3855 psi ($\Delta P = +929$ psi), the elevation of the GOC was still located at -9046.4 ft ($\Delta E = +3.4$ ft). Therefore, regardless of the grid adaptation, a gas cap remains as the reservoir is repressured.

Effect of Limited Resolution on Gas Cap During Repressuring

EFFECT OF LIMITED RESOLUTION ON GAS CAP DURING REPRESSURING

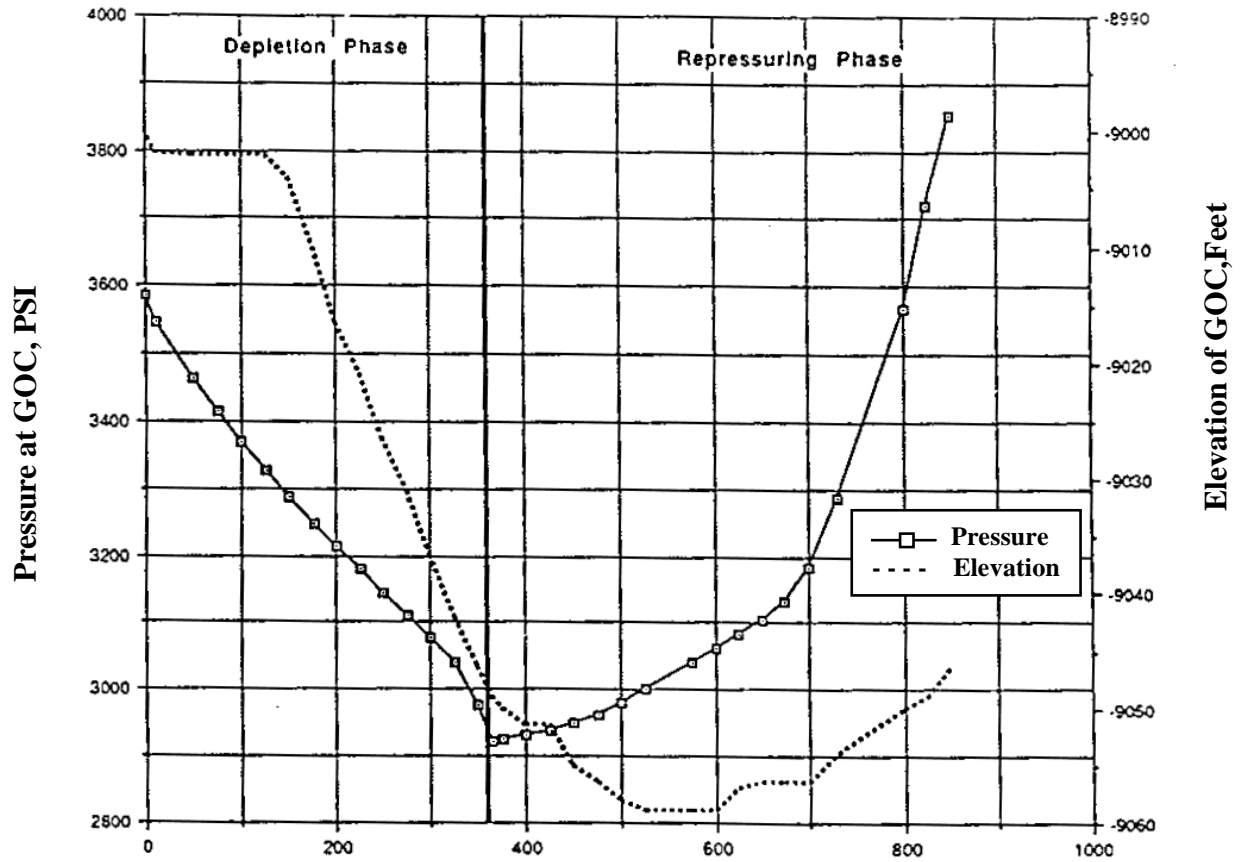


Fig. 20

A Simulated Waterflood of a Depleted Reservoir

Problem Description and Objective. The way that Tibu field was produced can be simplified as two periods: 1) primary production and 2) waterflooding. One of the interesting phenomena encountered when Tibu field was produced is that after certain period of water injection, the gas oil ratio (GOR) increased for a short period of time and then it decreased. Intuitively, we would expect that the water injection created a gas bank before an oil bank. It was the gas bank that caused the GOR to increase before the oil bank reached the production well. We simply call this phenomena Tibu field phenomena which can be best depicted by the following simplified plot (Fig. 21).

The objective of this project is to study this phenomena and investigate whether waterflooding can create this gas bank before the oil bank and under what conditions this gas bank can be created. This study is conducted using the VIP numerical simulator.

Simulation Input Data Setup (Reservoir Properties and Grid System). The SPE 2 data were used to conduct this study. A quadrant of a five-spot pattern was simulated by a 2-D homogeneous model. The grid system we used was 21x21 which is shown in Fig. 22. More detailed information can be found in the attached input data file.

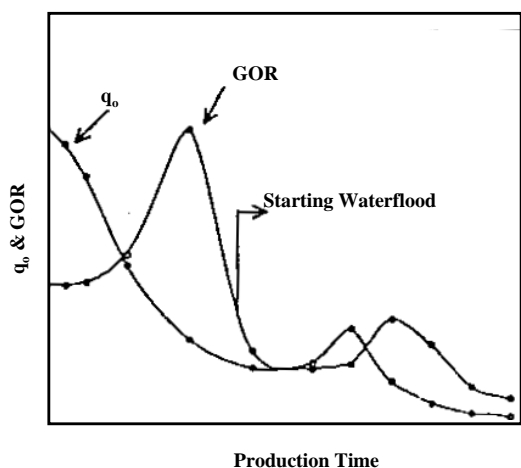


Fig. 21 - Simplified plot of GOR & q_o Performance for Waterflood.

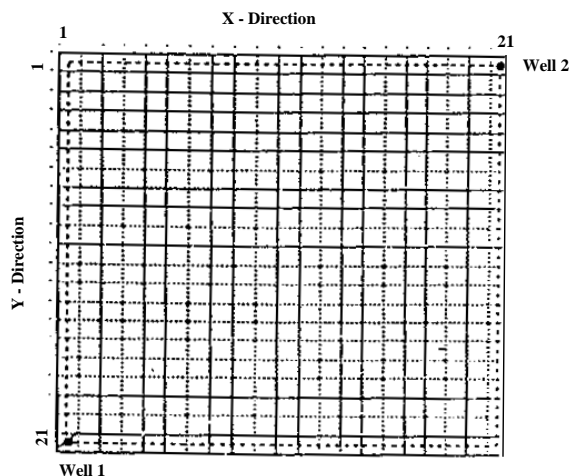


Fig. 22 - 2-D Simulation Model, Quadrant of 5-Spot Pattern, 20 acre.

Production and Injection Schedule. We set the bottomhole pressure at 100 psia and restricted the maximum production rate of 2000 STB per day per well. We first depleted reservoir to an average pressure of 200 psia then started water injection by converting the Well 1 into an injector and at the same time kept the Well 2 producing at a constant bottomhole pressure of 100 psia. For comparative purpose, we ran another case in which the reservoir was depleted in the same way as the previous case to an average pressure of 200 psia. Then, instead of injecting water, we shutin Well 1 and allowed Well 2 to continue production until the average reservoir pressure reached 100 psia.

Results and Discussions. Fig. 23 shows the GOR and q_o vs. production time from simulation runs. The solid line represents the case without water injection; the circles represent the case with water

injection. For the reference purpose, we also include the oil production rate from water injection case in which it clearly shows the time the oil bank reached the production well. For water injection case, we started water injection after 400 days of primary depletion. After 120 days of water injection, the oil bank reached Well 2. It can be seen from the figure that before the oil bank reached Well 2, the GOR performances with water injection and without water injection agree very well. For water injection case, after the oil bank reached the production well, the GOR dropped dramatically because of substantial oil coming out with little free gas. The GOR behavior was not affected by the water injection until the oil bank reached the production well. Therefore it is clear that no gas bank was created by water injection. This can be explained as follows: because the mobility of gas is very high compared to that of the oil behind, the free gas keeps flowing until it stop moving without establishing a gas bank. Fig. 4 shows the behavior of reservoir pressure and wellbore pressure for water injection case. This plot provides more information about how the reservoir was depleted and then repressurized. The solid line represents the reservoir pressure and the dash line represents the wellbore pressure.

To study how the oil viscosity affects the reservoir performance, we ran another two similar cases by changing the oil viscosity only to 10 times of the original values. The reason for changing viscosity of oil is that we expected that the oil viscosity would play an important role in reservoir performance. Fig. 25 and Fig. 26 present the similar information as Fig. 23 and Fig. 24. It also shows that no gas bank was created by the water injection.

In addition to the above simulation runs, we also varied some other reservoir properties and process parameters attempting to simulate the GOR behavior observed in Tibu Field. The results we obtained are very similar to those of above cases without finding Tibu field phenomena. The following parameters and reservoir properties were changed:

- 1) wellbore pressures (for constant pressure production);
- 2) maximum injection rate and maximum production rate;
- 3) reservoir pressures (depleted to different reservoir pressure before water injection);
- 4) permeability;
- 5) gas viscosity,
- 6) pseudo relative permeability curve for segregation.

Conclusion and Recommendation. Using SPE 2 data and 2-D homogeneous model, we did not see the similar phenomena encountered in the Tibu field. Since the mobility of gas is much high than that of oil, water injection can not create a gas bank before oil bank. We conclude that the Tibu field phenomena is not a simple phenomena which can be simulated using above 2-D model.

Since Tibu field is a multilayered reservoir with a high degree of heterogeneity, we would expect that the phenomena observed in Tibu Field might be caused by reservoir heterogeneity and multilayer system. Our 2-D, homogeneous reservoir simulation model could not model thiwaterflood performance for such complicated reservoir. A 3-D model is recommended to simulate the Tibu field phenomena.

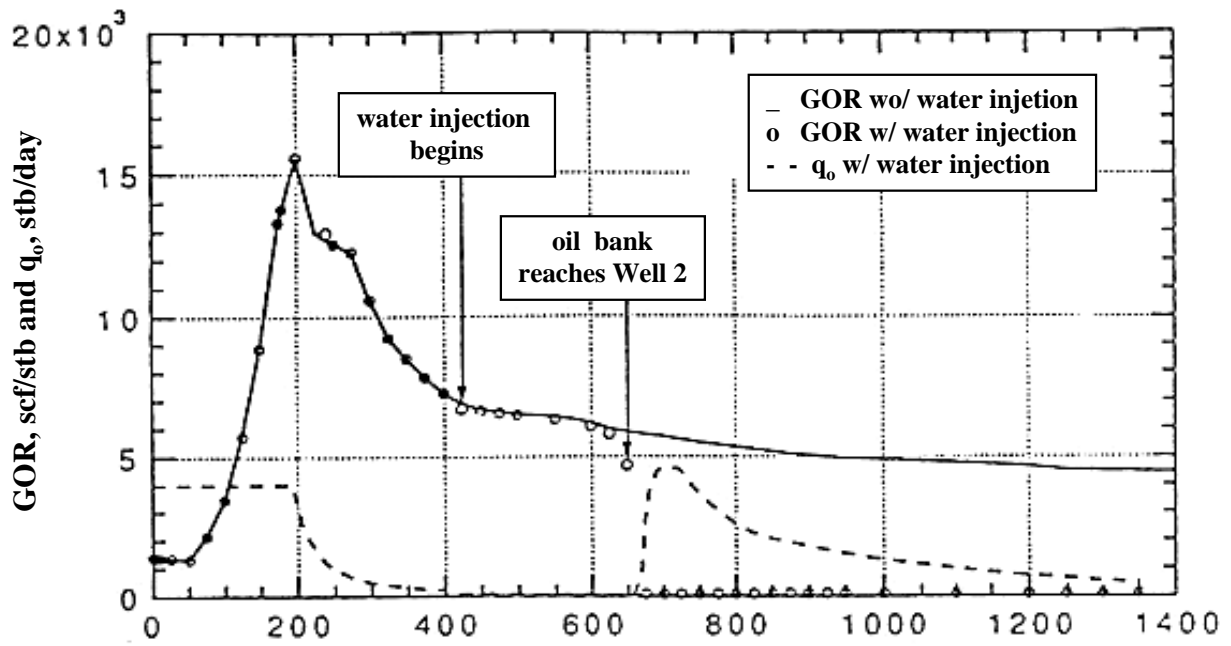


Fig. 23 - Comparison of GOR: with and without water injection (SPE2 data).

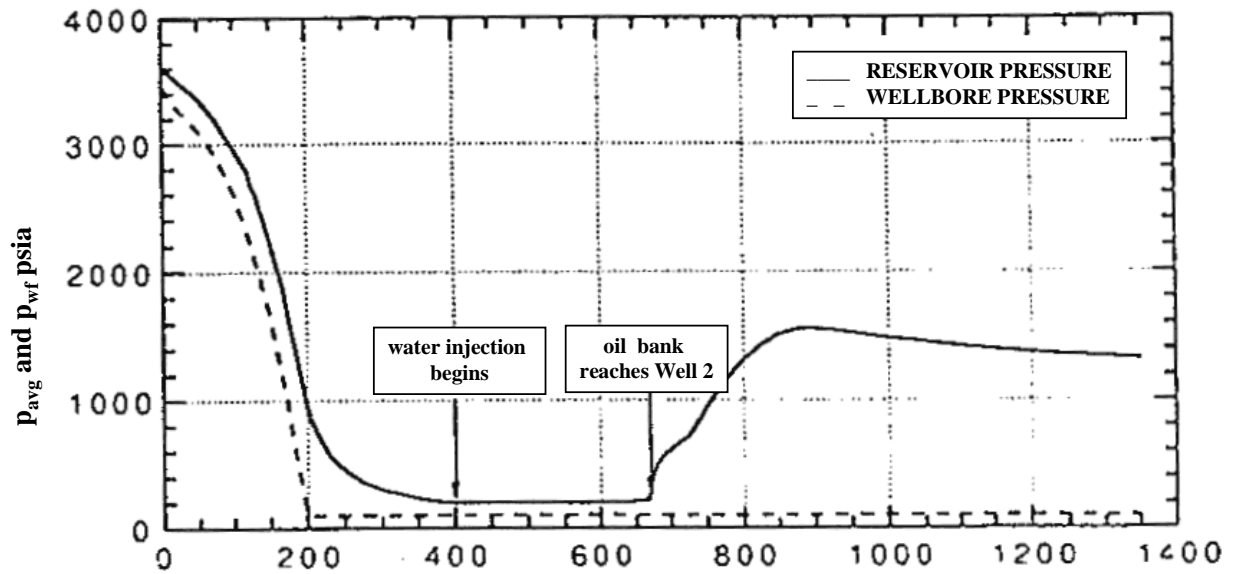


Fig. 24 - Reservoir pressure performance: for the case with water injection.

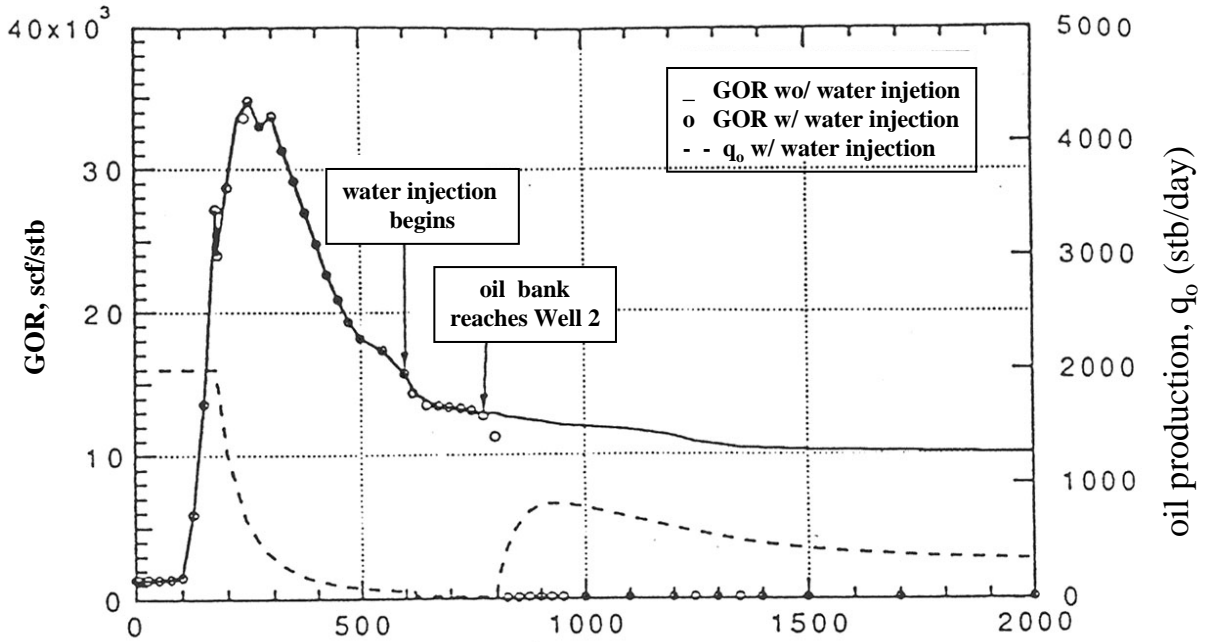


Fig. 25 - Comparison of GOR: with and without water injection (SPE2 data with oil viscosity increased 10 times).

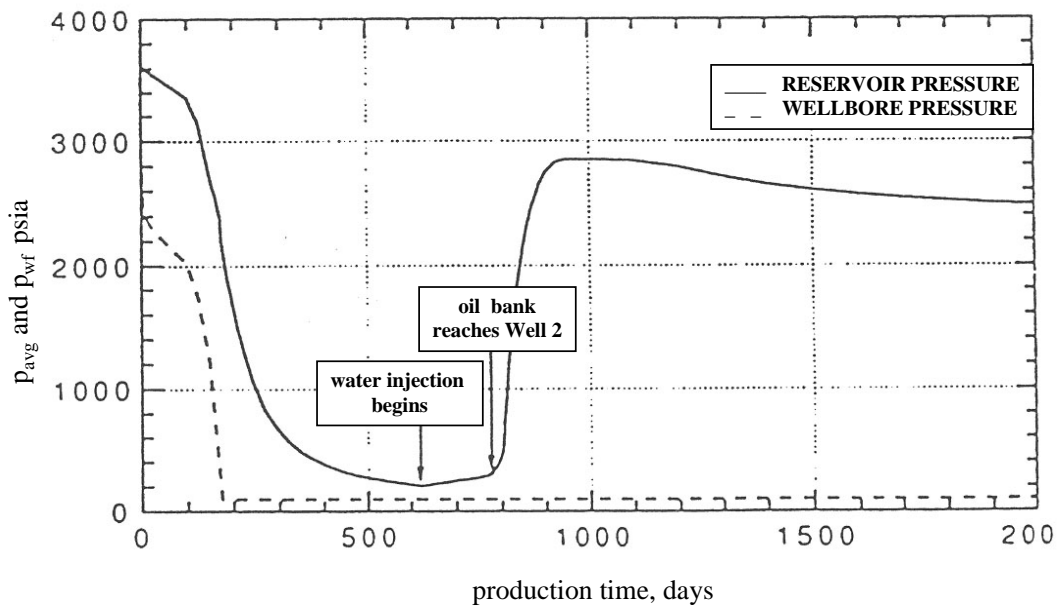


Fig. 26 - Reservoir pressure performance: for the case with water injection (SPE2 data with oil viscosity increased 10 times).

Exercises

Class Problem No. 90 (Repressuring)

A cell of a "black oil" simulator is being repressured following the original R_s curve. Consider the cell to be isolated from other cells. Use Odeh's data to solve the following problems.

The following conditions were observed for the cell at a lower pressure:

$$\begin{array}{rcl} S_g & = & 0.10 \\ S_o & = & 0.50 \\ p & = & 1,000 \text{ psia} \end{array}$$

- (1) Find the new bubble point that will be obtained during repressuring.
- (2) Find the correct values of μ_o and B_o at a pressure of 2,000 psia.

Class Problem No. 91 (Repressuring)

Use problem no. 90 to:

- (1) Compute the total compressibility (c_t) with gas going back into solution (Odeh's case A).
- (2) Compute total compressibility (c_t) without gas going back into solution (Odeh's case B).

CHAPTER 3

History Matching

- Technique
- Purpose
- Quality of Data
- Production Allocation
- Wrong Rate Problem
- Pressure Analysis
- Determining OOIP from Depletion History
- Continuity Problem
- Parameters to Be Changed in History Matching
- History Matching Procedures

History Matching

History matching is the part of reservoir simulation which often requires most of the time and money. This is a process of trying to reconstruct a field's past performance with model runs. An example of a history matching comparison is shown below, in which the model pressures are compared with actual pressures from the field build-up tests. After the history match is completed within the desired tolerances, or within the time and money constraints allowed for history matching, then prediction runs are performed. In this case three prediction runs are made (Cases A, B, and C), all beginning at the end of the history matching period.

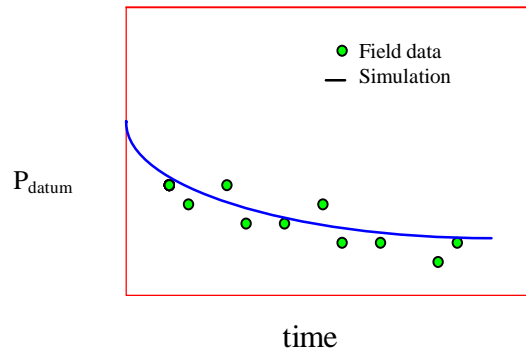


Fig. 1 - Datum pressure as a function of time.

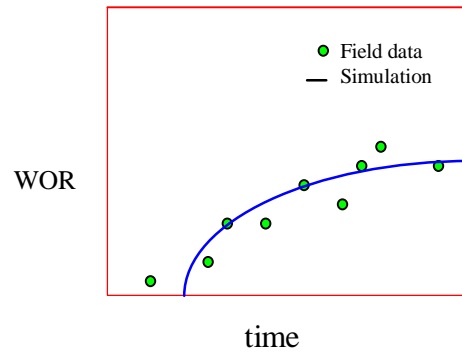


Fig. 2 - Water oil ratio as a function of time.

Technique

The usual technique is to input actual oil production and compare the model values of gas and water production against the field values. When simulating the behavior of oil reservoirs, oil production data will always be the most accurate because it is the value that must be accurately measured for sales purposes. This comparison is also made for bottom-hole flowing pressure, individual cell pressures, and average reservoir pressure. The oil production is usually available in monthly periods, but for the purposes of data input, the monthly production is allocated on a daily basis using a simple average unless detailed well records are available.

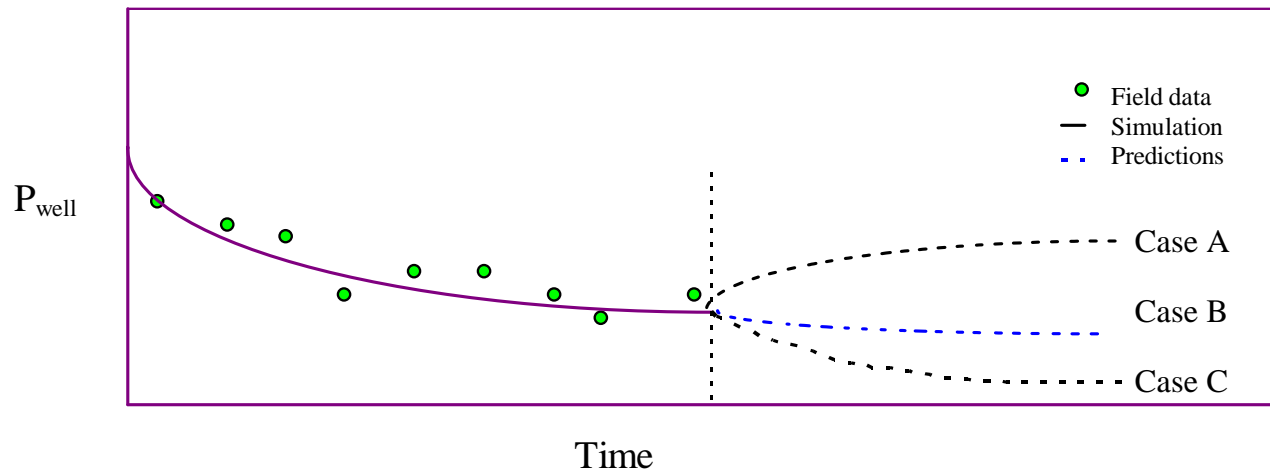


Fig. 3 - Prediction of different cases after history matching of well.

Purpose

The purpose of history matching is to validate the model for use in predictions and also to understand the reservoir mechanisms better. We will have much more confidence in the validity of our model if past reservoir performance data is available. In some cases, the complications that arise from history matching might make it necessary to acquire additional field data or to analyze the existing data differently. Very often the information learned during the history match process leads to a re-interpretation of the geologic study. Another purpose of the history matching procedure is to simply provide initial reservoir conditions for the predictive runs.

Purpose of history matching:

- 1) Calibration of model.
 - a) To make predictions
 - b) To understand reservoir mechanisms and geology.
- 2) Provide initial conditions for predictions.

Many simulation projects have been completed without field performance history. These projects are much easier to perform because the tedious history matching procedure is eliminated. In these cases the simulator should be updated as field data becomes available, otherwise the actual performance of the reservoir may not be modeled accurately. Reservoir simulation is usually used in these cases because it is capable of providing more accurate results and including more aspects of reservoir description and operating conditions than could be done by hand methods, and minor adjustments may be done easily.

Quality of Data

Accuracy of Model vs. Its Importance. An interesting comparison can be made between the accuracy of a model, as determined by history matching, and the importance of having a good reservoir simulation study. At the time of abandonment of a field, it is possible to get the most complete description of a reservoir from performance history matching. However, at that time a reservoir study has little value. At the beginning of production, the need for accurate predictions and reservoir description is the most important. It is at this time that important capital expenditures are made and perhaps irreversible decisions are made about how the field should be produced. At the beginning of production we do not have the benefit of performance history matching so we can say that the model has the least accuracy at this time.

Pressure Data. It is important to realize that the performance data that is being matched might have significant errors in it. The quantity and accuracy of the pressure data, for example, is limited by money available for testing and the sensitivity and the accuracy of the pressure measuring device. Pressure errors can also be made because of poor calibration of the tool or incorrect analysis of test results.

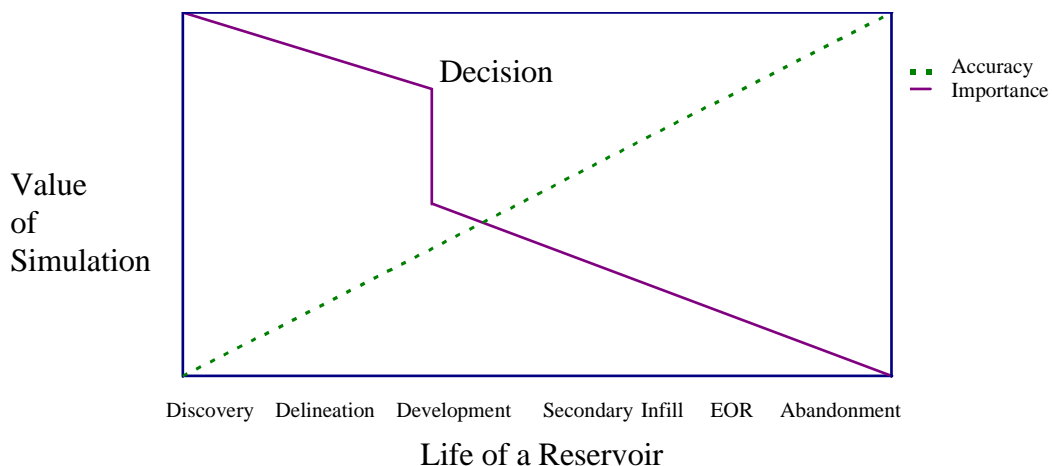


Fig. 4 - Relative importance and accuracy of a simulation study during the life of a producing well.

Pressure Data:

- (a) Quantity of data.
- (b) Sensitivity/Accuracy of tool.
- (c) Calibration of tool.
- (d) Analysis of test.

Production Data. It is also important to realize that production data, even oil production data, is not always accurate. The overall lease or tract production might be considered to be accurate, but

individual well production rates are usually allocated from field tests that are done periodically, if at all. Sometimes testing procedures are not frequent enough or accurate enough. For oil reservoirs, the gas and water production rates are likely to be in greater error than the oil production rate. The engineer should know whether these rates were metered during tests and whether they were metered monthly at the tank battery. In many cases water production is not needed but is estimated from production tests of brief duration and sometimes questionable accuracy. If wrong rates are input into the simulator, then the simulator rates and the resulting pressures will be of questionable accuracy.

Production data:

- (a) Frequency of test.
- (b) Accuracy of test.
- (c) Available equipment/meters.
- (d) Allocation of rates.

Production Allocation

The sketch below shows how production might be allocated in a typical production setup. Each of the wells will have an individual flow line that goes to the manifold at a common point. Each well can then be directed towards the production separator, along with the other wells, or to the test separator by itself. The normal procedure is to test a well for 24 hours at a frequency of, perhaps, once a month. The monthly production from all of the wells will be the most accurate measured value but there are other complications such as wells being “down” during periods of the month. The monthly production rates at the sales point are allocated to individual wells based on their test rates and the producing time of each well. The allocated rates would not usually be exactly the same as the test production rates. Then it is necessary to apply some correction factor to make the monthly well production add up to that measured at the sales point.

The same procedure is, more or less, followed for the gas and water phases. These values will be more accurate if the rates are metered at the tank battery during normal operation and adjusted with test production data.

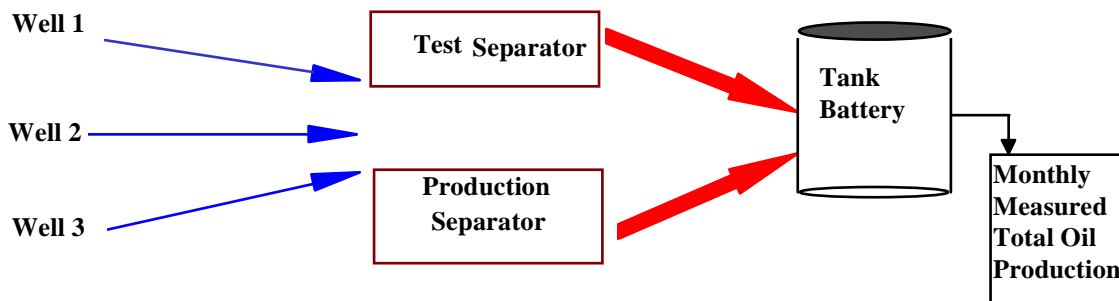


Fig. 5 - Surface Production System

Example of Production Allocation

Well No.	Test Separator Data	
	q_o (B/D)	q_w (B/D)
1	100	0
2	250	10
3	125	15
Total (B/D)	475	25

Metered or monthly values at tank battery: $q_o = 450$ B/D, $q_w = 20$ B/D

Wrong Rate Problem

There are some problems to avoid in history matching that might not be obvious to an inexperienced engineer. One of the most common problems is the “wrong rate problem”.

In the example reservoir in Figure 6, a number of wells are producing from the oil leg of the reservoir at low solution gas/oil ratios. One well is near the gas/oil contact and produces at high gas/oil ratios. The simulator run is made with a fixed oil production rate and the gas/oil ratio is calculated from the cell saturations. In this case, the calculated gas/oil ratio is much too high because the model oil saturation is approaching residual oil saturation. The model gas/oil ratio approaches infinity and so does the gas production rate since the oil production rate is fixed. We find that the pressure behavior of the model is meaningless because the gas rate in this one well is extremely high.

In order to solve this problem, the total production rate must not be controlled by the lower rate phase (oil in this case) if the total reservoir production rate is to be accurately matched. This total production rate must be matched before the reservoir pressure can be matched.

A simple check to make at the end of a history match run is to make sure that all three phases produce about the same cumulative production as observed in the field. If one of the phases is significantly off, then that rate must be adjusted before pressure can be matched.

Some simulators make an automatic adjustment of the rates to honor the observed total reservoir rates, rather than the oil rates. This requires data input of oil, gas, and water production rates. At each timestep, the total reservoir production rate is calculated and matched with the observed field rate. When this calculation is performed, the total reservoir production rate will be correct and the pressure match can then be performed.

Solution. The problem is that q_g approaches infinity since the model k_{ro} approaches zero. We can see the effect on q_t by remembering that:

$$q_t = q_o B_o + q_w B_w + (q_g - R_s q_o) B_g$$

When using the total production rate, input a value of $(q_g)_{\max}$, which is the highest value of q_g seen in the field. A second solution method is to input q_g instead of q_o when $GOR > 4,000$ scf/bbl and subsequently calculate q_o . A third method is to input q_t (or q_o , q_w , and q_g) observed and then match $(q_t)_{\text{model}}$ as shown in the following table:

	q_o	q_w	WOR	q_t
FIELD	50	100	2.0	150
MODEL	50	150	3.0	200
MODEL (Adjusted)	37.5	112.5	3.0	150

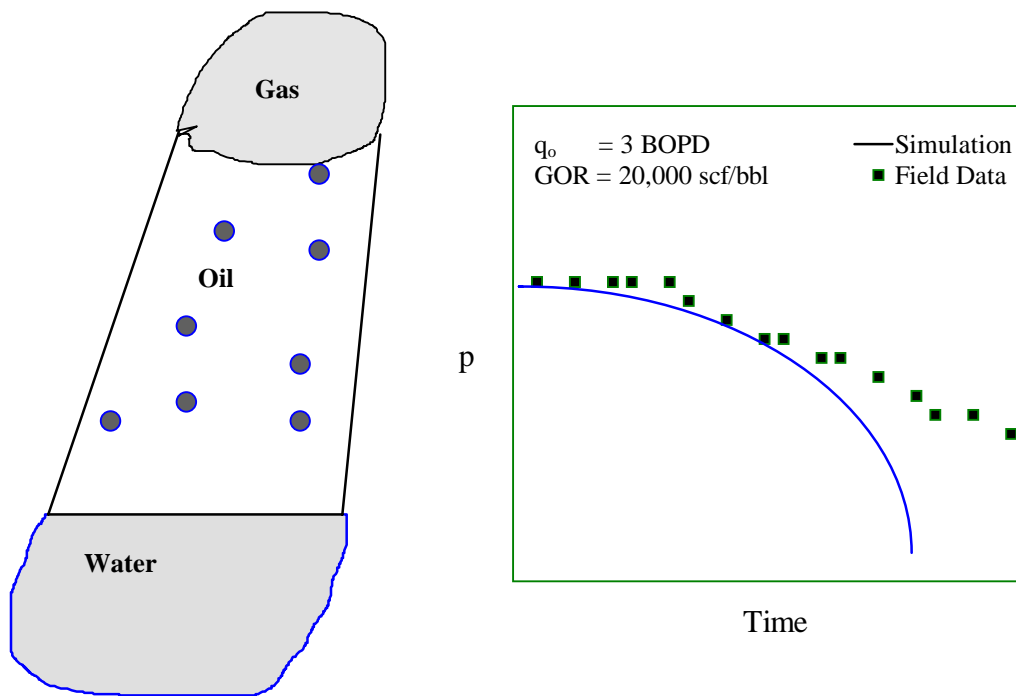


Fig. 6 - Wrong rate problem for the well near gas-oil contact (GOC).

Pressure Analysis

We can analyze different aspects of pressure performance and make some generalities about how this may be adjusted.

Gradients (Cross-Section). The pressure gradients can be observed from pressure profiles constructed at particular times where field data is available. The gradients may lead to information about the continuity of the formation or the transmissibility of the reservoir.

$$a) u_t = -\left(\frac{k}{\mu}\right)\nabla\Phi$$

- b) faults
- c) h contour

In figure 7, the model shows different trend than the field data. One of the probable cause for the difference is that high absolute permeability used in the simulation model. Decreasing absolute permeability in the simulation may improve the match.

Pseudosteady-State (Closed reservoir). Pseudosteady-state behavior can be analyzed when it occurs in the model and in the field. The matching of this data requires that the total reservoir production rate be correct. History matching can lead to better estimates of pore volume or total compressibility.

$$\frac{dp}{dt} = -\frac{q_t}{V_p c_t} \quad (1)$$

(at all points)

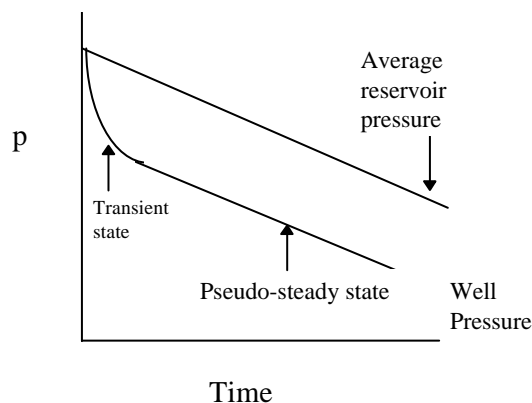


Fig. 8 - Pressure versus time.

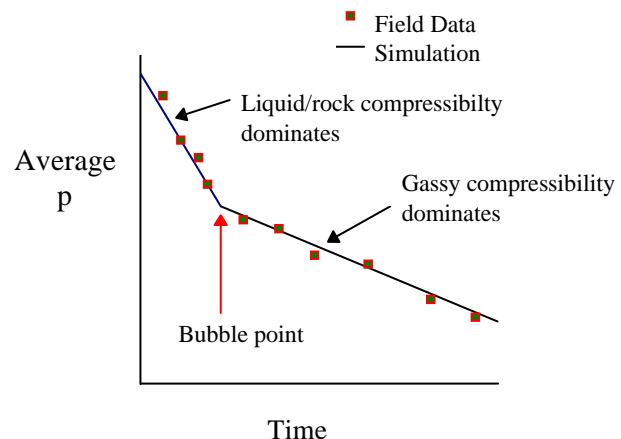


Fig. 9 - Average pressure versus time.

Tank Material Balance:

$$\frac{d\bar{p}}{dt} = - \frac{q_t}{V_p c_t} \quad (2)$$

After the reservoir pressure goes below bubble point, total compressibility increases drastically because of increase in oil compressibility and generation of gas saturation and gas compressibility. Below bubble point, oil compressibility dominates over other terms.

Transient Pressure Behavior. Transient behavior can be analyzed using the dimensionless pressure and dimensionless time and the results can be used as another tool in the parameter adjustment process during history matching. The results of this analysis apply **only** to transient flow periods.

It should be noted that mobility is a factor in the magnitude of the pressure drop (as indicated by the dimensionless pressure equation) and the timing at which a particular feature occurs (from dimensionless time). The thickness only affects the magnitude of pressure drop. The porosity or total compressibility affect only the timing.

$$p_D = \frac{kh(p_i - p_{wf})}{141.2 q B \mu} \quad t_D = \frac{0.000264 k t_{hrs}}{\phi \mu c_t r_w^2} \quad (3)$$

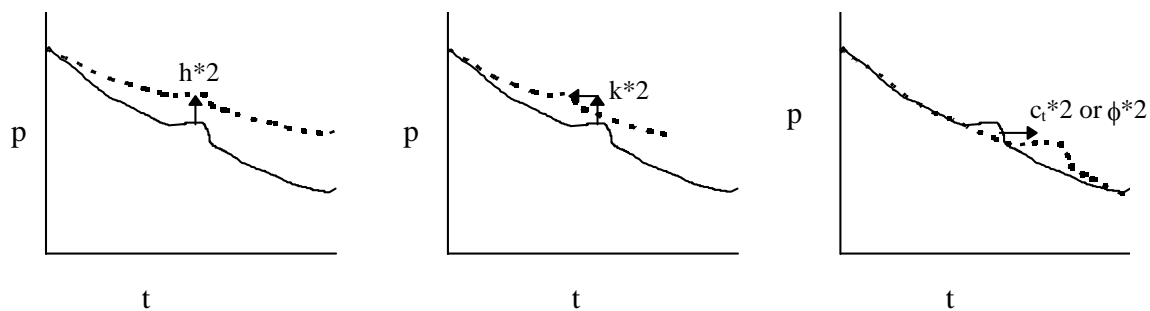


Fig. 10 - Effect of different variables during transient time.

Determining OOIP from Depletion History (when available)

$$OOIP = \frac{V_p S_o}{B_o} \quad (4)$$

$$\frac{dp}{dt} = - \frac{q_t}{V_p c_t} \quad (5)$$

OOIP can be accurately determined when the following conditions are met:

- If (1) good depletion history
 (a) good data
 (b) significant pressure decline
 (c) volumetric (closed) reservoir
 and (2) c_t is dominated by $c_o S_o$
 and (3) good PVT data for oil

Assume:

$$c_t = c_f + c_o S_o + c_w S_w + c_g S_g \quad (6)$$

$$c_t \approx c_o S_o \quad (7)$$

Then,

$$\frac{dp}{dt} = \frac{-q_t}{V_p c_o S_o} \approx - \frac{q_t}{c_o B_o} \frac{1}{OOIP} \quad (8)$$

Or:

$$OOIP = \left(\frac{-q_t}{c_o B_o} \right) / \left(\frac{dp}{dt} \right) \quad (9)$$

Notes:

- (1) c_o is more likely to dominate below the bubble point. Above the bubble point c_f and c_w become important and data may not be accurate.
- (2) Original gas in place (OGIP) is measured by extrapolating a plot of p/z versus G_p . Hence, if a strong water drive is present in the reservoir, wrong OGIP will be obtained.
- (3) If a good history match is obtained, it does **not** necessarily mean a good prediction of OOIP can be obtained.

- (4) Generally, values of permeability and porosity used in the simulation are obtained from the core analysis. During core analysis, permeability is calculated by establishing a steady state flow through the core. The porosity is obtained by expansion process following Boyle's law. Good evaluation during core analysis will lead to good history matching and OOIP calculation.
- (5) If injection has been started at the beginning of the life of the reservoir, then it is highly unlikely that a good prediction of OOIP can be obtained.

Continuity Problem

Sometimes, it is difficult to predict the continuity of the reservoir. For example, suppose, two identical wells are producing at the same rate as shown in figure 11. In this case, we cannot conclude about the continuity at the "no flow boundary" which is midway between the two wells. Presence of continuity at the no flow boundary may not be important during primary depletion. However, continuity is important during secondary recovery when one of the wells may be changed to an injection well. Interference well testing can determine continuity. This type of factor should be taken into account for successful prediction using simulator.

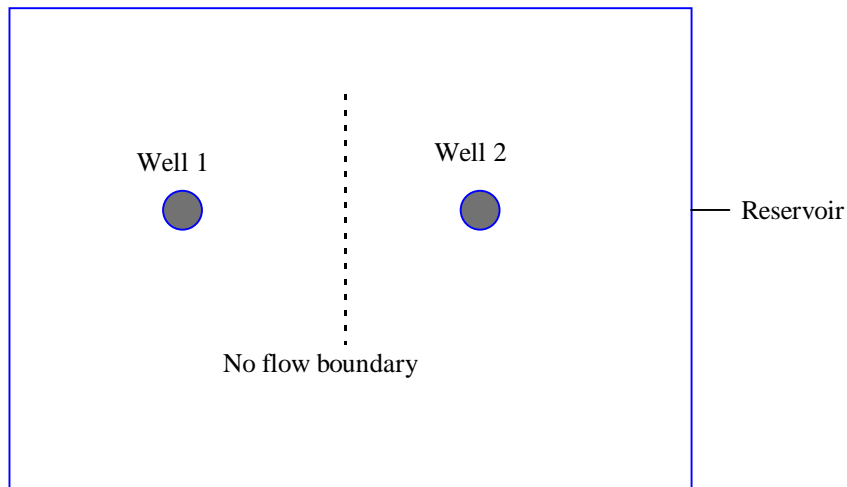


Fig. 11 - Two identical wells producing in a reservoir.

Parameters to be Changed in History Matching

1) One rule that should be observed in history matching is that the parameter with the lowest degree of reliability (or highest degree of uncertainty) should be changed first. The reservoir and aquifer properties in approximate order of uncertainty are: (1) aquifer transmissibility, kh ; (2) aquifer storage, $\phi h c_i$; (3) reservoir kh ; (4) relative permeability and capillary pressure functions; (5) reservoir thickness; (6) reservoir permeability; (7) reservoir porosity; (8) structural definitions (datums); (9) rock compressibility; (10) oil and gas fluid properties; (11) water-oil and gas-oil contacts; and (12) water fluid properties.

2) Some useful practical observations are worth noting: (1) increasing model permeability, k , will decrease cell pressure; (2) increasing model porosity, ϕ , will increase cell pressure; (3) increasing model reservoir thickness, h , will increase cell pressure; and (4) on the pressure-distance graph, increasing model permeability, k , will decrease the absolute value of pressure gradient.

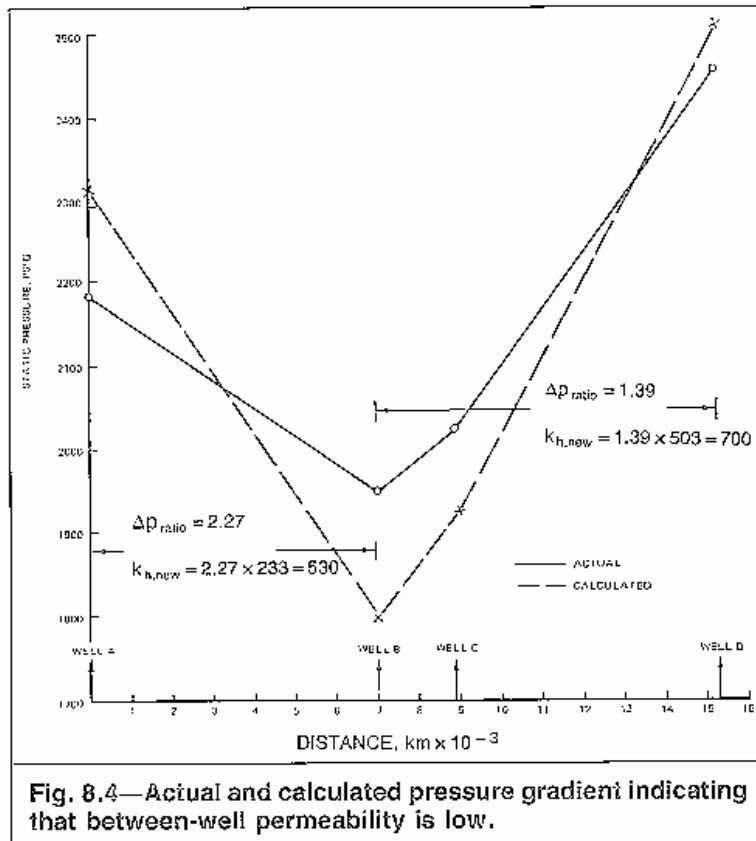


Fig. 12 - (from Fig. 8.4, SPE Monograph 13).
Calculated pressure gradients greater than actual data.
Increasing model permeability will yield match.

History Matching Procedures

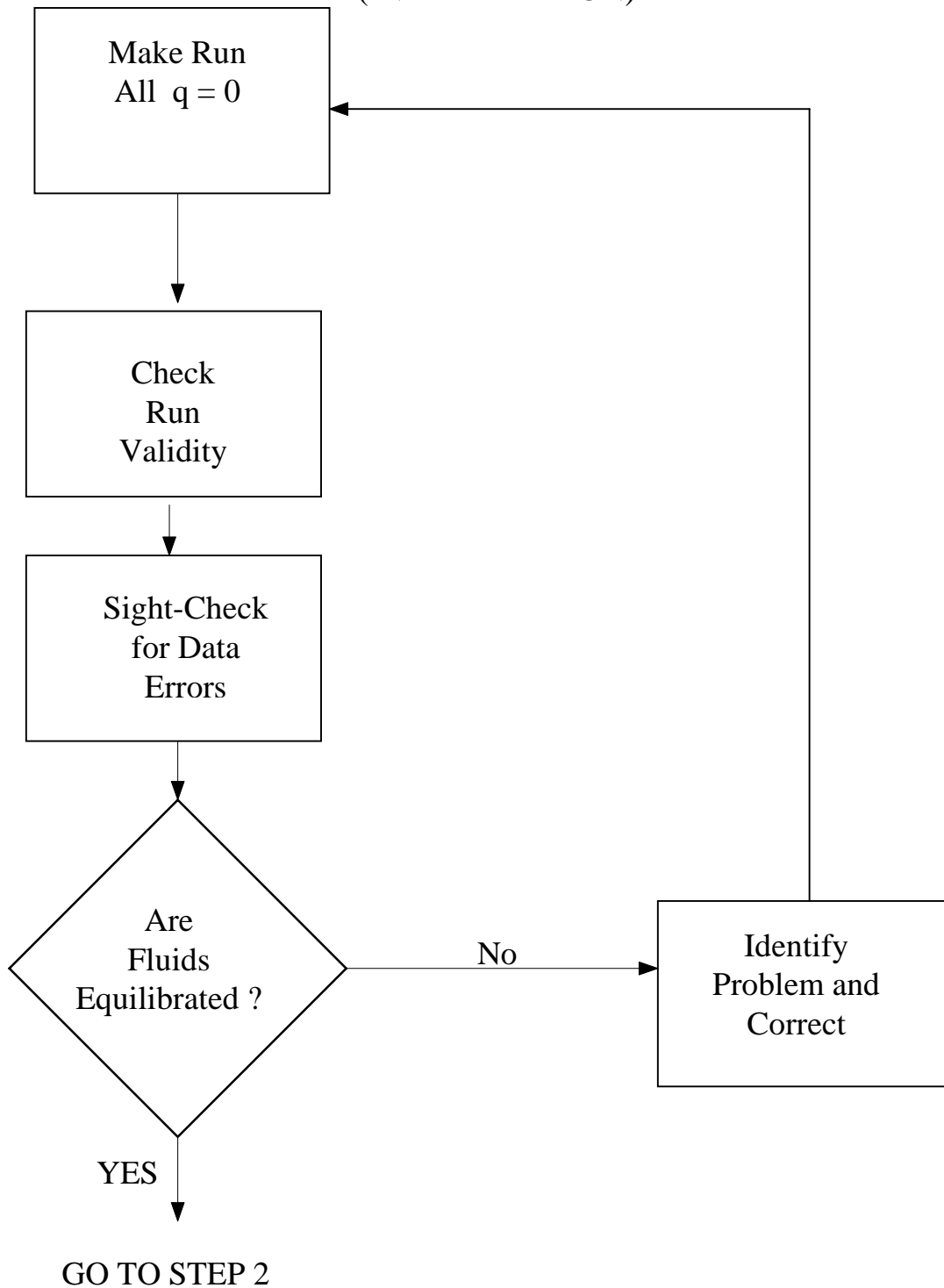
The history matching process can be systematized to some degree if a four-step procedure is followed. This procedure allows us to focus our attention on particular aspects of the model accuracy when making model adjustments during any step.

Step 1 is the initialization of the model. In addition to checking the data for input errors, a good initial check is to perform an “equilibration run” to make sure that the initial conditions are static. This is done by running the model over the period of time of interest with zero production rate. If the model is equilibrated properly, saturations and pressures will not change. If there are some changes, the engineer must judge whether these changes can be avoided and whether they are significant compared to the expected changes during reservoir performance.

HISTORY MATCHING PROCEDURES

STEP 1

(INITIALIZATION)



Step 2 is the pressure match. During this step it is required that the total reservoir production rate be specified for each well so that the “wrong rate problem” can be avoided. The producing ratios may be in error, but the total reservoir production rate must be correct. When we have accomplished this, then we can think of modeling Martin's equation using total mobility, total compressibility, and total reservoir production rate.

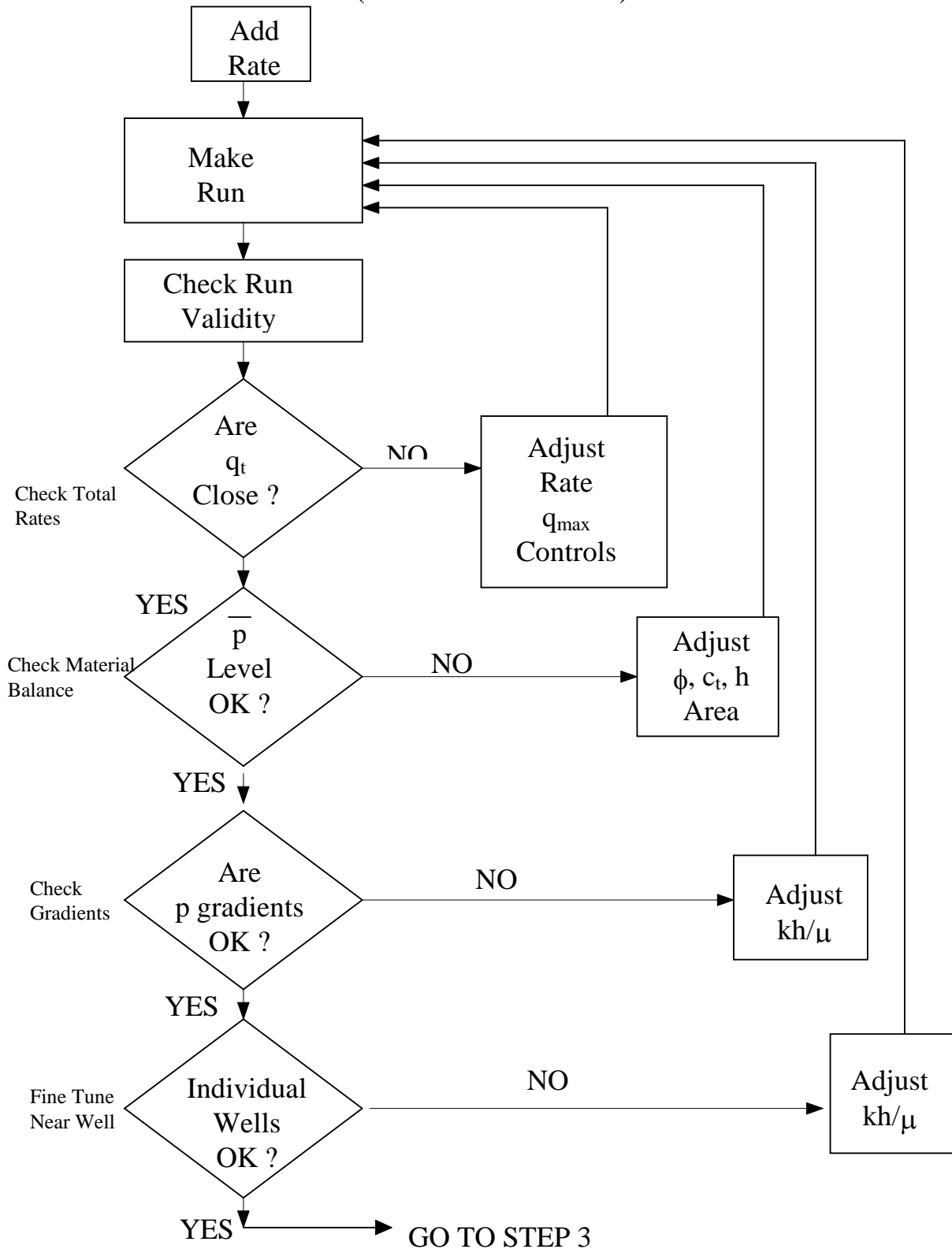
The first step is to match the average reservoir pressure. This is equivalent to checking the material balance for the reservoir. Adjustment in the pore volume or compressibility must be made at this point. If an aquifer exists, then the level of aquifer support will be matched at this point.

The next step is to check pressure gradients at particular times to see if the reservoir continuity and transmissibility are correct.

Finally, when the gross reservoir adjustments are completed, then individual well areas can be adjusted.

After step 2 is completed, then we can go to step 3.

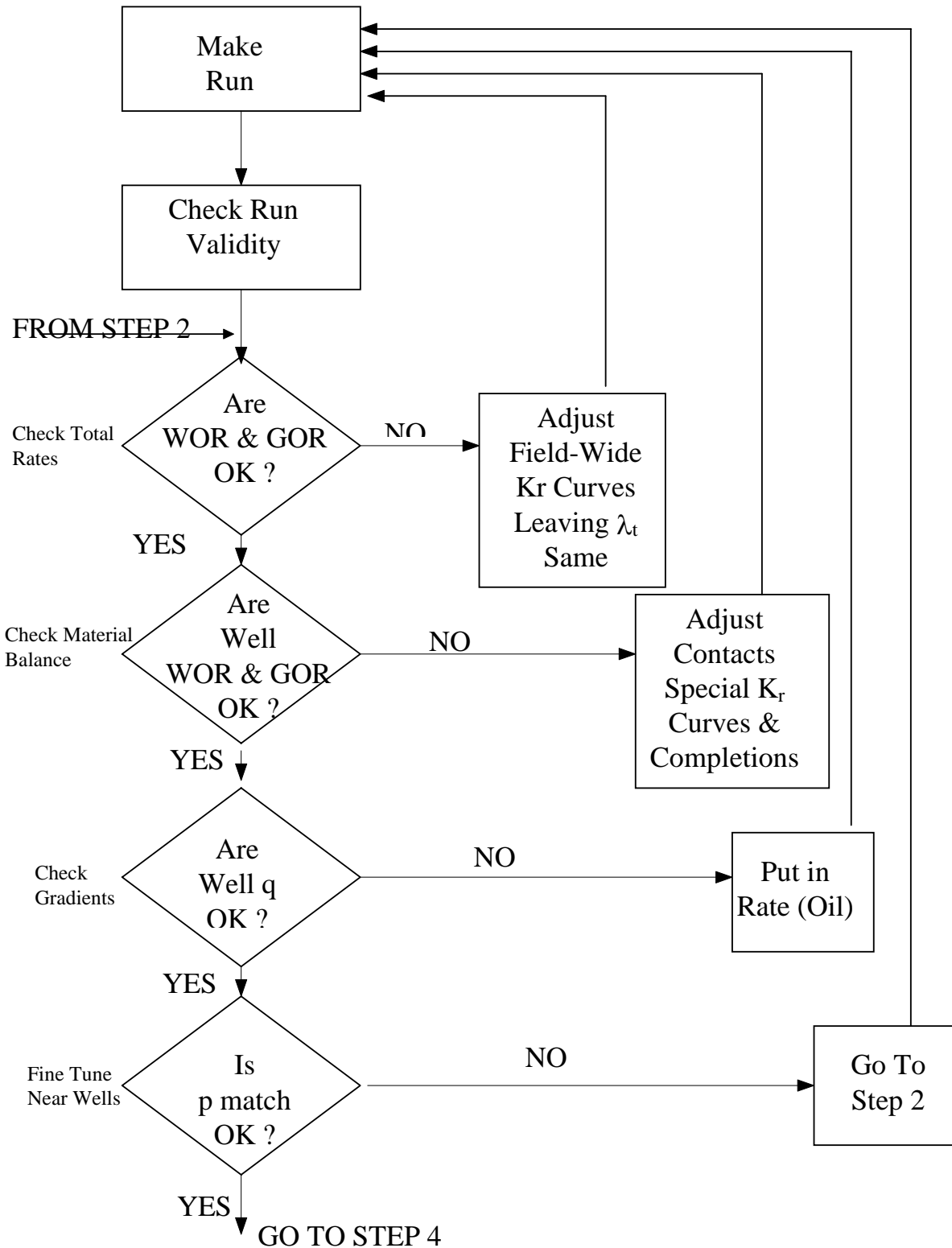
HISTORY MATCHING PROCEDURES
STEP 2
(PRESSURE MATCH)



We enter step 3 with the correct total reservoir producing rates, but may have erroneous producing ratios. The adjustments in step 3 are ones that involve saturations, relative permeabilities, water/oil contacts, and gas/oil contacts. The relative permeability adjustments that are required to match the producing ratios may be done with pseudo relative permeabilities if a 2-D model or a coarse 3-D model is used.

HISTORY MATCHING PROCEDURES

STEP 3 (S MATCH)



Step 4 is the final step in history matching. Once the pressures and producing ratios have been matched then the productivity indices can be matched. This is done by adjusting the model's productivity index (PI) to give the actual field bottom hole flowing pressures at the end of the history period. The bottom hole flowing pressure must be accurate at this point because it will usually control the producing rates during the prediction period.

For a 2-D model, the productivity index adjustment can be made by hand without even making a simulator run. The bottom hole pressure calculation is external to the cell pressure calculation in the simulator and is not involved in the matching of cell pressures.

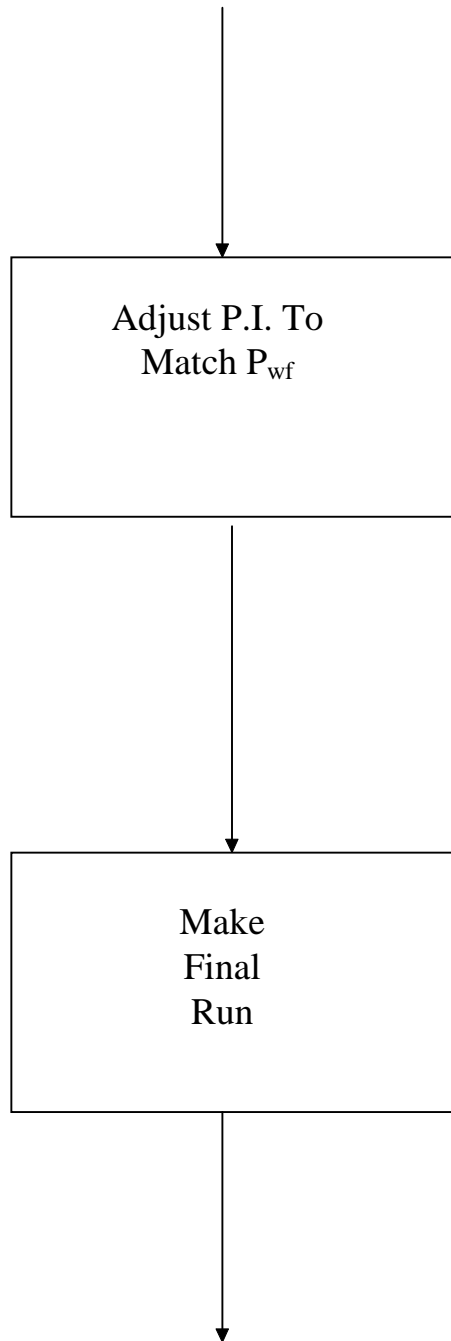
If the model is a 3-D model with commingled wells, then the adjustment of productivity indices has to be done on an individual layer basis. This affects the “flow splitting” from the different producing intervals in the model wells, which may in turn affect the pressure behavior. This type of adjustment can be tedious but can be aided by downhole producing information that indicates rates from different producing intervals (i.e., tracer surveys or flowmeter surveys).

HISTORY MATCHING PROCEDURES

STEP 4

(P_{wf} MATCH)

FROM STEP 3



GO TO PREDICTION

Synthetic History Matching

A series of synthetic history matching exercises has been set up. These are relatively simple exercises in which analysis skills for history matching are required.

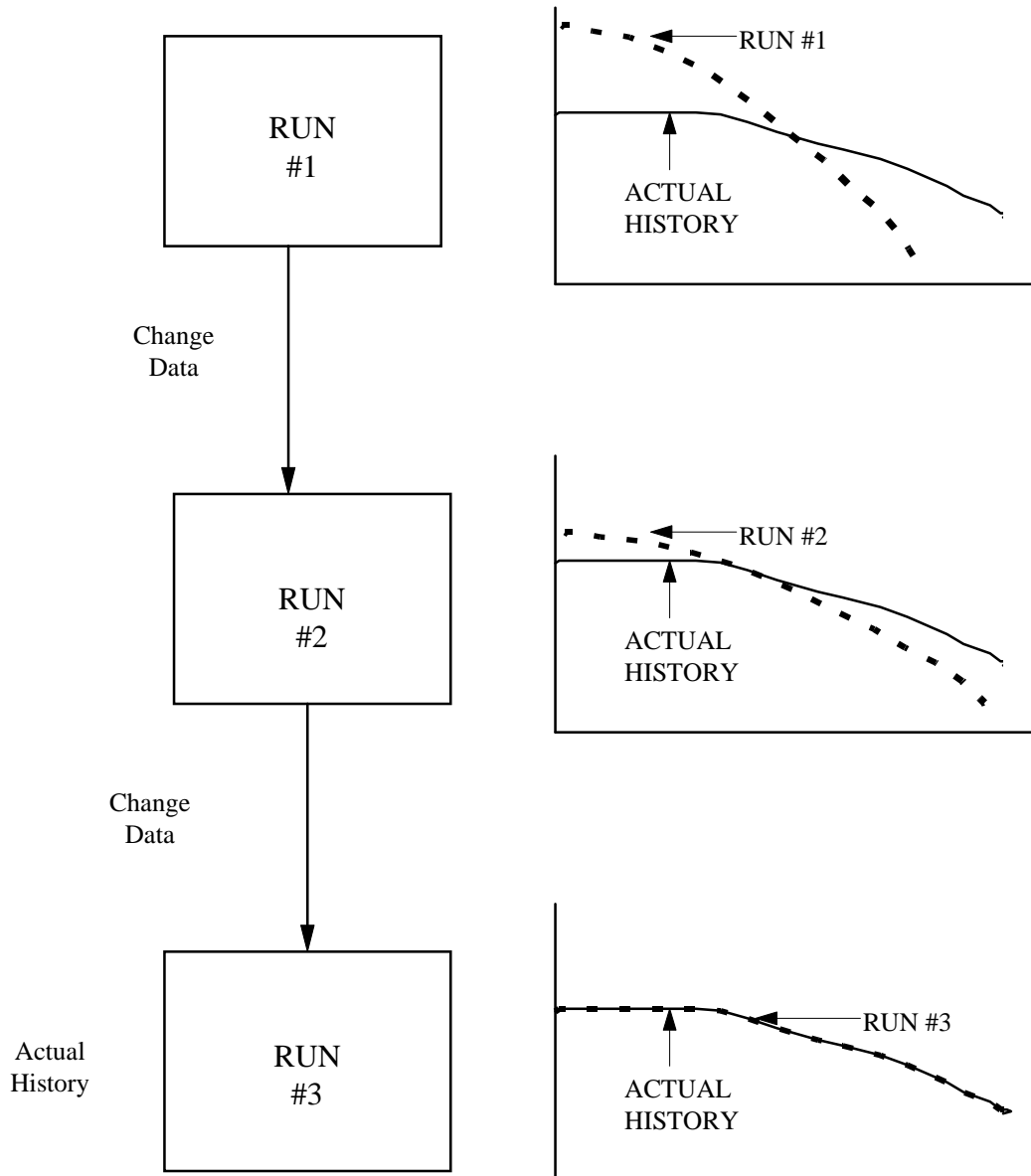
A series of three simulator runs is made with changes in the data between runs. The final run is considered to be the “actual history” of the reservoir. When the results of the first run are compared to this “actual history” the engineer must analyze the reservoir mechanics of the performance and try to determine what data has been changed between the first and third run. After the first run is analyzed and the proper data has been changed, then the second run is analyzed to try to determine the last change in data which gave the “actual history”.

The skills involved in analyzing this type of problem are exactly the same skills used in analyzing an actual field history match. As we try to match history in a field case, we are called upon to predict the effect of each data change that we propose to make. It is common that the resulting data changes are not of the magnitude that the engineer predicted. If this is the case, then the engineer's skill of relating data changes to changes in performance are inhibiting his ability to match history.

A good rule to follow is to not make too many changes in a single history run. Concentrate on adjusting one parameter at a time. Since the results of data changes are not always the same as anticipated, it is better to isolate each type of data change and observe its effect before changing another type of data. It is also advisable, in many cases, to make data changes larger than the engineer expects is necessary. If the resulting performance changes are too severe, then interpolation of the required parameter change will be easier than extrapolation.

Another rule that might be considered is to work from “left to right” on the time scale of field performance. In other words, to match the early history before matching the later history. This means we can often begin our history matching with shorter runs.

SYNTHETIC HISTORY MATCHING



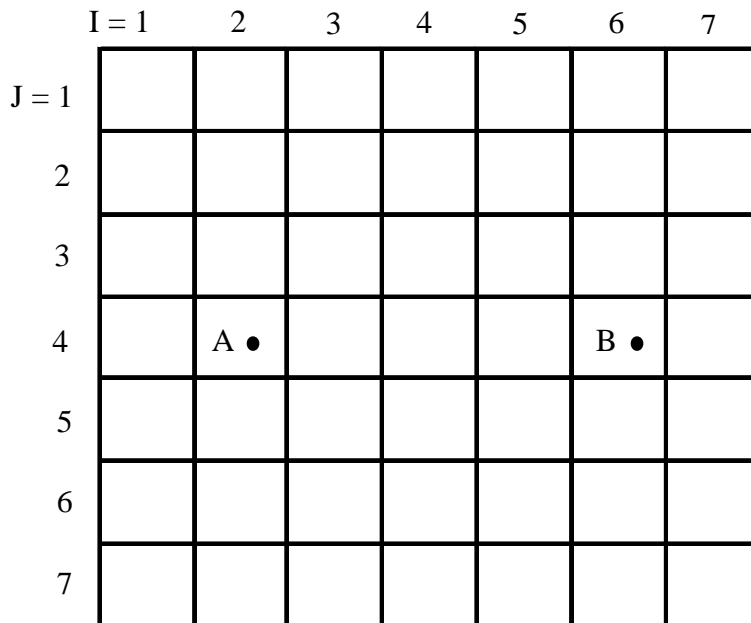
EXERCISES

RESERVOIR SIMULATION CLASS PROBLEM NO. 62

The reservoir shown below is homogeneous, isotropic, and 2-D. Wells A and B are producing at a constant rate for 5 years. At that time, well A is converted to an injection well. The injection rate in Well A and the production rate in well B are held constant over the remaining 5 years.

The observed pressure data and the results of history match run #1 are attached. The input and output data files for the simulation runs are also provided.

Analyze the pressure performance and recommend the changes required in reservoir parameters to match the pressure behavior.



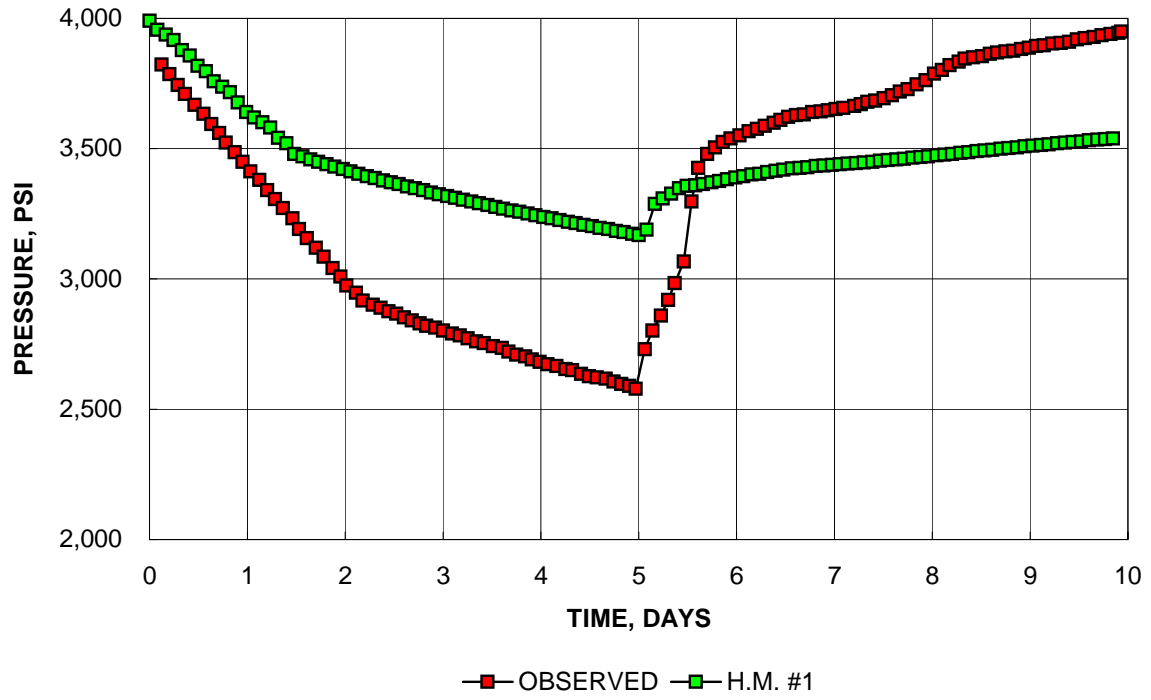
PROB_62

TIME, YRS Well A	Obs. Press. Well A	TIME, YRS Well B	Obs. Press. Well B	TIME, YRS	H.M. #1 Well A	H.M. #1 Well B
0.12	3821.9	0.14	3854.8	0.003	3991.3	3991.3
0.2	3784.6	0.23	3817.8	0.08	3957.1	3957.1
0.29	3744.7	0.31	3778.1	0.16	3937.1	3937.1
0.36	3710.1	0.39	3738.5	0.25	3917.1	3917.1
0.46	3667.5	0.49	3698.9	0.33	3877.2	3877.2
0.55	3632.8	0.57	3661.9	0.41	3857.3	3857.3
0.63	3595.6	0.64	3624.9	0.49	3817.4	3817.4
0.71	3561	0.74	3587.9	0.58	3797.5	3797.5
0.78	3523.7	0.8	3548.3	0.66	3757.6	3757.6
0.87	3486.4	0.9	3511.2	0.74	3737.6	3737.6
0.95	3449.2	0.98	3476.9	0.82	3717.7	3717.7
1.03	3411.9	1.06	3439.9	0.90	3677.8	3677.8
1.12	3379.9	1.14	3397.6	0.99	3640.6	3640.6
1.2	3340	1.23	3360.6	1.07	3620.7	3620.7
1.28	3305.4	1.31	3321	1.15	3600.7	3600.7
1.36	3270.8	1.38	3284	1.23	3580.8	3580.8
1.46	3233.5	1.48	3244.4	1.32	3540.9	3540.9
1.53	3190.9	1.56	3207.4	1.40	3520.9	3520.9
1.61	3156.3	1.64	3173	1.48	3480	3480
1.7	3119	1.73	3130.7	1.56	3469	3469
1.78	3084.4	1.81	3096.4	1.64	3458.9	3458.9
1.87	3041.8	1.89	3059.4	1.73	3449.1	3449.1
1.95	3009.9	1.97	3022.4	1.81	3439.4	3439.4
2.01	2975.3	2.05	2982.7	1.89	3429.9	3429.9
2.11	2946	2.13	2958.9	1.97	3420.7	3420.7
2.18	2916.7	2.22	2927.2	2.05	3411.9	3411.9
2.28	2900.6	2.3	2916.6	2.14	3403.3	3403.3
2.36	2889.9	2.38	2900.7	2.22	3394.9	3394.9
2.44	2876.6	2.47	2887.5	2.30	3386.6	3386.6
2.52	2865.9	2.54	2876.9	2.38	3378.7	3378.7
2.6	2852.5	2.62	2866.3	2.47	3370.8	3370.8
2.68	2841.8	2.7	2855.6	2.55	3363	3363
2.76	2828.4	2.79	2842.4	2.63	3355.3	3355.3
2.83	2820.4	2.85	2834.4	2.71	3347.7	3347.7
2.92	2812.3	2.96	2823.8	2.79	3340.1	3340.1
3	2801.6	3.03	2810.6	2.88	3332.7	3332.7
3.09	2790.9	3.11	2800	2.96	3325.3	3325.3
3.17	2782.8	3.2	2792	3.04	3318	3318
3.25	2772.1	3.29	2778.7	3.12	3310.8	3310.8
3.34	2761.4	3.36	2770.8	3.21	3303.8	3303.8
3.42	2753.4	3.44	2760.2	3.29	3296.8	3296.8
3.51	2742.6	3.53	2746.9	3.37	3290.1	3290.1
3.6	2734.6	3.61	2738.9	3.45	3283.4	3283.4
3.67	2721.2	3.68	2731	3.53	3276.8	3276.8
3.75	2710.5	3.78	2720.3	3.62	3270.2	3270.2
3.84	2702.5	3.86	2712.4	3.70	3263.7	3263.7
3.91	2691.8	3.94	2701.8	3.78	3257.2	3257.2
3.99	2681	4.02	2693.8	3.86	3250.8	3250.8
4.07	2673	4.09	2685.8	0.00	3244.4	3244.4
4.16	2664.9	4.18	2677.8	4.03	3238.1	3238.1
4.25	2654.2	4.27	2664.6	4.11	3231.9	3231.9
4.32	2648.8	4.35	2656.6	4.19	3225.7	3225.7
4.41	2635.5	4.43	2648.6	4.27	3219.6	3219.6
4.49	2627.4	4.51	2640.7	4.36	3213.5	3213.5
4.57	2622	4.6	2627.4	4.44	3207.5	3207.5
4.66	2616.6	4.68	2622.1	4.52	3201.7	3201.7
4.74	2605.9	4.77	2616.8	4.60	3195.9	3195.9
4.82	2597.8	4.85	2608.8	4.68	3190.1	3190.1
4.9	2589.8	4.93	2598.2	4.77	3184.3	3184.3
4.97	2579.1	5.01	2590.2	4.85	3178.6	3178.6
5.06	2730.4	5.08	2582.2	4.93	3173	3173
5.14	2802	5.17	2576.9	5.00	3168.3	3168.3
5.23	2860.4	5.26	2571.6	5.08	3188.3	3166.6
5.3	2918.7	5.33	2568.9	5.16	3288.3	3162.9

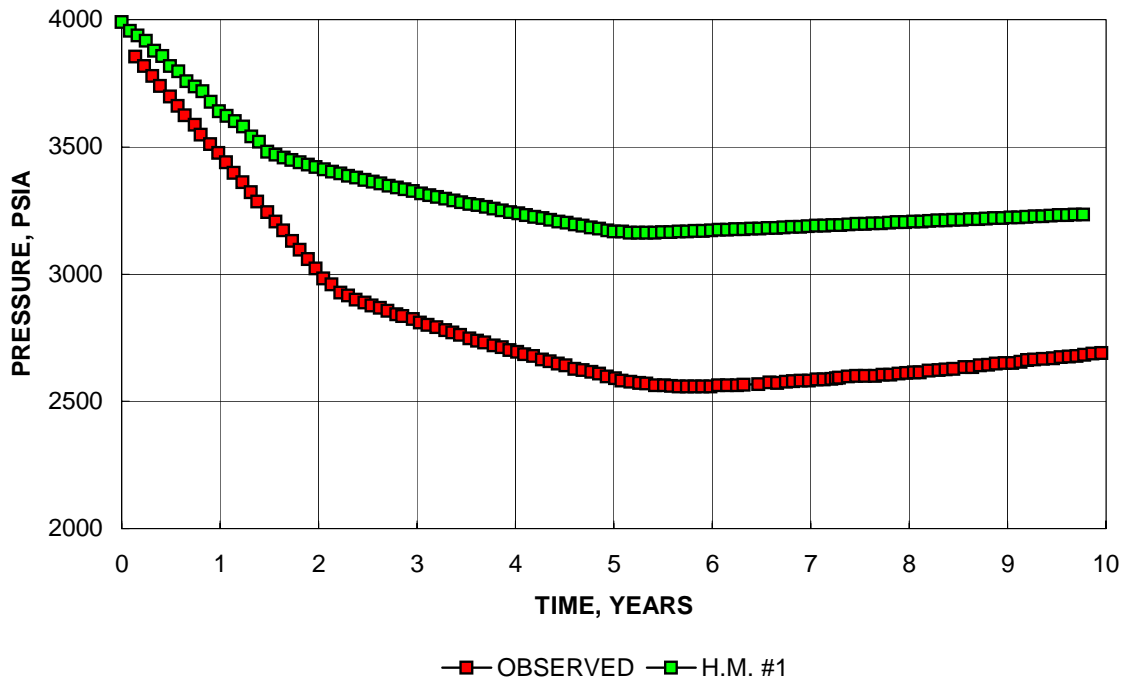
PROB_62

TIME, YRS Well A	Obs. Press. Well A	TIME, YRS Well B	Obs. Press. Well B	TIME, YRS	H.M. #1 Well A	H.M. #1 Well B
5.37	2985	5.42	2563.5	5.25	3308.3	3162.4
5.46	3067.3	5.51	2563.5	5.33	3328.3	3162.4
5.54	3298.3	5.58	2560.8	5.41	3348.3	3162.9
5.61	3425.7	5.66	2558.1	5.49	3356.5	3164
5.7	3478.7	5.74	2558	5.58	3360.5	3165.2
5.78	3505.2	5.82	2558	5.66	3365	3166.6
5.86	3526.3	5.9	2557.9	5.74	3370	3167.9
5.94	3539.5	5.98	2557.9	5.82	3375.6	3169.3
6.03	3550.1	6.06	2563.1	5.90	3381.8	3170.6
6.12	3565.9	6.15	2563	5.99	3388.6	3171.8
6.21	3576.4	6.25	2563	6.07	3394.2	3173.1
6.29	3587	6.32	2565.6	6.15	3400.1	3174.4
6.38	3600.2	6.47	2568.1	6.23	3404.2	3175.7
6.45	3610.7	6.58	2573.3	6.32	3409.5	3177
6.53	3621.3	6.66	2573.2	6.40	3415	3178.2
6.61	3629.1	6.75	2575.8	6.48	3420.3	3179.4
6.69	3631.7	6.82	2578.4	6.56	3423.9	3180.7
6.77	3639.6	6.9	2581	6.64	3426.9	3182.1
6.86	3642.1	6.98	2580.9	6.73	3429.7	3183.5
6.93	3647.4	7.06	2586.1	6.81	3432.2	3184.9
7.01	3652.6	7.13	2586.1	6.89	3434.6	3186.4
7.09	3657.8	7.21	2588.7	6.97	3436.9	3187.8
7.2	3663	7.26	2591.3	7.05	3439.4	3189.3
7.27	3670.9	7.29	2593.9	7.14	3441.9	3190.7
7.34	3678.8	7.38	2596.5	7.22	3444.5	3192.1
7.42	3684.1	7.46	2599.1	7.30	3447.3	3193.5
7.5	3694.6	7.55	2599	7.38	3450.1	3195
7.59	3705.1	7.65	2598.9	7.47	3452.9	3196.4
7.67	3718.3	7.73	2604.2	7.55	3455.8	3197.8
7.75	3728.9	7.81	2604.1	7.63	3458.9	3199.2
7.84	3747.4	7.89	2609.3	7.71	3461.7	3200.6
7.93	3763.2	7.97	2611.9	7.79	3464.6	3202
8.02	3787	8.05	2614.5	7.88	3467.6	3203.3
8.1	3802.9	8.11	2614.4	7.96	3470.6	3204.7
8.18	3821.4	8.2	2619.7	8.04	3473.7	3206.1
8.27	3834.6	8.3	2622.2	8.12	3476.9	3207.4
8.33	3845.1	8.37	2624.8	8.21	3480.1	3208.7
8.42	3850.3	8.45	2627.4	8.29	3483.4	3210
8.51	3855.5	8.56	2635.2	8.37	3486.7	3211.3
8.59	3863.4	8.64	2635.2	8.45	3489.9	3212.7
8.66	3868.7	8.72	2640.4	8.53	3493.1	3214
8.75	3873.9	8.8	2643	8.62	3496.2	3215.4
8.83	3876.5	8.88	2648.2	8.70	3499.3	3216.8
8.91	3881.7	8.97	2650.8	8.78	3502.4	3218.2
8.99	3886.9	9.05	2650.7	8.86	3505.7	3219.5
9.06	3894.8	9.13	2656	8.95	3508.6	3220.9
9.14	3897.4	9.2	2661.2	9.03	3511.5	3222.3
9.23	3902.6	9.27	2663.8	9.11	3514.3	3223.7
9.31	3905.2	9.36	2666.4	9.19	3517.2	3225.1
9.4	3910.4	9.46	2668.9	9.27	3520	3226.5
9.48	3918.3	9.54	2674.1	9.36	3522.8	3227.9
9.56	3923.5	9.62	2676.7	9.44	3525.6	3229.3
9.65	3928.7	9.7	2679.3	9.52	3528.4	3230.7
9.73	3936.6	9.78	2681.9	9.60	3531.2	3232
9.82	3939.2	9.86	2687.1	9.68	3534	3233.4
9.9	3944.4	9.95	2689.7	9.77	3536.8	3234.9
9.93	3949.7			9.85	3539.6	3236.3
				9.93	3542.4	3237.8
				10.00	3544.6	3239

CELL PRESSURES - WELL A



CELL PRESSURES - WELL B



```

/          SIMULATOR INPUT DATA
/  Problem 62
/  Run 1
/
/  SINGLE VALUE DATA
/
IMAX  7      /Number of grid blocks in X-direction
JMAX  7      /Number of grid blocks in Y-direction

PREF  4000   /Reference Pressure, psia
CROC  3.5E-6 /Formation Compressibility, psi-1
CWAT  2.0E-6 /Water Compressibility, psi-1
COIL  26.9E-6 /Oil Compressibility, psi-1
CRVO  62.162E-6 / Slope of undersaturated oil viscosity curve, cp/psi
VISW  0.3355 /Water viscosity, cp

DENO  .312 /Oil Density, psi/ft
DENG  .000368 /Gas Density, psi/ft
DENW  .433 /Water Density, psi/ft

METH 1      / D-4 solution method
STONE      /Method for 3-phase Kr calculation
END
/
/  TABULAR DATA
/
KRW
/  Sw    Krw    Krow  Pcow
    0.0   0.0    1.00  0.0
    0.10  0.0    0.98  0.0
    0.20  0.0    0.94  0.0
    0.30  0.01  0.86  0.0
    0.40  0.045 0.37  0.0      /Water-Oil Kr table
    0.50  0.08  0.05  0.0
    0.60  0.115 0.01  0.0
    0.70  0.15  0.0   0.0
    0.80  0.29  0.0   0.0
    0.90  0.57  0.0   0.0
    1.0   1.0   0.0   0.0

KRG
/  Sg    Krg    Krog  Pcog
    0.0   0.0    1.0   0.0
    0.5   0.0    1.0   0.0      /Gas-Oil Kr table
    0.9   0.0    1.0   0.0
    1.00  1.0   0.0   0.0

```

```

PRES
/   P   Bo   Bg   Vo   Vg   Rs
/   psi rb/stb rcf/scf cp   cp   scf/stb
      500  1.19 .04  0.75 .0118 350
      1000 1.25 .015 0.56 .0132 475
      2000 1.41 .007 0.38 .0168 850      /PVT table
      3000 1.61 .005 0.27 .0215 1250
      3500 1.77 .004 0.25 .024  1575
END
/
/   GRID DATA
/
DX 7*600      /Reference depth for top of grid blocks
DY 7*600
/           H   Por   Perm  Elev
GRID  0 0 0   30   0.25  50   -5000      /Thickness, porosity, perm, & elev.
PO     0 0 0   4000      /Initial reservoir pressure
PSAT  0 0 0.3500      /Bubble point pressure
SW     0 0 0.3      /Initial water saturation
SG     0 0 0   0.0      /Initial gas saturation
END
/
/   SCHEDULE DATA
/
NAME 1      I = 2, J = 4, K =1 PI = 3.375      /Well location and productivity index
QO 1        150.0      /Initial production rate
PLIM 1      100.0      /BHP constraint
NAME 2      I = 6, J = 4, K =1 PI = 3.375
QO 2        150.0
PLIM 2      100.0
WLRT 1      PSRT 1
DELT        30      /Timestep increment
DTMAX       30
TIME        1825
QW 2        -400.0      /Well status changed to water injection
PLIM 2      20000
TIME        3650
END

```

Problem No. 62

History Match Run 1 - Output

REGION	NUMBER OF GRIDS ACTIVE	INACTIVE	*****	INITIAL FLUID IN PLACE			*****	PORE	AVERAGE SATURATIONS									
			OIL (MMSTB)	GAS (MMMSCF)	WATER (MMSTB)	SOLVENT (MMMSCF)	VOLUME (MMRCF)	OIL (FRC)	GAS (FRC)	WATER (FRC)	SOLVENT (FRC)							
TOTAL	49	0	9.44359	14.8747	7.12491	.000000	132.300	.700	.000	.300	.000							
STEP	TIME DAYS	DELT DAYS	PAVG PSI	FIELD OIL B/D	PRODUCTION GAS MCF/D	WATER B/D	FIELD GAS MCF/D	INJECTION WATER B/D	MATERIAL OIL FRC	BALANCE GAS FRC	ERROR WATER FRC	MAXIMUM SATURATION ERROR	I	J	K	NWT	SOR	CUT
TS 1	30	30.00	3970	300	473	5	0	0	-.1E-05	-.1E-05	-.9E-07	.000	2	4	1	1	1	0
TS 2	60	30.00	3941	300	473	5	0	0	-.1E-05	-.1E-05	.3E-06	.000	6	4	1	1	1	0
TS 3	90	30.00	3911	300	473	5	0	0	-.1E-05	-.8E-06	-.2E-07	.000	2	4	1	1	1	0
TS 4	120	30.00	3881	300	473	5	0	0	-.1E-05	-.1E-05	.2E-06	.000	2	4	1	1	1	0
TS 5	150	30.00	3852	300	473	5	0	0	-.9E-06	-.1E-05	-.4E-07	.000	2	4	1	1	1	0
TS 6	180	30.00	3822	300	473	5	0	0	-.1E-05	-.1E-05	-.2E-06	.000	2	4	1	1	1	0
TS 7	210	30.00	3792	300	472	5	0	0	-.9E-06	-.9E-06	-.7E-07	.000	2	4	1	1	1	0
TS 8	240	30.00	3762	300	473	5	0	0	-.7E-06	-.1E-05	-.8E-07	.000	2	4	1	1	1	0
TS 9	270	30.00	3733	300	473	5	0	0	-.1E-05	-.1E-05	.7E-08	.000	2	4	1	1	1	0
TS 10	300	30.00	3703	300	473	5	0	0	-.1E-05	-.1E-05	-.6E-08	.000	2	4	1	1	1	0
TS 11	330	30.00	3673	300	472	5	0	0	-.1E-05	-.7E-06	-.1E-06	.000	6	4	1	1	1	0
TS 12	360	30.00	3643	300	473	5	0	0	-.5E-06	-.1E-05	-.3E-07	.000	2	4	1	1	1	0
TS 13	390	30.00	3613	300	472	5	0	0	-.8E-06	-.7E-06	-.1E-06	.000	6	4	1	1	1	0
TS 14	420	30.00	3584	300	472	5	0	0	-.7E-06	-.1E-05	-.6E-07	.000	6	4	1	1	1	0
TS 15	450	30.00	3554	300	472	5	0	0	-.7E-06	-.9E-06	.7E-06	.000	2	4	1	1	1	0
TS 16	480	30.00	3524	300	473	5	0	0	-.8E-06	-.1E-05	.2E-07	.000	6	4	1	1	1	0
TS 17	510	30.00	3494	300	468	5	0	0	.3E-03	.3E-03	-.1E-06	-.001	2	4	1	1	1	0
TS 18	540	30.00	3487	300	467	5	0	0	.7E-05	.6E-05	-.2E-06	.000	6	4	1	1	1	0
TS 19	570	30.00	3476	300	465	5	0	0	.1E-04	.1E-04	.2E-08	.000	6	4	1	1	1	0
TS 20	600	30.00	3466	300	463	5	0	0	.1E-04	.1E-04	.2E-06	.000	6	4	1	1	1	0
TS 21	630	30.00	3455	300	461	5	0	0	.1E-04	.1E-04	-.1E-06	.000	6	4	1	1	1	0
TS 22	660	30.00	3446	300	459	5	0	0	.1E-04	.1E-04	-.1E-06	.000	2	4	1	1	1	0
TS 23	690	30.00	3436	300	457	5	0	0	.1E-04	.1E-04	-.8E-08	.000	2	4	1	1	1	0
TS 24	720	30.00	3426	300	455	5	0	0	.1E-04	.1E-04	-.1E-07	.000	6	4	1	1	1	0
TS 25	750	30.00	3417	300	453	5	0	0	.1E-04	.1E-04	.2E-06	.000	2	4	1	1	1	0
TS 26	780	30.00	3408	300	452	5	0	0	.1E-04	.1E-04	-.1E-06	.000	2	4	1	1	1	0
TS 27	810	30.00	3399	300	450	5	0	0	.1E-04	.1E-04	-.1E-06	.000	2	4	1	1	1	0
TS 28	840	30.00	3390	300	448	5	0	0	.1E-04	.9E-05	-.1E-06	.000	2	4	1	1	1	0
TS 29	870	30.00	3382	300	446	5	0	0	.9E-05	.9E-05	.2E-06	.000	2	4	1	1	1	0
TS 30	900	30.00	3373	300	445	5	0	0	.9E-05	.9E-05	.2E-06	.000	6	4	1	1	1	0
TS 31	930	30.00	3365	300	443	5	0	0	.9E-05	.9E-05	.2E-06	.000	2	4	1	1	1	0
TS 32	960	30.00	3357	300	442	5	0	0	.9E-05	.8E-05	-.2E-07	.000	6	4	1	1	1	0
TS 33	990	30.00	3349	300	440	5	0	0	.9E-05	.8E-05	-.2E-06	.000	2	4	1	1	1	0
TS 34	1020	30.00	3341	300	439	5	0	0	.8E-05	.8E-05	.3E-06	.000	6	4	1	1	1	0
TS 35	1050	30.00	3334	300	437	5	0	0	.8E-05	.8E-05	-.1E-06	.000	6	4	1	1	1	0
TS 36	1080	30.00	3326	300	436	5	0	0	.9E-05	.7E-05	-.1E-07	.000	2	4	1	1	1	0
TS 37	1110	30.00	3319	300	434	5	0	0	.8E-05	.7E-05	-.1E-07	.000	2	4	1	1	1	0
TS 38	1140	30.00	3311	300	433	5	0	0	.8E-05	.7E-05	.9E-07	.000	2	4	1	1	1	0
TS 39	1170	30.00	3304	300	431	5	0	0	.7E-05	.7E-05	-.1E-06	.000	2	4	1	1	1	0
TS 40	1200	30.00	3297	300	430	5	0	0	.7E-05	.7E-05	-.1E-07	.000	6	4	1	1	1	0
TS 41	1230	30.00	3290	300	429	5	0	0	.7E-05	.7E-05	-.1E-07	.000	6	4	1	1	1	0
TS 42	1260	30.00	3283	300	427	5	0	0	.7E-05	.6E-05	-.2E-06	.000	6	4	1	1	1	0
TS 43	1290	30.00	3276	300	426	5	0	0	.7E-05	.6E-05	-.7E-08	.000	2	4	1	1	1	0
TS 44	1320	30.00	3269	300	425	5	0	0	.7E-05	.6E-05	.2E-06	.000	2	4	1	1	1	0
TS 45	1350	30.00	3263	300	423	5	0	0	.7E-05	.6E-05	-.1E-06	.000	2	4	1	1	1	0
TS 46	1380	30.00	3256	300	422	5	0	0	.6E-05	.6E-05	-.2E-06	.000	6	4	1	1	1	0
TS 47	1410	30.00	3250	300	421	5	0	0	.6E-05	.6E-05	.2E-06	.000	2	4	1	1	1	0
TS 48	1440	30.00	3243	300	419	5	0	0	.6E-05	.6E-05	.1E-08	.000	2	4	1	1	1	0
TS 49	1470	30.00	3237	300	418	5	0	0	.6E-05	.6E-05	-.3E-06	.000	2	4	1	1	1	0
TS 50	1500	30.00	3231	300	417	5	0	0	.6E-05	.5E-05	.2E-06	.000	2	4	1	1	1	0
TS 51	1530	30.00	3225	300	416	5	0	0	.6E-05	.5E-05	.1E-06	.000	2	4	1	1	1	0
TS 52	1560	30.00	3219	300	415	5	0	0	.6E-05	.6E-05	.2E-06	.000	6	4	1	1	1	0
TS 53	1590	30.00	3213	300	414	5	0	0	.6E-05	.5E-05	.1E-07	.000	2	4	1	1	1	0
TS 54	1620	30.00	3207	300	412	5	0	0	.6E-05	.5E-05	-.2E-06	.000	6	4	1	1	1	0
TS 55	1650	30.00	3201	300	411	5	0	0	.6E-05	.5E-05	.1E-06	.000	2	4	1	1	1	0
TS 56	1680	30.00	3195	300	410	5	0	0	.5E-05	.5E-05	.2E-07	.000	6	4	1	1	1	0
TS 57	1710	30.00	3189	300	409	5	0	0	.5E-05	.5E-05	.1E-06	.000	6	4	1	1	1	0
TS 58	1740	30.00	3184	300	408	5	0	0	.6E-05	.5E-05	.2E-07	.000	2	4	1	1	1	0
TS 59	1770	30.00	3178	300	407	5	0	0	.6E-05	.5E-05	-.2E-06	.000	6	4	1	1	1	0
TS 60	1798	27.50	3173	300	406	5	0	0	.5E-05	.4E-05	-.1E-06	.000	2	4	1	1	1	0

TIMESTEP 61 AT 1825.0 DAYS

REGION	**** CURRENT FLUID IN PLACE ****			PORE VOLUME	AVERAGE SATURATIONS			PORE VOLUME
	OIL (MMSTB)	GAS (BSCF)	WATER (MMSTB)	(MMRCF)	OIL (FRC)	GAS (FRC)	WATER (FRC)	AVERAGED PRESSURE
TOTAL	8.89613	14.0652	7.11621	131.915	.630	.069	.301	3167.9

NAME	I	J	K	STAT	PI	PWF (PSI)	* * * WELL RATES * * *			GOR (SCF/B)	WCT (PCT)	CUMULATIVE PRODUCTION			SATURATIONS		
							OIL (B/D)	GAS (MCF/D)	WATER (B/D)			OIL MB	GAS MMCF	WATER MB	SO (FRC)	SG (PORVOL)	SW (PORVOL)
1	2	4	1	QO	3.4	3130.0	150.0	202.4	2.4	1349.3	1.6	274	405	4	.62	.08	.30
2	6	4	1	QO	3.4	3130.0	150.0	202.4	2.4	1349.3	1.6	274	405	4	.62	.08	.30
FIELD TOTALS - PRODUCED:							300.0	404.8	4.8	1349.3	1.6	547	810	9			
INJECTED:							.0	.0	.0			0	0	0			

CONTROL	WELLS	NUMBER OF WELLS	...
QO	2	2	2

I=	PRESSURE (PSI)							TIME= 1825.00
	1	2	3	4	5	6	7	
1	3171.37	3171.44	3171.82	3172.03	3171.82	3171.44	3171.37	
2	3169.47	3169.29	3170.17	3170.63	3170.17	3169.29	3169.47	
3	3165.90	3164.24	3167.10	3168.30	3167.10	3164.24	3165.90	
J 4	3162.15	3152.77	3163.85	3166.54	3163.85	3152.77	3162.15	
5	3165.90	3164.24	3167.10	3168.30	3167.10	3164.24	3165.90	
6	3169.47	3169.29	3170.17	3170.63	3170.17	3169.29	3169.47	
7	3171.37	3171.44	3171.82	3172.03	3171.82	3171.44	3171.37	

STEP	TIME DAYS	DELT DAYS	PAVG PSI	FIELD PRODUCTION			FIELD INJECTION		MATERIAL BALANCE ERROR			MAXIMUM SATURATION ERROR				NWT	SOR	CUT
				OIL B/D	GAS MCF/D	WATER B/D	GAS MCF/D	WATER B/D	OIL FRC	GAS FRC	WATER FRC	I	J	K				
TS 61	1825	27.50	3168	300	405	5	0	0	.5E-05	.4E-05	.1E-06	.000	2	4	1	1	1	0
TS 62	1855	30.00	3170	150	202	2	0	-400	.1E-04	.1E-04	.4E-07	.000	6	4	1	1	1	0
TS 63	1885	30.00	3171	150	202	2	0	-400	.4E-05	.3E-05	.5E-07	.000	6	4	1	1	1	0
TS 64	1915	30.00	3173	150	202	2	0	-400	.2E-05	.1E-05	-.1E-06	.000	6	4	1	1	1	0
TS 65	1945	30.00	3175	150	202	2	0	-400	.1E-05	.1E-05	.1E-06	.000	6	4	1	1	1	0
TS 66	1975	30.00	3176	150	202	2	0	-400	.1E-05	.1E-05	.4E-07	.000	6	4	1	1	1	0
TS 67	2005	30.00	3178	150	202	2	0	-400	.1E-05	.1E-05	.4E-07	.000	6	4	1	1	1	0
TS 68	2035	30.00	3180	150	202	2	0	-400	.1E-05	.1E-05	.4E-07	.000	6	4	1	1	1	0
TS 69	2065	30.00	3182	150	202	2	0	-400	.4E-07	.2E-06	.3E-05	.000	6	4	1	1	1	0
TS 70	2095	30.00	3183	150	202	2	0	-400	.2E-06	.1E-06	.5E-05	.000	6	4	1	1	1	0
TS 71	2125	30.00	3185	150	203	2	0	-400	-.2E-06	.4E-06	.8E-05	.000	6	4	1	1	1	0
TS 72	2155	30.00	3187	150	203	2	0	-400	.3E-06	.1E-06	.2E-05	.000	6	4	1	1	1	0
TS 73	2185	30.00	3189	150	203	2	0	-400	.3E-06	.4E-06	.6E-06	.000	6	4	1	1	1	0
TS 74	2215	30.00	3191	150	203	2	0	-400	.6E-06	.4E-06	.3E-06	.000	6	4	1	1	1	0
TS 75	2245	30.00	3192	150	203	2	0	-400	.5E-07	.2E-06	.1E-06	.000	2	4	1	1	1	0
TS 76	2275	30.00	3194	150	203	2	0	-400	.5E-06	.4E-06	.3E-06	.000	2	4	1	1	1	0
TS 77	2305	30.00	3196	150	203	2	0	-400	.5E-06	.5E-07	.2E-06	.000	2	4	1	1	1	0
TS 78	2335	30.00	3198	150	204	2	0	-400	.2E-06	.7E-07	.1E-06	.000	2	4	1	1	1	0
TS 79	2365	30.00	3199	150	204	2	0	-400	.4E-06	.9E-07	.5E-07	.000	2	4	1	1	1	0
TS 80	2395	30.00	3201	150	204	2	0	-400	.4E-06	.5E-06	.1E-06	.000	2	4	1	1	1	0
TS 81	2425	30.00	3203	150	204	2	0	-400	.6E-06	.3E-06	.2E-06	.000	2	4	1	1	1	0
TS 82	2455	30.00	3205	150	204	2	0	-400	.3E-06	.4E-06	.5E-07	.000	2	4	1	1	1	0
TS 83	2485	30.00	3206	150	204	2	0	-400	.4E-06	.5E-06	.1E-06	.000	2	4	1	1	1	0
TS 84	2515	30.00	3208	150	205	2	0	-400	.3E-06	.3E-06	-.2E-06	.000	2	4	1	1	1	0
TS 85	2545	30.00	3210	150	205	2	0	-400	.6E-06	.7E-07	.1E-06	.000	2	4	1	1	1	0
TS 86	2575	30.00	3212	150	205	2	0	-400	.3E-06	.5E-06	.4E-07	.000	2	4	1	1	1	0
TS 87	2605	30.00	3213	150	205	2	0	-400	.3E-06	.6E-06	-.6E-07	.000	2	4	1	1	1	0
TS 88	2635	30.00	3215	150	205	2	0	-400	.3E-06	.3E-06	-.2E-06	.000	2	4	1	1	1	0
TS 89	2665	30.00	3217	150	205	2	0	-400	.3E-06	.5E-06	.1E-06	.000	2	4	1	1	1	0
TS 90	2695	30.00	3219	150	206	2	0	-400	.6E-06	.2E-06	-.2E-06	.000	2	4	1	1	1	0
TS 91	2725	30.00	3221	150	206	2	0	-400	.5E-06	.5E-06	.2E-06	.000	2	4	1	1	1	0
TS 92	2755	30.00	3222	150	206	2	0	-400	.3E-06	.2E-06	.4E-07	.000	2	4	1	1	1	0
TS 93	2785	30.00	3224	150	206	2	0	-400	.3E-06	.6E-06	.1E-06	.000	2	4	1	1	1	0
TS 94	2815	30.00	3226	150	206	2	0	-400	.5E-06	.3E-06	-.6E-07	.000	2	4	1	1	1	0
TS 95	2845	30.00	3228	150	206	2	0	-400	.3E-06	.3E-06	.4E-07	.000	2	4	1	1	1	0
TS 96	2875	30.00	3230	150	207	2	0	-400	.3E-06	.6E-06	.1E-06	.000	2	4	1	1	1	0
TS 97	2905	30.00	3231	150	207	2	0	-400	.5E-06	.4E-06	-.2E-06	.000	2	4	1	1	1	0
TS 98	2935	30.00	3233	150	207	2	0	-400	.4E-06	.4E-06	.4E-06	.000	2	4	1	1	1	0
TS 99	2965	30.00	3235	150	207	2	0	-400	.4E-06	.3E-06	-.2E-06	.000	2	4	1	1	1	0
TS 100	2995	30.00	3237	150	207	2	0	-400	.1E-06	.3E-06	.2E-06	.000	2	4	1	1	1	0
TS 101	3025	30.00	3239	150	207	2	0	-400	.4E-06	.4E-06	-.2E-06	.000	2	4	1	1	1	0
TS 102	3055	30.00	3241	150	208	2	0	-400	.6E-06	.8E-06	-.6E-07	.000	2	4	1	1	1	0
TS 103	3085	30.00	3243	150	208	2	0	-400	.3E-06	.4E-06	.1E-06	.000	2	4	1	1	1	0
TS 104	3115	30.00	3244	150	208	2	0	-400	.4E-06	.3E-06	.4E-07	.000	2	4	1	1	1	0
TS 105	3145	30.00	3246	150	208	2	0	-400	.3E-06	.4E-06	.5E-06	.000	2	4	1	1	1	0
TS 106	3175	30.00	3248	150	208	2	0	-400	.6E-06	.2E-06	.1E-06	.000	2	4	1	1	1	0
TS 107	3205	30.00	3250	150	208	2	0	-400	.4E-06	.2E-06	.5E-06	.000	2	4	1	1	1	0
TS 108	3235	30.00	3252	150	209	2	0	-400	.2E-06	.2E-06	.5E-06	.000	2	4	1	1	1	0
TS 109	3265	30.00	3254	150	209	2	0	-400	.3E-06	.3E-06	.5E-06	.000	2	4	1	1	1	0
TS 110	3295	30.00	3256	150	209	2	0	-400	.3E-06	.2E-06	.6E-06	.000	2	4	1	1	1	0
TS 111	3325	30.00	3258	150	209	2	0	-400	.2E-06	.5E-06	.6E-06	.000	2	4	1	1	1	0

TS 112	3355	30.00	3260	150	209	2	0	-400	-.1E-06	.2E-06	.8E-06	.000	2	4	1	1	1	0
TS 113	3385	30.00	3262	150	209	2	0	-400	.3E-06	.2E-06	.8E-06	.000	2	4	1	1	1	0
TS 114	3415	30.00	3264	150	209	2	0	-400	.2E-06	.2E-06	.4E-06	.000	2	4	1	1	1	0
TS 115	3445	30.00	3266	150	210	2	0	-400	.2E-06	.3E-06	.5E-06	.000	2	4	1	1	1	0
TS 116	3475	30.00	3268	150	210	2	0	-400	.2E-06	.1E-06	.2E-06	.000	2	4	1	1	1	0
TS 117	3505	30.00	3270	150	210	2	0	-400	.4E-07	.9E-07	.6E-06	.000	2	4	1	1	1	0
TS 118	3535	30.00	3272	150	210	2	0	-400	.3E-06	.6E-06	.3E-06	.000	2	4	1	1	1	0
TS 119	3565	30.00	3274	150	210	2	0	-400	.3E-06	.3E-06	.2E-06	.000	2	4	1	1	1	0
TS 120	3595	30.00	3276	150	211	2	0	-400	-.3E-07	.4E-06	.4E-06	.000	2	4	1	1	1	0
TS 121	3623	27.50	3278	150	211	2	0	-400	.7E-07	.5E-06	.2E-06	.000	2	4	1	1	1	0

TIMESTEP 122 AT 3650.0 DAYS

REGION	**** CURRENT FLUID IN PLACE ****			PORE VOLUME (MMRCF)	AVERAGE SATURATIONS			PORE VOLUME AVERAGED PRESSURE
	OIL (MMSTB)	GAS (BSCF)	WATER (MMSTB)		OIL (FRC)	GAS (FRC)	WATER (FRC)	
TOTAL	8.62240	13.6893	7.84180	131.966	.623	.046	.331	3279.5

NAME	I	J	K	STAT	PI	PWF (PSI)	* * * WELL RATES * * *			GOR (SCF/B)	WCT (PCT)	CUMULATIVE PRODUCTION			SATURATIONS		
							OIL (B/D)	GAS (MCF/D)	WATER (B/D)			OIL MB	GAS MMCF	WATER MB	SO (FRC)	SG (PORVOL)	SW
1	2	4	1	QO	3.4	3217.1	150.0	210.9	2.4	1405.9	1.6	548	781	9	.64	.06	.30
2	6	4	1	QWI	3.4	3520.3	.0	.0	-400.0	.0	.0	274	405	-726	.31	.03	.66
FIELD TOTALS - PRODUCED:							150.0	210.9	2.4	1405.9	1.6	821	1185	13			
INJECTED:							.0	.0	-400.0			0	0	-730			

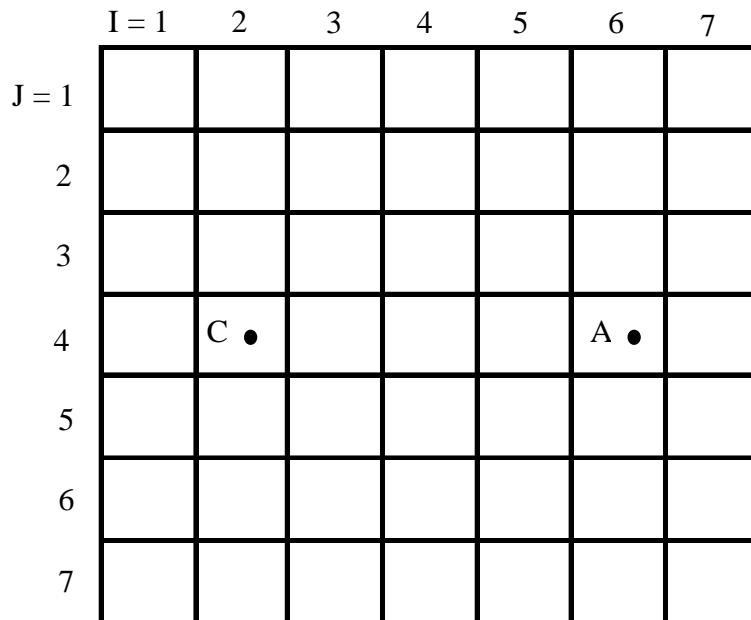
CONTROL	WELLS	NUMBER OF WELLS	...	2
---	---	NUMBER OF NODES	...	2
QO	1			
QWI	1			

I=	PRESSURE (PSI)							TIME= 3650.00
	1	2	3	4	5	6	7	
1	3255.99	3258.37	3263.29	3269.98	3277.48	3284.36	3288.60	
2	3254.16	3256.37	3262.05	3269.69	3278.65	3287.94	3293.39	
3	3250.65	3251.44	3259.37	3268.63	3281.93	3338.40	3306.47	
J 4	3246.88	3239.89	3255.92	3267.37	3327.44	3480.76	3362.86	
5	3250.65	3251.44	3259.37	3268.63	3281.93	3338.40	3306.47	
6	3254.16	3256.37	3262.05	3269.69	3278.65	3287.94	3293.39	
7	3255.99	3258.37	3263.29	3269.98	3277.49	3284.36	3288.60	

STEP	TIME DAYS	DELT DAYS	PAVG PSI	FIELD PRODUCTION			FIELD INJECTION		MATERIAL BALANCE ERROR			MAXIMUM SATURATION ERROR			I	J	K	NWT	SOR	CUT
				OIL B/D	GAS MCF/D	WATER B/D	GAS MCF/D	WATER B/D	OIL FRC	GAS FRC	WATER FRC	ERROR								
TS 122	3650	27.50	3280	150	211	2	0	-400	.4E-06	.6E-06	.2E-06	.000	2	4	1	1	1	1	0	

NORMAL END OF RUN

RESERVOIR SIMULATION
 CLASS PROBLEM NO. 63 (SYNTHETIC HISTORY MATCHING)



Attached is the pressure versus time history of well C, which produced oil at constant rate from the above reservoir. Well A displayed the same behavior. The reservoir is 2-D, homogeneous, and isotropic.

The pressure versus time plot for history match # 1 is also given.

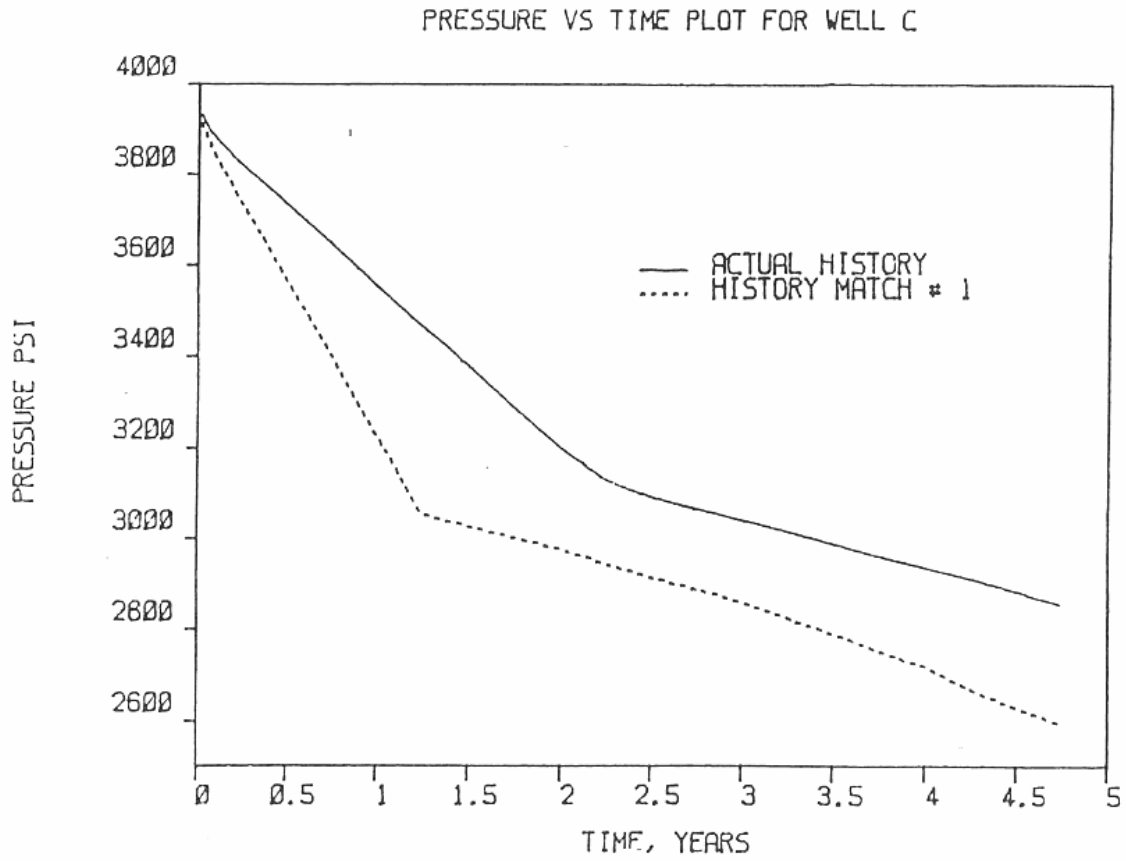
Analyze the pressure histories and recommend data changes.


```

CMNT
END      END OF EMPIRICAL DATA
CMNT
CMNT      GRID DATA
CMNT
DIS      C      -1
PHI      C      0.18
KXY      C      10
H        C      30
ZTB      C      -5000
POI      C      4000
SOI      C      0.70
SGI      C      0.00
DX       C      600
DY       C      600
BPT      C      3200
END      END OF GRID DATA
CMNT
CMNT      SCHEDULE DATA
NAME     2  4  COSAN      100
NAME     6  4  AYAN      100
RATE     COSAN      150
RATE     AYAN      150
PRESS    0
SATO     0
SATG     0
SATW     0
TAPE     0
WELREP   2
OUTPUT   2
TIME     10
TIME     30
TIME     90
TIME     180
TIME     270
TIME     365
TIME     1  90
TIME     1  100
TIME     1  110
TIME     1  120
TIME     1  130
TIME     1  140
TIME     1  150
TIME     1  160
TIME     1  170
TIME     1  180
TIME     1  270
TIME     1  365
TIME     2  60
TIME     2  70
TIME     2  80
TIME     2  90
TIME     2  100
TIME     2  110
TIME     2  120
TIME     2  130
TIME     2  140
TIME     2  150
TIME     2  160
TIME     2  170
TIME     2  180

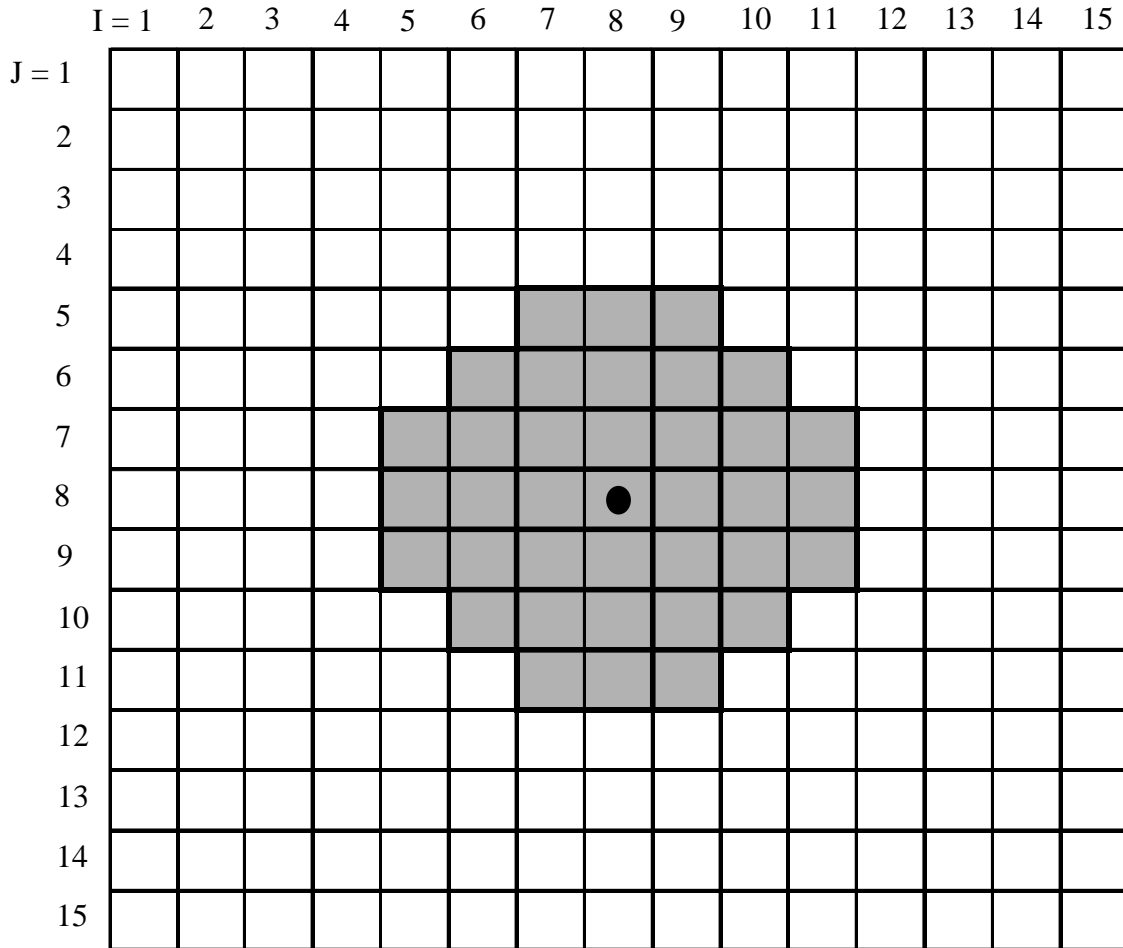
```

TIME	2	270
TIME	2	365
TIME	3	90
TIME	3	180
TIME	3	270
TIME	3	365
TIME	4	90
TIME	4	180
TIME	4	270
TIME	4	365
END	END OF SCHEDULE DATA	



Pressure vs time plot for Well C

RESERVOIR SIMULATION
 CLASS PROBLEM NO. 65 (SYNTHETIC HISTORY MATCHING)



Well GE-209, located in the center of the reservoir's oil zone (shown above), has been producing at a constant rate for 1.5 years. The reservoir is homogeneous, isotropic, and effectively 2-D.

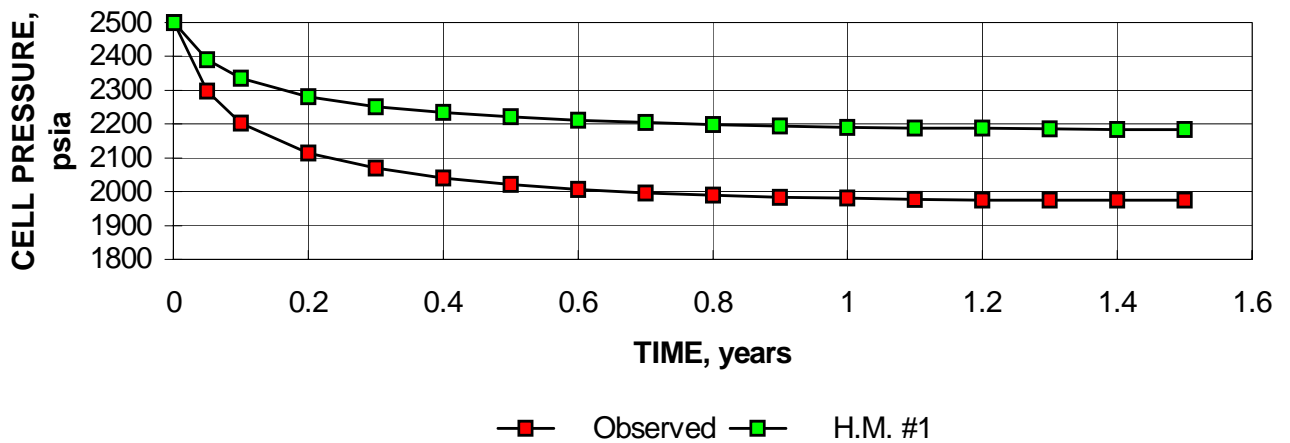
Observed pressure data, as well as the results of history match run #1, are attached.

PROBLEM NO. 65

Gridblock Pressure (psia)

TIME,yrs	H.M. #1	Observed
0.001	2500	2500
0.05	2391	2298
0.1	2335	2202
0.2	2280	2114
0.3	2252	2069
0.4	2234	2041
0.5	2221	2021
0.6	2212	2007
0.7	2204	1997
0.8	2199	1990
0.9	2194	1984
1.0	2191	1981
1.1	2189	1978
1.2	2187	1976
1.3	2185	1975
1.4	2184	1975
1.5	2183	1974

PROBLEM 65 - SYNTHETIC HISTORY MATCHING



```

/          SIMULATOR INPUT DATA
/   Problem 65
/   Run 1
/   SINGLE VALUE DATA
/
IMAX  15   /number of grids in X-direction
JMAX  15   /number of grids in Y-direction

PREF      2500          /reference pressure, psia
CROC      3.0E-6       /rock compressibility, psi-1
CWAT      3.3E-6       /water compressibility, psi-1
COIL      16.95E-6     /oil compressibility, psi-1
CRVO      62.162E-6   / slope of undersaturated oil viscosity curve, cp/psi
VISW      0.4          /water viscosity, cp

METH 1 / D-4 solution method      /matrix solution method
STONE                                       /method for 3-phase Kr calculation
END
/
/   TABULAR DATA
/
KRW
/   Sw   Krw   Krow   Pcow
      0.0   0.0   1.00   0.0
      0.10  0.0   1.00   0.0
      0.24  0.0   1.00   0.0
      0.40  0.07  0.19   0.0          /water-oil Kr table
      0.50  0.13  0.10   0.0
      0.60  0.19  0.02   0.0
      0.76  0.254 0.0    0.0
      0.80  0.27  0.0    0.0
      1.0   1.0   0.0    0.0

KRG
/   Sg   Krg   Krog   Pcog
      0.0   0.0   1.0    0.0
      1.0   1.0   0.0    0.0          /gas-oil Kr table

PRES
/   P     Bo           Bg           Vo     Vg     Rs
/   (psi) (rb/stb)(rcf/scf) (cp) (cp) (scf/stb)
      100  1.13           0.17          17.0  0.02  150
      1000 1.21           0.017         17.0  0.0   350
      4000 1.15           0.004         17.0  0.10  350          /PVT table

END
/
/   GRID DATA

```

```

/
DX 12800 6400 3200 1600 800 400 400 400 400 400 800 1600 3200 6400 9000
DY 12800 6400 3200 1600 800 400 400 400 400 400 800 1600 3200 6400 9000

```

```

/
GRID      0 0 0   H   Por   Perm   Elev      /thickness, porosity, perm, & elev.
PO        0 0 1   2500      /initial reservoir pressure, psia
PSAT      0 0 0   1000      /bubble point pressure, psia
SW        0 0 0   1.0      /initial water saturation
SG        0 0 0   0.0      /initial gas saturation

```

```

/.....Input Sw in the oil region
/

```

```

WINDOW I = 7 TO 9, J = 5 TO 5, K = 1 TO 1
SW 0 0 0 0.24
WINDOW I = 6 TO 10, J = 6 TO 6, K = 1 TO 1
SW 0 0 0 0.24
WINDOW I = 5 TO 11, J = 7 TO 9, K = 1 TO 1      /set initial water saturations in oil block
SW 0 0 0 0.24
WINDOW I = 6 TO 10, J = 10 TO 10, K = 1 TO 1
SW 0 0 0 0.24
WINDOW I = 7 TO 9, J = 11 TO 11, K = 1 TO 1
SW 0 0 0 0.24
END

```

```

/
/ SCHEDULE DATA
/

```

```

NAME 1    I = 8   J = 8   K = 1   PI = 3.375   /well location and productivity index
QO 1      100.0      /initial production rate
PLIM 1    1000.0     /BHP constraint

```

```

WLRT 1 PSRT 1
DSTAR    0.05
DSLIM    0.05

```

```

OMEGA    1.1
DELT     10
DTMAX    10
TIME 18.2625 / .05 years
TIME 36.525  / .10 years
TIME 73.05   / .20 years
TIME 109.575 / .30 years
TIME 146.1   / .40 years
TIME 182.625 / .50 years
TIME 219.15  / .60 years
TIME 255.675 / .70 years

```

TIME 292.2 / .80 years
TIME 328.725 / .90 years
TIME 365.25 / 1.00 years
TIME 401.775 / 1.10 years
TIME 438.3 / 1.20 years
TIME 474.825 / 1.30 years
TIME 511.35 / 1.40 years
TIME 547.875 / 1.50 years

Problem No. 65

History Match Run 1 - Output

TABLE OF PRESSURE-RELATED VARIABLES

PRESSURE (PSIA)	BO (RB/STB)	BG (RCF/SCF)	OIL VISC (CP)	GAS VISC (CP)	RS (SCF/STB)
100.0	1.130	.1700	17.000	.020	150.0
1000.0	1.210	.0170	17.000	.060	350.0
4000.0	1.150	.0040	17.000	.100	350.0

OIL RELATIVE PERMEABILITIES (STONE)

KRO = (KRW+KROW) (KRG+KROG) - KRW - KRG

USING FIRST WATER AND GAS RELATIVE PERMEABILITY TABLES

KRO	: .000	.100	.240	.400	.500	.600	.760	.800	1.000
.000	: 1.000	1.000	1.000	.190	.100	.020	.000	.000	.000
SG1.000	: .000								

GAS/OIL RELATIVE PERMEABILITY TABLE NO. 1

SG	KRG	KROG	PCOG
.000	.0000	1.0000	.000
1.000	1.0000	.0000	.000

WATER/OIL RELATIVE PERMEABILITY TABLE NO. 1

SW	KRW	KROW	PCOW
.000	.0000	1.0000	.000
.100	.0000	1.0000	.000
.240	.0000	1.0000	.000
.400	.0700	.1900	.000
.500	.1300	.1000	.000
.600	.1900	.0200	.000
.760	.2540	.0000	.000
.800	.2700	.0000	.000
1.000	1.0000	.0000	.000

REGION	NUMBER OF GRIDS ACTIVE	INACTIVE	OIL (MMSTB)	GAS (MMMSCF)	WATER (MMSTB)	SOLVENT (MMMSCF)	PORE VOLUME (MMRCF)	AVERAGE OIL (FRC)	GAS (FRC)	WATER (FRC)	SOLVENT (FRC)	SATURATIONS I	J	K	NWT	SOR	CUT
TOTAL	225	0	21.7627	7.61750	9902.27	.000000	55293.1	.003	.000	.997	.000						

FIELD	PRODUCTION STEP	TIME DAYS	DELT DAYS	PAVG PSI	OIL B/D	GAS MCF/D	WATER B/D	GAS MCF/D	ERROR	MAXIMUM WATER B/D	OIL FRC	GAS FRC	WATER FRC	SATURATION ERROR	I	J	K	NWT	SOR	CUT
TS	1	9	9.13	2500	100	35	0	0	0	-.3E-06	-.4E-06	-.2E-09	.000	8	8	1	1	1	1	0

..... TIMESTEP 2 AT 18.3 DAYS

REGION	OIL (MMSTB)	GAS (BSCF)	WATER (MMSTB)	PORE VOLUME (MMRCF)	AVERAGE OIL (FRC)	GAS (FRC)	WATER (FRC)	AVERAGED PRESSURE
TOTAL	21.7609	7.61687	9902.27	55293.1	.003	.000	.997	2500.0

NAME	I	J	K	STAT	PI	PWF (PSI)	OIL (B/D)	GAS (MCF/D)	WATER (B/D)	GOR (SCF/B)	WCT (PCT)	CUMULATIVE PRODUCTION OIL MB	GAS MMCF	WATER MB	SATURATIONS SO SG SW (FRC PORVOL)
1	8	8	1	QO	3.4	1742.8	100.0	35.0	.4	350.0	.4	2	1	0	.76 .00 .24
FIELD TOTALS - PRODUCED:							100.0	35.0	.4	350.0	.4	2	1	0	
INJECTED:							.0	.0	.0	0	0	0	0	0	

CONTROL	WELLS	NUMBER OF WELLS ...	NUMBER OF NODES ...
QO	1	1	1

STEP	TIME DAYS	DELT DAYS	PAVG PSI	OIL B/D	GAS MCF/D	WATER B/D	GAS MCF/D	ERROR	MAXIMUM WATER B/D	OIL FRC	GAS FRC	WATER FRC	SATURATION ERROR	I	J	K	NWT	SOR	CUT
TS	2	18	9.13	2500	100	35	0	0	0	-.6E-07	.5E-07	-.4E-09	.000	8	8	1	1	1	0
TS	3	27	9.13	2500	100	35	0	0	0	-.3E-06	-.2E-06	-.4E-09	.000	8	8	1	1	1	0

..... TIMESTEP 4 AT 36.5 DAYS

REGION	**** CURRENT FLUID IN PLACE ****			PORE VOLUME	AVERAGE SATURATIONS			PORE VOLUME
	OIL (MMSTB)	GAS (BSCF)	WATER (MMSTB)	(MMRCF)	OIL (FRC)	GAS (FRC)	WATER (FRC)	AVERAGED PRESSURE
TOTAL	21.7591	7.61623	9902.27	55293.1	.003	.000	.997	2500.0

NAME	I	J	K	STAT	PI	PWF (PSI)	* * * WELL RATES * * *			GOR (SCF/B)	WCT (PCT)	CUMULATIVE PRODUCTION			SATURATIONS		
							OIL (B/D)	GAS (MCF/D)	WATER (B/D)			OIL MB	GAS MMCF	WATER MB	SO (FRC)	SG	SW (PORVOL)
1	8	8	1	QO	3.4	1688.5	100.0	35.0	.6	350.0	.5	4	1	0	.76	.00	.24
FIELD TOTALS - PRODUCED:							100.0	35.0	.6	350.0	.5	4	1	0			
INJECTED:							.0	.0	.0			0	0	0			

CONTROL	WELLS	NUMBER OF WELLS	NUMBER OF NODES
-----	-----
QO	1	1	1

STEP	TIME DAYS	DELT DAYS	PAVG PSI	OIL B/D	GAS MCF/D	WATER B/D	FIELD GAS MCF/D	INJECTION WATER B/D	MATERIAL OIL FRC	BALANCE GAS FRC	ERROR WATER FRC	MAXIMUM SATURATION			NWT	SOR	CUT	
TS 4	37	9.13	2500	100	35	1	0	0	-.6E-07	-.8E-07	-.1E-06	.000	8	8	1	1	1	0
TS 5	47	10.00	2500	100	35	1	0	0	-.2E-06	-.4E-07	-.6E-09	.000	8	8	1	1	1	0
TS 6	57	10.00	2500	100	35	1	0	0	.2E-06	.2E-06	-.6E-09	.000	8	8	1	1	1	0
TS 7	65	8.26	2500	100	35	1	0	0	-.6E-07	-.2E-06	-.6E-09	.000	8	8	1	1	1	0

..... TIMESTEP 8 AT 73.1 DAYS

REGION	**** CURRENT FLUID IN PLACE ****			PORE VOLUME	AVERAGE SATURATIONS			PORE VOLUME
	OIL (MMSTB)	GAS (BSCF)	WATER (MMSTB)	(MMRCF)	OIL (FRC)	GAS (FRC)	WATER (FRC)	AVERAGED PRESSURE
TOTAL	21.7554	7.61495	9902.27	55293.1	.003	.000	.997	2499.9

NAME	I	J	K	STAT	PI	PWF (PSI)	* * * WELL RATES * * *			GOR (SCF/B)	WCT (PCT)	CUMULATIVE PRODUCTION			SATURATIONS		
							OIL (B/D)	GAS (MCF/D)	WATER (B/D)			OIL MB	GAS MMCF	WATER MB	SO (FRC)	SG	SW (PORVOL)
1	8	8	1	QO	3.4	1635.5	100.0	35.0	.7	350.0	.7	7	3	0	.76	.00	.24
FIELD TOTALS - PRODUCED:							100.0	35.0	.7	350.0	.7	7	3	0			
INJECTED:							.0	.0	.0			0	0	0			

CONTROL	WELLS	NUMBER OF WELLS	NUMBER OF NODES
-----	-----
QO	1	1	1

STEP	TIME DAYS	DELT DAYS	PAVG PSI	OIL B/D	GAS MCF/D	WATER B/D	FIELD GAS MCF/D	INJECTION WATER B/D	MATERIAL OIL FRC	BALANCE GAS FRC	ERROR WATER FRC	MAXIMUM SATURATION			NWT	SOR	CUT	
TS 8	73	8.26	2500	100	35	1	0	0	-.1E-06	.1E-07	-.6E-09	.000	8	8	1	1	1	0
TS 9	83	10.00	2500	100	35	1	0	0	.1E-06	-.2E-06	-.7E-09	.000	8	8	1	1	1	0
TS 10	93	10.00	2500	100	35	1	0	0	-.2E-06	-.1E-06	.1E-06	.000	8	8	1	1	1	0
TS 11	101	8.26	2500	100	35	1	0	0	.7E-07	.2E-06	.7E-06	.000	8	8	1	1	1	0

..... TIMESTEP 12 AT 109.6 DAYS

REGION	**** CURRENT FLUID IN PLACE ****			PORE VOLUME	AVERAGE SATURATIONS			PORE VOLUME
	OIL (MMSTB)	GAS (BSCF)	WATER (MMSTB)	(MMRCF)	OIL (FRC)	GAS (FRC)	WATER (FRC)	AVERAGED PRESSURE
TOTAL	21.7518	7.61367	9902.26	55293.1	.003	.000	.997	2499.9

NAME	I	J	K	STAT	PI	PWF (PSI)	* * * WELL RATES * * *			GOR (SCF/B)	WCT (PCT)	CUMULATIVE PRODUCTION			SATURATIONS		
							OIL (B/D)	GAS (MCF/D)	WATER (B/D)			OIL MB	GAS MMCF	WATER MB	SO (FRC)	SG	SW (PORVOL)
1	8	8	1	QO	3.4	1608.4	100.0	35.0	.7	350.0	.7	11	4	0	.76	.00	.24
FIELD TOTALS - PRODUCED:							100.0	35.0	.7	350.0	.7	11	4	0			
INJECTED:							.0	.0	.0			0	0	0			

CONTROL	WELLS	NUMBER OF WELLS	NUMBER OF NODES
-----	-----
QO	1	1	1

TIME	DELT	PAVG	OIL	GAS	WATER	FIELD GAS	INJECTION WATER	MATERIAL OIL	BALANCE GAS	ERROR WATER	MAXIMUM SATURATION
------	------	------	-----	-----	-------	-----------	-----------------	--------------	-------------	-------------	--------------------

STEP	DAYS	DAYS	PSI	B/D	MCF/D	B/D	MCF/D	B/D	FRC	FRC	FRC	ERROR	I	J	K	NWT	SOR	CUT
TS 12	110	8.26	2500	100	35	1	0	0	-.5E-06	-.1E-06	-.6E-09	.000	8	8	1	1	1	0
TS 13	120	10.00	2500	100	35	1	0	0	.1E-07	.2E-06	-.7E-09	.000	8	8	1	1	1	0
TS 14	130	10.00	2500	100	35	1	0	0	.1E-06	-.3E-06	.7E-07	.000	8	8	1	1	1	0
TS 15	138	8.26	2500	100	35	1	0	0	.7E-07	.3E-06	.7E-07	.000	8	8	1	1	1	0

..... TIMESTEP 16 AT 146.1 DAYS

REGION	OIL (MMSTB)	CURRENT GAS (BSCF)	FLUID IN PLACE WATER (MMSTB)	PLACE ****	PORE VOLUME (MMRCF)	AVERAGE OIL (FRC)	SATURATIONS GAS (FRC)	WATER (FRC)	PORE VOLUME AVERAGED PRESSURE
TOTAL	21.7481	7.61239	9902.26	55293.1	.003	.000	.997	2499.9	

NAME	I	J	K	STAT	PI	PI (PSI)	WELL RATES OIL (B/D)	GAS (MCF/D)	WATER (B/D)	GOR (SCF/B)	WCT (PCT)	CUMULATIVE OIL MB	GAS MMCF	WATER MB	SATURATIONS SO (FRC)	SG	SW (PORVOL)
1	8	8	1	QO	3.4	1590.9	100.0	35.0	.7	350.0	.7	15	5	0	.76	.00	.24
FIELD TOTALS	- PRODUCED:						100.0	35.0	.7	350.0	.7	15	5	0			
	INJECTED:						.0	.0	.0			0	0	0			
CONTROL	WELLS						NUMBER OF WELLS ...		1			NUMBER OF NODES ...		1			
	QO	1															

STEP	TIME DAYS	DELT DAYS	PAVG PSI	OIL B/D	GAS MCF/D	WATER B/D	MATERIAL GAS MCF/D	WATER B/D	ERROR OIL FRC	GAS FRC	WATER FRC	SATURATION ERROR	I	J	K	NWT	SOR	CUT
TS 16	146	8.26	2500	100	35	1	0	0	.8E-08	.1E-07	-.1E-06	.000	4	3	1	1	1	0
TS 17	156	10.00	2500	100	35	1	0	0	.8E-07	-.3E-06	.2E-06	.000	5	2	1	1	1	0
TS 18	166	10.00	2500	100	35	1	0	0	-.5E-07	.2E-06	-.7E-09	.000	8	8	1	1	1	0
TS 19	174	8.26	2500	100	35	1	0	0	-.6E-07	.1E-06	-.6E-09	.000	7	7	1	1	1	0

..... TIMESTEP 20 AT 182.6 DAYS

REGION	OIL (MMSTB)	CURRENT GAS (BSCF)	FLUID IN PLACE WATER (MMSTB)	PLACE ****	PORE VOLUME (MMRCF)	AVERAGE OIL (FRC)	SATURATIONS GAS (FRC)	WATER (FRC)	PORE VOLUME AVERAGED PRESSURE
TOTAL	21.7445	7.61111	9902.26	55293.1	.003	.000	.997	2499.8	

NAME	I	J	K	STAT	PI	PI (PSI)	WELL RATES OIL (B/D)	GAS (MCF/D)	WATER (B/D)	GOR (SCF/B)	WCT (PCT)	CUMULATIVE OIL MB	GAS MMCF	WATER MB	SATURATIONS SO (FRC)	SG	SW (PORVOL)
1	8	8	1	QO	3.4	1578.3	100.0	35.0	.7	350.0	.7	18	6	0	.76	.00	.24
FIELD TOTALS	- PRODUCED:						100.0	35.0	.7	350.0	.7	18	6	0			
	INJECTED:						.0	.0	.0			0	0	0			
CONTROL	WELLS						NUMBER OF WELLS ...		1			NUMBER OF NODES ...		1			
	QO	1															

STEP	TIME DAYS	DELT DAYS	PAVG PSI	OIL B/D	GAS MCF/D	WATER B/D	MATERIAL GAS MCF/D	WATER B/D	ERROR OIL FRC	GAS FRC	WATER FRC	SATURATION ERROR	I	J	K	NWT	SOR	CUT
TS 20	183	8.26	2500	100	35	1	0	0	-.6E-07	.1E-06	-.3E-06	.000	2	2	1	1	1	0
TS 21	193	10.00	2500	100	35	1	0	0	.2E-06	-.2E-06	-.1E-06	.000	4	1	1	1	1	0
TS 22	203	10.00	2500	100	35	1	0	0	-.1E-06	.2E-06	.1E-06	.000	13	8	1	1	1	0
TS 23	211	8.26	2500	100	35	1	0	0	.2E-06	-.6E-07	-.6E-09	.000	4	1	1	1	1	0

..... TIMESTEP 24 AT 219.2 DAYS

REGION	OIL (MMSTB)	CURRENT GAS (BSCF)	FLUID IN PLACE WATER (MMSTB)	PLACE ****	PORE VOLUME (MMRCF)	AVERAGE OIL (FRC)	SATURATIONS GAS (FRC)	WATER (FRC)	PORE VOLUME AVERAGED PRESSURE
TOTAL	21.7408	7.60984	9902.26	55293.1	.003	.000	.997	2499.8	

NAME	I	J	K	STAT	PI	PI (PSI)	WELL RATES OIL (B/D)	GAS (MCF/D)	WATER (B/D)	GOR (SCF/B)	WCT (PCT)	CUMULATIVE OIL MB	GAS MMCF	WATER MB	SATURATIONS SO (FRC)	SG	SW (PORVOL)
1	8	8	1	QO	3.4	1568.9	100.0	35.0	.7	350.0	.7	22	8	0	.76	.00	.24
FIELD TOTALS	- PRODUCED:						100.0	35.0	.7	350.0	.7	22	8	0			

INJECTED: .0 .0 .0 0 0 0

CONTROL WELLS NUMBER OF WELLS ... 1

 QO 1 NUMBER OF NODES ... 1

STEP	TIME DAYS	DELT DAYS	PAVG PSI	FIELD PRODUCTION			FIELD INJECTION		MATERIAL BALANCE ERROR			MAXIMUM SATURATION			NWT	SOR	CUT	
				OIL B/D	GAS MCF/D	WATER B/D	GAS MCF/D	WATER B/D	OIL FRC	GAS FRC	WATER FRC	ERROR	I	J				K
TS 24	219	8.26	2500	100	35	1	0	0	-.6E-07	-.2E-06	-.6E-09	.000	3	1	1	1	1	0
TS 25	229	10.00	2500	100	35	1	0	0	.1E-06	.3E-06	-.7E-09	.000	13	1	1	1	1	0
TS 26	239	10.00	2500	100	35	1	0	0	-.5E-07	.2E-06	-.7E-07	.000	11	1	1	1	1	0
TS 27	247	8.26	2500	100	35	1	0	0	.3E-06	-.3E-06	-.3E-06	.000	3	1	1	1	1	0

..... TIMESTEP 28 AT 255.7 DAYS

REGION	OIL (MMSTB)	CURRENT GAS (BSCF)	FLUID IN PLACE (MMSTB)	WATER (MMSTB)	PORE VOLUME (MMRCF)	AVERAGE OIL (FRC)	SATURATIONS GAS (FRC)	WATER (FRC)	PORE VOLUME AVERAGED PRESSURE
TOTAL	21.7372	7.60855	9902.27	55293.1	.003	.000	.997	2499.7	

NAME	I	J	K	STAT	PI	PWF (PSI)	* * * WELL RATES * * *			GOR (SCF/B)	WCT (PCT)	CUMULATIVE PRODUCTION			SATURATIONS		
							OIL (B/D)	GAS (MCF/D)	WATER (B/D)			OIL MB	GAS MMCF	WATER MB	SO (FRC)	SG (PORVOL)	SW
1	8	8	1	QO	3.4	1561.8	100.0	35.0	.7	350.0	.7	26	9	0	.76	.00	.24
FIELD TOTALS - PRODUCED:							100.0	35.0	.7	350.0	.7	26	9	0			
INJECTED:							.0	.0	.0			0	0	0			

CONTROL WELLS NUMBER OF WELLS ... 1

 QO 1 NUMBER OF NODES ... 1

STEP	TIME DAYS	DELT DAYS	PAVG PSI	FIELD PRODUCTION			FIELD INJECTION		MATERIAL BALANCE ERROR			MAXIMUM SATURATION			NWT	SOR	CUT	
				OIL B/D	GAS MCF/D	WATER B/D	GAS MCF/D	WATER B/D	OIL FRC	GAS FRC	WATER FRC	ERROR	I	J				K
TS 28	256	8.26	2500	100	35	1	0	0	-.1E-06	.1E-06	-.1E-06	.000	15	13	1	1	1	0
TS 29	266	10.00	2500	100	35	1	0	0	-.2E-06	-.4E-07	-.7E-09	.000	3	1	1	1	1	0
TS 30	276	10.00	2500	100	35	1	0	0	-.5E-07	.3E-07	-.7E-09	.000	2	1	1	1	1	0
TS 31	284	8.26	2500	100	35	1	0	0	.7E-07	.1E-07	-.6E-09	.000	15	2	1	1	1	0

..... TIMESTEP 32 AT 292.2 DAYS

REGION	OIL (MMSTB)	CURRENT GAS (BSCF)	FLUID IN PLACE (MMSTB)	WATER (MMSTB)	PORE VOLUME (MMRCF)	AVERAGE OIL (FRC)	SATURATIONS GAS (FRC)	WATER (FRC)	PORE VOLUME AVERAGED PRESSURE
TOTAL	21.7335	7.60728	9902.27	55293.1	.003	.000	.997	2499.7	

NAME	I	J	K	STAT	PI	PWF (PSI)	* * * WELL RATES * * *			GOR (SCF/B)	WCT (PCT)	CUMULATIVE PRODUCTION			SATURATIONS		
							OIL (B/D)	GAS (MCF/D)	WATER (B/D)			OIL MB	GAS MMCF	WATER MB	SO (FRC)	SG (PORVOL)	SW
1	8	8	1	QO	3.4	1556.3	100.0	35.0	.7	350.0	.7	29	10	0	.76	.00	.24
FIELD TOTALS - PRODUCED:							100.0	35.0	.7	350.0	.7	29	10	0			
INJECTED:							.0	.0	.0			0	0	0			

CONTROL WELLS NUMBER OF WELLS ... 1

 QO 1 NUMBER OF NODES ... 1

STEP	TIME DAYS	DELT DAYS	PAVG PSI	FIELD PRODUCTION			FIELD INJECTION		MATERIAL BALANCE ERROR			MAXIMUM SATURATION			NWT	SOR	CUT	
				OIL B/D	GAS MCF/D	WATER B/D	GAS MCF/D	WATER B/D	OIL FRC	GAS FRC	WATER FRC	ERROR	I	J				K
TS 32	292	8.26	2500	100	35	1	0	0	-.6E-07	.1E-07	-.3E-06	.000	2	1	1	1	1	0
TS 33	302	10.00	2500	100	35	1	0	0	.3E-06	-.4E-07	-.1E-06	.000	3	1	1	1	1	0
TS 34	312	10.00	2500	100	35	1	0	0	-.3E-06	-.1E-06	-.7E-09	.000	15	7	1	1	1	0
TS 35	320	8.26	2500	100	35	1	0	0	.2E-06	-.2E-06	-.6E-09	.000	7	1	1	1	1	0

..... TIMESTEP 36 AT 328.7 DAYS

REGION	OIL (MMSTB)	CURRENT GAS (BSCF)	FLUID IN PLACE (MMSTB)	WATER (MMSTB)	PORE VOLUME (MMRCF)	AVERAGE OIL (FRC)	SATURATIONS GAS (FRC)	WATER (FRC)	PORE VOLUME AVERAGED PRESSURE
--------	-------------	--------------------	------------------------	---------------	---------------------	-------------------	-----------------------	-------------	-------------------------------

TOTAL 21.7299 7.60600 9902.27 55293.0 .003 .000 .997 2499.6

NAME	I	J	K	STAT	PI	PWF (PSI)	* * * WELL RATES * * *			GOR (SCF/B)	WCT (PCT)	CUMULATIVE PRODUCTION			SATURATIONS		
							OIL (B/D)	GAS (MCF/D)	WATER (B/D)			OIL MB	GAS MMCF	WATER MB	SO (FRC)	SG (PORVOL)	SW
1	8	8	1	QO	3.4	1552.1	100.0	35.0	.7	350.0	.7	33	12	0	.76	.00	.24
FIELD TOTALS - PRODUCED:							100.0	35.0	.7	350.0	.7	33	12	0			
INJECTED:							.0	.0	.0			0	0	0			

CONTROL WELLS NUMBER OF WELLS ... 1

 QO 1 NUMBER OF NODES ... 1

STEP	TIME DAYS	DELT DAYS	PAVG PSI	FIELD PRODUCTION			FIELD INJECTION		MATERIAL BALANCE ERROR			MAXIMUM SATURATION			NWT	SOR	CUT	
				OIL B/D	GAS MCF/D	WATER B/D	GAS MCF/D	WATER B/D	OIL FRC	GAS FRC	WATER FRC	ERROR	I	J				K
TS 36	329	8.26	2500	100	35	1	0	0	-.1E-06	.2E-06	-.6E-09	.000	13	12	1	1	1	0
TS 37	339	10.00	2500	100	35	1	0	0	.3E-06	.9E-07	-.7E-07	.000	15	9	1	1	1	0
TS 38	349	10.00	2500	100	35	1	0	0	-.2E-06	.9E-07	.7E-07	.000	4	2	1	1	1	0
TS 39	357	8.26	2500	100	35	1	0	0	-.2E-06	-.2E-06	-.5E-09	.000	9	1	1	1	1	0

..... TIMESTEP 40 AT 365.3 DAYS

REGION	OIL (MMSTB)	GAS (BSCF)	WATER (MMSTB)	PORE VOLUME (MMRCF)	AVERAGE OIL (FRC)	GAS (FRC)	WATER (FRC)	PORE VOLUME AVERAGED PRESSURE
TOTAL	21.7262	7.60472	9902.27	55293.0	.003	.000	.997	2499.5

NAME	I	J	K	STAT	PI	PWF (PSI)	* * * WELL RATES * * *			GOR (SCF/B)	WCT (PCT)	CUMULATIVE PRODUCTION			SATURATIONS		
							OIL (B/D)	GAS (MCF/D)	WATER (B/D)			OIL MB	GAS MMCF	WATER MB	SO (FRC)	SG (PORVOL)	SW
1	8	8	1	QO	3.4	1549.0	100.0	35.0	.7	350.0	.6	37	13	0	.76	.00	.24
FIELD TOTALS - PRODUCED:							100.0	35.0	.7	350.0	.6	37	13	0			
INJECTED:							.0	.0	.0			0	0	0			

CONTROL WELLS NUMBER OF WELLS ... 1

 QO 1 NUMBER OF NODES ... 1

STEP	TIME DAYS	DELT DAYS	PAVG PSI	FIELD PRODUCTION			FIELD INJECTION		MATERIAL BALANCE ERROR			MAXIMUM SATURATION			NWT	SOR	CUT	
				OIL B/D	GAS MCF/D	WATER B/D	GAS MCF/D	WATER B/D	OIL FRC	GAS FRC	WATER FRC	ERROR	I	J				K
TS 40	365	8.26	2500	100	35	1	0	0	.8E-08	.8E-07	-.5E-09	.000	12	2	1	1	1	0
TS 41	375	10.00	2500	100	35	1	0	0	.1E-07	-.4E-07	.7E-07	.000	8	3	1	1	1	0
TS 42	385	10.00	2499	100	35	1	0	0	.1E-07	-.4E-07	-.1E-06	.000	7	2	1	1	1	0
TS 43	394	8.26	2499	100	35	1	0	0	.7E-07	.8E-07	-.1E-06	.000	5	2	1	1	1	0

..... TIMESTEP 44 AT 401.8 DAYS

REGION	OIL (MMSTB)	GAS (BSCF)	WATER (MMSTB)	PORE VOLUME (MMRCF)	AVERAGE OIL (FRC)	GAS (FRC)	WATER (FRC)	PORE VOLUME AVERAGED PRESSURE
TOTAL	21.7226	7.60344	9902.27	55293.0	.003	.000	.997	2499.5

NAME	I	J	K	STAT	PI	PWF (PSI)	* * * WELL RATES * * *			GOR (SCF/B)	WCT (PCT)	CUMULATIVE PRODUCTION			SATURATIONS		
							OIL (B/D)	GAS (MCF/D)	WATER (B/D)			OIL MB	GAS MMCF	WATER MB	SO (FRC)	SG (PORVOL)	SW
1	8	8	1	QO	3.4	1546.5	100.0	35.0	.6	350.0	.6	40	14	0	.76	.00	.24
FIELD TOTALS - PRODUCED:							100.0	35.0	.6	350.0	.6	40	14	0			
INJECTED:							.0	.0	.0			0	0	0			

CONTROL WELLS NUMBER OF WELLS ... 1

 QO 1 NUMBER OF NODES ... 1

STEP	TIME DAYS	DELT DAYS	PAVG PSI	FIELD PRODUCTION			FIELD INJECTION		MATERIAL BALANCE ERROR			MAXIMUM SATURATION			NWT	SOR	CUT	
				OIL B/D	GAS MCF/D	WATER B/D	GAS MCF/D	WATER B/D	OIL FRC	GAS FRC	WATER FRC	ERROR	I	J				K
TS 44	402	8.26	2499	100	35	1	0	0	.8E-08	-.1E-06	-.1E-06	.000	4	2	1	1	1	0
TS 45	412	10.00	2499	100	35	1	0	0	.3E-06	.3E-07	.4E-06	.000	15	2	1	1	1	0

TS 46	422	10.00	2499	100	35	1	0	0	-.3E-06	.2E-06	.1E-06	.000	15	2	1	1	1	0
TS 47	430	8.26	2499	100	35	1	0	0	.8E-08	-.6E-07	-.5E-09	.000	1	1	1	1	1	0

..... TIMESTEP 48 AT 438.3 DAYS

REGION	**** CURRENT FLUID IN PLACE ****			PORE VOLUME	AVERAGE SATURATIONS			PORE VOLUME
	OIL (MMSTB)	GAS (BSCF)	WATER (MMSTB)	(MMRCF)	OIL (FRC)	GAS (FRC)	WATER (FRC)	AVERAGED PRESSURE
TOTAL	21.7189	7.60216	9902.27	55293.0	.003	.000	.997	2499.4

NAME	I	J	K	STAT	PI	PWF (PSI)	*** WELL RATES ***			GOR (SCF/B)	WCT (PCT)	CUMULATIVE PRODUCTION			SATURATIONS			
							OIL (B/D)	GAS (MCF/D)	WATER (B/D)			OIL MB	GAS MMCF	WATER MB	SO (FRC)	SG (FRC)	SW (FRC)	PORVOL)
1	8	8	1	QO	3.4	1544.7	100.0	35.0	.6	350.0	.6	44	15	0	.76	.00	.24	
FIELD TOTALS - PRODUCED:							100.0	35.0	.6	350.0	.6	44	15	0				
INJECTED:							.0	.0	.0			0	0	0				

CONTROL	WELLS	NUMBER OF WELLS ...		1
-----	-----	NUMBER OF NODES ...		1
QO	1			

STEP	TIME DAYS	DELT DAYS	PAVG PSI	FIELD PRODUCTION			FIELD INJECTION		MATERIAL BALANCE ERROR			MAXIMUM SATURATION						
				OIL B/D	GAS MCF/D	WATER B/D	GAS MCF/D	WATER B/D	OIL FRC	GAS FRC	WATER FRC	ERROR	I	J	K	NWT	SOR	CUT
TS 48	438	8.26	2499	100	35	1	0	0	-.2E-06	-.1E-06	-.5E-09	.000	1	1	1	1	1	0
TS 49	448	10.00	2499	100	35	1	0	0	-.5E-07	-.2E-06	.1E-06	.000	1	1	1	1	1	0
TS 50	458	10.00	2499	100	35	1	0	0	-.1E-06	-.1E-06	.7E-07	.000	6	1	1	1	1	0
TS 51	467	8.26	2499	100	35	1	0	0	.3E-06	-.2E-06	-.6E-06	.000	15	1	1	1	1	0

..... TIMESTEP 52 AT 474.8 DAYS

REGION	**** CURRENT FLUID IN PLACE ****			PORE VOLUME	AVERAGE SATURATIONS			PORE VOLUME
	OIL (MMSTB)	GAS (BSCF)	WATER (MMSTB)	(MMRCF)	OIL (FRC)	GAS (FRC)	WATER (FRC)	AVERAGED PRESSURE
TOTAL	21.7153	7.60089	9902.27	55293.0	.003	.000	.997	2499.3

NAME	I	J	K	STAT	PI	PWF (PSI)	*** WELL RATES ***			GOR (SCF/B)	WCT (PCT)	CUMULATIVE PRODUCTION			SATURATIONS			
							OIL (B/D)	GAS (MCF/D)	WATER (B/D)			OIL MB	GAS MMCF	WATER MB	SO (FRC)	SG (FRC)	SW (FRC)	PORVOL)
1	8	8	1	QO	3.4	1543.3	100.0	35.0	.6	350.0	.6	47	17	0	.76	.00	.24	
FIELD TOTALS - PRODUCED:							100.0	35.0	.6	350.0	.6	47	17	0				
INJECTED:							.0	.0	.0			0	0	0				

CONTROL	WELLS	NUMBER OF WELLS ...		1
-----	-----	NUMBER OF NODES ...		1
QO	1			

STEP	TIME DAYS	DELT DAYS	PAVG PSI	FIELD PRODUCTION			FIELD INJECTION		MATERIAL BALANCE ERROR			MAXIMUM SATURATION						
				OIL B/D	GAS MCF/D	WATER B/D	GAS MCF/D	WATER B/D	OIL FRC	GAS FRC	WATER FRC	ERROR	I	J	K	NWT	SOR	CUT
TS 52	475	8.26	2499	100	35	1	0	0	-.6E-07	.2E-06	.1E-06	.000	5	1	1	1	1	0
TS 53	485	10.00	2499	100	35	1	0	0	.1E-07	.3E-07	.7E-07	.000	6	1	1	1	1	0
TS 54	495	10.00	2499	100	35	1	0	0	-.1E-06	-.4E-07	.1E-06	.000	11	1	1	1	1	0
TS 55	503	8.26	2499	100	35	1	0	0	.1E-06	-.3E-06	.1E-06	.000	15	5	1	1	1	0

..... TIMESTEP 56 AT 511.3 DAYS

REGION	**** CURRENT FLUID IN PLACE ****			PORE VOLUME	AVERAGE SATURATIONS			PORE VOLUME
	OIL (MMSTB)	GAS (BSCF)	WATER (MMSTB)	(MMRCF)	OIL (FRC)	GAS (FRC)	WATER (FRC)	AVERAGED PRESSURE
TOTAL	21.7116	7.59961	9902.27	55293.0	.003	.000	.997	2499.3

NAME	I	J	K	STAT	PI	PWF (PSI)	*** WELL RATES ***			GOR (SCF/B)	WCT (PCT)	CUMULATIVE PRODUCTION			SATURATIONS			
							OIL (B/D)	GAS (MCF/D)	WATER (B/D)			OIL MB	GAS MMCF	WATER MB	SO (FRC)	SG (FRC)	SW (FRC)	PORVOL)
1	8	8	1	QO	3.4	1542.2	100.0	35.0	.6	350.0	.6	51	18	0	.76	.00	.24	
FIELD TOTALS - PRODUCED:							100.0	35.0	.6	350.0	.6	51	18	0				
INJECTED:							.0	.0	.0			0	0	0				

CONTROL	WELLS	NUMBER OF WELLS ...		1
---------	-------	---------------------	--	---

----- 1
 QO 1 NUMBER OF NODES ... 1

STEP	TIME DAYS	DELT DAYS	PAVG PSI	FIELD PRODUCTION			FIELD INJECTION		MATERIAL BALANCE ERROR			MAXIMUM SATURATION			NWT	SOR	CUT	
				OIL B/D	GAS MCF/D	WATER B/D	GAS MCF/D	WATER B/D	OIL FRC	GAS FRC	WATER FRC	ERROR	I	J				K
TS 56	511	8.26	2499	100	35	1	0	0	.8E-08	.2E-06	-.5E-09	.000	5	1	1	1	1	0
TS 57	521	10.00	2499	100	35	1	0	0	.2E-06	-.3E-06	-.7E-07	.000	15	7	1	1	1	0
TS 58	531	10.00	2499	100	35	1	0	0	-.5E-07	.2E-06	.7E-07	.000	4	1	1	1	1	0
TS 59	540	8.26	2499	100	35	1	0	0	.8E-08	-.6E-07	.1E-06	.000	5	1	1	1	1	0

..... TIMESTEP 60 AT 547.9 DAYS

REGION	**** CURRENT FLUID IN PLACE ****			PORE VOLUME (MMRCF)	AVERAGE SATURATIONS			PORE VOLUME AVERAGED PRESSURE
	OIL (MMSTB)	GAS (BSCF)	WATER (MMSTB)		OIL (FRC)	GAS (FRC)	WATER (FRC)	
TOTAL	21.7080	7.59833	9902.27	55293.0	.003	.000	.997	2499.2

NAME	I	J	K	STAT	PI	PWF (PSI)	* * * WELL RATES * * *			GOR (SCF/B)	WCT (PCT)	CUMULATIVE PRODUCTION			SATURATIONS		
							OIL (B/D)	GAS (MCF/D)	WATER (B/D)			OIL MB	GAS MMCF	WATER MB	SO (FRC PORVOL)	SG	SW
1	8	8	1	QO	3.4	1541.5	100.0	35.0	.6	350.0	.6	55	19	0	.76	.00	.24
FIELD TOTALS - PRODUCED:							100.0	35.0	.6	350.0	.6	55	19	0			
INJECTED:							.0	.0	.0			0	0	0			

CONTROL WELLS

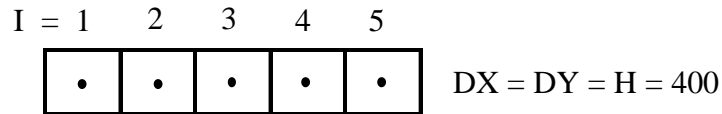
 QO 1 NUMBER OF WELLS ... 1

 NUMBER OF NODES ... 1

STEP	TIME DAYS	DELT DAYS	PAVG PSI	FIELD PRODUCTION			FIELD INJECTION		MATERIAL BALANCE ERROR			MAXIMUM SATURATION			NWT	SOR	CUT	
				OIL B/D	GAS MCF/D	WATER B/D	GAS MCF/D	WATER B/D	OIL FRC	GAS FRC	WATER FRC	ERROR	I	J				K
TS 60	548	8.26	2499	100	35	1	0	0	.8E-08	.8E-07	-.7E-07	.000	3	1	1	1	1	0

NORMAL END OF RUN

RESERVOIR SIMULATION
CLASS PROBLEM NO. 66 (SYNTHETIC HISTORY MATCHING)



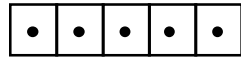
The above homogeneous, isotropic, 1-D, oil zone is attached to an aquifer of uncertain properties and dimensions. Geological work has shown that there are five possible aquifer structures. They are represented by Reservoirs “A” through “E” in Figure 1.

The reservoir is produced at a variable rate as shown by figure 2. Figure 3 shows the production cell pressure response versus time for six years of production for the base case (no aquifer). Also shown in Figure 3 is a pressure plot for a six year simulation run of the oil zone with an aquifer in communication.

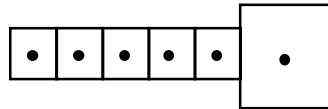
Reservoirs “A” through “E” (Figure 1) are the same oil zone, but with aquifers of different sizes and configurations attached. The data set for the base case and grid modifications for each of the aquifers are given in Tables A and B respectively.

Analyze Figure 2. Decide which aquifer case (A-E) is plotted, then make a computer run to confirm your choice.

BASE RESERVOIR

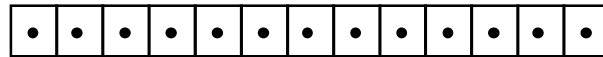


RESERVOIR "A"



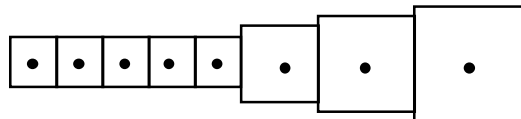
IMAX = 6

RESERVOIR "B"



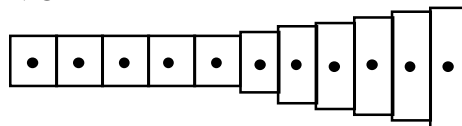
IMAX = 13

RESERVOIR "C"



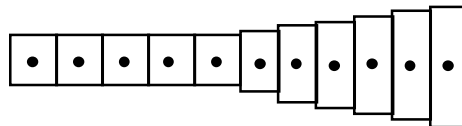
IMAX = 8

RESERVOIR "D"



IMAX = 11

RESERVOIR "E"



IMAX = 11

Oil Production Rate vs. Time, Problem 66

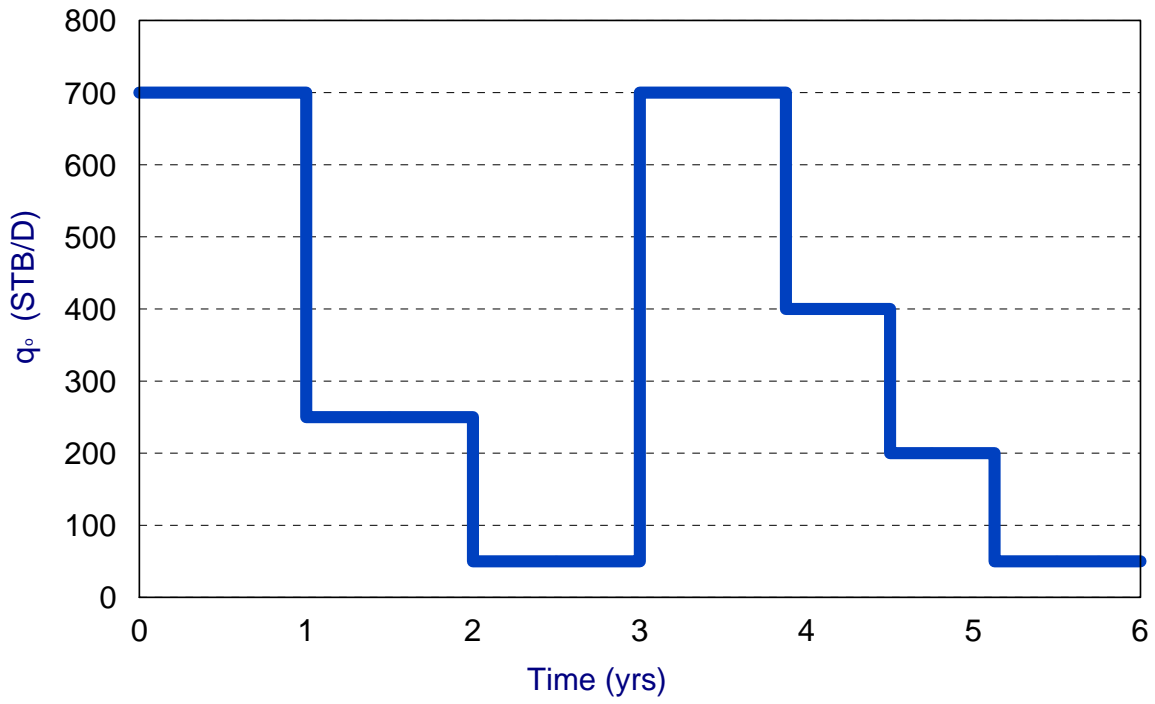


TABLE A

```

/      Problem 66 - BASE CASE
/      3DSIM - WATTENBARGER AND ASSOCIATES
/      8/14/85
/
/
IMAX   5
CROC   3.0E-6      /Formation Compressibility, psi-1
CWAT   3.1E-6      /Water Compressibility, psi-1
COIL   18E-6       /Oil Compressibility, psi-1
CRVO   46E-6       / Slope of undersaturated oil viscosity curve, cp/psi
VISW   0.310       /Water viscosity, cp

DENO   .32114      /Oil Density, psi/ft
DENG   .0004493    /Gas Density, psi/ft
DENW   .4384       /Water Density, psi/ft

METH   2           / D-4 solution method
STONE = T       /Method for 3-phase Kr calculation
NOMAPS
NOTABS
END
/
/      .....TABLE SECTION
/
KRW
/      Sw      Krw      Krow      Pcow
0.0     0.0     1.00     0.0
0.20    0.06    0.7      0.0
0.25    0.016   0.465   0.0
0.30    0.026   0.283   0.0
0.35    0.039   0.187   0.0
0.40    0.055   0.127   0.0
0.45    0.073   0.085   0.0
0.50    0.095   0.060   0.0
0.55    0.121   0.040   0.0
0.60    0.153   0.027   0.0
0.65    0.198   0.018   0.0
0.70    0.254   0.010   0.0
0.75    0.325   0.007   0.0
0.80    0.420   0.0      0.0
1.00    1.000   0.0      0.0
/
KRG
/      Sg      Krg      Krog      Pcog
0.0     0.0     1.0      0.0
1.00    0.0     1.0      0.0

PRES
/      P      Bo      Bg      Vo      Vg      Rs
/      psi     rb/stb  rcf/scf  cp      cp      scf/stb
14.7    1.0620  0.935829 1.040    0.0080  1.1
264.7   1.1500  0.067902 0.9750   0.00960 90.4
514.7   1.2070  0.035229 0.9100   0.01120 180.2
1014.7  1.2950  0.018007 0.8300   0.01400 371.1

2014.7  1.4350  0.009063 0.6950   0.01890 636.1
2514.7  1.5000  0.007266 0.6410   0.02080 774.8
3014.7  1.5650  0.006064 0.5940   0.02280 929.8
4014.7  1.6950  0.004554 0.5100   0.02680 1270.0
9014.7  1.5790  0.002167 0.7400   0.47000 1270.0
5014.7  1.8270  0.003644 0.4490   0.03090 1618.0
9014.7  2.3570  0.002167 0.2030   0.04700 2984.0

```

```

END
/
/      GRID DATA
/
WINDOW  I=1 TO 5 J = 1 TO 1 K = 1 TO 1
ELEV    0      0      0      .7200
H       0      0      0      400
POR     0      0      0      .25
WSAT   0      0      0      .20
GSAT   0      0      0      .0
PSAT   0      0      0      1000
PO     0      0      0      5000
PERM   0      0      0      10
DX           5*400
DY           1*400
END

```

```

/      SCHEDULE DATA
OMEGA=1.0
WLRT      2
PSRT      2
DELT=10
DTCUT=0.5
DTFAC=2.0
DTMIN=1
SGMAX=0.04
SWMAX=0.04
DOUT=365
DTMAX=60
WELL=1    I=1      J=1      K=1
M=1  QO=700    PI=10.59
TIME 365
M=1  QO=250
TIME 730
M=1  QO=50
TIME 1095
M=1  QO=700
TIME 1460
M=1  QO=400
TIME 1642
M=1  QO=200
TIME 1825
M=1  QO=50
TIME 2190
END

```

TABLE B
MODIFICATIONS FOR DIFFERENT CASES
PROBLEM NO. 66

	CELL	DI	K	H	POR	SOI
CASE A:	6	1500		1500	0.1	0
CASE B:	6		1	1500		0
	7		1	1500		0
	8		1	1500		0
	9		1	1500		0
	10		1	1500		0
	11		1	1500		0
	12		1	1500		0
	13		1	1500		0
CASE C:	6	600	0.1	600		0
	7	700	0.1	700		0
	8	800	0.1	800		0
CASE D:	6		1000	600		0
	7		0.5	700		0
	8		1000	800		0
	9		1000	900		0
	10		1000	1000		0
	11		1000	1100		0
CASE E:	6		1	600		0
	7		1000	700		0
	8		1000	800		0
	9		1000	900		0
	10		1000	1000		0
	11		1000	1100		0

NOTE: Blank data is same as oil reservoir.

REFERENCES

1. Mattax, C.C. and Dalton, R.L.: *Reservoir Simulation*, SPE Monograph **13**, Richardson, TX (1990) 87-98.
2. Peaceman, D.W.: "Interpretation of Well-Block Pressures in Numerical Reservoir Simulation," *SPEJ* (June 1978) 183-194; *Trans.*, AIME, **265**.
3. van Poollen, H.K., Breitenbach, E.A., and Thurnau, D.H.: "Treatment of Individual Wellsand Grids in Reservoir Modeling," *SPEJ* (Dec. 1968) 341-46.
4. Slater, G.E. and Durrer, E.: "Adjustment of Reservoir Simulator Models to Match Field Performance," *SPEJ* (Sept. 1971) 295-305; *Trans.*, AIME, **251**.
5. Carter, R.D. *et al.*: "Performance Matching With Constraints," *SPEJ* (April 1974) 187-91; *Trans.*, AIME, **257**.
6. Veatch, R.W. Jr. and Thomas, G.W.: "A Direct Approach for History Matching," paper SPE 3515 presented at the 1971 Annual Meeting, New Orleans, Oct. 3-6.
7. Coats, K.H. and Dempsey, J.R.: "A New Approach for Determining Reservoir Description from Field Performance" *SPEJ* (March 1970) 66-74; *Trans.*, AIME, **249**.
8. Bradford, R.N. and Hrkel, E.J.: "Evaluation of a Reservoir Simulation Study: West Civit Dykeman Sand Unit," *JPT* (Dec. 1979) 1599-1604.
9. Brummett, W.M. *et al.*: "Reservoir Description by Simulation at SACROC- A Case History," *JPT* (Oct. 1976) 1241-1255.

CHAPTER 4

Coning

- Introduction
- Analysis of Forces
- Critical Coning Rate
- Coning Simulation
- Addington's Method
- References
- Exercises
- Appendix

Coning

Introduction

Water coning. Many wells produce from oil zones underlain by "bottom water". When the well is produced, water moves up toward the wellbore in a cone shape. At certain conditions, water breaks through into the well and concurrent oil and water production begins. The phenomena is referred to as 'water coning'.

The phenomenon of coning was studied analytically by Muskat and several key factors were determined. However this analysis was for steady state and also assumed with no multi-phase flow or saturation gradients occur. The main result of the analysis was that a critical rate exists above which the cone reaches the perforations and the water or gas is produced. Below this critical rate, the cone reaches a certain height depending on the rate and other parameters.

Some of the factors affecting coning are listed. Coning increases with:

- (a) increasing λ_w/λ_o (=M)
- (b) increasing k_v/k_h (or continuity)
- (c) increasing q
- (d) decreasing h_w
- (e) decreasing $(\Delta\rho)/144$
- (f) decreasing (kh)
- (g) increasing P_c

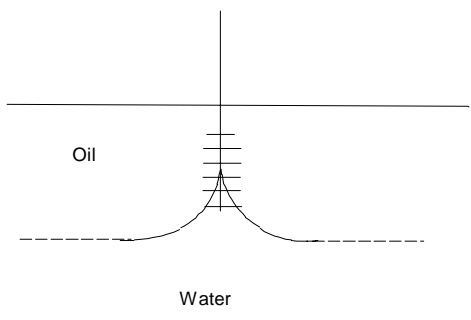


Fig. 1 - Water Coning

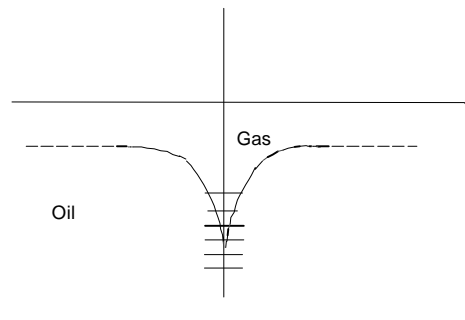


Fig. 2 - Gas Coning

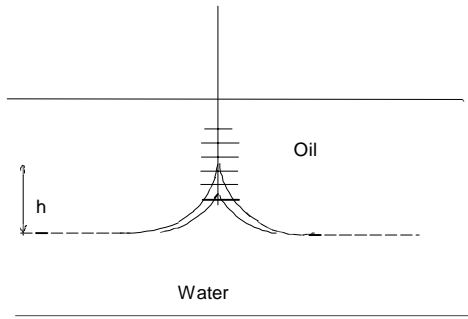


Fig. 3 - Water Coning, Muskat

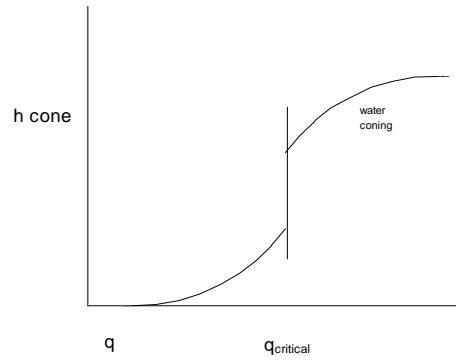


Fig. 4 - h_{cone} vs q_{critical} (steady state)

Analysis of forces

(a) Gravity forces $\frac{\Delta\rho}{144}h_{ap}$ (psi) - 1 (1)

(b) Viscous forces - $(\Delta p)_{viscous}$ (psi)

Coning condition:

(2)
$$(\Delta p)_{gravity} = (\Delta\rho/144)h_{ap}$$

Estimation of $(\Delta p)_{viscous}$:

2
$$qB = \frac{0.00708kh\frac{\bar{h}}{\mu_o}(\Delta p)_{viscous}}{\ln\frac{r_e}{r_w} + S_{partial\ penetration}}$$
 (3)

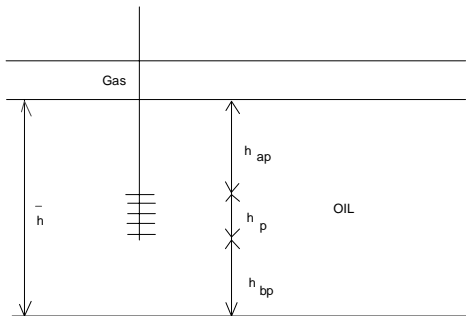


Fig. 5 - Schematic

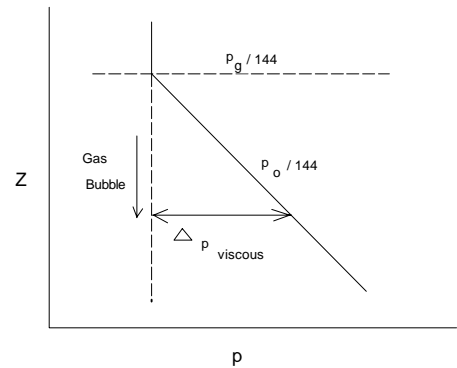


Fig. 6 - Z vs p plot

where h_{ap} - height above perforation
 h_p - perforation height
 h_{bp} - height below perforation

Gravity Number

N_{grav} = gravity force/viscous force

$$N_{\text{grav}} = \frac{0.0078 (\Delta\rho / 144) k_h \bar{h} h_{\text{ap}}}{q_o B_o \mu_o \left(\ln \frac{r_e}{r_w} + S_{\text{pp}} \right)} \quad (4)$$

or,

$$N_{\text{grav}} = \frac{\left(\frac{\Delta\rho}{144} \right)}{\frac{q\mu_w}{0.00633 A k_{\text{avg}}}} \quad (5)$$

from these, the higher the flow rate the lower the gravity number.

Coning conditions

$$N_{\text{grav}} < 1$$

critical rate: @ q_c , $q_o = q_c$, $N_{\text{grav}} = 1$

$$(q_o)_c = \frac{0.00708 (\Delta\rho / 144) k_h \bar{h} h_{\text{ap}}}{B_o \mu_o \left(\ln \frac{r_e}{r_w} + S_{\text{pp}} \right)} \quad (6)$$

Critical coning rate

After Muskat analytical study several attempts have been made to develop a relationship to obtain the rate above which the cone reaches the perforations and the water is produced. Table 1 gives a summary of some equations obtained analytically, experimentally or simulated.

Table 1
Critical Coning Rate Equations
(from Weiping Yang's M.S. thesis, 1990)

Steady-state:

(a) Muskat & Wyckoff 4
(Analytical)

$$q_c = \frac{4\pi\Delta\rho\Sigma a_n b_n}{\mu_o \left[\phi_e - \frac{4}{h} \Sigma a_n b_n \log \frac{4h}{r_e} \right]}$$

(b) Meyer & Garder

$$q_c = \frac{3.5425 \times 10^{-3} (\Delta\rho / 144) (h^2 - h_p^2) k_o}{\mu_o B_o \ln \frac{r_e}{r_w}} \quad 5(\text{Analytical})$$

(c) Chaney *et. al.*

$$q_c = \frac{0.00708 k_o (\Delta\rho / 144) q_{\text{curve}}}{\mu_o B_o} \quad 6(\text{Analytical\&Experimental})$$

(d) Schols 7

$$q_c = \left(\frac{(\Delta\rho / 144) k_o (h^2 - h_p^2)}{887.89 \mu_o B_o} \right) \left(0.432 + \frac{\pi}{\ln \frac{r_e}{r_w}} \right)^{\left(\frac{h}{r_e} \right)^{0.14}} \quad (\text{Experimental})$$

(e) Chierici *et. al.* 8

$$q_c = \frac{7.0915 \times 10^{-3} h^2 (\Delta\rho / 144) k_o}{B_o \mu_o} \Psi(r_{D_e}, \epsilon, \delta)$$

(where: Ψ 9 is the potential function calculated from diagrams.)

(f) Wheatly 10

$$q_c = \left(\frac{0.0142 h^2 k_h (\Delta\rho / 144)}{\mu_o} \right)^{q_{cD}}$$

from an iterative scheme.)

(Analytical, q_{cD} is calculate

(g) Høyland *et. al.* 11

$$q_c = \frac{k_o (\Delta\rho / 144)}{75.15 B_o \mu_o} \left[1 - \left(\frac{h_p}{h} \right)^2 \right]^{1.325} (h_t)^{2.238} [\ln r_e]^{1.99}$$

(Simulation for isotropic case and simulation for anisotropic case.)

12

$$q_c = \left(\frac{h^2 (\Delta\rho / 144) k_h}{282.41 B_o \mu_o} \right) q_{cD} \quad (q_{cD} \text{ is calculated from diagrams.})$$

Non-Steady-State:

(a) Addington13

$$q_c = \frac{1}{(137.9)^2} \frac{k_h \sqrt{h_p} h_{ap}^2}{B_o \left(\frac{k_v}{k_h}\right)^{0.1} \mu_o F_1 F_2} \quad (\text{Simulation})$$

Coning simulation

A special type of simulation is required to model the coning of water or gas into a producing well. The phenomenon is only local to the vicinity of the wellbore and the simulation must be concentrated around the wellbore area. For this region a radial geometry must be used.

The reservoir simulation of coning behavior will predict the changes with time and give a complete performance prediction for a well. The purpose of a coning study is usually to predict the performance of a well after matching history. In some reservoir studies, the purpose of a coning simulation is to study the completion of the well and try to determine the effects of various workover, stimulation, and recompletion plans. Coning simulation has been performed to set field rules for conservation in some cases.

Another common use of coning simulation is to develop pseudo-relative permeability curves for use in field scale 2-D or 3-D models. Since the field scale model cannot predict accurately coning behavior, this behavior must be studied separately in radial coordinates and the results of the coning study must then be put into the field scale model in the form of pseudo-relative permeabilities or other calculation procedure.

The purposes of coning study are to match history & describe the reservoir, predict, study workovers, set field rules, and develop kr curves for 2-D/3-D models.

A special type of reservoir simulator is required for coning simulation. It is necessary to use "implicit saturation" calculations in order to make practical simulation runs. We will describe the reason for this.

A typical simulation grid has small grids near the wellbore. These small grids are required to model the rapidly changing saturations and flow rates near the wellbore. An evenly spaced logarithmic spacing is usually used which represents the pressure gradient as a straight line with the logarithm of radius, at least for an ideal problem. This improves the accuracy of the calculations. Care should be taken not to take the first cell unduly small because this is the cell which has the highest velocities and is the most likely to be unstable.

We note that the velocity of the fluid flow is the greatest near the wellbore. But the pore volumes of the cells have the smallest values near the wellbore. this results in an extremely high through-put of fluids through a cell near the wellbore during a timestep. It is not unusual to have several hundreds of pore volumes of throughput in a cell during a timestep. the IMPES method tends to be very unstable with these high throughput rates. this instability results in oscillating solution values such as saturations. This oscillation usually leads to the solution "blowing up" and the solution becomes meaningless.

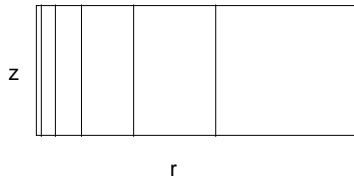


Fig. 7 - r vs Z plot

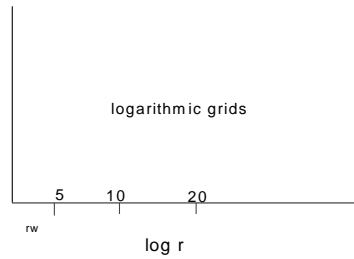


Fig. 8 - Logarithmic grids

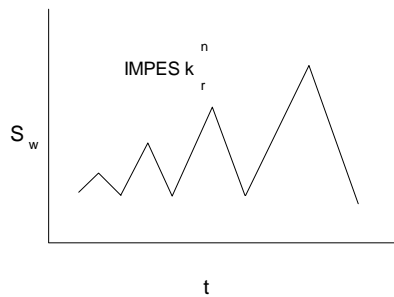


Fig. 9 - t vs S_w plot

Implicit simulators.

The solution to the stability problem is to treat relative permeability and capillary pressure implicitly. That is, to solve the timesteps with these values evaluated at the end of the timestep rather than at the beginning of the timestep. There are a number of published methods of performing the implicit calculations. The fundamentals of most of the methods involves extrapolating the old relative permeability to a new value by using a "chord slope" of the relative permeability curves multiplied times the saturation change.

The typical results from a coning simulation will be plots such as water/oil ratio versus time. If two or more rates are used for the simulation, it is important to re-plot the results on a cumulative production basis. If the water/oil ratio is the same for two rate cases when plotted on a cumulative oil production basis, then we would say that the cases are not rate sensitive. The higher rate does not damage the water/oil ratio performance of the well.

Implicit methods.

- (a) Solving k_r^{n+1} implicitly.
- (b) Solving P_c^{n+1} implicitly.

$$k_r^{n+1} = k_r^n + [(k_r^{n+1} - k_r^n)/(S_{n+1} - S_n)]*(S_{n+1} - S_n) \quad (7)$$

$$k_r^{n+1} = k_r^n + (\Delta k_r / \Delta S)*(S^{n+1} - S^n) \quad (8)$$

Solve this by various methods which solve ΔS simultaneously with Δp .

Types of Results

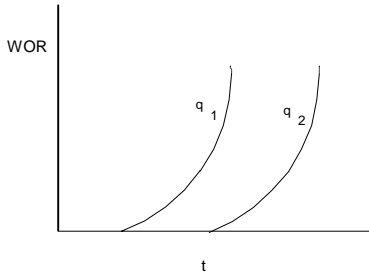


Fig. 10 - WOR vs Time plot

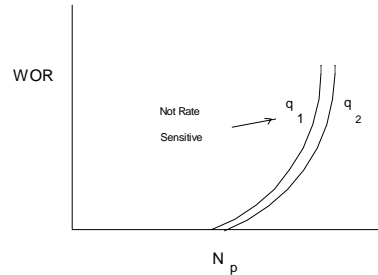


Fig. 11 - WOR vs N_p plot

An example of the application of a coning simulator can be found in an actual coning study that was performed. The reservoir was producing large amounts of water and it was important to determine whether a workover or recompletion was desirable.

In this case the water/oil ratio was not accurately known nor was the stratification of the reservoir known, at least away from the wellbore. Whether cross-flow was predominant or whether the layers were isolated was also not known. The stimulation runs were made with these uncertain variables varied for different cases. This is called a "sensitivity analysis". A number of simulation runs were made varying the rate, and completion interval along with different values of the uncertain reservoir parameters. The result of this sensitivity analysis was that none of the variables had much effect on the water/oil ratio performance within the limits that were investigated. Therefore, it was decided that a reduction in rate or a workover was not called for in this case.

Several rules can be applied to coning simulation. In the radial direction the spacing should be evenly spaced logarithmically near the wellbore. This the same as having each cell radius equal to the previous radius times a factor. For example, values of 2, 4, 8 would be an example of geometric spacing with a factor of 2.0. Near the outer boundary of the radial direction, the spacing should be more evenly spaced on a coordinate basis, because the pressure gradients tend to flatten rather than

being a semi-log straight with radius. The total number of grids in the radial direction is normally around eight to ten.

The vertical direction is very important in a coning simulation. Normally a well is stratified with layers that are roughly normal to the wellbore, so the vertical flow is similar to serial flow going through various layers of transmissibility. The vertical grid spacing should be chosen in a manner which describes the stratification of the well accurately. If the permeability profile of the wellbore can be represented by a "stair step" such as in the diagram in the sketch, then the vertical grids should coincide with the stair steps. If an impermeable break is identified, it should be located between cells, rather than in the middle of the cell.

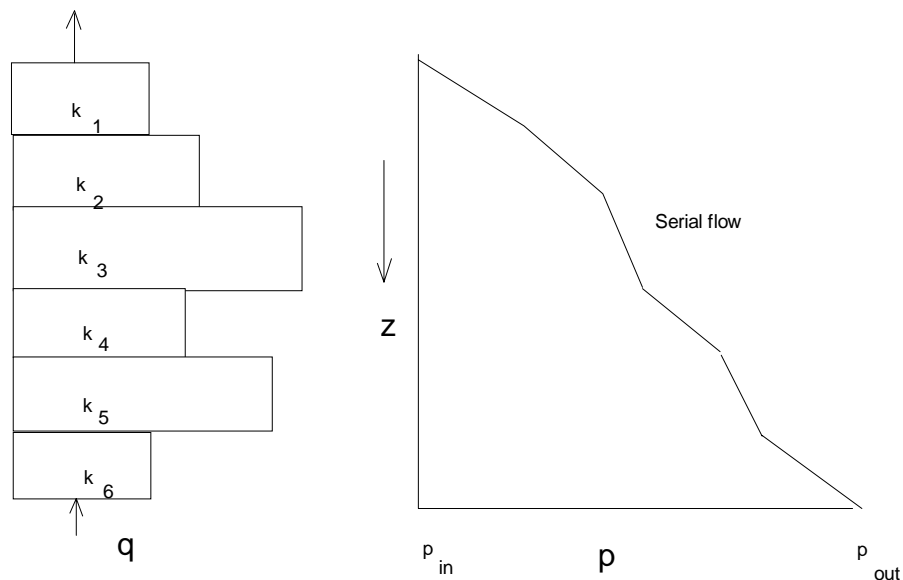


Fig. 12 - During Serial Flow add Δp 's

Because of the layered nature of a typical reservoir, horizontal flow tends to be parallel along the layers and the average horizontal permeability should include all of the layers that are contained within a cell.

The vertical flow in the layered reservoir tends to be serial flow through the layers. The correct vertical permeability for flow between vertical cells in a 3 -D model or radial model should be a harmonic average of the reservoir layers between the mid-points of adjacent simulator cells.

3-D or RADIAL

Horizontal:

$$\bar{k}_h = \frac{\sum k_h h}{\sum h} \quad (\text{arithmetic})$$

(9)

Vertical:

$$\bar{k}_v = \frac{\sum h}{\sum \left(\frac{h}{k_w} \right)} \quad (\text{harmonic})$$

(10)

The smallest permeability value dominates.

Addington's Method

This method shows how to obtain a correlation to predict gas coning behavior based on a radial numerical model which can be used in a 3-D coarse simulator. The correlation allows to predict not only the critical coning rate but also the GOR of a well after coning has been achieved.

Purpose - To develop a method to use in a 3-D coarse simulator.

- (a) Coning correlation for coarse 3-D.
- (b) Calibrate method with r-z coning runs.
- (c) Rate dependent GOR's above critical rate q_c .

Methodology

- (a) Do sensitivity analysis with coning simulator.

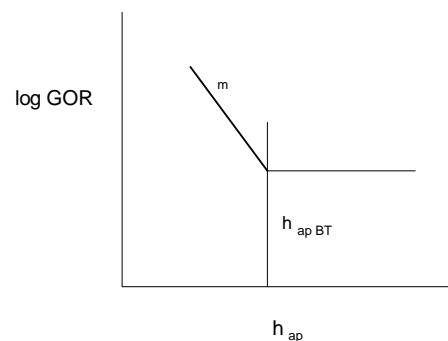


Fig. 13 - $\log(\text{GOR})$ vs h_{ap} plot

- (b) Do regression with h_{BT} , m for model parameters (q_t , h_p , k_h , k_v/k_h , etc.).
- (c) Correlate h_{BT} , m with these (model parameters).

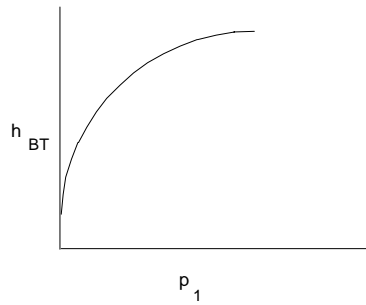


Fig. 14 - h_{BT} vs P_1 plot

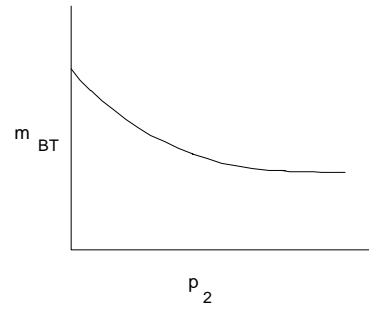


Fig. 15 - m_{BT} vs P_2 plot

$$P1 = q_t(k_v/k_h)^{0.1} \mu_o f_1 f_2 / (k_h * h_p^{1/2}) \quad (11)$$

$$F1 = (h_p + h_{ap}) / (h_p + h_{ap} + h_{bp}) \quad (12)$$

$$F2 = (\text{Acres}/160)^{0.1} \quad (13)$$

$$P2 = q_t(k_v/k_h)^{0.5} \mu_o F_1 F_3 / (k_h * h_p^{1/2}) \quad (14)$$

$$F3 = (\text{Acres}/160)^{0.5} \quad (15)$$

During 3-D simulation; each time step:

(a) Calculate h_{BT} , m , for q .

(b) Calculate elevation of current gas-oil contact GOC from saturations.

$$\sum_{k=1}^{k_{\max}} S_g V_p = \text{gas volume} \quad (15)$$

14

$$S_g = 1 - S_{wc} \quad (16)$$

$$S_g = 1 - S_{wc} - S_{or} \quad (17)$$

$$S_g = S_{gc} \quad (18)$$

Now suppose a fixed gas rate, $(q_g)_{\max}$, is produced from the same field. In this case, an optimal allocation of gas rates to individual wells would maximize total field oil rates. This problem can be stated as:

$$\text{Objective function:} \quad \text{maximize} \quad \sum (q_o)_i \quad (23)$$

$$\text{Constrain :} \quad \sum (q_g)_i = (q_g)_{\max} \quad (24)$$

The maximum field rate for oil might be a pipeline capacity, and the maximum field rate for gas might be a plant processing capacity.

Optimization criterion

The development of an optimization algorithm requires that the optimal solution be recognized by some criterion. This criterion was developed by deduction and was stated as follows:

$$(dq_g / dq_o)_i = (dq_g / dq_o)_j \quad i, j = 1, \dots, n \quad (25)$$

It should be pointed out that $(dq_g/dq_o)_i$ is a derivative and not a GOR. This derivative shows the change in the gas rate with an incremental change in the oil rate and changes with rate under gas coning conditions.

This optimization algorithm can optimize actual field rates using well test data and can be used in a general 3-dimensional reservoir simulator to optimize well rates during simulation.

A typical plot obtained from this method:

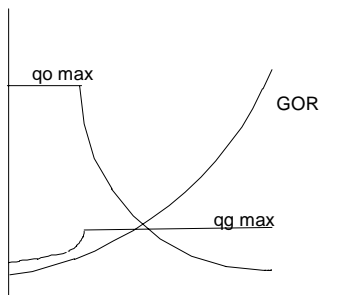


Fig. 17 - q_o , q_w , & GOR vs Time plot

Yang's approach to water coning problem

Following the same procedure as Addington did, Yang performed an extensive sensitivity analysis of water coning using numerical simulation. From this analysis an empirical coning correlation was developed; it predicts critical rate, breakthrough time and WOR after breakthrough.

This correlation provides a hand calculation method of coning prediction for both vertical and horizontal wells. It can also be used as a coning function for 3-D coarse grid reservoir simulation. The correlation was tested and found to be reliable in predicting WOR, critical rate, and breakthrough time when water-oil mobility ratio is smaller than 5 or viscous forces are not dominating.

As production proceeds, h_{bp} (height below perforations) decreases. At some point on time, water breaks into the wellbore, the average oil column height below perforation at this time is termed average oil column height below perforation at breakthrough, denoted by h_{wb} . After water breaks into the well, WOR increases as h_{bp} decreases.

As water cone moves up, critical rate gradually decreases. The following equations predict this **critical rate** for vertical and horizontal wells.

Vertical wells :

$$q_c = \frac{k_h k'_{ro} h^2 \Delta\rho / 144}{\mu_o} q_{cD} \quad (26)$$

Horizontal wells:

$$q_c = \frac{\sqrt{k_v k_h} k'_{ro} L h \Delta\rho / 144}{\mu_o} q_{cD} \quad (27)$$

where,

- q_c = critical coning rate, stb/D
- k_h = horizontal permeability, md
- k'_{ro} = oil relative permeability at S_{wc}
- μ_o = oil viscosity, cp
- $\Delta\gamma$ = water-oil gravity difference, psi/ft
- h = initial oil formation thickness, ft
- q_{cD} = dimensionless critical coning rate
- L = length of horizontal well, ft

For a tank reservoir, the h_{wb} correlation can be used to calculate water breakthrough time for vertical and horizontal wells.

$$t_{bt} = \frac{(N_p)_{bt}}{q_t} \quad (28)$$

For constant rate cases, WOR after breakthrough can be predicted from

Vertical wells:

$$\log(WOR + 0.02) = m (h_{bp} - h_{wb}) + \log(0.02) \quad h_{bp} \leq h_{wb} \quad (29)$$

Horizontal wells:

$$\log(WOR + 0.25) = m (h_{bp} - h_{wb}) + \log(0.25) \quad h_{bp} \leq h_{wb} \quad (30)$$

REFERENCES

1. Addington, D.V., "An approach to Gas-Coning Correlations for a Large Grid Cell Reservoir Simulator" JPT November 1981.
2. Yang W., Wattenbarger R.A., "Water Coning Calculations for Vertical and Horizontal Wells" SPE 22931
3. Urbanczyk, Christopher H., Wattenbarger, R.A., "Optimization of Well Rates under Gas Coning Conditions" SPE 21677

EXERCISES

RESERVOIR SIMULATION

CLASS PROBLEM NO. 41 (CONING FUNCTIONS)

Use the Addington method and correlation to do the following:

- a. Calculate q_o critical
- b. Draw GOR curve for this rate
- c. Calculate GOR at $2 \times q_o$ critical
- d. Draw the GOR vs h_{ap} curves for both rates

Data:

$$k_v / k_h = 0.1$$

$$\mu_o = 5.0 \text{ cp}$$

$$kh = 1200 \text{ md-feet}$$

$$h_t = 500 \text{ feet}$$

$$h_{bp} = 0$$

$$h_p = 60 \text{ feet}$$

$$h_{ap} = 100 \text{ feet}$$

$$\text{Area} = 160 \text{ acres}$$

$$R_s = 850 \text{ scf/stb}$$

$$B_o = 1.42 \text{ rb/stb}$$

Reinject producing gas

RESERVOIR SIMULATION

CLASS PROBLEM NO. 95

Find k_h and k_v for each layer from the following core analysis.

layer	h	k_h	k_v
1	1	50	25
	1	10	5
	1	20	10
	1	100	50
2	1	200	100
	1	300	150
	1	50	25
	1	20	10
	1	10	5
3	1	5	2.5
	1	6	3
	1	8	4
	1	10	5
4	1	20	10
	1	100	50
	1	500	250
	1	10	5
5	1	50	25
	1	60	30
	1	80	40
	1	90	45

APPENDIX

- SPE 22931 "Water Coning Calculations for Vertical and Horizontal Wells"
- SPE 21677 "Optimization of Well Rates under Gas Coning Conditions"

CHAPTER 5

Compositional Simulation

- Introduction
- Applications
- PVT Behavior
- Equations for Compositional Simulation
- Regression of EOS Parameters
- Modeling of Surface Facilities
- Lab Tests
- Gas Cycling in Volatile Oil and Gas Condensate Reservoirs
- Vaporizing Gas Drive (VGD)
- Field Examples
- Fundamentals
 - Heavy Fraction Characterization
 - Pseudoization
 - Regrouping Scheme of Heavy Components
- Compositional Simulation
 - Heavy Ends Characterization
 - Default Fluid Predictions
 - Pre - Regression
 - Component Pseudoization
 - Regression
 - Initialization Data for VIP
 - Run Data for VIP
- Data Files

PVT Matching

- Fundamentals
 - Heavy Fraction Characterization
 - Pseudoization
 - Regrouping Scheme of Heavy Components
- Compositional Simulation
 - Heavy Ends Characterization
 - Default Fluid Predictions
 - Pre - regression
 - Component Pseudoization
 - Regression
 - Initialization Data For VIP
 - Run Data For VI
- Data Files
 - Heavy.dat
 - Heavy.eos
 - Default.dat
 - Regression.dat
 - Pseudo.dat
 - Pseudo.eos
 - Final.dat
 - Final.eos
 - Spe3i.dat
 - Spe3r.dat

Compositional Simulation

Introduction

In compositional simulation of oil and gas reservoirs equation-of-state (EOS) methods are seeing increasing usage over more traditional K-value methods for phase equilibrium calculations. It has been found by several authors that equations-of-state are, in general, not able to accurately predict reservoir fluid behavior using theoretical EOS parameters. It has been found that "tuning" the EOS (by modifying the EOS parameters) is required to adequately match laboratory derived PVT data.

In this chapter, we describe how an equation-of-state is "tuned" to match laboratory data using nonlinear regression. We present partial justification for modification of EOS parameters and then discuss some practical guidelines for efficient and meaningful fluid characterization. Although we will mention component pseudoization (lumping) since it is usually part of the fluid characterization process, the emphasis of this section will be on regression and not on pseudoization.

Most of the material presented in this text was obtained from Coats and Smart.¹

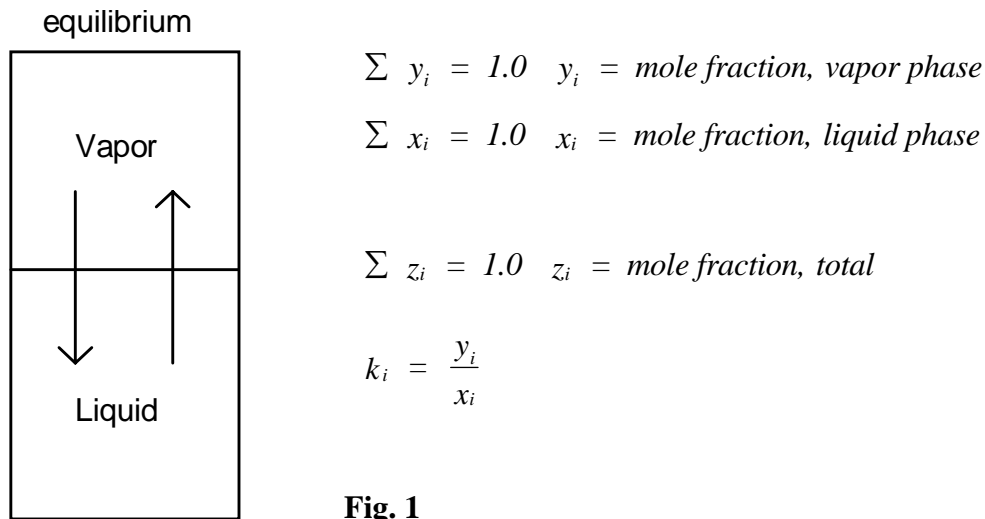
Applications

A compositional simulator is used in a variety of situations in which a black oil simulator does not adequately describe the fluid behavior. Each of the applications listed requires a special phase behavior computation and may require special laboratory analysis to determine the behavior of the fluids. Some applications are as follows:

- A) Volatile oil ($^{\circ}$ API changes, oil vaporizes)
- B) Miscible, EOR (CO_2 , LPG)
- C) Condensate (cycling, oil flows)
- D) Gas cycling (injection of dry gas)
- E) Injecting new fluid (N_2)

PVT Behavior

The PVT behavior of the reservoir fluids must be well understood in order to do a competent job of compositional simulation. We will briefly review some of the fundamentals. At any particular time, a mixture of fluids may be in a vapor-liquid equilibrium at a particular temperature and pressure. For most reservoirs the temperature can be considered to be constant. The variation of the equilibrium with pressure and also with composition is also important. When the vapor and liquid phases are in equilibrium, the molecules of each component are condensing and vaporizing at the same rate as shown in Fig. 1. The equilibrium can be described by x , y , and z values for all the components. A K-value can be calculated for the equilibrium for each component.



Prediction of PVT Behavior. The K-values have different patterns that can be observed. It is common to see a log-log plot of K vs. p which shows a family of curves tending to converge to a K-value of 1.0 at a "convergence pressure" as in Fig. 2. The behavior of this family of curves depends on the composition as well as on temperature and pressure. For example, the amount of intermediate hydrocarbons has a significant effect on convergence pressure.

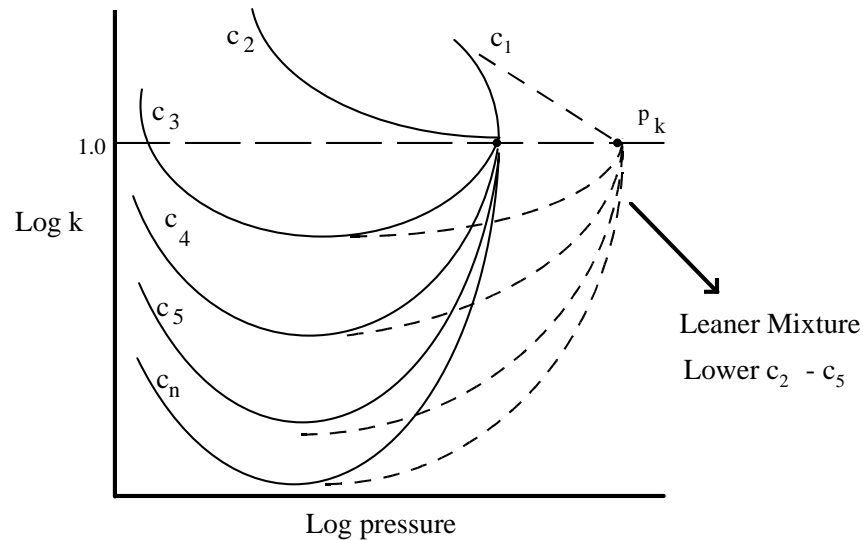


Fig. 2

Several methods are commonly used in compositional simulators to model the phase behavior. K-value methods can be used with a systematic method of modifying convergence pressures with compositions. Equation of state methods are also in common usage and have the advantage of predicting densities as well as the molecular equilibrium.

Much research has been directed toward predicting phase behavior given temperature, pressure and composition. However, for reservoir simulation studies laboratory composition data is almost always available for the mixtures expected to occur in the reservoir. For that reason, it is not as important to predict fluid behavior because the computational procedure must be modified to match the laboratory data. All of the phase behavior methods use various parameters that can be adjusted to accomplish the match of the laboratory data. It should be noted that a simulator using an equation of state method can run as much as ten times slower than a simulator using the K-value methods. This loss of computer efficiency tends to offset the advantages of the equation of state methods. Some simulation engineers use equation of state methods to match laboratory data and then convert to K-value methods with independent density calculation methods for the reservoir simulation runs.

PVT Prediction Methods. The methods used for PVT prediction are as follows:

- 1) K-value, p_k (convergence pressure) method.(This method is faster and can be matched with lab data and EOS , but it needs correction for the density of oil and the density of gas)
- 2) Equation of State method (EOS).(It matches more accurate with the lab data and we can get the density of oil and gas)
 - a) Peng-Robinson
 - b) Redlich-Kwong

Equations for Compositional Simulation

Mass Balance. The basic equations for compositional simulation are mass balance equations for each of the components. In addition to these mass balances, it is required that saturations sum to 1.0 and the phase behavior be consistent with temperature, pressure and compositions at each cell. The mass balance equation and other conditions applicable for component i are:

1) Mass balance equation :

$$\nabla \bullet (\hat{y}_i \rho_g \vec{u}_g) + \nabla \bullet (\hat{x}_i \rho_o \vec{u}_o) = - \frac{\partial}{\partial t} [\phi (S_o \rho_o \hat{x}_i + S_g \rho_g \hat{y}_i)] \quad (1)$$

vapor flow + liquid flow = storage

$\hat{y}_i, \hat{x}_i = \text{mass fractions of vapor, liquid}$

where

2) The saturation relationship is:

$$\sum S_{o, g} = 1.0 \quad (2)$$

3) Darcy's Law and Martin's Equation apply.

4) The phase behavior is:

$$\rho_o, \rho_g, \mu_o, \mu_g = f(p, T, x_i, y_i, z_i) \quad (3)$$

Equations of State. An equation-of-state (EOS) is an equation which expresses the relationship between pressure, temperature and volume of a gas or liquid. These equations are usually of cubic form. Two EOS widely used in the petroleum industry today are the Peng-Robinson² (PR) and Soave-Redlich-Kwong³ (SRK) EOS.

Van der Waals Equation. One of the earliest attempts to represent the behavior of real gases by an EOS was by van der Waals. His equation was:

$$(p + a/V_M^2)(V_M - b) = RT \quad (4)$$

where a and b are characteristics of the particular gas, R is the universal gas constant, and V_M is the molar volume.

Peng - Robinson Equation. Peng and Robinson later proposed the following:

$$\left[p + \frac{a_T}{V_M(V_M + b) + b(V_M - b)} \right] (V_M - b) = RT \quad (5)$$

The coefficients for Eq.5 are calculated by:

$$a_T = a_c \alpha \quad (6)$$

$$A_C = 0.45724 \frac{R^2 T_C^2}{P_C} \quad (7)$$

$$\alpha^{1/2} = 1 + m(1 - T_r^{1/2}) \quad (8)$$

$$b = 0.07780 \frac{RT_c}{P_c} \quad (9)$$

$$m = 0.37464 + 1.54226\omega - 0.26992\omega^2 \quad (10)$$

Soave-Redlich-Kwong Equation. The Soave-Redlich-Kwong equation has the form:

$$\left[p + \frac{a_T}{V_M(V_M + b)} \right] (V_M - b) = RT \quad (11)$$

$$a_c = 0.42747 \frac{R^2 T_c^2}{P_c} \quad (12)$$

$$b = 0.08664 \frac{RT_c}{P_c} \quad (13)$$

$$m = 0.480 + 1.574\omega - 0.176 \omega^2 \quad (14)$$

where the Pitzer acentric factor is given by:

$$\omega = -(\log p_{vr} + 1) \quad (15)$$

Here p_{vr} is the reduced vapor pressure, evaluated at $T_r = 0.7$.

These EOS contain coefficients and parameters which have theoretically derived values. For example, the theoretical values of Ω_a , Ω_b in the PR and SRK EOS are roughly 0.4572, 0.0778 and 0.4275, 0.0866, respectively. EOS also contain parameters, called binary interaction coefficients, which govern the interaction between all pairs of components in the mixture. These also have theoretically or experimentally determined values.

Regression of EOS Parameters.

It has been found by several authors that, in general, EOS with theoretical parameter values are incapable of accurately predicting fluid behavior of hydrocarbon mixtures commonly encountered in oil and gas reservoirs. Flexibility in the use of the EOS can be obtained by altering the EOS parameters or allowing them to change by component. The parameters most commonly changed are Ω_a , Ω_b and the binary interaction coefficients. By changing these parameters, the EOS can be forced to match laboratory measured data.

Although EOS parameters can be modified manually, they are usually determined using a nonlinear regression algorithm. One algorithm that is used in commercial software packages is an extension of the least-squares, linear programming (LSLP) method.⁴ The linear programming algorithm places global upper and lower limits on each regression variable v_i . Subject to these limits, the regression determines values of $\{v_i\}$ that minimize the objective function F defined as

$$F = \sum_{j=1}^{n_j} W_j \left| \left(d_j - d_{jC} \right) / d_j \right| \quad (16)$$

where d_{jC} and d_j are calculated and observed values of observation j , respectively, and W is a weighting factor.

Using the regression algorithm above and the guidelines contained in this text, it has been found that agreement between laboratory data and regressed EOS results is generally good to excellent.

Justification for Altering Theoretical EOS Parameters. Thus far, no justification has been given for alteration of the theoretical values of EOS parameters. In the following sections we present partial justification for the modification of EOS parameters for methane and the plus fraction.

Methane Fraction. The theoretical Ω_a and Ω_b values in both the PR and SRK EOS are based on the van der Waals conditions of $\partial p / \partial V = \partial^2 p / \partial V^2 = 0$ at the critical point. The component temperature functions in the SRK and PR EOS essentially reflect satisfaction of pure-component density and vapor-pressure data below critical temperature. At reservoir conditions, methane is usually well above its critical point, where there is no theory or clear-cut guide to selection or alteration of Ω 's. Since the theoretical values are based on p and T conditions far removed from the p and T conditions of interest, one could argue that the Ω 's for methane should be determined from matching of laboratory-derived PVT data in the p and T ranges of interest.

Plus Fraction. The primary argument for altering EOS parameters of the plus fraction is that the plus fraction, unlike all other components, is a mixture of many components.

General Procedure for Fluid Characterization. In this section, we describe the procedure commonly used to characterize a particular fluid for use in compositional simulation. Computer programs (such as Integrated Technologies' EOS-PAK) are available commercially which can

facilitate greatly the computations required in the following steps. Some or all of the following steps may be employed in a typical fluid characterization.

1. Decide if and how to split the plus fraction into extended fractions. The actual splitting is usually done using the method presented by Whitson⁵. There is some debate as to whether the mole fractions of the extended fractions should be roughly equal or decreasing (e.g., exponentially) with increasing molecular weight.

2. Pseudoize (lump) the components into a fewer number of pseudo-components. This is done primarily for economic reasons (fewer components results in faster run times and lower costs). The focus of this section is not on pseudoization; however, there are references available which offer some guidelines for optimal pseudoization.⁶

3. Match the laboratory expansion data using a nonlinear regression algorithm. The regression data set to be matched may include results from multiple fluid samples and results from tests run at different temperatures. In general, the regression data set should include all measured laboratory data. Any calculated data that are reported as part of a fluid analysis should not be included. The regression variable set should be chosen such that it possesses the characteristics of an optimal regression variable set.

4. Match the laboratory viscosity data using a nonlinear regression algorithm. The regression data set should include all measured viscosity data. The regression variable set should include only the critical z-factors (which affect viscosity only and do not affect the results of expansion tests).

5. At this point the EOS fluid characterization is complete, as all laboratory measured data have been matched. However, additional adjustments to the fluid data may be required before compositional simulation can be started. For example, it may be necessary to alter the initial fluid composition to match the initial saturation pressure or gas-oil ratio observed in the field. In addition, it may be necessary to determine the optimum separator conditions (only for predictive studies; for history matching, the actual separator conditions should be used).

Practical Considerations for Minimizing Splitting of C₇₊ Fraction. Coats and Smart found that extensive splitting of the C₇₊ fraction is not necessary to match laboratory data, in contrast to previous authors. In general, none to four splits of the C₇₊ fraction are all that are required. A general, *a priori* guide to the extent of C₇₊ splitting required can be obtained from the experimentally observed range of C₇₊ molecular weights during an expansion or multiple-contact test. The greater the range of C₇₊ molecular weights, the more C₇₊ fractions are required.

In addition, the degree of splitting is also affected by the anticipated recovery process. For example, gas cycling processes will require more splitting than depletion/waterflooding processes.

Minimizing Number of Regression Variables. Usually only five parameters - Ω_a and Ω_b for methane and the heaviest fraction and the methane/heaviest binary interaction coefficient - are necessary and sufficient for good matches of laboratory data. For the purposes of this discussion, the "heaviest" fraction is the heaviest single fraction used in the EOS calculations. For example, if the

original plus fraction, C_{7+} , is split into three components, say F_7 , F_8 , and F_9 , then F_9 is the new heaviest fraction as defined above.

A general rule for selecting regression variables is to exclude any EOS parameter that, by inspection, cannot affect significantly the calculated value of any of the regression data. For example, if the fluid composition in a regression data set has a very small amount of a particular component, then it would not make sense to include that particular component's Ω 's or binaries as regression variables. Conversely, it makes sense to include the EOS parameters of a component that is predominate (such as methane) in the fluid compositions.

Regression of Surface Separation Data. Coats and Smart found that regressed EOS surface separation results were the same regardless of whether surface separation data were included in the regression data set. In other words, an EOS tuned with only data at reservoir conditions will, in general, adequately predict surface separation data.

They did not address the opposite situation, i.e. whether including the surface separation data in the regression data set could harm the match of data at reservoir conditions. They implied that there was nothing wrong with including the separation data, but that it was not necessary. Of course, this applies only if the surface separation data are measured in the laboratory. Surface separation data presented in standard fluid analysis reports are commonly calculated (using K-values) and not measured. In general, calculated data (such as surface separation data) should not be included in a regression data set; only measured data should be included.

Characteristics of an Optimal Regression Variable Set. The characteristics of an optimal regression variable set are:

1. The regression converges,
2. The values that the variables converge upon are realistic (reasonably close to theoretical values),
3. Deletion of any member of the variable set results in either or both of (a) significantly worse data match and (b) unrealistic variable values, and
4. Addition of any other EOS parameter results in either or both of (a) nonconvergence and (b) insignificantly better data matches.

Nonconvergence is dependent on both the variable set and the regression data set. It may be possible to solve a nonconvergence problem by adding more data to the regression data set. For a fixed regression data set, the general remedy for nonconvergence is to simply remove one of the regression variables.

The general remedy for convergence to unrealistic variable values is to add another variable to the regression variable set. For example, although negative values of binary interaction coefficients may result in a good match of lab data, negative values are not reasonable. It may be possible, by adding another regression variable, to obtain an equally good match of the lab data with more reasonable positive interaction coefficients.

From personal experience, it has also been determined that (1) convergence and (2) realistic variable values are also affected by the weighting factors assigned to the various regression data items. It may be possible to fix problems with either or both of these characteristics by changing the weighting factors assigned to certain data items (e.g. assigning lower weighting factors to data that are suspect).

If a poor data match results from a regression that satisfies the above criteria for an optimal regression variable set, then this indicates either erroneous data or inadequacy of the EOS to match the particular fluid data (it may be difficult to distinguish between the two). It is sometimes possible to detect erroneous data by simple mass balances on CVD data and/or surface separation data.

Example Applications. Examples of EOS regression to match laboratory data are presented by Coats and Smart¹ and the third SPE comparative solution project, SPE 12278.⁷

Modeling of Surface Facilities

Fig. 3 shows how a compositional simulator models the surface facilities as well as the reservoir performance.

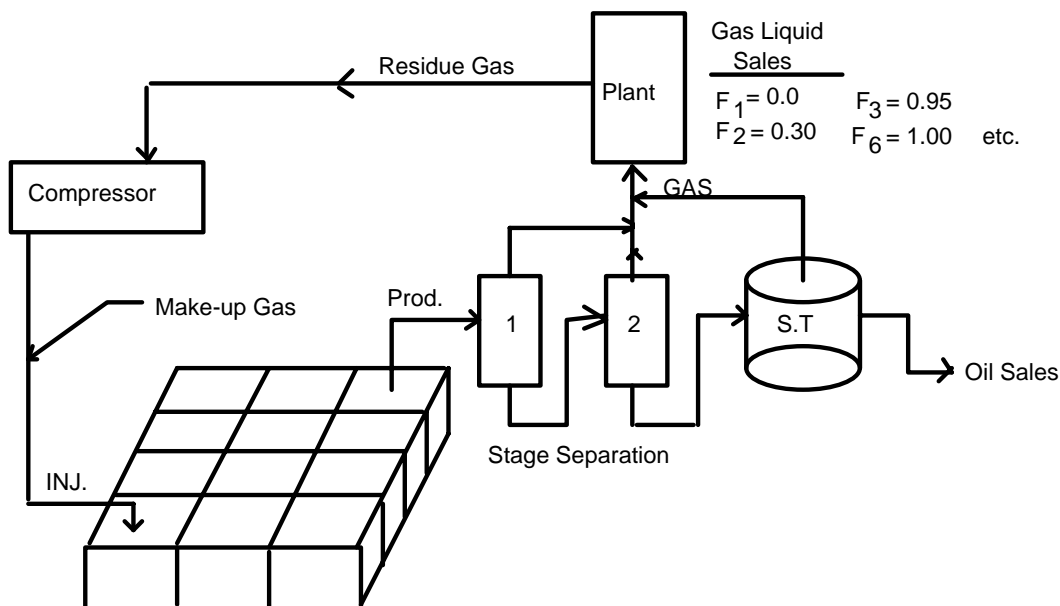


Fig. 3

The producing fluid is separated with stage separation to improve the oil recovery. The separator calculation must be performed at the separator temperature and pressure given. The separator liquid goes to the stock tank and is sold as oil.

The separator gas then continues to a gas liquids plant which strips the gas liquids from the input stream. This is modeled by specifying a fraction of each component which is recovered as gas liquids.

The remaining residue gas may be re-injected into the reservoir after compression to a suitable injection pressure. It may be necessary to add make-up gas to the gas injection in order to compensate for shrinkage after liquid removal.

The simulation of the surface facilities as well as the reservoir performance makes this a very interesting project. The optimization of the operations might include runs in which the plant configuration is modified as well as runs with the usual injection and production parameters modified.

would result in no residual oil saturation if this could be accomplished in the reservoir, but this test is only applicable for constant composition.

Fig. 5 shows a phase diagram for a constant composition fluid. For this fluid, the nature of constant composition expansion depends on the temperature of the fluid. This figure shows a bubble point fluid at low temperatures and a fairly dry condensate which vaporizes completely during pressure decreases at higher temperatures.

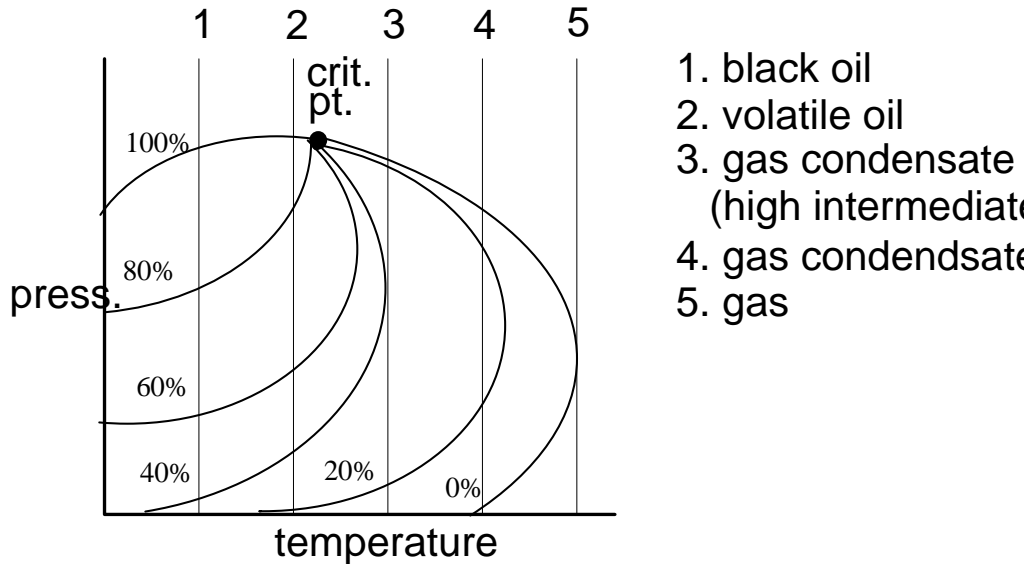


Fig. 5

Fig. 6 presents a family of curves which represent the pressure traverses of the various temperatures shown in Fig. 5. For the first two temperatures, bubble points are observed. The second temperature has greater shrinkage since it is closer to the critical point. At temperatures above the critical temperature, the dew point elevates with increases in temperature and then decreases with further increases in temperature. At the highest temperature, the liquid completely vaporizes with pressure reduction.

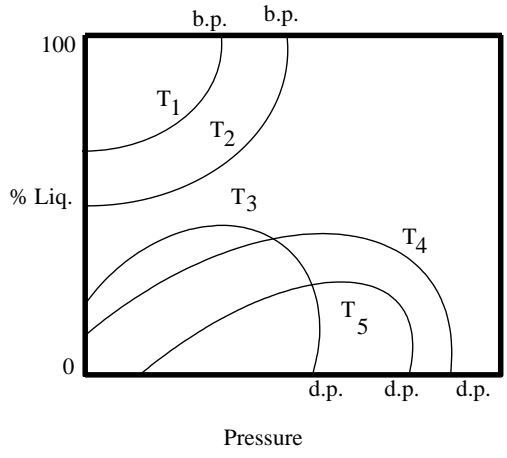


Fig. 6

Behavior of the constant composition expansion is useful in understanding reservoir fluid behavior. It is important to match this behavior with the simulator. However, the composition of the reservoir fluid during depletion usually changes dramatically when two phase flow occurs.

Constant Volume Depletion Test. Fig. 7 depicts a constant volume depletion test (or simply, depletion test). This test is normally done for a dew point fluid. This is a test which approximates the constant reservoir volume fluid expansion.

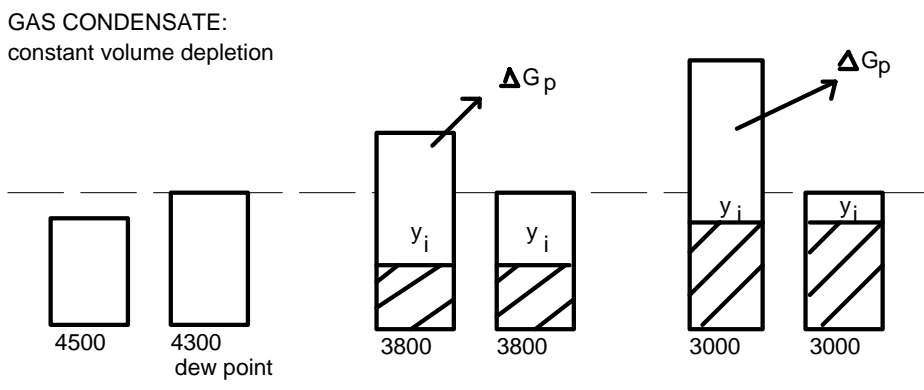


Fig. 7

For this case, gas is withdrawn at pressures below the dew point, representing gas production from the reservoir. Liquid is not taken out of the PVT cell because liquid usually does not flow in the reservoir. Rather than "bleeding off" the reservoir gas, the gas production is taken out of the PVT cell at discrete intervals. By performing the test in this manner the exact composition of the equilibrium gas is known at the pressure at which the gas is withdrawn. This composition is measured from the produced gas at that particular pressure. The liquid composition cannot be

measured without destroying the sample, but it can be calculated from a material balance. Experimental errors affect the accuracy of the material balance, however.

The standard results of this test are direct measurements which are represented by three sketches shown in Fig. 8.

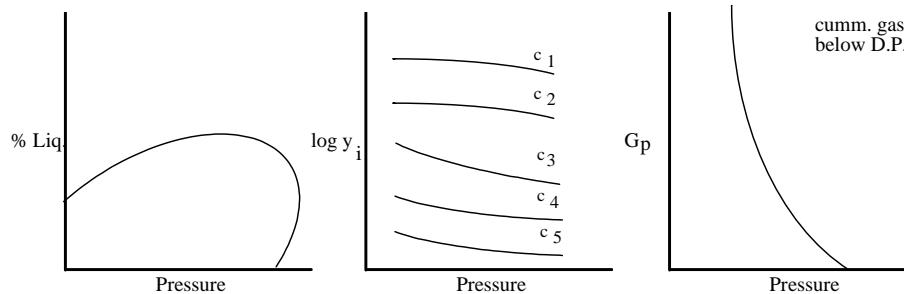


Fig. 8

The liquid percent curve can be modified to show oil saturation by accounting for the connate water saturation. The composition of the producing gas stream is presented and can be used to calculate the gas-oil ratio or gas-liquid ratio in the producing stream during depletion. And finally, the cumulative gas production shows how pressure declines with gas production. These three curves must be matched with the simulator to validate the phase behavior and fluid property calculations. The liquid density is not measured directly, nor is the gas density. The validation of the simulator includes the density calculations as well as the phase equilibrium calculations.

The surface separation and calculation of the gas-oil ratio must also be calculated by the simulator during the simulation runs. This information is usually reported in the depletion laboratory test results. These calculations are relatively simple because NGAA K-values can usually be used at surface conditions.

Gas Cycling in Volatile Oil and Gas Condensate Reservoirs

Introduction. Gas cycling is a process used widely in volatile oil and condensate reservoirs for primarily two reasons - for pressure maintenance, where pressures have fallen off due to depletion and to enforce a miscible displacement process to achieve higher recoveries. In principle, the process involves re-injection of produced gas into the reservoir so that reservoir pressures are increased and a miscible displacement is initiated. A schematic of the gas cycling process is shown in Fig. 9. Volatile oil and condensate reservoirs are characterized by reservoir fluids that are composed primarily of a light oil and a rich gas. Typically these fluids are composed of 50-70 mole percent of methane (C_1), 20-30 mole percent of intermediates (C_2-C_6) and 10-20 mole percent of heavies (C_{7+}). Gravity of the stock tank oil ranges from 42° to 60° API. Characteristic gas-oil ratios range from 1200-3500 SCF/STB for volatile oil reservoirs and from 8000-30000 SCF/STB for retrograde condensates. Approximate ranges of reservoir and fluid characteristics are summarized in Table 1 (page 20). When the reservoir pressure falls below saturation pressure, due to depletion, the reservoir oil is in equilibrium with a rich gas. The oil tends to be heavy with high viscosities and low mobilities. The process of gas cycling is designed to exploit the gas phase mobility compared to that of the oil. Methane from the produced gas is recycled back into the reservoir. Sometimes, methane is mixed with small fractions of intermediate gases before re-injection. Surface facilities required for this include a gas plant to which part or all of the separator gas is sent, which is pressurized with a compressor and re-injected into the reservoir.

Displacement Process. The injected lean gas miscibility displaces the in-situ rich gas toward the producing well. The liquid generally does not move due to unfavorable mobility ratios. Also the oil saturation can drop below the residual oil saturation. However, the oil vaporizes behind the displacement front. The intermediates in the oil vaporize due to the contact with the injected lean gas. This vaporization process "strips" the reservoir liquid of its intermediates which are then transported in the gas phase to the producer. This miscible process is referred to as a multiple contact miscible process (also called developed miscibility) as opposed to a first contact miscible process. If the reservoir fluid is considered as being composed of three pseudo components (C_1), intermediates (C_{2-6}) and heavies (C_{7+}), a ternary diagram can be used to represent the reservoir fluid and the displacement process at a given temperature and pressure. Two fluids are considered first contact miscible if all possible mixtures of the two yield a single phase fluid at a given pressure and temperature. If the path connecting the injected gas composition and the reservoir oil composition does not pass through the two phase region, the process is termed first contact miscible. This path is known as the dilution path and represents the composition changes as the injected gas displaces reservoir oil. In doing so, we are neglecting the pressure change that is, of course, an essential ingredient in making the fluids flow in the reservoir. Ternary diagrams represent constant pressure and temperature conditions, but illustrate the mechanics of a miscible displacement process.

An Example of Compositional Simulation - Gas Cycling. A typical example of compositional simulation is found in gas cycling performance. Fig. 9 shows that the reservoir pressure has dropped below the dew point and an oil saturation has developed. Below the dew point the reservoir liquid will be in equilibrium with a rich reservoir gas. During gas cycling a dry gas (mostly methane) is

injected. The dry gas miscibly displaces the rich gas toward the producing wells. The liquid normally does not move because it is below the residual oil saturation. However, the oil does vaporize behind the displacement front. The lighter ends of the oil vaporize because of the contact with the dry injection gas instead of the rich reservoir gas that it previously contacted. As this vaporization continues, the oil saturation decreases and a significant amount of the oil components are transported to the producing wells in the gas phase.

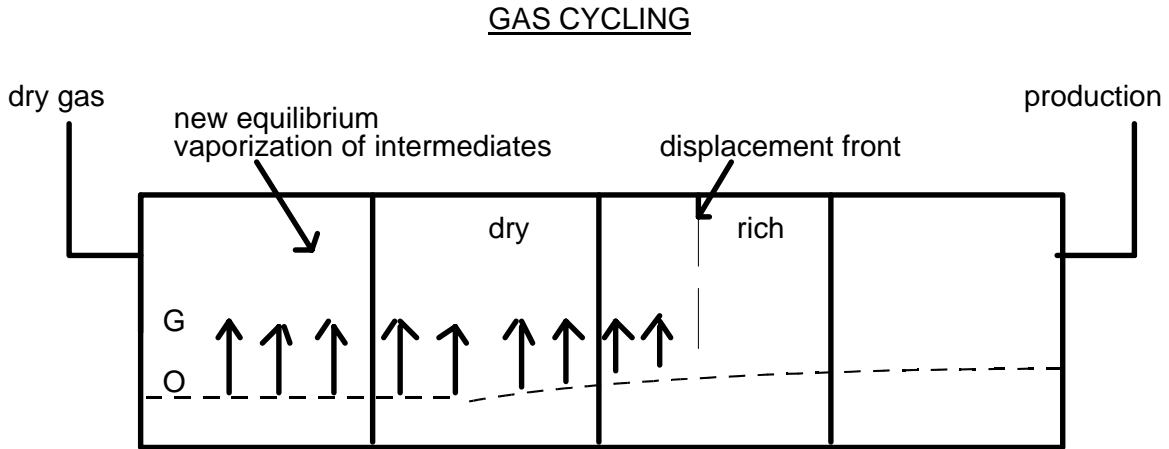


Fig. 9

This gas cycling process is modeled with a compositional simulator. The displacement mechanism is modeled simultaneously with the phase behavior.

Vaporizing Gas Drive (VGD)

If the dilution path does pass through the two phase region, the process is no longer first contact miscible. Imagine a series of well mixed cells that represent the permeable medium in a one dimensional displacement. The first cell initially contains crude to which we add an amount of solvent so that the overall composition is given by M_1 . The mixture will split into two phases, a gas G_1 and a liquid L_1 , determined by equilibrium tie lines. The gas G_1 will have a much higher mobility than L_1 , and this phase moves preferentially into the second mixing cell to form mixture M_2 . Liquid L_1 remains behind to mix with more pure solvent (injected gas). In the second cell mixture, M_2 splits into gas G_2 and liquid L_2 (again determined by the equilibrium tie lines), G_2 flows into the third cell to form mixture M_3 , and so forth. At some cell beyond the third (for this diagram), the gas phase will no longer form two phases on mixing with the crude. From this point onward, all compositions in the displacement will be on a straight dilution path between a crude and a point tangent to the binodal curve. The displacement from here on will be first contact miscible, with the solvent composition given by the point of tangency. The process has developed miscibility since the solvent has been enriched in intermediate components to be miscible with the crude. Since the intermediates are vaporized from crude, the process is a vaporizing gas drive. Miscibility will develop in this process as long as the injected solvent and crude are on opposite sides of the critical tie line. A schematic of vaporizing gas drive is shown in Fig. 9.

The injected fluid and reservoir fluids form a "mixing zone" in the reservoir, as the injected solvent moves further into the reservoir. The point of miscibility is at the front of the mixing zone. The key characteristics of a VGD can be summarized as:

- 1) Reservoir oil transfers intermediates to injected lean gas.
 - 2) Point of miscibility is at front of the mixing zone.
 - 3) Miscibility is achieved by progressively contacting generated gas composition with fresh oil.
- Figure 9 shows a saturation profile of the injected gas as it travels from the injector toward the producer. Note the vaporization of the intermediates, the location of the mixing zone and the point of miscibility in the reservoir.

Reservoir Simulation Aspects. Simulation of gas cycling processes requires a compositional model to track the phase behavior of the fluids along with modeling displacement fronts. Current compositional models are highly sophisticated; they use both equation-of-state and K-value options to model phase equilibria within the reservoir. A major part of such a study is phase behavior matching, where laboratory tests on reservoir fluids are simulated by forcing equation-of-state parameters or K-value correlations to match observed laboratory behavior.

Economic Considerations. As in all oil field operations, economic considerations dictate whether gas cycling should be employed over other methods, i.e. waterflooding. Gas cycling involves investment in surface facilities: gas plant to re-inject residue gas. However, in volatile oil and condensate reservoirs, gas cycling has potential to yield higher ultimate recoveries than a waterflood and has greater long term profit potential. Reservoir simulation is an important tool in such cases to assess the viability of different recovery schemes.

Field Examples

Three field simulation studies are summarized in this section. All three reservoirs are retrograde reservoirs. In each case, gas cycling was used for a variety of reasons. However the underlying mechanism of displacement is the vaporizing gas drive as described earlier.

Carson Creek Field, Alberta. The Carson Creek field is a retrograde gas condensate field of Central Alberta, discovered in 1957. The field encompasses about 18,000 acres and has two gas pools, "A" and "B". The original gas-in-place in the two pools was about 400 BSCF. Methane constituted 70.2 mole percent of the original reservoir fluid. Gas cycling operations began in 1962; original gas cycling operations consisted of processing between 70 and 90 MMSCF/D raw gas to extract about 4,000 STB/D condensate and re-injecting all residue gases into the reservoir. The cycling also processed 5 to 10 MMSCF/D solution gas from an adjacent field and was re-injected. Gas cycling was employed in this field for both pressure maintenance and to carry out a miscible flood.

A compositional simulator was used to simulate gas cycling in this field. The model uses K-values as a function of temperature, pressure and composition to model phase equilibrium. Density, viscosity and compressibility of the fluids were treated as functions of composition and pressure. History matches of production, injection and pressure in each well were obtained. Also, a match of the pentanes-plus composition of each produced well stream was obtained.

Bonnie Glen D 3-A Pool Model, Alberta. The Bonnie Glen D 3-A pool, is one of the most prolific fields in Canada. The original oil in place is estimated at 6.57 MMSTB, with an initial gas cap of 44.5 MMSCF. Since simultaneous production of gas cap during the life of the oil column could be detrimental to oil recovery, gas cap production would normally be deferred until depletion of the oil column. Gas cycling can however, can be carried out concurrently with continued depletion of oil column with a beneficial effect on the overall recovery of hydrocarbon liquids. The increase in recovery results from vaporization of retrograde liquids in the gas cap plus vaporization of lighter components from the original oil column.

A three dimensional three phase black oil simulation study was first conducted to history match the reservoir performance. This was followed by conversion to a compositional formulation. The compositional formulation used K-value correlations to model phase equilibria.

Kaybob South Field , Alberta. The Kaybob South Field is one of the largest oil fields in Canada. Initial gas in place in the field was estimated at 4,000 BSCF. The reservoir encompasses an area of 57,000 acres and is totally underlain by water (bottom water drive). Because of the possibility of significant retrograde liquid losses upon depletion, it was decided to implement gas cycling in the field. Reservoir simulation was used to design the gas cycling project and study its potential impact. The design and planning of the cycling project began in 1967, without full delineation of the reservoir limits. Several cycling patterns were simulated (involving different injection well patterns). The effect of different cycling rates was also studied by simulating various cases. Studies were undertaken to determine the degree of revaporization expected from cycling with residue gas.

Table 1

Reservoir Fluid Characteristics for
Volatile Oils and Retrograde Condensates

Fluid Classification	Volatile Oils	Gas Condensates
Stock tank oil color	Greenish to orange	Yellowish
Stock tank oil gravity °API	42-45	45-60
Gas-oil ratio, SCF/STB	1200-3500	8000-30000
Formation volume factor, B _o	1.7-3.0	6.0-20.0
Typical reservoir temperature, °F	150-300	150-300
Typical saturation pressure, Psia	3000-7500 (Bubble Point)	1500-9000 (Dew Point)

PVT MATCHING

Fundamentals:

Heavy Fraction Characterization. During the development of the application of EOS's to naturally occurring hydrocarbon mixtures, it has become clear that insufficient description of heavier hydrocarbons (e.g., heptanes and heavier) reduces the accuracy of PVT predictions. Volatile oil and gas-condensate volumetric phase behavior is particularly sensitive to composition and properties of the heaviest components. Therefore we have to develop a comprehensive method to characterize compositional variation, which we call "molar distribution". A three-parameter gamma function was chosen for describing molar distribution.

$$p(x) = \frac{(x-h)^{a-1} \exp[-(x-h)/b]}{b^a \Gamma(a)} \quad (1)$$

$p(x)$ is called the probability density function (or three parameter gamma function). Whereas x corresponds to measured C_{7+} molecular weight. For $a = 1$, the distribution is exponential. Values less than one give accelerated exponential distribution, while values greater than one yield left-skewed distributions. Note that as 'a' approaches infinity, the distribution becomes normal, though "folded" at h , the minimum molecular weight included in the C_{7+} fraction.

a , b , and h are parameters defining the distribution. h can be estimated accurately since it represents the minimum molecular weight to be included in the fraction. If a is given, b is found directly from h , a , and the measured C_{7+} molecular weight, M_{7+} . a can be fitted to measured molar- and weight-distribution data, or estimated using an empirical relation.

The parameter h is defined as the minimum molecular weight expected to occur in the C_{n+} fraction. That is, there is zero probability [$p(x) = 0$] for occurrence of compounds with molecular weight less than h . If the C_{7+} is considered, then $h = 92$ (the molecular weight of toluene) would be a good estimate for h . Experience has shown that a good approximation of h is given by

$$h = 14n - 6 \quad (2)$$

for a C_{n+} fraction. Eq. 2 is a useful empirical relation but should not be considered a restraint on the model.

Considering the remaining two parameters in Eq. 1, a and b , a useful property of the three-parameter gamma function is that the product ab equals the arithmetic average molecular weight, M_{n+} , minus h .

$$M_{n+} - h = ab \quad (3)$$

where M_{n+} is measured directly.

There are several empirical correlations available for estimating a from randomly sampled data such as fully extended molar distribution. b is easily calculated from the other variables.

$$b = (M_{n+} - h)/a \quad (4)$$

An estimate of a can be calculated using the following proposed empirical relation.

$$a = Y^{-1} (0.5000876 + 0.1648852Y - 0.0544174Y^2) \quad (5)$$

where,

$$Y = \ln[(M_{n+} - h)/m_G] \quad (6)$$

and

$$m_G = \left[\prod_{i=n}^N (M_i - h)^{Z_i} \right]^{1/Z_{n+}} \quad (7)$$

Eq. 5 is valid for $0 < Y < 0.5772$ (i.e., $a \geq 1.0$). The variable m_G merely represents a geometric average molecular-weight variable. For Eq. 5 to be useful for the molar distribution problem, it is necessary to have measured SCN (single-carbon-number) mole fractions and molecular weights accurately. They should also constitute a full compositional analysis, preferably having a diminishing or negligible quantity of the last fraction, N. Since such analyses are nearly nonexistent, a set of correction tables has been developed when only partial analyses are available (the limitation of $a \geq 1.0$ mentioned previously is also lifted in the present use of Eq. 5).

Due to the limitation of the Eq. 5, we may determine a by minimization of a error function. The error function, $E(a)$, used to optimize a is defined as the sum of the squares of differences in measured and calculated compositions and is given by

$$E(a) = \sum_{i=n}^N (Z_i - \bar{Z})^2 \quad (8)$$

If a molar distribution is to fit, and

$$E(a) = \sum_{i=n}^N (f_{wi} - \bar{f})^2 \quad (9)$$

if a weight distribution is to fit (the more common case). Calculated values are marked with a tilde.

The minimization of E may proceed by a simple secant or half-interval method. Two procedures for performing the minimization have proved useful. Reasonable limits for a are 0.5 to 3.0.

The probabilistic model is not a true physical model. One assumption is the continuous relation between molecular weight and mole fraction. This assumption, however, along with others implicit in its mathematical form, seems as reasonable as, for example, the assumption in distillation (TBP) analysis that cumulative volume and boiling point have a continuous relation.

In the DESKTOP-PVT package, at least three numbers, molecular weight, specific gravity and mole (or weight) fraction of the heavy fraction must be entered for heavy fraction characterization.

The extended analysis can be entirely predictive or can be compared to experimental distillation data. If distillation data of mole (or weight) fraction distillation are available, an option can be activated to compute an optimal. This will minimize the differences between the experimental and calculated distributions.

The gamma distribution function gives the mole (or weight) fraction and molecular weight for each single carbon number (SCN) of the extended fractions. The calculated mole fraction and molecular weight of the last carbon number in the extended analysis are adjusted so the computed mole fraction and molecular weight of the heavy fraction are matched to the observed data. The gamma function can be calculated using either a constant molecular weight interval or variable molecular weight intervals.

A constant Watson characterization factor, K , is used for all carbon numbers in the heavy fraction. K defines relative paraffinicity of a hydrocarbon fraction, with a typical range from 10.0 (highly aromatic) to 13.0 (highly paraffinic). If a Watson factor is entered, the input number is used to compute the specific gravity of all carbon numbers. If a Watson factor is not entered, this number is adjusted so the computed specific gravity of the heavy fraction is matched to the observed.

Pseudoization. The term "pseudoization" here denotes the reduction in number of components used in EOS calculations for reservoir fluids. Pseudoization is important in reservoir calculations because of the large number of real components (e.g. in C_{7+} fraction) in reservoir fluids. Compositional model computing times can increase significantly with number of components used.

Pseudoization must satisfy the following conditions:

- 1) EOS calculation will yield identical density (Z -factor) and viscosity for each pseudo component whether performed in a) single-component mode, or b) n -component mode.
- 2) For all mixtures of the m pseudo components (including the original mixture z), the EOS calculations will yield identical mixture density and viscosity whether performed in a) m -pseudo component mode or b) n -component mode.

The first of the two pseudoization conditions is satisfied by defining pseudo component properties as:

$$A^{(l)} = \Omega_a^l p (T_c^{(l)})^2 / T^2 p_c^{(l)} = \sum_{i=1}^n \sum_{j=1}^n x_i^{(l)} x_j^{(l)} (1 - d_{ij}) (A_i A_j)^{0.5} \quad (10)$$

$$B^{(l)} = \Omega_b^l p T_c^{(l)} / T p_c^{(l)} = \sum_{j=1}^n x_j^{(l)} B_j \quad (11)$$

$$P_c^{(l)} = \sum_{j=1}^n x_j^{(l)} P_{cj} \quad (12)$$

$$T_c^{(l)} = \sum_{j=1}^n x_j^{(l)} T_{cj} \quad (13)$$

$$v_c^{(l)} = \sum_{j=1}^n x_j^{(l)} v_{cj} \quad (14)$$

$$M^{(l)} = \sum_{j=1}^n x_j^{(l)} M_j \quad (15)$$

$$m^{*(l)} = \sum_{j=1}^n x_j^{(l)} m_j^* M_j^{0.5} / \sum_{j=1}^n (x_j^{(l)} M_j^{0.5}) \quad (16)$$

The Ω_a and Ω_b appearing in Eqs. are "theoretically" universal constants, determined by forcing the EOS to satisfy the Van der Waals conditions: $(dp/dv)_{T_c}$ and $(d^2p/dv^2)_{T_c} = 0$ at the critical point. In practice, however, the Ω_a , Ω_b values are generally treated as component-dependent functions of temperature.

The second condition of pseudoization is satisfied by Eqs. 10 through 16 and the additional requirement that for each pair of pseudo components, the pseudo binary interaction coefficient is given by

$$\sum_{i=1}^2 \sum_{j=1}^2 a_i a_j (1 - d^{ij}) (A^{(i)} A^{(j)})^{0.5} = \sum_{i=1}^n \sum_{j=1}^n x_i x_j (1 - d_{ij}) (A_i A_j)^{0.5} \quad (17)$$

The pair of pseudo components are arbitrarily labeled components 1 and 2 on the left-hand side of Eq. 17. $\{x_i\}$ is the n-component composition of an arbitrary mixture of the two pseudo components, i.e.

$$x_i = a_1 x_i^1 + a_2 x_i^2 \quad (18)$$

where $a_1 + a_2 = 1$ and $0 < a_j < 1$ for $j = 1, 2$.

The only unknown in Eq. 17, after use of Eqs. 13 and 14, is d^{12} , i.e. the (pseudo) binary interaction coefficient between pseudo components 1 and 2. This coefficient d^{12} , is independent of temperature regardless of temperature-dependence of Ω_{ai} and /or Ω_{bi} , provided, of course, that the d_{ij} are independent of temperature.

Regrouping Scheme of Heavy Components. A method is proposed for estimating the number of multiple-carbon-number(MCN) groups needed for adequate plus-fraction description, as well as which SCN groups belong to the MCN group. It is based on Sturge's rule and the observation that the proposed distribution model is similar to a folded log-normal distribution. The number of MCN groups, N_g , is given by

$$N_g = \text{Int} [1 + 3.3 \log_{10}(N - n)] \quad (19)$$

For black-oil system, this number probably can be reduced by one.

The molecular weights separating each MCN group are taken as

$$M_I = M_n \{ \exp[(1/N_g) \ln(M_N/M_n)] \}^I \quad (20)$$

where M_N is the molecular weight of the last SCN group (which may actually be a plus fraction), and $I = 1, 2, \dots, N_g$. Molecular weights of SCN groups falling within the boundaries of these values are included in the MCN group, I.

Compositional Simulation:

There are two basic steps to work on compositional simulation. One is the PVT match, the other is the simulation of the compositional model. The following are the step-wise procedures and the corresponding data files. DESKTOP_PVT package was used for PVT match, compositional simulator is VIP. Data are from “Third SPE Comparative Solution Project: Gas Cycling of Retrograde Condensate Reservoirs”¹ (we name this paper as SPE3).

1- Heavy Ends Characterization. This is the first step for PVT matching. The following procedure is to be followed:

- a- Invoke DESKTOP_PVT. The Peng-Robinson EOS is selected by picking **CONFIG** from the main menu, then **EOS** submenu, then typing **PR**. (noted as **CONFIG/EOS, PR**).
- b- Turn on heavy end characterization by choosing **CONFIG/Heavy, Y**.
- c- Enter heavy end parameters by selecting (from main menu) **HEAVY/Parameter**. At least three numbers must be input to complete this step, they are: molecular weight, specific gravity, and mole fraction of C_{7+} . These numbers can be found in SPE3.
- d- Specify the names and number of heavy component groups by choosing **PSEUDO-COMPONENT NO. AND NAME**.
- e- Select “cut-off molecular weights” and specify 130 for bracket 1 and 180 for bracket 2.
- f- After inputting these data, you click **CALCULATE** option in the **HEAVY** menu.
- g- Inspect the data by selecting **HEAVY/Review**.
- h- Save the calculated EOS parameters by selecting **HEAVY/Save EOS**. Name the file “*heavy.eos*”.
- i- Save the data by choosing **FILE/Save** and name the file “*heavy.dat*”.

Molecular Weight	=	140
Specific gravity	=	0.774
Mole Fraction	=	0.0659
Cut-off Molecular Weight		130 180
Names of Heavy Components:		HVY1 HVY2 HVY3
Output:		HEAVY.DAT, HEAVY.EOS

2- Default Fluid Predictions. At this step, all components from SPE3 should be input except heavy components. The following procedure is to be followed:

- a- Choose **CONFIG/Test Type**.
- b- Select, **Cnst Composition, Cnst Volume, and/or Swelling**.
- c- Choose **CONFIG/Heavy, N**, to turn off the heavy components option.
- d- Choose **COMPONENT/System**, and highlight the components required (do not include the C_{7+}).
- e- Load The EOS for the heavy component by choosing **COMPONENT/Append EOS**, “*heavy.eos*”.
- f- Enter pure component mole fraction by choosing **COMPONENT/Composition**.
- g- Enter the data for the tests by choosing **TESTS/Cnst Composition**.
- h- Repeat for the **Cnst Volume** and **Swelling** tests.

- i- Run the program by Choosing **RUN/Go**.
- j- View the data by choosing **REPORT/Graphics**.
- k- Save the data by choosing **FILE/Save**. Name the file “*default.dat*”.

Components: CO₂,N₂,C1,C2,C3,NC4,IC4,NC5,IC5,NC6,HVY1,HVY2,HVY3
 Test Types: Constant Composition Expansion, Constant Volume Depletion and Swelling
 Output: default.dat

3- Pre-regression. Before pseudoization, we make regression for EOS properties. We call this step as pre-regression. We first need to pick regression variables, then run the program based on the previous data file default.dat. After doing this, we save two files. One is regress.dat, and the other is regress.eos. The updated EOS properties are included in regress.eos. The following procedure is to be followed:

- a- Choose **CONFIG/Regression, Y**, to turn on regression.
- b- Choose (from main menu) **REGRES/Variable**. Choose **EOS Property** and enter the number for the regression variable in the appropriate place. Then Choose **Binary Coeff** and enter the number for the regression variable in the appropriate place. Then **Exit**.
- c- Choose **REGRES/Limits** and change the minimum to 0.7 and maximum to 1.3.
- d- Choose **REGRES/Control** and change the no. of iterations to 20.
- e- Run the program by Choosing **RUN/Go**.
- f- View the data by choosing **REPORT/Graphics**.
- g- Save the calculated EOS parameters by selecting **REPORT/Save EOS**. Name the file “*regress.eos*”.
- h- Save the data by choosing **FILE/Save** and name the file “*regress.dat*”.

Components: CO₂,N₂,C1,C2,C3,NC4,IC4,NC5,IC5,NC6,HVY1,HVY2,HVY3

Regress Variables:

C1-OMEGAA	1
C1-OMEGAB	2
HVY1-OMEGAA	3
HVY2-OMEGAA	4
HVY3-OMEGAA	5
HVY1-OMEGAB	6
HVY2-OMEGAB	7
HVY3-OMEGAB	8
DJK C1-HVY1	9
DJK C1-HVY2	10
DJK C2-HVY3	11
Output:	REGRESS.DAT, REGRESS.EOS

4- Component Pseudoization. This step is called the pseudoization. The pseudo components are listed below. Once you give the names of pseudo components and components included in them, the program is capable of calculating regrouped lab data. Test data must be reentered for the new pseudo components. New files will be generated: “pseudo.dat” and “pseudo.eos”. The following procedure is to be followed:

- a- Choose **COMPONENT/Load EOS**, “*regress.eos*”. This will load the regressed EOS.
- b- Turn off regression by choosing **CONFIG/Regression, N**.
- c- Turn Pseudoization on by selecting **CONFIG/Pseudoization, Y**.
- d- Choose **PSEUDO/Pseudo Name**. Give names to the new pseudo components.
- e- Choose **PSEUDO/Parameter**. Specify the components in **Pseudo-COMP P1 Lump**. Repeat for all pseudo components.
- f- Choose **PSEUDO/Calculate**.
- g- Save the calculated EOS parameters by selecting **PSEUDO/Save EOS**. Name the file “*pseudo.eos*”.
- h- Choose **PSEUDO/Replace EOS**. This replaces the active EOS.
- i- Turn off pseudoization by choosing **CONFIG/Pseudoization, N**.
- j- Reenter the test data by choosing **TESTS/Const Composition**. Press F2 and load the global reference composition. Repeat for other tests.
- k- Run the program by selecting **RUN/Go**.
- l- Save the data by choosing **FILE/Save** and name the file “*pseudo.dat*”.

Pseudo Components:

P1	C1 + N2
P2	C2 + CO2
P3	C3 + NC4 + IC4
P4	C6 + NC5 + IC5
P5	HVY1
P6	HVY2
P7	HVY3

Test Types: Constant Composition Expansion, Constant Volume Depletion and Swelling

Output: PSEUDO.DAT, PSEUDO.EOS

5- Regression. This is the final step for PVT match. Procedures are the same as we did in the step 3. Regression is based on the data obtained in the step 4. The main problem is the selection of variables to be regressed in order to obtain a good match. There is no definite way to proceed. In this case trial and error method was used to get a good match. Selecting proper variables is a time consuming effort. The following procedure is to be followed:

- a- Choose **CONFIG/Regression, Y**, to turn on regression.
- b- Choose (from main menu), **REGRES/Variable**. Choose **EOS Property** and enter the number for the regression variable in the appropriate place (delete old numbers if present). Then Choose **Binary Coeff** and enter the number for the regression variable in the appropriate place. Then **Exit**.

- c- Choose **REGRES/Limits** and change the minimum to 0.7 and maximum to 1.3.
- d- Choose **REGRES/Control** and change the no. of iterations to 20.
- e- Run the program by Choosing **RUN/Go**.
- f- View the data by choosing **REPORT/Graphics**.
- g- Save the calculated EOS parameters by selecting **REPORT/Save EOS**. Name the file "*final.eos*".
- h- Choose **COMPONENT/Load EOS, final.eos**. This will overwrite the old EOS.
- i- Choose **CONFIG/Regression, N**, to turn off regression.
- j- Run the program by Choosing **RUN/Go**.
- k- Save the data by choosing **FILE/Save** and name the file "*final.dat*".

Pseudo Components:

P1	C1 + N2
P2	C2 + CO2
P3	C3 + NC4 + IC4
P4	C6 + NC5 + IC5
P5	HVY1
P6	HVY2
P7	HVY3

Regress Variables:

P1-ZC	1
P2-ZC	2
P5-ZC	3
P6-ZC	4
P7-ZC	5
P1-OMEGGA	6
P1-OMEGAB	7
P5,P6,P7-OMEGAA	8
P5,P6,P7-OMEGAB	9
DJK P1-P7	10

Output: FINAL.DAT, FINAL.EOS

6- Initialization Data for Compositional Simulation. After step 5, the adjusted EOS properties are obtained. These data are considered as the "correct values" and input in the initialization file along with other data from SPE3. The format of initialization file is attached in the following pages. VIP will create a spe3i.rst file when you type: "corerun" in the terminal. It should be noted that you should check the "corefil.dat" in the current directory before you type command "corerun."

Data Sources: SPE12278 paper, FINAL.DAT
 File Name: spe3i.dat

7- Run Data for Compositional Simulation. This is the last step for compositional simulation. After creating the simulation run data file-spe3r.dat and having a proper restart file-spe3i.rst from step 6. you can type the command "execrun", VIP will automatically produce the information specified by the user in the spe3r.dat. The format of the run data file spe3r.dat is attached in the following pages.

Data Sources: SPE12278, Final.dat
File Name: spe3r.dat

Data Files

The following pages contain the data files and the output files from the VIP simulator. Below is a list of the enclosed material.

Heavy.dat
Heavy.eos
Default.dat
Regression.dat
Regression.eos
Pseudo.dat
Pseudo.eos
Final.dat
Final.eos
Spe3i.dat
Spe3r.dat

(Input data file for Step 1 - Heavy Ends Characterization)

HEAVY.DAT

SPLIT

MWPLUS GPLUS ZPLUS NG MWGRP

140.00 0.7740 0.06590 3 130.00 180.00

PROPERTY CORRELATION SIMULATION

TC RIAZI-DAUBERT

PC RIAZI-DAUBERT

ACENTRIC EDMISTER

ZC RIAZI-DAUBERT

CONMWI

MWC6C7 92.00

MWINC 12.000

END

(Output data file for Step 1 - Heavy Ends Characterization)

HEAVY.EOS

EOS PR

COMPONENTS

HVY1 HVY2 HVY3

C

C PLUS FRACTION PSEUDO COMPONENT PROPERTIES

C

PROPERTIES

COMP	MW	TC	PC	ZC	Accentric	OMEGA A	OMEGA B
HVY1	107.77	561.98	410.55	26239	.31504	X	X
HVY2	148.05	677.63	325.18	24598	.41381	X	X
HVY3	224.01	843.58	244.42	23072	.57895	X	X

DJK C1

HVY1 .036113

HVY2 .041436

HVY3 .049070

ENDEOS

C

C PLUS FRACTION PSEUDO COMPONENT COMPOSITIONS

C

COMPOSITION

.034766 .019684 .011451

(Input data file for Step 2 - Default Fluid Predictions)

DEFAULT.DAT

```

EOS PR
COMPONENTS
CO2 N2 C1 C2 C3 NC4 IC4 NC5 IC5 NC6 HVY1 HVY2 HVY3
NCV 13
PROPERTIES F PSIA
COMP MW TC PC ZC ACENTRIC OMEGAA OMEGAB PCHOR
CO2 44.010 87.90 1070.9 .27420 .22250 .457236 .077796 49.60
N2 28.013 -232.40 493.0 .29100 .03720 .457236 .077796 35.00
C1 16.043 -116.60 667.8 .28900 .01260 .457236 .077796 71.00
C2 30.070 90.10 707.8 .28500 .09780 .457236 .077796 111.00
C3 44.097 206.00 616.3 .28100 .15410 .457236 .077796 151.00
NC4 58.124 305.70 550.7 .27400 .20150 .457236 .077796 191.00
IC4 58.124 275.00 529.1 .28300 .18400 .457236 .077796 191.00
NC5 72.151 385.70 488.6 .26200 .25240 .457236 .077796 231.00
IC5 72.151 369.10 490.4 .27300 .22860 .457236 .077796 231.00
NC6 86.178 453.70 436.9 .26400 .29980 .457236 .077796 271.00
HVY1 107.770 561.98 410.5 .26239 .31504 .457236 .077796 353.20
HVY2 148.050 677.63 325.2 .24598 .41381 .457236 .077796 474.02
HVY3 224.010 843.58 244.4 .23072 .57895 .457236 .077796 677.90
DJK CO2
N2 .000000
C1 .150000
C2 .150000
C3 .150000
NC4 .150000
IC4 .150000
NC5 .150000
IC5 .150000
NC6 .150000
HVY1 .150000
HVY2 .150000
HVY3 .150000
DJK N2
C1 .120000
C2 .120000
C3 .120000
NC4 .120000
IC4 .120000
NC5 .120000
IC5 .120000
NC6 .120000
HVY1 .120000
HVY2 .120000
HVY3 .120000
DJK C1
C2 .000000
C3 .000000
NC4 .020000
IC4 .020000
NC5 .020000
IC5 .020000
NC6 .025000
HVY1 .036113
HVY2 .041436
HVY3 .049070
DJK C2
C3 .000000
NC4 .010000
IC4 .010000
NC5 .010000
IC5 .010000
NC6 .010000
HVY1 .010000

```

```

HVY2 .010000
HVY3 .010000
DJK C3
NC4 .010000
IC4 .010000
NC5 .010000
IC5 .010000
NC6 .010000
HVY1 .010000
HVY2 .010000
HVY3 .010000
DJK NC4
IC4 .000000
NC5 .000000
IC5 .000000
NC6 .000000
HVY1 .000000
HVY2 .000000
HVY3 .000000
DJK IC4
NC5 .000000
IC5 .000000
NC6 .000000
HVY1 .000000
HVY2 .000000
HVY3 .000000
DJK NC5
IC5 .000000
NC6 .000000
HVY1 .000000
HVY2 .000000
HVY3 .000000
DJK IC5
NC6 .000000
HVY1 .000000
HVY2 .000000
HVY3 .000000
DJK NC6
HVY1 .000000
HVY2 .000000
HVY3 .000000
DJK HVY1
HVY2 .000000
HVY3 .000000
DJK HVY2
HVY3 .000000
HIDEAL
CO2 2.1028E+02 5.0361E+00 4.4507E-03 -1.1658E-06 1.5274E-10 -5.7829E-15
N2 -2.6164E+01 7.1489E+00 -4.9835E-04 4.4513E-07 -9.0210E-11 4.4521E-15
C1 -1.1193E+02 9.1718E+00 -4.7216E-03 6.7887E-06 -2.4493E-09 3.1208E-13
C2 -6.3147E-01 7.9649E+00 -7.5217E-04 8.7905E-06 -3.8672E-09 5.4789E-13
C3 -3.2544E+01 7.6111E+00 4.1469E-03 9.5048E-06 -4.7227E-09 7.0237E-13
NC4 4.3186E+02 5.7293E+00 1.5646E-02 3.0120E-06 -2.4420E-09 3.8132E-13
IC4 6.6831E+02 2.7132E+00 1.9460E-02 8.3832E-07 -1.8392E-09 3.1555E-13
NC5 1.9605E+03 -2.0202E-01 3.1752E-02 -6.2257E-06 5.8994E-10 -1.4225E-14
IC5 1.9930E+03 -2.2728E+00 3.3903E-02 -7.0911E-06 7.4305E-10 -2.1274E-14
NC6 -6.3694E+02 1.9744E+01 -7.0295E-03 3.9020E-05 -2.1744E-08 4.0917E-12
HVY1 0.0000E+00 4.4727E+00 4.4674E-02 -6.3579E-06 0.0000E+00 0.0000E+00
HVY2 0.0000E+00 2.7007E+00 5.8820E-02 -7.8301E-06 0.0000E+00 0.0000E+00
HVY3 0.0000E+00 4.9001E+00 8.9064E-02 -1.1580E-05 0.0000E+00 0.0000E+00
ENDEOS
C
PVTFILE
KVFILE
C
CCEXP RUN1
COMPOSITION

```

```

.012100 .019400 .659900 .086900 .059100 .027800 .023900
.011200 .015700 .018100 .034766 .019684 .011451
TEMP 200.0 F
DEWPT 3428.0 PSIG
PRES VREL XLIQ ZG
6000.0 0.8045 0.0 1.129
5500.0 0.8268 0.0 1.063
5000.0 0.8530 0.0 0.9980
4500.0 0.8856 0.0 0.9930
4000.0 0.9284 0.0 0.8690
3600.0 0.9745 0.0 0.8220
3428.0 1.000 0.0 0.0
3400.0 1.004 0.009000 0.0
3350.0 1.014 0.02700 0.0
3200.0 1.047 0.08100 0.0
3000.0 1.100 0.1500 0.0
2800.0 1.164 0.0 0.0
2400.0 1.341 0.0 0.0
2000.0 1.611 0.0 0.0
1600.0 2.041 0.0 0.0
1300.0 2.554 0.0 0.0
1030.0 3.293 0.0 0.0
836.00 4.139 0.0 0.0

```

```

C
CVDEP RUN1
COMPOSITION
.012100 .019400 .659900 .086900 .059100 .027800 .023900
(Input data file for Step 2 - Default Fluid Predictions p. 1/4)

```

```

.011200 .015700 .018100 .034766 .019684 .011451
TEMP 200.0 F
DEWPT 3428.0 PSIG
PRES 3428.0 3000.0 2400.0 1800.0 1200.0 700.0
MW HVY1 HVY3 140.00 127.00 118.00 111.00 106.00 105.00
ZGAS 0.8030 0.7980 0.8020 0.8300 0.8770 0.9240
VPROD 0.0 0.09095 0.2470 0.42026 0.59687 0.7402
SLIQ 0.0 0.1500 0.1990 0.1920 0.1710 0.1520

```

```

C
SWELL RUN1
COMPOSITION
.012100 .019400 .659900 .086900 .059100 .027800 .023900
.011200 .015700 .018100 .034766 .019684 .011451
YINJ
.000000 .000000 .946800 .052700 .000500 .000000 .000000
.000000 .000000 .000000 .000000 .000000 .000000

```

```

TEMP 200.0 F
PSIG
ZINJ VREL PSAT TYPE
0.0 1.000 3428.0 DEWPT
0.1271 1.122 3635.0 DEWPT
0.3046 1.354 4015.0 DEWPT
0.5384 1.925 4610.0 DEWPT
0.6538 2.504 4880.0 DEWPT

```

```

C
END

```

(Input data file for Step 3 - Pre-regression)

REGRESS.DAT

```
REGRESS
VARIABLE MIN INIT MAX
1 .8000 1.0000 1.2000
2 .8000 1.0000 1.2000
3 .8000 1.0000 1.2000
4 .8000 1.0000 1.2000
5 .8000 1.0000 1.2000
6 .8000 1.0000 1.2000
7 .8000 1.0000 1.2000
8 .8000 1.0000 1.2000
9 .8000 1.0000 1.2000
10 .8000 1.0000 1.2000
11 .8000 1.0000 1.2000
IMAX IPRINT H TOL1 TOL2 TOL3
20 1 .200000 .001000 .001000 .010000
COMP MW TC PC ZC ACENTRIC OMEGAA OMEGAB PCHOR
C1 X X X X X 1 2 X
HVY1 X X X X X 3 6 X
HVY2 X X X X X 4 7 X
HVY3 X X X X X 5 8 X
DJK C1
HVY1 9
HVY2 10
HVY3 11
ENDREG
C
C
EOS PR
COMPONENTS
CO2 N2 C1 C2 C3 NC4 IC4 NC5 IC5 NC6 HVY1 HVY2 HVY3
NCV 13
PROPERTIES F PSIA
COMP MW TC PC ZC ACENTRIC OMEGAA OMEGAB PCHOR
CO2 44.010 87.90 1070.9 .27420 .22250 .457236 .077796 49.60
N2 28.013 -232.40 493.0 .29100 .03720 .457236 .077796 35.00
C1 16.043 -116.60 667.8 .28900 .01260 .457236 .077796 71.00
C2 30.070 90.10 707.8 .28500 .09780 .457236 .077796 111.00
C3 44.097 206.00 616.3 .28100 .15410 .457236 .077796 151.00
NC4 58.124 305.70 550.7 .27400 .20150 .457236 .077796 191.00
IC4 58.124 275.00 529.1 .28300 .18400 .457236 .077796 191.00
NC5 72.151 385.70 488.6 .26200 .25240 .457236 .077796 231.00
IC5 72.151 369.10 490.4 .27300 .22860 .457236 .077796 231.00
NC6 86.178 453.70 436.9 .26400 .29980 .457236 .077796 271.00
HVY1 107.770 561.98 410.5 .26239 .31504 .457236 .077796 353.20
HVY2 148.050 677.63 325.2 .24598 .41381 .457236 .077796 474.02
HVY3 224.010 843.58 244.4 .23072 .57895 .457236 .077796 677.90
DJK CO2
N2 .000000
C1 .150000
C2 .150000
C3 .150000
NC4 .150000
IC4 .150000
NC5 .150000
IC5 .150000
NC6 .150000
HVY1 .150000
HVY2 .150000
HVY3 .150000
DJK N2
C1 .120000
```

```

C2 .120000
C3 .120000
NC4 .120000
IC4 .120000
NC5 .120000
IC5 .120000
NC6 .120000
HVV1 .120000
HVV2 .120000
HVV3 .120000
DJK C1
C2 .000000
C3 .000000
NC4 .020000
IC4 .020000
NC5 .020000
IC5 .020000
NC6 .025000
HVV1 .036113
HVV2 .041436
HVV3 .049070
DJK C2
C3 .000000
NC4 .010000
IC4 .010000
NC5 .010000
IC5 .010000
NC6 .010000
HVV1 .010000
HVV2 .010000
HVV3 .010000
DJK C3
NC4 .010000
IC4 .010000
NC5 .010000
IC5 .010000
NC6 .010000
HVV1 .010000
HVV2 .010000
HVV3 .010000
DJK NC4
IC4 .000000
NC5 .000000
IC5 .000000
NC6 .000000
HVV1 .000000
HVV2 .000000
HVV3 .000000
DJK IC4
NC5 .000000
IC5 .000000
NC6 .000000
HVV1 .000000
HVV2 .000000
HVV3 .000000
DJK NC5
IC5 .000000
NC6 .000000
HVV1 .000000
HVV2 .000000
HVV3 .000000
DJK IC5
NC6 .000000
HVV1 .000000
HVV2 .000000
HVV3 .000000
DJK NC6

```

```

HVY1 .000000
HVY2 .000000
HVY3 .000000
DJK HVY1
HVY2 .000000
HVY3 .000000
DJK HVY2
HVY3 .000000
HIDEAL
CO2 2.1028E+02 5.0361E+00 4.4507E-03 -1.1658E-06 1.5274E-10 -5.7829E-15
N2 -2.6164E+01 7.1489E+00 -4.9835E-04 4.4513E-07 -9.0210E-11 4.4521E-15
C1 -1.1193E+02 9.1718E+00 -4.7216E-03 6.7887E-06 -2.4493E-09 3.1208E-13
C2 -6.3147E-01 7.9649E+00 -7.5217E-04 8.7905E-06 -3.8672E-09 5.4789E-13
C3 -3.2544E+01 7.6111E+00 4.1469E-03 9.5048E-06 -4.7227E-09 7.0237E-13
NC4 4.3186E+02 5.7293E+00 1.5646E-02 3.0120E-06 -2.4420E-09 3.8132E-13
IC4 6.6831E+02 2.7132E+00 1.9460E-02 8.3832E-07 -1.8392E-09 3.1555E-13
NC5 1.9605E+03 -2.0202E-01 3.1752E-02 -6.2257E-06 5.8994E-10 -1.4225E-14
IC5 1.9930E+03 -2.2728E+00 3.3903E-02 -7.0911E-06 7.4305E-10 -2.1274E-14
NC6 -6.3694E+02 1.9744E+01 -7.0295E-03 3.9020E-05 -2.1744E-08 4.0917E-12
HVY1 0.0000E+00 4.4727E+00 4.4674E-02 -6.3579E-06 0.0000E+00 0.0000E+00
HVY2 0.0000E+00 2.7007E+00 5.8820E-02 -7.8301E-06 0.0000E+00 0.0000E+00
HVY3 0.0000E+00 4.9001E+00 8.9064E-02 -1.1580E-05 0.0000E+00 0.0000E+00
ENDEOS
C
PVTFILE
KVFILE
C
CCEXP RUN1
COMPOSITION
.012100 .019400 .659900 .086900 .059100 .027800 .023900
.011200 .015700 .018100 .034766 .019684 .011451
TEMP 200.0 F
DEWPT 3428.0 PSIG
PRES VREL XLIQ ZG
6000.0 0.8045 0.0 1.129
5500.0 0.8268 0.0 1.063
5000.0 0.8530 0.0 0.9980
4500.0 0.8856 0.0 0.9930
4000.0 0.9284 0.0 0.8690
3600.0 0.9745 0.0 0.8220
3428.0 1.000 0.0 0.0
3400.0 1.004 0.009000 0.0
3350.0 1.014 0.02700 0.0
3200.0 1.047 0.08100 0.0
3000.0 1.100 0.1500 0.0
2800.0 1.164 0.0 0.0
2400.0 1.341 0.0 0.0
2000.0 1.611 0.0 0.0
1600.0 2.041 0.0 0.0
1300.0 2.554 0.0 0.0
1030.0 3.293 0.0 0.0
836.00 4.139 0.0 0.0
C
CVDEP RUN1
COMPOSITION
.012100 .019400 .659900 .086900 .059100 .027800 .023900
.011200 .015700 .018100 .034766 .019684 .011451
TEMP 200.0 F
DEWPT 3428.0 PSIG
PRES 3428.0 3000.0 2400.0 1800.0 1200.0 700.00
MW HVY1 HVY3 140.00 127.00 118.00 111.00 106.00 105.00
ZGAS 0.8030 0.7980 0.8020 0.8300 0.8770 0.9240
VPROD 0.0 0.09095 0.2470 0.42026 0.59687 0.7402
SLIQ 0.0 0.1500 0.1990 0.1920 0.1710 0.1520
C
SWELL RUN1
COMPOSITION

```

```
.012100 .019400 .659900 .086900 .059100 .027800 .023900
.011200 .015700 .018100 .034766 .019684 .011451
YINJ
.000000 .000000 .946800 .052700 .000500 .000000 .000000
.000000 .000000 .000000 .000000 .000000 .000000
TEMP 200.0 F
PSIG
ZINJ VREL PSAT TYPE
0.0 1.000 3428.0 DEWPT
0.1271 1.122 3635.0 DEWPT
0.3046 1.354 4015.0 DEWPT
0.5384 1.925 4610.0 DEWPT
0.6538 2.504 4880.0 DEWPT
C
END
```

(Output data file for Step 3 - Pre-regression)

REGRESS.EOS

```
EOS PR
COMPONENTS
CO2 N2 C1 C2 C3 NC4 IC4 NC5 IC5 NC6 HVY1 HVY2 HVY3
NCV 13
PROPERTIES F PSIA
COMP MW TC PC ZC ACENTRIC OMEGAA OMEGAB PCHOR
CO2 44.01 87.90 1070.90 .2742 .2225 .4572360 .0777960 49.6
N2 28.01 -232.40 493.00 .2910 .0372 .4572360 .0777960 35.0
C1 16.04 -116.60 667.80 .2890 .0126 .3776518 .0727877 71.0
C2 30.07 90.10 707.80 .2850 .0978 .4572360 .0777960 111.0
C3 44.10 206.00 616.30 .2810 .1541 .4572360 .0777960 151.0
NC4 58.12 305.70 550.70 .2740 .2015 .4572360 .0777960 191.0
IC4 58.12 275.00 529.10 .2830 .1840 .4572360 .0777960 191.0
NC5 72.15 385.70 488.60 .2620 .2524 .4572360 .0777960 231.0
IC5 72.15 369.10 490.40 .2730 .2286 .4572360 .0777960 231.0
NC6 86.18 453.70 436.90 .2640 .2998 .4572360 .0777960 271.0
HVY1 107.77 561.98 410.50 .2624 .3150 .4169631 .0933548 353.2
HVY2 148.05 677.63 325.20 .2460 .4138 .5486750 .0883512 474.0
HVY3 224.01 843.58 244.40 .2307 .5789 .5344757 .0933546 677.9
DJK N2
CO .0000000
DJK C1
CO2 .1500000
N2 .1200000
DJK C2
CO2 .1500000
N2 .1200000
C1 .0000000
DJK C3
CO2 .1500000
N2 .1200000
C1 .0000000
C2 .0000000
DJK NC4
CO2 .1500000
N2 .1200000
C1 .0200000
C2 .0100000
C3 .0100000
DJK IC4
CO2 .1500000
N2 .1200000
C1 .0200000
C2 .0100000
C3 .0100000
NC4 .0000000
DJK NC5
CO2 .1500000
N2 .1200000
C1 .0200000
C2 .0100000
C3 .0100000
NC4 .0000000
IC4 .0000000
DJK IC5
CO2 .1500000
N2 .1200000
C1 .0200000
C2 .0100000
C3 .0100000
```

```

NC4 .000000
IC4 .000000
NC5 .000000
DJK NC6
CO2 .150000
N2 .120000
C1 .025000
C2 .010000
C3 .010000
NC4 .000000
IC4 .000000
NC5 .000000
IC5 .000000
DJK HVY1
CO2 .150000
N2 .120000
C1 -.1638391
C2 .010000
C3 .010000
NC4 .000000
IC4 .000000
NC5 .000000
IC5 .000000
NC6 .000000
DJK HVY2
CO2 .150000
N2 .120000
C1 -.1585253
C2 .010000
C3 .010000
NC4 .000000
IC4 .000000
NC5 .000000
IC5 .000000
NC6 .000000
HVY1 .000000
DJK HVY3
CO2 .150000
N2 .120000
C1 .2490480
C2 .010000
C3 .010000
NC4 .000000
IC4 .000000
NC5 .000000
IC5 .000000
NC6 .000000
HVY1 .000000
HVY2 .000000
C
HSTAR
CO2 2.10280E+02 5.03610E+00 4.45070E-03 -1.16580E-06 1.52740E-10
-5.78290E-15
N2 -2.61640E+01 7.14890E+00 -4.98350E-04 4.45130E-07 -9.02100E-11
4.45210E-15
C1 -1.11930E+02 9.17180E+00 -4.72160E-03 6.78870E-06 -2.44930E-09
3.12080E-13
C2 -6.31470E-01 7.96490E+00 -7.52170E-04 8.79050E-06 -3.86720E-09
5.47890E-13
C3 -3.25440E+01 7.61110E+00 4.14690E-03 9.50480E-06 -4.72270E-09
7.02370E-13
NC4 4.31860E+02 5.72930E+00 1.56460E-02 3.01200E-06 -2.44200E-09
3.81320E-13
IC4 6.68310E+02 2.71320E+00 1.94600E-02 8.38320E-07 -1.83920E-09
3.15550E-13
NC5 1.96050E+03 -2.02020E-01 3.17520E-02 -6.22570E-06 5.89940E-10
-1.42250E-14

```

IC5 1.99300E+03 -2.27280E+00 3.39030E-02 -7.09110E-06 7.43050E-10
-2.12740E-14
NC6 -6.36940E+02 1.97440E+01 -7.02950E-03 3.90200E-05 -2.17440E-08
4.09170E-12
HVY1 0.00000E+00 4.47270E+00 4.46740E-02 -6.35790E-06 0.00000E+00
0.00000E+00
HVY2 0.00000E+00 2.70070E+00 5.88200E-02 -7.83010E-06 0.00000E+00
0.00000E+00
HVY3 0.00000E+00 4.90010E+00 8.90640E-02 -1.15800E-05 0.00000E+00
0.00000E+00

C

ENDEOS

C

C Global Reference Component Composition

COMPOSITION

.012100 .019400 .659900 .086900 .059100 .027800 .023900 .011200
.015700 .018100 .034766 .019684 .011451

(Input data file for Step 4 - Component Pseudoization)

PSEUDO.DAT

```
EOS PR
COMPONENTS
P1 P2 P3 P4 P5 P6 P7
NCV 7
PROPERTIES F PSIA
COMP MW TC PC ZC ACENTRIC OMEGAA OMEGAB PCHOR
P1 16.382 -119.91 662.8 .28883 .01330 .376528 .072862 69.97
P2 31.774 89.83 752.2 .28944 .11304 .451923 .079260 103.50
P3 50.642 245.90 581.0 .28180 .17244 .459850 .078437 169.66
P4 77.793 407.26 468.4 .26789 .26316 .460949 .078234 247.09
P5 107.770 561.98 410.5 .26240 .31500 .416963 .093355 353.20
P6 148.050 677.63 325.2 .24600 .41380 .548675 .088351 474.00
P7 224.010 843.58 244.4 .23070 .57890 .534476 .093355 677.90
DJK P1
P2 .000947
P3 .007835
P4 .021885
P5 -.160885
P6 -.155665
P7 .244672
DJK P2
P3 .003695
P4 .010541
P5 .010541
P6 .010541
P7 .010541
DJK P3
P4 .002281
P5 .002281
P6 .002281
P7 .002281
DJK P4
P5 .000000
P6 .000000
P7 .000000
DJK P5
P6 .000000
P7 .000000
DJK P6
P7 .000000
HIDEAL
P3 0.0000E+00 3.0481E+00 2.2327E-02 -3.1330E-06 0.0000E+00 0.0000E+00
P4 0.0000E+00 1.3339E+00 3.0999E-02 -4.1340E-06 0.0000E+00 0.0000E+00
P6 0.0000E+00 2.5153E+01 7.7904E-02 -1.2416E-05 0.0000E+00 0.0000E+00
ENDEOS
C
PVTFILE
KVFILE
C
CCEXP RUN1
COMPOSITION
.679300 .099000 .110800 .045000 .034766 .019684 .011451

TEMP 200.0 F
DEWPT 3428.0 PSIG
PRES VREL XLIQ ZG
6000.0 0.8045 0.0 1.129
5500.0 0.8268 0.0 1.063
5000.0 0.8530 0.0 0.9980
4500.0 0.8856 0.0 0.9930
4000.0 0.9284 0.0 0.8690
```

3600.0 0.9745 0.0 0.8220
3428.0 1.000 0.0 0.0
3400.0 1.004 0.009000 0.0
3350.0 1.014 0.02700 0.0
3200.0 1.047 0.08100 0.0
3000.0 1.100 0.1500 0.0
2800.0 1.164 0.0 0.0
2400.0 1.341 0.0 0.0
2000.0 1.611 0.0 0.0
1600.0 2.041 0.0 0.0
1300.0 2.554 0.0 0.0
1030.0 3.293 0.0 0.0
836.00 4.139 0.0 0.0

C

CVDEP RUN1

COMPOSITION

.679300 .099000 .110800 .045000 .034766 .019684 .011451

TEMP 200.0 F

DEWPT 3428.0 PSIG

PRES 3428.0 3000.0 2400.0 1800.0 1200.0 700.00
MW P5 P7 140.00 127.00 118.00 111.00 106.00 105.00
ZGAS 0.8030 0.7980 0.8020 0.8300 0.8770 0.9240
VPROD 0.0 0.09095 0.2470 0.42026 0.59687 0.7402
SLIQ 0.0 0.1500 0.1990 0.1920 0.1710 0.1520

C

SWELL RUN1

COMPOSITION

.679300 .099000 .110800 .045000 .034766 .019684 .011451

YINJ

.946800 .052700 .000500 .000000 .000000 .000000 .000000

TEMP 200.0 F

PSIG

ZINJ VREL PSAT TYPE
0.0 1.000 3428.0 DEWPT
0.1271 1.122 3635.0 DEWPT
0.3046 1.354 4015.0 DEWPT
0.5384 1.925 4610.0 DEWPT
0.6538 2.504 4880.0 DEWPT

C

END

(Output data file for Step 4 - Component Pseudoization)

PSEUDO.EOS

C EQUATION OF STATE DATA PRODUCED BY DESKTOP-PVT FOR PSEUDO COMPONENTS

C

EOS PR

COMPONENTS

P1 P2 P3 P4 P5 P6 P7

PROPERTIES F PSIA

COMP	MW	TC	PC	ZC	ACENTRIC	OMEGAA	OMEGAB	PCHOR
------	----	----	----	----	----------	--------	--------	-------

P1	16.38	-119.91	662.81	.2888	.0133	.3765281	.0728615	70.0
----	-------	---------	--------	-------	-------	----------	----------	------

P2	31.77	89.83	752.18	.2894	.1130	.4519229	.0792598	103.5
----	-------	-------	--------	-------	-------	----------	----------	-------

P3	50.64	245.90	581.03	.2818	.1724	.4598499	.0784368	169.7
----	-------	--------	--------	-------	-------	----------	----------	-------

P4	77.79	407.26	468.43	.2679	.2632	.4609493	.0782338	247.1
----	-------	--------	--------	-------	-------	----------	----------	-------

P5	107.77	561.98	410.50	.2624	.3150	.4169631	.0933548	353.2
----	--------	--------	--------	-------	-------	----------	----------	-------

P6	148.05	677.63	325.20	.2460	.4138	.5486750	.0883512	474.0
----	--------	--------	--------	-------	-------	----------	----------	-------

P7	224.01	843.58	244.40	.2307	.5789	.5344757	.0933546	677.9
----	--------	--------	--------	-------	-------	----------	----------	-------

DJK P2

P1	.0009470
----	----------

DJK P3

P1	.0078346
----	----------

P2	.0036951
----	----------

DJK P4

P1	.0218854
----	----------

P2	.0105413
----	----------

P3	.0022813
----	----------

DJK P5

P1	-.1608847
----	-----------

P2	.0105413
----	----------

P3	.0022813
----	----------

P4	.0000000
----	----------

DJK P6

P1	-.1556652
----	-----------

P2	.0105413
----	----------

P3	.0022813
----	----------

P4	.0000000
----	----------

P5	.0000000
----	----------

DJK P7

P1	.2446722
----	----------

P2	.0105413
----	----------

P3	.0022813
----	----------

P4	.0000000
----	----------

P5	.0000000
----	----------

P6	.0000000
----	----------

C

HSTAR

P1	0.00000E+00	0.00000E+00	0.00000E+00	0.00000E+00	0.00000E+00	0.00000E+00
----	-------------	-------------	-------------	-------------	-------------	-------------

	0.00000E+00
--	-------------

P2	0.00000E+00	0.00000E+00	0.00000E+00	0.00000E+00	0.00000E+00	0.00000E+00
----	-------------	-------------	-------------	-------------	-------------	-------------

	0.00000E+00
--	-------------

P3	0.00000E+00	3.04810E+00	2.23275E-02	-3.13303E-06	0.00000E+00	0.00000E+00
----	-------------	-------------	-------------	--------------	-------------	-------------

	0.00000E+00
--	-------------

P4	0.00000E+00	1.33391E+00	3.09992E-02	-4.13396E-06	0.00000E+00	0.00000E+00
----	-------------	-------------	-------------	--------------	-------------	-------------

	0.00000E+00
--	-------------

P5	0.00000E+00	0.00000E+00	0.00000E+00	0.00000E+00	0.00000E+00	0.00000E+00
----	-------------	-------------	-------------	-------------	-------------	-------------

	0.00000E+00
--	-------------

P6	0.00000E+00	2.51533E+01	7.79036E-02	-1.24159E-05	0.00000E+00	0.00000E+00
----	-------------	-------------	-------------	--------------	-------------	-------------

	0.00000E+00
--	-------------

P7	0.00000E+00	0.00000E+00	0.00000E+00	0.00000E+00	0.00000E+00	0.00000E+00
----	-------------	-------------	-------------	-------------	-------------	-------------

	0.00000E+00
--	-------------

C

ENDEOS

C

C Pseudoized Component Composition

C

COMPOSITION

.679300 .099000 .110800 .045000 .034766 .019684 .011451

(Input data file for Step5 - Regressio)

FINAL.DAT

```
REGRESS
VARIABLE MIN INIT MAX
1 .8000 1.0000 1.2000
2 .8000 1.0000 1.2000
3 .8000 1.0000 1.2000
4 .8000 1.0000 1.2000
5 .8000 1.0000 1.2000
6 .8000 1.0000 1.2000
7 .8000 1.0000 1.2000
8 .8000 1.0000 1.2000
9 .8000 1.0000 1.2000
10 .8000 1.0000 1.2000
11 .8000 1.0000 1.2000
12 .8000 1.0000 1.2000
13 .8000 1.0000 1.2000
IMAX IPRINT H TOL1 TOL2 TOL3
20 1 .200000 .001000 .001000 .010000
COMP MW TC PC ZC ACENTRIC OMEGAA OMEGAB PCHOR
P1 X X X 1 X 6 7 X
P2 X X X 2 X X X X
P5 11 X X 3 X 8 9 X
P6 12 X X 4 X 8 9 X
P7 13 X X 5 X 8 9 X
DJK P1
P7 10
ENDREG
C
EOS PR
COMPONENTS
P1 P2 P3 P4 P5 P6 P7
NCV 7
PROPERTIES F PSIA
COMP MW TC PC ZC ACENTRIC OMEGAA OMEGAB PCHOR
P1 16.382 -119.91 662.8 .28883 .01330 .376528 .072862 69.97
P2 31.774 89.83 752.2 .28944 .11304 .451923 .079260 103.50
P3 50.642 245.90 581.0 .28180 .17244 .459850 .078437 169.66
P4 77.793 407.26 468.4 .26789 .26316 .460949 .078234 247.09
P5 107.770 561.98 410.5 .26240 .31500 .416963 .093355 353.20
P6 148.050 677.63 325.2 .24600 .41380 .548675 .088351 474.00
P7 224.010 843.58 244.4 .23070 .57890 .534476 .093355 677.90
DJK P1
P2 .000947
P3 .007835
P4 .021885
P5 -.160885
P6 -.155665
P7 .244672
DJK P2
P3 .003695
P4 .010541
P5 .010541
P6 .010541
P7 .010541
DJK P3
P4 .002281
P5 .002281
P6 .002281
P7 .002281
DJK P4
P5 .000000
```

P6 .000000
 P7 .000000
 DJK P5
 P6 .000000
 P7 .000000
 DJK P6
 P7 .000000
 HIDEAL
 P3 0.0000E+00 3.0481E+00 2.2327E-02 -3.1330E-06 0.0000E+00 0.0000E+00
 P4 0.0000E+00 1.3339E+00 3.0999E-02 -4.1340E-06 0.0000E+00 0.0000E+00
 P6 0.0000E+00 2.5153E+01 7.7904E-02 -1.2416E-05 0.0000E+00 0.0000E+00
 ENDEOS
 C
 PVTFILE
 KVFILE
 C
 CCEXP RUN1
 COMPOSITION
 .679300 .099000 .110800 .045000 .034766 .019684 .011451

TEMP 200.0 F
 DEWPT 3428.0 PSIG
 PRES VREL XLIQ ZG
 6000.0 0.8045 0.0 1.129
 5500.0 0.8268 0.0 1.063
 5000.0 0.8530 0.0 0.9980
 4500.0 0.8856 0.0 0.9930
 4000.0 0.9284 0.0 0.8690
 3600.0 0.9745 0.0 0.8220
 3428.0 1.000 0.0 0.0
 3400.0 1.004 0.009000 0.0
 3350.0 1.014 0.02700 0.0
 3200.0 1.047 0.08100 0.0
 3000.0 1.100 0.1500 0.0
 2800.0 1.164 0.0 0.0
 2400.0 1.341 0.0 0.0
 2000.0 1.611 0.0 0.0
 1600.0 2.041 0.0 0.0
 1300.0 2.554 0.0 0.0
 1030.0 3.293 0.0 0.0
 836.00 4.139 0.0 0.0

C
 CVDEP RUN1
 COMPOSITION
 .679300 .099000 .110800 .045000 .034766 .019684 .011451
 TEMP 200.0 F
 DEWPT 3428.0 PSIG
 PRES 3428.0 3000.0 2400.0 1800.0 1200.0 700.0
 MW P5 P7 140.00 127.00 118.00 111.00 106.00 105.00
 ZGAS 0.8030 0.7980 0.8020 0.8300 0.8770 0.9240
 VPROD 0.0 0.09095 0.2470 0.42026 0.59687 0.7402
 SLIQ 0.0 0.1500 0.1990 0.1920 0.1710 0.1520

C
 SWELL RUN1
 COMPOSITION
 .679300 .099000 .110800 .045000 .034766 .019684 .011451

YINJ
 .946800 .052700 .000500 .000000 .000000 .000000 .000000

TEMP 200.0 F
 PSIG
 ZINJ VREL PSAT TYPE
 0.0 1.000 3428.0 DEWPT
 0.1271 1.122 3635.0 DEWPT
 0.3046 1.354 4015.0 DEWPT
 0.5384 1.925 4610.0 DEWPT

0.6538 2.504 4880.0 DEWPT
C
END

(Output data file for Step5 - Regression)

FINAL.EOS

EOS PR
COMPONENTS
P1 P2 P3 P4 P5 P6 P7
NCV 7
PROPERTIES F PSIA
COMP MW TC PC ZC ACENTRIC OMEGAA OMEGAB PCHOR
P1 16.38 -119.91 662.80 .2888 .0133 .3528063 .0710390 70.0
P2 31.77 89.83 752.20 .2894 .1130 .4519230 .0792600 103.5
P3 50.64 245.90 581.00 .2818 .1724 .4598500 .0784370 169.7
P4 77.79 407.26 468.40 .2679 .2632 .4609490 .0782340 247.1
P5 102.03 561.98 410.50 .2624 .3150 .4192163 .0950905 353.2
P6 150.30 677.63 325.20 .2460 .4138 .5516401 .0899935 474.0
P7 233.65 843.58 244.40 .2307 .5789 .5373643 .0950905 677.9
DJK P2
P1 .0009470
DJK P3
P1 .0078350
P2 .0036950
DJK P4
P1 .0218850
P2 .0105410
P3 .0022810
DJK P5
P1 -.1608850
P2 .0105410
P3 .0022810
P4 .0000000
DJK P6
P1 -.1556650
P2 .0105410
P3 .0022810
P4 .0000000
P5 .0000000
DJK P7
P1 .2481725
P2 .0105410
P3 .0022810
P4 .0000000
P5 .0000000
P6 .0000000
C
HSTAR
P1 0.00000E+00 0.00000E+00 0.00000E+00 0.00000E+00 0.00000E+00
0.00000E+00
P2 0.00000E+00 0.00000E+00 0.00000E+00 0.00000E+00 0.00000E+00
0.00000E+00
P3 0.00000E+00 3.04810E+00 2.23270E-02 -3.13300E-06 0.00000E+00
0.00000E+00
P4 0.00000E+00 1.33390E+00 3.09990E-02 -4.13400E-06 0.00000E+00
0.00000E+00
P5 0.00000E+00 0.00000E+00 0.00000E+00 0.00000E+00 0.00000E+00
0.00000E+00
P6 0.00000E+00 2.51530E+01 7.79040E-02 -1.24160E-05 0.00000E+00
0.00000E+00
P7 0.00000E+00 0.00000E+00 0.00000E+00 0.00000E+00 0.00000E+00
0.00000E+00
C

ENDEOS

C

C Global Reference Component Composition

C

COMPOSITION

.679300 .099000 .110800 .045000 .034766 .019684 .011451

(Input data for Step 6 - Initialization for simulation)

Spe3i.dat

```
C VIP-EXEC COMPOSITIONAL EXAMPLE #1
C
C DATA SET NAME: SPE3I.DAT
C
C FEATURES DEMONSTRATED:
C (1) RECTANGULAR GRID 9X9X4
C (2) GAS CONDENSATE, GAS CYCLING
C
C -----
C
INIT
TITLE1
SPE COMPARATIVE PROJECT 3
TITLE2
DATA SET NAME: SPE3I.DAT
TITLE3
    SINGLE WELL RECTANGULAR GRID GAS CONDENSATE
C
NCOL  80
NLINES 60
C
PRINT ALL
C
C INITIAL SIMULATION DATE:
DATE 01 01 1992
C

C

NX NY NZ  NCOMP
9  9  4   7
C
C CONSTANT RESERVOIR PROPERTIES
DWB BWI VW CW  CR TRES TS PS
1.  .9813 .3 3.0E-6 4.0E-6 200. 60. 14.7
C
C
C
NOLIST
TABLES
IEQUIL  PINIT    DEPTH  PCWOC WOC  PCGOC  GOC    PSAT
1       3543    7500    0     7500  0     7500   3443
C

C
SWT 1
  SW  KRW      KROW PCWO
  0.00 0.0  0.801 75.0
  0.04 0.0  0.8005 71.0
  0.08 0.0  0.8003 70.0
  0.12 0.0  0.8001 60.0
  0.16 0.00 0.80  50.0
  0.2  0.002 0.65 30.0
  0.24 0.01 0.513 21.0
  0.28 0.02 0.4  15.5
  0.32 0.033 0.315 12.0
  0.36 0.049 0.25 9.20
  0.40 0.066 0.196 7.00
  0.44 0.090 0.15 5.30
  0.48 0.119 0.112 4.20
  0.52 0.15 0.082 3.40
```

0.56	0.186	0.060	2.70
0.60	0.227	0.04	2.10
0.64	0.277	0.024	1.70
0.68	0.330	0.012	1.30
0.72	0.39	0.005	1.00
0.76	0.462	0.0	0.70
0.80	0.54	0.0	0.50
0.84	0.62	0.0	0.40
0.88	0.71	0.0	0.30
0.92	0.80	0.0	0.20
0.96	0.90	0.0	0.10
1.00	1.00	0.0	0.00

C

SGT 1

SG	KRG	KROG	PCGO
0.0	0.0	0.801	0.0
0.04	0.005	0.650	0.0
0.08	0.013	0.513	0.0
0.12	0.026	0.400	0.0
0.16	0.040	0.315	0.0
0.20	0.058	0.250	0.0
0.24	0.078	0.196	0.0
0.28	0.100	0.150	0.0
0.32	0.126	0.112	0.0
0.36	0.156	0.082	0.0
0.40	0.187	0.060	0.0
0.44	0.222	0.040	0.0
0.48	0.260	0.024	0.0
0.52	0.300	0.012	0.0
0.56	0.348	0.005	0.0
0.60	0.400	0.00	0.0
0.64	0.450	0.00	0.0
0.68	0.505	0.00	0.0
0.72	0.562	0.00	0.0
0.76	0.620	0.00	0.0
0.80	0.680	0.0	0.0
0.84	0.74	0.0	0.0
0.88	0.74	0.0	0.0
0.92	0.74	0.0	0.0
0.96	0.74	0.0	0.0
1.00	0.74	0.0	0.0

C EQUATION OF STATE DATA

C

C

EOS PR

COMPONENTS

P1 P2 P3 P4 P5 P6 P7

PROPERTIES F PSIA

COMP	MW	TC	PC	ZC	ACENTRIC	OMEGAA	OMEGAB
P1	16.38	-119.91	662.80	.2888	.0133	.352806	.071039
P2	31.77	89.83	752.20	.2894	.1130	.451923	.079260
P3	50.64	245.90	581.00	.2818	.1724	.459850	.0784370
P4	77.79	407.26	468.40	.2679	.2532	.460949	.078234
P5	102.03	561.98	410.50	.2624	.3150	.419216	.095091
P6	150.30	677.63	325.20	.2460	.4138	.551640	.089993
P7	233.65	843.58	244.40	.23070	.57890	.537364	.095091

DJK P1

P2	.000947
P3	.007835
P4	.021885
P5	-.160885
P6	-.155665
P7	.248173

DJK P2

P3	.003695
P4	.010541

```

P5 .010541
P6 .010541
P7 .010541
DJK P3
P4 .002281
P5 .002281
P6 .002281
P7 .002281
DJK P4
P5 .000000
P6 .000000
P7 .000000
DJK P5
P6 .000000
P7 .000000
DJK P6
P7 .000000
C
ENDEOS
C
C
GASMF
.679300 .099000 .110800 .045000 .034766 .019684 .011451
OILMF
X X X X X X X
C
C
C RESERVOIR DESCRIPTION ARRAYS FOLLOW:
ARRAYS
C
DX CON
293.3
DY CON
293.3
DZ ZVAR
30 30 50 50
MDEPTH ZVAR
7330 7360 7400 7450
POR CON
.13
C
KX ZVAR
130 40 20 150
KY ZVAR
130 40 20 150
KZ ZVAR
13 4 2 15
C
RUN
STOP
END

```

(Input data for Step 7 - Simulation)

Spe3r.dat

```
C VIP-EXEC COMPOSITIONAL EXAMPLE #1
C
C DATA SET NAME: spe3r.DAT
C
C FEATURES DEMONSTRATED:
C (1) IMPLICIT
C (2) GAUSS
C
C -----
RUN
C
DIM NAMAX
      300000
C
IMPLICIT
C
RESTART 0 3
C
TITLE2
      DATA SET NAME: spe3r.DAT
TITLE3
      SINGLE WELL - RICH GAS CONDENSATE,GAS CYCLING
C
C START CARD DEFINES WHERE DATA PROCESSING BEGINS
START
C
C USE GAUSS AS SOLUTION METHOD
GAUSS
C
C WELL DEFINITION DATA
WELL N IW JW IGC IBAT
      1  7  7  1  1
      2  7  1  1  1
C
C DEFINE WELL 1 AS A PRODUCER
PROD G 1
INJ G 2
YINJ 2
      0.8036 0.1052 0.08 0.0112 0.0 0.0 0.0
FPERF
WELL  L IW JW KH
      1  3  7  7 1000
      1  4  7  7 7500
      2  1  1  1 3900
      2  2  1  1 1200
C FLOW CHARACTERISTICS FOR WELL 1!
WI 1
1.55
C FLOW CHARACTERISTICS FOR WELL 2
WI 2
1.55
C
C PRESSURE AND RATE CONTROLS FOR WELL 1
BHP 1
500
7400
QMAX 1
6200
QMAX 2
4700
C
C SURFACE SEPARATION DATA FOR WELL 1
SEPARATOR 1
```

STAGE	TEMP	PRES	VFRAC	VDEST	LFRAC	LDEST
1	80.	815.	1.	GAS	1.	2
2	80.	65	1.	GAS	1.	3
3	60	14.6	1.	GAS	1.	OIL

NEWSEP 1
1
1
2500

STAGE	TEMP	PRES	VFRAC	VDEST	LFRAC	LDEST
1	80.	315	1.	GAS	1.	2
2	80.	65.	1.	GAS	1.	3
3	80.	14.6	1.	GAS	1.	OIL

C
C
C TIME STEP CONTROLS
DT -10 1. 365. 200. .2 .2 .03
C
C ITERATION CONTROLS
ITNLIM 1 8 300. .2 .2 .02
C OUTPUT CONTROLS
PRINT WELL TIME
OUTPUT SO
C
TIME 10
C SWITCH tO BLITZ
BLITZ
TIME 25
TIME 50
TIME 100
TIME 200
TIME 300
TIME 400
TIME 500
TIME 600
TIME 800
TIME 1000
TIME 1200
TIME 1500
TIME 1825
TIME 2000
TIME 2500
TIME 3000
TIME 3050
TIME 3100
TIME 3150
TIME 3200
TIME 3250
TIME 3300
TIME 3350
TIME 3400
TIME 3450
TIME 3500
TIME 3650
QMAX 2
0.0
TIME 4000
TIME 4500
TIME 5000
TIME 5500
TIME 6000
STOP
END

REFERENCES:

1. Coats, K.H. and Smart, G.T.: " Application of a Regression Based EOS PVT Program to Laboratory Data," *SPEE* (May 1986) 277-299.
2. Peng, D.-Y. and Robinson, D.B.: "A New Two-Constant Equation of State," *Ind. Eng. Chem. Fundam.* (1976) 15, 59.
3. Soave, G.: "Equilibrium Constants From a Modified Redlich Kwong Equation of State," *Chem. Eng. Sci.* (1972) 27, 1197-1203.
4. Coats, K.H., Dempsey, J.R., and Henderson, J.H.: "A New Technique for Determining Reservoir Description from Field Performance Data," *SPEJ* (March 1970) 66-74.
5. Whitson, C.H.: "Characterizing Hydrocarbon Plus Fractions," *SPEJ* (Aug. 1983) 683-94.
6. Coats, K.H.: "Simulation of Gas Condensate Reservoir Performance," *JPT* (Oct. 1985) 1870-86.
7. Kenyon, D.E. and Behie, A.: "Third Comparative Solution Project: Gas Cycling of Retrograde Condensate Reservoirs," SPE 12278, *JPT* (August 1987), 981-997.
8. Abel, W., Jackson, R.F. and Wattenbarger, R.A.: "Simulation of a Partial Pressure Maintenance Gas Cycling Project with a Compositional Model, Carson Creek Field, Alberta", *Numerical Simulation*, SPE Reprint Series No. 11, 285-293.
9. Thompson, F.R.: "Compositional Simulation of a Gas Cycling Project, Bonnie Glen D-3A Pool, Alberta, Canada", *Numerical Simulation*, SPE Reprint Series No. 11, 314-329.
10. Field, M.B., Givens, J.W. and Paxman, D.S.: "Kaybob South - Reservoir Simulation of a Gas Cycling Project with Bottom Water Drive", *Numerical Simulation*, SPE Reprint Series No. 11, 294-305.
11. Course notes, PETE 605, PETE 607 AND PETE 611, Texas A&M University.
12. Lake, L.W.: *Enhanced Oil Recovery*, Prentice Hall, 1989.
13. Stalkup, F.I.: *Miscible Flooding Fundamentals*, SPE Monograph Series, 1983.